



**Sónia Maria Gomes  
Pires**

**Oxidação catalítica de compostos orgânicos: uma  
abordagem sustentável**

**Catalytic oxidation of organic compounds: a  
sustainable approach**



**Sónia Maria Gomes  
Pires**

**Oxidação catalítica de compostos orgânicos: uma  
abordagem sustentável**

**Catalytic oxidation of organic compounds: a  
sustainable approach**

Tese apresentada à Universidade de Aveiro para cumprimento dos requisitos necessários à obtenção do grau de Doutor em Química, realizada sob a orientação científica da Doutora Maria da Graça de Pinho Morgado Silva Neves e do Doutor Mário Manuel Quialheiro Simões, respectivamente Professora Associada com Agregação e Professor Auxiliar do Departamento de Química da Universidade de Aveiro.

Apoio financeiro da FCT e do FSE no âmbito do III Quadro Comunitário de Apoio.



Aos meus Pais e Irmãos e à minha princesa Leonor

*“Porque eu sou do tamanho do que vejo  
E não do tamanho da minha altura...”*

Alberto Caeiro (heterónimo de Fernando Pessoa)

## **o júri**

presidente

**José Rodrigues Ferreira da Rocha**  
Professor Catedrático da Universidade de Aveiro

**Prof. Doutora Maria Miguéns Pereira**  
Professora Associada com Agregação, Faculdade de Ciências e Tecnologia, Universidade de Coimbra

**Prof. Doutora Maria da Graça de Pinho Morgado da Silva Neves**  
Professora Associada com Agregação, Universidade de Aveiro (Orientadora)

**Prof. Doutor Augusto Costa Tomé**  
Professor Associado com Agregação, Universidade de Aveiro

**Prof. Doutor Joaquim Luís Bernardes Martins de Faria**  
Professor Associado, Faculdade de Engenharia, Universidade do Porto

**Doutora Susana Luísa Henriques Rebelo**  
Investigadora, Faculdade de Ciências, Universidade do Porto

## agradecimentos

Gostaria de agradecer em primeiro lugar aos meus orientadores Doutora Graça Neves e Doutor Mário Simões pelos valiosos ensinamentos, constante motivação, amizade e disponibilidade que me dispensaram durante todo este percurso. Contribuíram de forma decisiva para o sucesso deste trabalho. Um agradecimento especial ao Doutor Artur Silva, não só pela preciosa ajuda na interpretação dos espectros de RMN, como pelo que me “obrigou” a estudar na grande parte das unidades curriculares do Programa Doutoral em que foi meu professor.

Não posso também deixar de expressar o meu agradecimento a todos os técnicos do Departamento de Química a quem tive que recorrer, não só pela colaboração no trabalho como pela simpatia com que sempre me trataram. A todas as pessoas que tiveram participação activa no trabalho apresentado nesta dissertação, nomeadamente a Doutora Isabel Vieira, Doutora Susana Rebelo, Doutora Rosário Domingues, Doutora Paula Alexandrina, Doutora Vera Silva, Gil Gonçalves, Tiago Duarte, Gustavo Silva e Doutor Filipe Paz, muito obrigada.

Aos meus colegas de laboratório... Começando pelos que já cá estavam quando iniciei esta aventura e me acompanharam até terminar: Diana, Leandro, Flávio, João, Maria Clara, Joana Costa; mais que colegas de trabalho, foram amigos, companheiros de “luta”, com vocês ri (muito), chorei, viajei, festejamos vitórias, conquistas, partilhamos desilusões e momentos difíceis... Por tudo isto e muito mais que não consigo expressar por palavras, OBRIGADA!!!!

Às minhas “babes” Joana Ferreira, Carla Santos (Màriza) e Cláudia Bispo o meu agradecimento pela compreensão, carinho e grande amizade que nos une.

Muitos mais nomes deveriam estar aqui... mas de modo a não tornar estes agradecimentos demasiados extensos e não querendo correr o risco de me esquecer de alguém, agradeço a todos os restantes membros que compõem o grupo de investigação do QOPNA, e aos que passaram por cá e que pelos mais diversos motivos já não estão, com quem tive o prazer de trabalhar!

Por último (mas não menos importante), o agradecimento à minha família, aos meus pais, irmãos e ao novo membro da família (nascida durante esta aventura), a minha sobrinha e minha princesinha Leonor. Vocês são aquilo que tenho de mais importante, os meus pilares, o meu refúgio... Obrigada por tudo!

**palavras-chave**

catalisadores, metaloporfirinas, oxidação, peróxido de hidrogénio, compostos organosulfurados, benzofuranos, naftoquinonas, polioxometalatos, óxido de grafeno

**resumo**

Um dos maiores desafios para os investigadores da área da química orgânica prende-se com o desenvolvimento de sistemas catalíticos capazes de promover, mesmo sob condições moderadas e ambientalmente sustentáveis, a oxidação selectiva de compostos orgânicos. Esta é uma transformação que a natureza realiza de uma forma extraordinária mas que se reveste de tremenda dificuldade tanto no meio académico como a nível industrial. As metaloporfirinas, consideradas modelos biomiméticos do citocromo P450, revestem-se por isso de um enorme potencial em catálise.

Assim, nesta dissertação, após o primeiro capítulo introdutório, onde os conceitos mencionados acima são apresentados, no capítulo 2 são abordados alguns dos principais aspectos relativos às propriedades, síntese e reactividade das porfirinas. São ainda descritas neste capítulo as rotas sintéticas para todas as metaloporfirinas de Mn(III) e de Fe(III) usadas durante o trabalho.

O capítulo 3 reporta-se à aplicação de complexos metaloporfirínicos de Mn(III) e de Fe(III) na catálise oxidativa de compostos organosulfurados (sulfuretos, benzotiofenos, dibenzotiofenos e 1,3-di-hidrobenzotiofenos) pelo peróxido de hidrogénio. Para além de se revelar uma metodologia altamente eficiente para a obtenção das correspondentes sulfonas, o uso de condições moderadas e atóxicas, torna esta abordagem segura para o meio ambiente. A potencialidade da metodologia desenvolvida só pode ser amplamente reconhecida através da heterogeneização do complexo porfirínico num suporte sólido. Desta forma, no capítulo 4 são apresentadas as estratégias de imobilização de diferentes macrociclos tetrapirrólicos na resina de Merrifield e na sílica funcionalizada. Foram preparados três materiais baseados em metaloporfirinas e os resultados dos ensaios catalíticos envolvendo o tioanisol como substrato e como oxidante o  $H_2O_2$  colocam em evidência a eficiência e a reciclabilidade de dois deles.

Os ensaios catalíticos com metaloporfirinas foram alargados a outras classes de substratos, nomeadamente os benzofuranos e as naftoquinonas, cujos resultados se apresentam nos capítulos 5 e 6, respectivamente. Apesar da complexidade de produtos obtida, a preferencial via de oxidação parece envolver, em ambos os casos, em primeiro lugar uma epoxidação.

Finalmente, foi ainda avaliada a eficiência de dois catalisadores não porfirínicos, nomeadamente um polioxometalato e um óxido de grafeno (testados em condições homogéneas e heterogéneas respectivamente) em processos de sulfoxidação pelo peróxido de hidrogénio, cujos resultados se descrevem no capítulo 7.

O último capítulo inclui as conclusões gerais e algumas perspectivas futuras para o trabalho desenvolvido.

**keywords**

Catalysts, metalloporphyrins, oxidation, hydrogen peroxide, organosulfur compounds, benzofurans, naphthoquinones, polyoxometalates, graphene oxide

**abstract**

One of the biggest challenges for organic chemistry researchers is the development of catalytic systems able to selectively oxidize organic compounds, under mild and environmental sustainable conditions. In fact, this is a transformation which nature operates with an extraordinary ability but is of remarkable difficulty for both academia and industry. Metalloporphyrins, as biomimetic models of cytochromes P450, are thus catalysts with great potential. After the first introductory chapter, where the above-mentioned concepts are fully discussed, some general features of porphyrin properties, synthetic methodologies and reactivity are presented in Chapter 2 of this dissertation. The synthetic routes to all the Mn(III) and Fe(III) porphyrins used as catalysts during the work are also described in this chapter. Chapter 3 is dedicated to the application of Mn(III) and Fe(III) metalloporphyrin complexes on the oxidative catalysis of organosulfur compounds (sulfides, benzothiophenes, dibenzothiophenes and 1,3-di-hydrobenzothiophenes) by hydrogen peroxide. Besides revealing a high efficient approach for the obtention of the corresponding sulfones, the use of mild and nontoxic conditions turns this approach environmentally safe. The potentiality of the developed methodology only can be fully recognized through the heterogenization of porphyrin complexes in a solid support. So, in chapter 4 the immobilization strategies of tetrapyrrolic macrocycles onto Merrifield resin and silica supports are presented. Three heterogeneous metalloporphyrin-based materials were prepared and the results of catalytic assays with thioanisole as substrate and H<sub>2</sub>O<sub>2</sub> as oxidant put in evidence the efficiency and recyclability of two of them. The catalytic experiments with metalloporphyrins were extended to other substrate classes, namely benzofurans and naphthoquinones, and the results are described and discussed in Chapters 5 and 6, respectively. Despite the complexity of the products obtained, the preferential oxidation route in both cases seems to involve first an epoxidation. Finally, the efficiency of two non-porphyrinic catalysts, namely a manganese polyoxometalate and graphene oxide (tested under homogeneous and heterogeneous conditions, respectively), was also evaluated in sulfoxidation processes by hydrogen peroxide, being the results described in Chapter 7. Graphene 3D oxide, whose catalytic performance was evaluated for the first time, demonstrates to be efficient and recyclable in the oxidation of thioanisole. The last chapter includes some general conclusions and future perspectives for the developed work.



## ABBREVIATIONS / ABREVIATURAS

a.u.	arbitrary units
CYP-450	cytochrome P450
<i>m</i> -CPBA	<i>m</i> -chloroperbenzoic acid
$\delta$	chemical shift in ppm
<i>d</i>	doublet
<i>dd</i>	doublet of doublets
<i>ddd</i>	double doublet of doublets
<i>o</i> -DCB	<i>ortho</i> -dichlorobenzene
DMD	dimethyldioxirane
DMF	dimethylformamide
DMSO	dimethylsulfoxide
equiv.	molar equivalents
ESI-MS	electrospray ionization mass spectrometry
Fe(TF <sub>4</sub> NMe <sub>2</sub> PP)Cl	chloro[ <i>meso</i> -tetrakis(4- <i>N,N</i> -dimethylamine-2,3,5,6-tetrafluorophenyl)porphyrinate] iron(III)
GC	gas chromatography
GC-FID	gas chromatograph equipped with a flame ionization detector
GC-MS	gas chromatograph equipped with a mass spectrometer
I.S.	internal standard
IUPAC	International Union of Pure and Applied Chemistry
<i>J</i>	coupling constant
$\lambda$	wavelength
$\lambda_{\max}$	wavelength of maximum absorbance
<i>m</i>	multiplet
MALDI(TOF/TOF)-MS	matrix assisted laser desorption ionization – time of flight – mass spectrometry
M-porph	metalloporphyrin
Mn(TDCPP)Cl	chloro[5,10,15,20-tetrakis(2,6-dichlorophenyl)porphyrinate]manganese (III)
Mn(TDMI <sub>m</sub> P)Cl	chloro[5,10,15,20-tetrakis(1,3-dimethylimidazolium-2-yl)porphyrinatomanganese(III)] tetraiodide
Mn(TPFPP)Cl	chloro[5,10,15,20-tetrakis(pentafluorophenyl)porphyrinate]manganese (III)

Mn(TMImP)Cl	chloro[5,10,15,20-tetrakis(1-methylimidazolium-2-yl)porphyrinate]manganese(III)
MW	molecular weight
MS (EI)	Mass spectrometry (electronic impact)
NMR	nuclear magnetic resonance
<sup>13</sup> C NMR	carbon ( <sup>13</sup> C) nuclear magnetic resonance
<sup>19</sup> F NMR	fluor ( <sup>19</sup> F) nuclear magnetic resonance
<sup>1</sup> H NMR	proton ( <sup>1</sup> H) nuclear magnetic resonance
PhIO	iodosylbenzene
ppm	part per million
<i>q</i>	quartet
R <sub>t</sub>	retention time in gas chromatography
<i>s</i>	singlet
<i>t</i>	triplet
TMS	tetramethylsilane
TPP	5,10,15,20-tetraphenylporphyrin
UV-Vis	ultraviolet-visible spectroscopy

# TABLE OF CONTENTS

<b>CHAPTER 1 INTRODUCTION</b> .....	<b>1</b>
<b>1. INTRODUCTION</b> .....	<b>3</b>
<b>1.1. CATALYSIS: GENERAL ASPECTS</b> .....	<b>4</b>
1.1.1. INTRODUCTORY CONCEPTS .....	4
1.1.2. TYPES OF CATALYSTS.....	6
1.1.3. CHOOSING HOMOGENEOUS/HETEROGENEOUS CATALYSTS .....	7
<b>1.2. OXIDATIVE CATALYSIS IN NATURE</b> .....	<b>8</b>
1.2.1. THE UBIQUITOUS PORPHYRIN SYSTEM.....	8
1.2.2. CYTOCHROME P450 .....	10
1.2.2.1. MECHANISM OF CYTOCHROME P450 CATALYZED OXIDATIONS .....	12
<b>1.3. SYNTHETIC MODELS OF CYTHOCROME P450 ENZYMES</b> .....	<b>15</b>
1.3.1. METALLOPORPHYRINS BASED BIOMIMETIC MODELS.....	16
1.3.1.1. EFFECT OF THE PORPHYRINIC LIGAND STRUCTURE.....	17
1.3.1.2. OXIDANT INFLUENCE .....	20
1.3.1.3. ROLE OF THE CO-CATALYST AND THE SOLVENT .....	21
1.3.1.4. MECHANISTIC CONSIDERATIONS.....	24
1.3.1.5. SUBSTRATE SCOPE .....	26
1.3.1.6. HETEROGENEOUS METALLOPORPHYRIN-BASED CATALYTIC SYSTEMS.....	36
<b>1.4. BIBLIOGRAPHY</b> .....	<b>41</b>
<b>CHAPTER 2 SYNTHESIS OF METALLOPORPHYRIN BASED CATALYSTS</b> .....	<b>49</b>
<b>2. SYNTHESIS OF METALLOPORPHYRIN BASED CATALYSTS</b> .....	<b>51</b>
<b>2.1. PORPHYRINS AND ANALOGUES: GENERAL ASPECTS</b> .....	<b>51</b>
2.1.1. NOMENCLATURE AND STRUCTURAL DEFINITIONS.....	51
2.1.2. AROMATICITY AND PRINCIPAL PHYSICO-CHEMICAL PROPERTIES .....	52
2.1.3. PROTON NMR SPECTROSCOPY .....	53
2.1.4. UV-VIS ABSORPTION SPECTROSCOPY .....	53
2.1.5. SYNTHETIC METHODOLOGIES.....	55
2.1.5.1. MESO-TETRAARYLPORPHYRINS .....	56
2.1.6. PORPHYRINIC MACROCYCLE REACTIVITY .....	58
<b>2.2. SYNTHETIC ROUTES TO PORPHYRINS AND ANALOGUES</b> .....	<b>60</b>
2.2.1. MESO-ARYLPORPHYRINS (2.1 AND 2.2).....	61
2.2.2. MESO-IMIDAZOL PORPHYRIN DERIVATIVE (2.3).....	63
2.2.1. SYNTHETIC ROUTES TO FREE BASE CHLORIN DERIVATIVES (2.4 AND 2.5) .....	63
<b>2.3. SYNTHESIS OF PORPHYRIN AND CHLORIN COMPLEXES (I-VII)</b> .....	<b>66</b>
2.3.1. SYNTHESIS OF THE MANGANESE COMPLEXES BASED ON THE STRUCTURE OF H <sub>2</sub> TPFPP (II E VII).....	67
2.3.2. SYNTHESIS OF THE CATIONIC CATALYST V .....	68
<b>2.4. EXPERIMENTAL</b> .....	<b>69</b>
2.4.1. SYNTHESIS OF PORPHYRINS 2.1 AND 2.2 .....	70
2.4.2. SYNTHESIS OF 5,10,15,20-TETRAKIS-(1-METHYLIMIDAZOLIUM-2-YL) PORPHYRIN 2.3 72	
2.4.3. SYNTHESIS OF FREE BASE CHLORIN DERIVATIVES 2.4 AND 2.5 .....	72
2.4.4. SYNTHESIS OF THE MANGANESE AND IRON PORPHYRIN-BASED CATALYSTS.....	74
2.4.4.1. GENERAL PROCEDURE FOR COMPLEXES I, III, IV AND VI.....	74
2.4.4.2. GENERAL PROCEDURE FOR COMPLEXES II AND VII .....	76
2.4.4.3. CATIONIC CATALYST COMPLEX-V .....	77
<b>2.5. BIBLIOGRAPHY</b> .....	<b>79</b>
<b>CHAPTER 3 HOMOGENEOUS BIOMIMETIC OXIDATION OF ORGANOSULFUR COMPOUNDS WITH H<sub>2</sub>O<sub>2</sub> CATALYZED BY METALLOPORPHYRINS</b> .....	<b>83</b>

<b>3. HOMOGENEOUS BIOMIMETIC OXIDATION OF ORGANOSULFUR COMPOUNDS WITH H<sub>2</sub>O<sub>2</sub> CATALYZED BY METALLOPORPHYRINS.....</b>	<b>85</b>
<b>3.1. OXIDATION OF SULFIDES, BENZOTHIOPHENES AND DIBENZOTHIOPHENES</b>	<b>85</b>
3.1.1. PRESENTATION OF THE WORK DEVELOPED.....	86
3.1.2. PART A- CATALYTIC EXPERIMENTS WITH MANGANESE(III) COMPLEXES .....	88
3.1.3. PART B- CATALYTIC EXPERIMENTS WITH IRON(III) COMPLEXES .....	93
3.1.4. CONCLUSIONS .....	103
<b>3.2. OXIDATION OF 1,3-DIHYDROBENZO[C]THIOPHENES.....</b>	<b>104</b>
3.2.1. RESULTS AND DISCUSSION .....	105
3.2.2. CONCLUSIONS .....	108
<b>3.3. EXPERIMENTAL .....</b>	<b>109</b>
3.3.1. GENERAL PROCEDURE FOR THE CATALYTIC EXPERIMENTS .....	109
3.3.2. GC-FID ANALYSES .....	110
3.3.3. OXIDATION OF SULFIDES, BENZOTHIOPHENES AND DIBENZOTHIOPHENES.....	110
3.3.3.1. CHARACTERIZATION OF THE COMPOUNDS .....	111
3.3.4. MODEL FUEL OXIDATION .....	116
3.3.5. OXIDATION OF 1,3-DIHYDROBENZO[C] THIOPHENES .....	116
3.3.5.1. SYNTHESIS OF THE STARTING 1,3-DIHYDROBENZO[C]THIOPHENES .....	116
3.3.5.2. OXIDATION OF 1,3-DIHYDROBENZO[C]THIOPHENES .....	116
<b>3.1. BIBLIOGRAPHY .....</b>	<b>118</b>
<b>CHAPTER 4 HETEROGENEOUS METALLOPORPHYRIN BASED CATALYTIC SYSTEMS FOR OXIDATION OF SULFUR DERIVATIVES .....</b>	<b>123</b>
<b>4. HETEROGENEOUS METALLOPORPHYRIN BASED CATALYTIC SYSTEMS FOR THE OXIDATION OF ORGANOSULFUR COMPOUNDS.....</b>	<b>125</b>
<b>4.1. OVERVIEW .....</b>	<b>125</b>
<b>4.2. CATALYTIC EXPERIMENTS WITH IMIDAZOLIUM PORPHYRIN DERIVATIVES</b>	<b>127</b>
4.2.1. ASSAYS UNDER HOMOGENEOUS CONDITIONS.....	127
4.2.2. SYNTHESIS OF THE HETEROGENEOUS CATALYSTS .....	130
4.2.3. ASSAYS UNDER HETEROGENEOUS CONDITIONS .....	131
<b>4.3. IMMOBILIZATION OF AN IRON PORPHYRIN ON A MERRIFIELD RESIN AND CATALYTIC EXPERIMENTS.....</b>	<b>136</b>
<b>4.4. CATALYTIC EXPERIMENTS WITH THE HETEROGENEOUS CHLORIN VI-SI ...</b>	<b>138</b>
<b>4.5. CONCLUSIONS .....</b>	<b>141</b>
<b>4.6. EXPERIMENTAL .....</b>	<b>142</b>
4.6.1. SYNTHESIS OF PORPHYRIN-BASED CATALYSTS IMMOBILIZED ON A MERRIFIELD RESIN	142
4.6.2. SYNTHESIS OF PORPHYRIN-BASED CATALYSTS IMMOBILIZED ON A FUNCTIONALIZED SILICA	143
4.6.3. CATALYTIC STUDIES .....	143
4.6.3.1. CATALYTIC TESTS USING CATIONIC CATALYST <b>V</b> UNDER HOMOGENEOUS CONDITIONS	143
4.6.3.2. CATALYTIC TESTS WITH METALLOPORPHYRIN-BASED MATERIALS UNDER HETEROGENEOUS CONDITIONS .....	144
<b>4.7. BIBLIOGRAPHY .....</b>	<b>145</b>
<b>CHAPTER 5 BIOMIMETIC OXIDATION OF BENZOFURAN DERIVATIVES.....</b>	<b>147</b>
<b>5. BIOMIMETIC OXIDATION OF BENZOFURAN DERIVATIVES.....</b>	<b>149</b>
<b>5.1. OVERVIEW .....</b>	<b>149</b>
<b>5.2. CATALYTIC EXPERIMENTS WITH BENZOFURAN SUBSTRATES.....</b>	<b>151</b>
5.2.1. CATALYTIC OXIDATION OF BENZOFURAN (5.6).....	153

5.2.2.	CATALYTIC OXIDATION OF 2-METHYLBENZOFURAN (5.7)	156
5.2.3.	CATALYTIC OXIDATION OF 3-METHYLBENZOFURAN (5.8)	158
<b>5.3.</b>	<b>CONCLUSIONS</b>	<b>161</b>
<b>5.4.</b>	<b>EXPERIMENTAL</b>	<b>162</b>
5.4.1.	CATALYTIC EXPERIMENTS	162
5.4.2.	CHARACTERIZATION OF THE ISOLATED OXIDATION PRODUCTS	162
<b>5.5.</b>	<b>BIBLIOGRAPHY</b>	<b>164</b>
<b>CHAPTER 6 BIOMIMETIC OXIDATION OF NAPHTHOQUINONES</b>		<b>167</b>
<b>6.</b>	<b>BIOMIMETIC OXIDATION OF NAPHTHOQUINONES</b>	<b>169</b>
<b>6.1.</b>	<b>OVERVIEW</b>	<b>169</b>
<b>6.2.</b>	<b>BIOMIMETIC OXIDATION OF LAPACHOL (6.1) WITH Mn(TDCPP)Cl AS CATALYST</b>	<b>171</b>
6.2.1.	BIOMIMETIC OXIDATION OF LAPACHOL 6.1 IN THE PRESENCE OF Mn(III) METALLOPORPHYRINS II AND V	178
<b>6.3.</b>	<b>BIOMIMETIC OXIDATION OF <i>nor</i>-LAPACHOL (6.2)</b>	<b>179</b>
<b>6.4.</b>	<b>CONCLUSIONS</b>	<b>180</b>
<b>6.5.</b>	<b>EXPERIMENTAL</b>	<b>181</b>
6.5.1.	GENERAL PROCEDURES	181
6.5.1.1.	OXIDATION OF LAPACHOL DERIVATIVES (6.1 AND 6.2) USING M-CPBA – ROUTE A	181
6.5.1.2.	GENERAL PROCEDURES OXIDATION OF LAPACHOL (6.1 AND 6.2) USING Mn(III) PORPHYRINS – ROUTE B	181
6.5.2.	CHARACTERIZATION OF THE COMPOUNDS	182
<b>6.6.</b>	<b>BIBLIOGRAPHY</b>	<b>185</b>
<b>CHAPTER 7 OTHER CATALYTIC SYSTEMS IN THE OXIDATION OF SULFUR COMPOUNDS</b>		<b>187</b>
<b>7.</b>	<b>OTHER CATALYTIC SYSTEMS IN THE OXIDATION OF ORGANOSULFUR COMPOUNDS</b>	<b>189</b>
<b>7.1.</b>	<b>OVERVIEW</b>	<b>189</b>
<b>7.2.</b>	<b>POLYOXOMETALATE CATALYSTS: POTENTIAL APPLICATION IN ODS</b>	<b>190</b>
7.2.1.	CATALYTIC EXPERIMENTS USING A BW <sub>11</sub> Mn	192
<b>7.3.</b>	<b>CATALYTIC EXPERIMENTS USING GRAPHENE OXIDE</b>	<b>197</b>
<b>7.4.</b>	<b>CONCLUSIONS</b>	<b>205</b>
<b>7.5.</b>	<b>EXPERIMENTAL</b>	<b>206</b>
7.5.1.	INSTRUMENTS AND METHODS	206
7.5.2.	SYNTHESIS OF Mn-POM AND GRAPHENE OXIDE CATALYSTS	206
7.5.3.	TYPICAL PROCEDURE FOR THE OXIDATION REACTIONS USING Mn-POM	206
7.5.4.	TYPICAL PROCEDURE FOR THE OXIDATION REACTIONS USING GRAPHENE OXIDE	207
<b>7.6.</b>	<b>BIBLIOGRAPHY</b>	<b>208</b>
<b>CHAPTER 8 GENERAL CONCLUSIONS AND FUTURE PERSPECTIVES</b>		<b>213</b>



# Chapter 1 INTRODUCTION





## 1. INTRODUCTION

The field of catalysis plays a role of crucial importance in contemporary society. In fact, in order to increase the yield and to lower the waste, over 85% of the currently manufactured products such as fuels, materials or drugs, involve the use of a catalyst in at least one step of production. Catalyzed processes are also absolutely vital in nature and probably life, as we know, could not exist, since the essential reactions of metabolism would be too slow.<sup>1</sup>

Thus, the crescent dissemination of catalyzed processes observed in the last decades is being mainly driven by the growing concerns associated to a sustainable development and, consequently, with the use of increasingly clean technologies. This led to the development of new and more efficient catalysts able to work properly, under mild conditions and in the presence of the so-called “green oxidants” (as air or hydrogen peroxide).<sup>2</sup> The developments in this area have been enormous and have inclusively been awarded with a Nobel Prize in 2001. The prize has been equally shared by William R. Knowles and Ryoji Noyori “for their work on chirally catalyzed hydrogenation reactions” and by K. Barry Sharpless “for his work on chirally catalyzed oxidation reactions”.<sup>3</sup> The “phenomenon” of oxidative catalysis is well evidenced by the number of publications that appeared over the last decades (Figure 1-1).

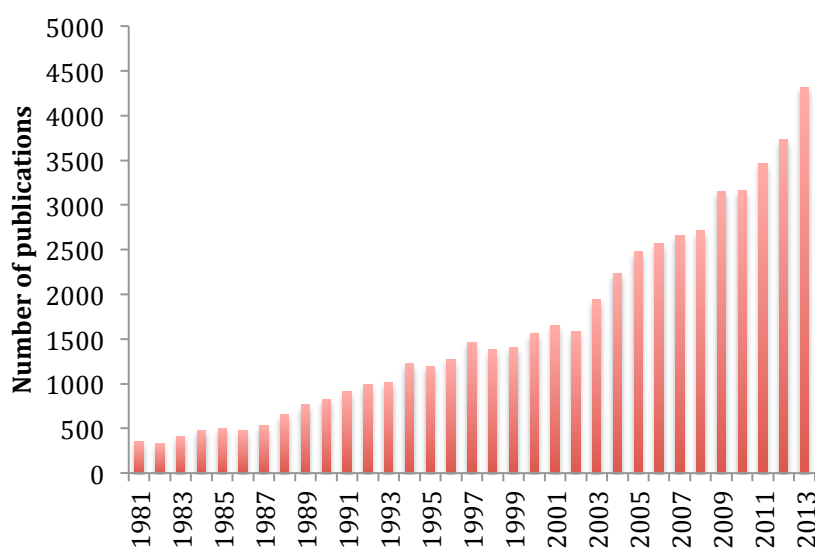


**Figure 1-1** Evolution of the number of publications in oxidative catalysis over the last 32 years (search at [www.sciencedirect.com](http://www.sciencedirect.com) with the keywords oxidative and catalysis)



Selective oxidation of organic compounds under mild conditions is one of the most relevant and, at the same time, most challenging transformations for modern industry and organic synthesis research. In biological systems, nature has its unique way of promoting selective oxidation processes with  $O_2$ .<sup>4</sup> Among the well-known and understood metalloenzymes capable of activate molecular oxygen are the cytochrome P-450 monooxygenases (CYP-450).<sup>4,5</sup> These ubiquitous and fascinating enzymes, containing an iron porphyrin core, are able to catalyze a wide variety of oxidation reactions: epoxidation, hydroxylation, dealkylation, dehydrogenation, oxidation of amines, sulfides, alcohols, aldehydes and even of unactivated hydrocarbons. Many efforts have been made towards the development of chemical biomimetic catalysts that surrogate the heme-containing active center of CYP-450's. In this sense metalloporphyrins are perhaps the best understood and most studied biomimetic models for oxidation reactions.<sup>6</sup> Since the first report by Groves<sup>7</sup> in 1979 considering the use of an iron(III) complex of 5,10,15,20-tetraphenylporphyrin (TPP) as catalyst in the oxidation of alkanes and alkenes, this field triggered the interest of several research groups spread all over the world and many advances have been reported in the last four decades. These findings are related with: i) the influence of the structure of the porphyrin ligand; ii) the metal ion in the inner core; iii) the role of the oxygen atom source; iv) the development of regio- and enantioselective oxidation catalysts v) the development of heterogeneous metalloporphyrin biomimetic systems.

In the next sections of this introductory chapter some general aspects on catalysis and on tetrapyrrolic macrocycles will be presented. The importance of metalloporphyrin synthetic biomimetic models will be also emphasized, along to the most relevant aspects that have been disclosed in literature in this field until today.

## 1.1. CATALYSIS: GENERAL ASPECTS

### 1.1.1. INTRODUCTORY CONCEPTS

Catalysis is a term created by the Swedish chemist Baron J. J. Berzelius in 1835 to describe the property of substances that facilitate chemical reactions without being consumed in them. At that time the catalytic phenomenon was described as a “new force” which he called the “catalytic force”.<sup>8</sup>

By definition, a catalyst is a substance that affects the normal velocity of the reaction providing a completely different pathway through the formation of intermediates and thus changing the necessary activation energy (Figure 1-2). The catalyst is not consumed in the process, being regenerated at the end. The presence of the catalyst does not affect the enthalpy energy, its effect is purely kinetic and not thermodynamic, thus the equilibrium state of the transformation remains unchanged.<sup>9</sup>

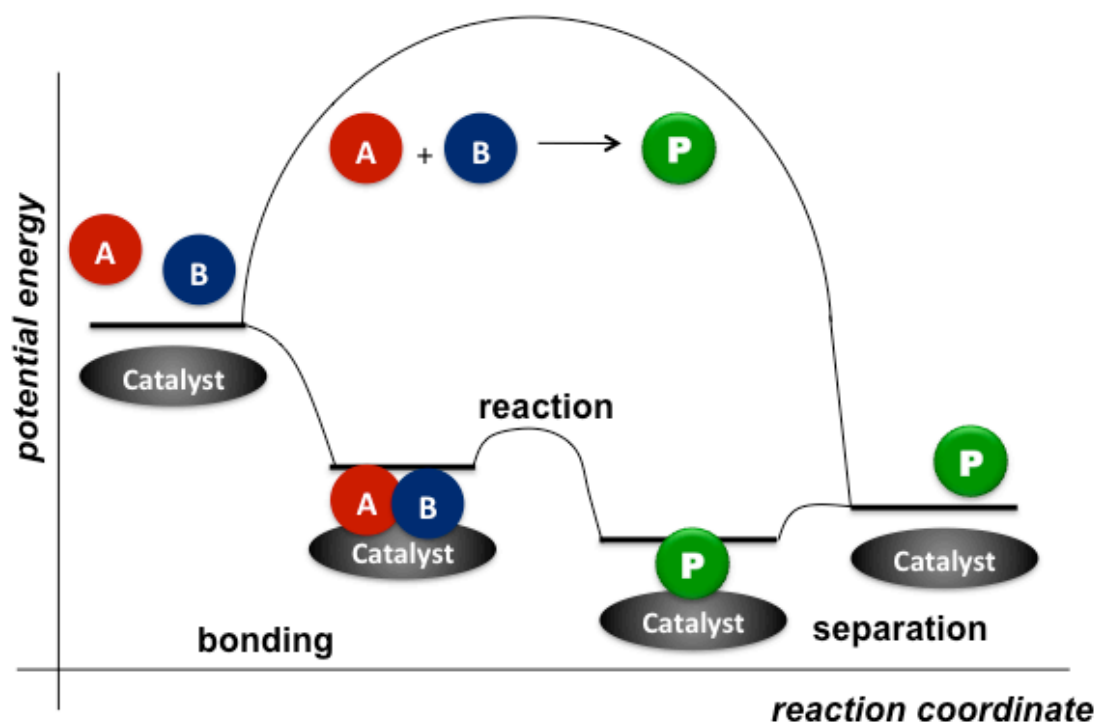


**Figure 1-2** Comparative energy diagrams of catalyzed and uncatalyzed processes

Generally a good catalyst should be easily accessible both from the synthetic and the economical point of view, must present enough stability under the reaction conditions, and of course has to demonstrate a high efficiency. Catalysts' efficiency can be evaluated either by the so-called turnover number (TON) or through the conversion of the substrate for a determined Substrate/Catalyst molar ratio. TON specifies the total amount of products that can be produced using a determined quantity of catalyst and is expressed by *mol Product(s)/mol Catalyst*. However, in order to make an acceptable comparison between two different sets of catalysts, is normally used the turnover frequency (TOF) defined by  $TOF = TON/\text{time of reaction}$ .<sup>10</sup> Relatively to the conversion, this is generally expressed in percentage and is obtained simply by *mol*



*Substrate consumed/mol Initial Substrate*. It is noteworthy that on the contrary of TOF (expressed as time unit<sup>-1</sup>), TON and conversion are dimensionless measures and, in order to be meaningful, reaction conditions must be cited.<sup>9, 11</sup>

Additionally, another important feature of a catalyst is its ability to direct the conversion of the reactants through a specific route, precisely its selectivity. Selectivity is defined as *mol of a specific product/mol of total formed products* when the conversion plateau is reached. It is important to understand that the formation and activation energies of substrate-catalyst intermediate are sensitive to the fine-tuning of catalyst structure. At least theoretically, it is possible to design a particular catalyst in order to obtain a specific product.<sup>11</sup>

### 1.1.2. TYPES OF CATALYSTS

The transition metal complexes are undoubtedly among the most used catalysts in industrial or laboratory organic synthesis. This is mainly due to the particular properties of transition metals which, presenting their valence d orbitals incompletely filled with electrons, can thus give or withdraw electrons depending on the nature of the reaction. Furthermore, they can easily form complexes with several compounds, and due to their ability to interchange between different oxidation states, make compounds based on transition metals very attractive catalysts.<sup>12</sup>

Enzymes, viewed as biological or natural catalysts, only gained importance in organic synthesis in the latter half of the 20th century; however, two major limitations are pointed to their use. First, many enzymes cannot be easily expressed in enough quantities for practical applications, although this situation was dramatically modified in the late 1970s with the development of recombinant DNA technology.<sup>13</sup> Second, many enzymes show often a narrow substrate scope, poor stereo- and/or regioselectivity and/or insufficient stability under operating conditions. With recent developments these problems can now be addressed and generally solved as demonstrated by several reports disclosed in the literature and also by the number of industrial applications. So, biocatalysis, with the referred improvements, turned to an area of great relevance also in organic synthesis. In fact, there are enzyme catalyzed transformations that simply are not possible or are extremely difficult even in the presence of the best nonbiological catalyst.<sup>14-17</sup>

Between organometallic catalysis and biocatalysis, after the year 2000 a third catalytical approach emerged, mainly for the production of enantiomerically pure organic compounds – organocatalysis. This field, driven by the independent reports of List, Lerner and Barbas and MacMillan and co-workers, concerns the use of small organic molecules, mainly composed of carbon, hydrogen, nitrogen, sulfur and phosphorous, to catalyze organic transformations.<sup>18</sup> Organocatalytic methods seem to be especially attractive in the synthesis of compounds in which the metal contamination must be avoided, e.g. pharmaceutical products.<sup>19, 20</sup> Besides, they also present other advantages as robustness, low-price (they are often naturally available), non-toxicity and environmental safety. Despite that, organocatalyzed reactions generally use higher catalyst loadings and, in order to obtain enantioselectivity, the reaction should be performed at room temperature, being thus much more time-consuming.<sup>21</sup>

All the three types of catalysis presented above have advantages and disadvantages, which means that a general solution to all the relevant problems cannot be expected with the exclusive use of one of them. Therefore, the research in all the three approaches needs to be intensified.

### 1.1.3. CHOOSING HOMOGENEOUS/HETEROGENEOUS CATALYSTS

Catalysts can be distinguished as homogeneous or heterogeneous. In homogeneous catalysis the catalyst is present in the same phase as the reactants, which normally means that they are present in a liquid reaction mixture. On the other hand, in heterogeneous catalysis, the catalyst is generally a solid being the reactants in a different phase, gaseous or liquid, and the overall process occurs at the surface of the support. The reactants are first adsorbed from the fluid phase to the solid surface, then occurring the catalyzed transformation involving the adsorbed species; finally, the products can be desorbed into the fluid phase.<sup>22</sup>

Commonly the main advantages on the use of heterogeneous catalysts lies on its easier separation from the reaction mixture and on their high tolerance to the extreme operating conditions, thus being widely used in industrial applications. On the other hand, homogeneous catalysts offer improved selectivity and increased activity, normally allowing the use of softer reaction conditions.<sup>23-25</sup>



Despite the advantages and disadvantages associated to each one of the catalytic systems, both play a significant role on chemical industry. In order to give answers to new challenges in the field, some research is focused on the development of catalysts that can combine the best of the two catalytic systems. In other words, the objective is to develop chemically homogeneous but physically heterogeneous catalysts;<sup>26</sup> this will be discussed in more detail afterwards.

## 1.2. OXIDATIVE CATALYSIS IN NATURE

The knowledge about the chemistry involved in biological oxidation reactions is fundamental for the understanding of natural processes such as the biosynthesis of endogenous compounds or the degradation of xenobiotics. Live organisms, over millions and millions of years of evolution, have developed extremely efficient and selective aerobic oxidation systems able to properly function even under mild conditions.<sup>27-29</sup>

Oxidations in biological systems are mainly catalyzed by metalloenzymes where the redox active site is structurally composed by a metalloporphyrin. Among the several enzymes able to catalyze oxidative processes, dehydrogenases, deoxygenases, peroxidases or monooxygenases, the cytochrome P450 monooxygenases have attracted a special attention of researchers.<sup>29-32</sup>

### 1.2.1. THE UBIQUITOUS PORPHYRIN SYSTEM

Present in almost all living organisms, porphyrins have a basic structure constituted by four pyrrolic type units linked by methinic bridges (Figure 1-3). These highly conjugated aromatic compounds are intensely coloured and the porphyrin designation derives from the Greek “πορφύρα”, porphyra, meaning "purple pigment". Not only the colour, but also the characteristic  $\pi$  system rule the main electronic and redox properties of these molecules.<sup>33</sup>

One of the most useful techniques to study this class of compounds is UV-Vis spectrophotometry and this point will be further discussed in chapter 2. The typical porphyrin spectrum shows an intense band around the 400 nm, denominated as the Soret band, and a set of weaker bands, designated as Q bands, between 500-700 nm. This spectrum reflects the structure of the macrocycle, the degree of saturation and

the substituents present, or the coordination to a metal center. The porphyrin macrocycle presents several functionalization sites, namely *meso* positions,  $\beta$ -pyrrolic positions, as well as the inner core (Figure 1-3).<sup>29, 30</sup>

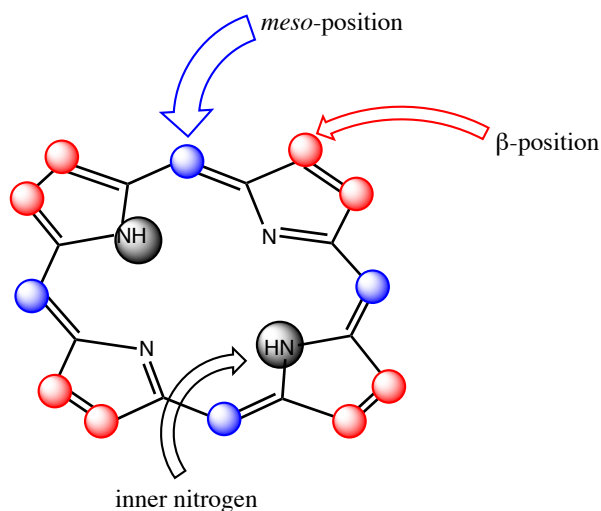


**Figure 1-3** Functionalization sites of the porphyrin macrocycle

Porphyrins and their analogue derivatives provide a vacant site at its center, ideally suited for metal incorporation. It is not surprising that they naturally occur as metal complexes and is in this form that they play the most critical roles in biological systems. Some of the most popular members of this family are represented on Figure 1-4: iron(II) complex of protoporphyrin IX (**1.1**), usually known as the heme group, and chlorophylls (**1.2**) disseminated in green plants.<sup>30</sup>

Derivative **1.1**, the most common prosthetic group, takes part in several cellular processes like oxygen transport and respiration (hemoglobin, myoglobin, cytochrome oxidase) and detoxification (cytochromes P450). Being present as the prosthetic group of all hemoproteins, iron porphyrin complexes were apparently naturally selected for dioxygen binding and activation. They can differ from each other in the peptidic component/axial ligand, and in the oxidation state of the iron (+2 or +3). These variations are the main reason for the several functions they display. For example, the reversible binding of dioxygen in hemoglobin, presenting a histidine residue as axial ligand and an iron(II) center, changes to dioxygen activation in cytochrome P450-dependent monooxygenases. In the latter, cysteine is the axial ligand and iron in the core is in the oxidation state +3. Chlorophylls **1.2**, structurally viewed as hydroporphyrin derivatives (also denominated chlorins), are responsible for the

captation of solar energy and its transformation into chemical energy in the photosynthetic process.<sup>32, 33</sup>

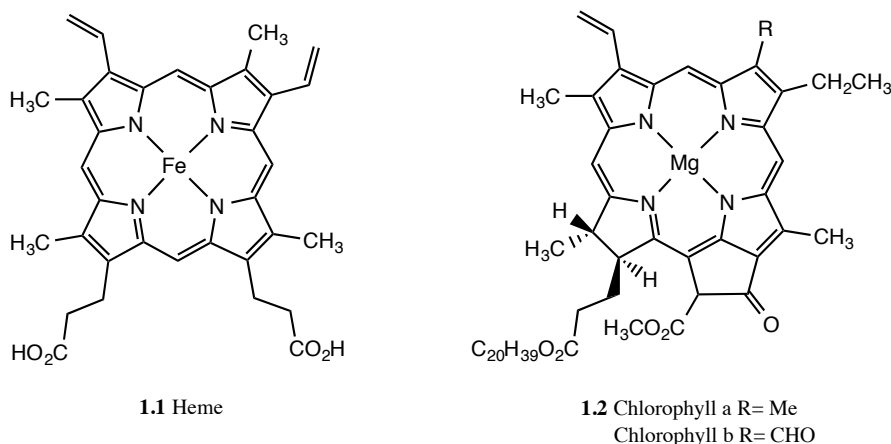


**Figure 1-4** Naturally occurring porphyrin derivatives

The structure of the heme group was firstly elucidated by Hans Fisher after promoting the synthesis of hematin in the laboratory. The importance of this achievement, along with further relationship to the green pigments of plants (chlorophylls) was recognized with the award of the Chemistry Nobel Prize in 1930.<sup>34</sup> After that, tetrapyrrolic macrocycles motivated a high multidisciplinary research interest from scientific community due to their intrinsic physical, chemical and biological properties.<sup>35</sup>

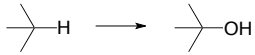
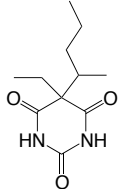
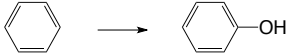
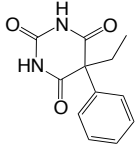
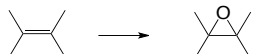
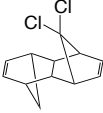
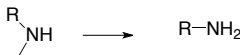
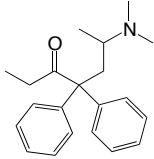
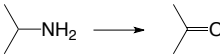
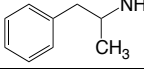
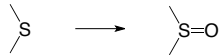
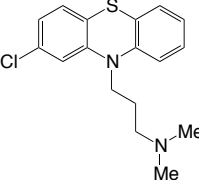
### 1.2.2. CYTOCHROME P450

Widely spread by all the five biological kingdoms (Animals, Plants, Fungi, Protists and Monera) cytochromes P450 constitute a superfamily of heme-containing monooxygenases counting already with more than 3000 members. They can be found in several mitochondrial tissues, in mammals however they are preferentially located in the endoplasmic reticulum of liver. Interestingly, from the already identified eighteen families of CYP-450, eleven were detected in the human liver. Moreover, from those eleven families, the five more largely expressed are responsible for the metabolism of approximately 95% of the drugs we ingest every day, clearly putting in evidence their high versatility.<sup>36-38</sup> Also in plants CYP-450 are considered essential in the production of some significant secondary metabolites, such as lignin, terpenoids,



steroids, essential oils, and opioid precursors. The ability demonstrated by these enzymes for the selective catalytic transference of one oxygen atom to the most diverse substrates, as exemplified in Table 1-1, inspired several important studies.<sup>38, 39</sup> Some important marks concerning the knowledge about CYP-450 were achieved, including the elucidation of its structure and novel understanding about the biological and chemical processes involved.<sup>40</sup>

**Table 1-1** Distinct processes catalyzed by cytochrome P-450 enzymes

Type of reaction	Simplified Example	Typical Substrate
Aliphatic Hydroxylation		<i>pentobarbital</i> 
Aromatic Hydroxylation		<i>phenobarbital</i> 
Alkenes Epoxidation		<i>aldrine</i> 
N,S,O-Dealkylation		<i>metadone</i> 
Oxidative Deamination		<i>amphetamine</i> 
S-Oxidation		<i>chlorpromazine</i> 

Martin Klingenberg first recognized CYP-450, in 1958, when he was studying the spectrophotometric properties of a microsomal fraction isolated from rat liver.<sup>41</sup> At that time, the author described that, when this same diluted fraction was treated with sodium dithionite, and then exposed to carbon monoxide, it was possible to observe a characteristic absorption band with a maximum at 450 nm. Six years later, Omura and Sato related this band with the iron(II) complex of protoporphyrin IX [P450-Fe<sup>2+</sup>-

CO]. The atypical position of the Soret band (at 450 nm) comparatively to other hemoproteins is in the origin of the name given to this particular cytochrome: cytochrome P450.<sup>42</sup>

The first cytochrome P450-dependent monooxygenase to be crystalized and having its X-ray structure solved was isolated from *Pseudomonas putida*.<sup>43</sup> Structurally, as it is possible to observe in Figure 1-5, besides the heme group, all CYP-450 have in the fifth coordination position of the metal a cysteine residue which establishes the linkage to the protein matrix through a disulfide bridge. The six and last position of the coordination sphere of iron(II) is occupied by a water molecule and is precisely where the molecular oxygen activation occurs. Both the thiolate axial ligand and the hydrophobic binding site seem to be determinant for the unique activity and selectivity of CYP-450. The cysteinyl ligand induces an effect known as “pull-push effect”, in the oxo-iron group responsible for the specific accessibility to the substrate and thus determining the catalytic properties of the system.<sup>44</sup>

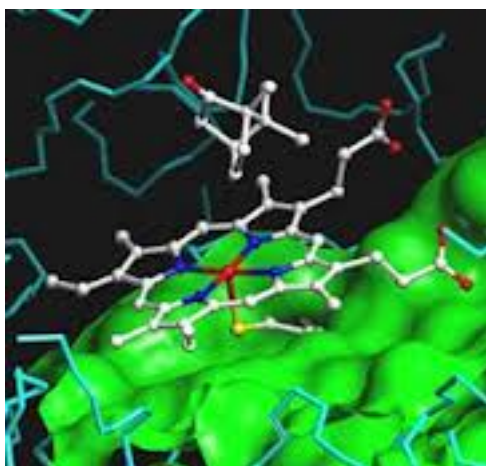
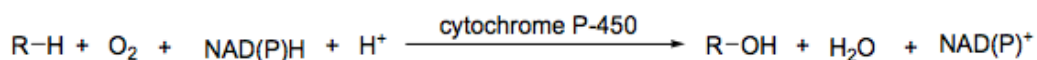


**Figure 1-5** Schematic representation of cytochrome P450 active center<sup>45</sup>

#### 1.2.2.1. MECHANISM OF CYTOCHROME P450 CATALYZED OXIDATIONS

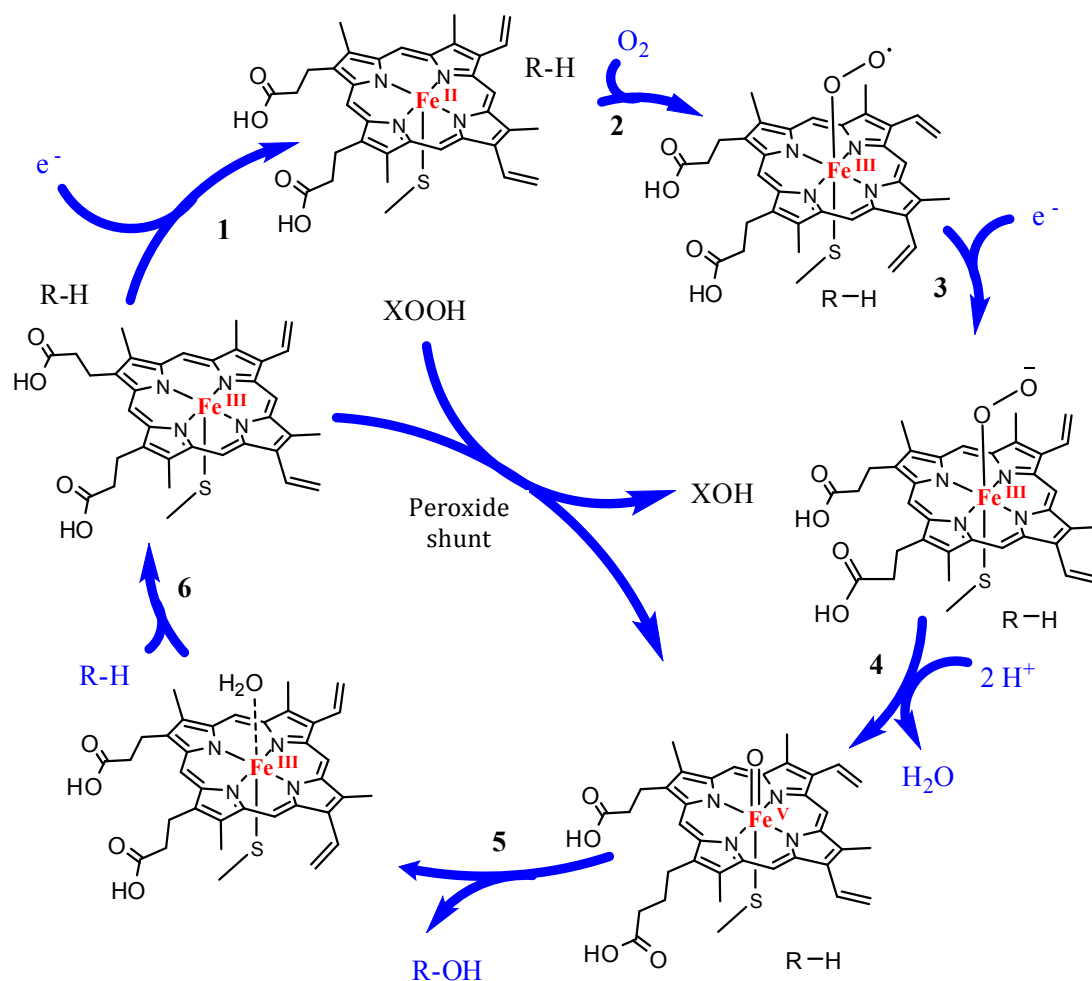
In the biotransformation processes promoted by these enzymes, generally a liposoluble xenobiotic or endobiotic compound is transformed into a polar, water-soluble, and extractable metabolite(s). It is nowadays accepted that despite the great versatility of CYP-450 in terms of the substrates, the same catalytic cycle is observed with all the members of these superfamily.<sup>38,46</sup> In the reactive processes CYP-450 enzymes take two reducing equivalents from NAD(P)H and deliver one atom from

dioxygen to the organic substrate and the other oxygen atom is released as water (Scheme 1-1).



**Scheme 1-1**

From the mechanistic point of view, it is now consensually accepted that the common catalytic cycle of CYP-450 involves a high-valent iron-oxo intermediate ((Por)Fe<sup>V</sup>=O or [(Por•)Fe<sup>IV</sup>=O]<sup>+</sup>) as the catalytic active species.<sup>47</sup> Regarding the catalytic cycle represented on Scheme 1-2, initially the binding of the substrate to the resting low-spin ferric enzyme induces structural changes, which may manifest in the dissociation of the distally coordinated water and on the conversion of the heme to a high spin form. The linkage of the substrate facilitates, in the first step of the cycle (**1**, Scheme 1-2) the reduction of the ferric enzyme, giving rise to the ferrous substrate bound form, allowing the delivery of the first electron. Next, the molecular oxygen binds to the ferrous heme and the ferric superoxide complex is formed (**2**, Scheme 1-2). The reduction of this species to ferric peroxo followed by protonation at the distal oxygen generates a ferric hydroperoxo complex, strongly evidenced by density functional calculations by EPR and ENDOR studies (**3**, Scheme 1-2). Finally, occurs the decomposition of this intermediate, the delivery of an additional proton to the distal oxygen permits the heterolytic cleavage of the O-O bond yielding the so-called *compound I* (the catalytic active species (Por)Fe<sup>V</sup>=O or [(Por•)Fe<sup>IV</sup>=O]<sup>+</sup>) (**4**, Scheme 1-2), responsible for the substrate oxidation.<sup>48</sup> This high electrophilic species, *compound I*, is able to transfer the oxygen atom to the substrate affording the corresponding oxidized product, an alcohol during alkanes oxidation, an epoxide in the case of alkenes oxidation, or other products depending on the oxidation reaction (**5**, Scheme 1-2).<sup>47</sup>



Scheme 1-2

As illustrated in Scheme 1-2, this catalytic cycle, mainly in the presence of reduced oxygen donors as iodossylbenzene, hypochlorites and peroxides, can occur through a shorter and simplified pathway named as the “peroxide shunt”.

Two determinant aspects have to be considered in the reactions where cytochrome P450 enzymes participate. The first one is the reductive activation of molecular oxygen, a step easily manipulated by nature but presenting great difficulties in biomimetic models chemistry. The second is related to the substrate oxidation itself, and with the intermediate reactions involving metal ions in higher oxidation states, with hydrocarbons.<sup>49</sup>

### 1.3. SYNTHETIC MODELS OF CYTHOCROME P450 ENZYMES

As previously referred, finding an efficient catalyst for the selective oxidation of organic molecules, under mild conditions, is one of the most challenging and at the same time, most important tasks in organic chemistry. Natural biological systems through the action of CYP-450 deal with this, in a unique and extraordinary way.<sup>50</sup> Therefore, based on the detailed knowledge of such enzymatic systems, the development of synthetic chemical models might therefore be a very useful tool to overcome the difficulty to work with enzymes *in vivo* and *in vitro*.<sup>51, 52</sup>

The use of synthetic models, beyond the accessibility issue, since they are much easier and rather available, is accompanied with other advantages. The study of the mechanisms and intermediates involved in the biomimetic models may provide new answers for the pathways involved in biological reactions, and otherwise validate the already existing proposals. Furthermore, different substituents and ligands in these synthetic analogues can provide more information concerning the structural and electronic aspects affecting their reactivity. Indeed, this can bring important contributions to the development of new bioinspired catalyst generations with improved selectivity, reactivity and stability.<sup>53</sup>

Good catalysts examples widely reported in the literature, able to efficiently mimic the catalytic active center of CYP-450, both structurally and functionally, are the metalloporphyrins and the Salen-type complexes, namely the Jacobsen catalyst. This type of catalysts find relevant applications, for example, in the study of biotransformations of new therapeutic agents, giving access to important metabolites and allowing to evaluate their toxicity. Although this non-enzymatic strategies are not able to simulate all the spectra of CYP-450 catalyzed reactions, they are considered as a relevant approach. Following the referred advantages, the use of this kind of models can contribute to decrease the number of animals used in clinical tests and discard the problems commonly associated with the isolation of natural enzymes or cells.<sup>35c, 54</sup>

The growing number of drug candidates provided every year to the market constrains the urgent development of rapid screening techniques, which may allow a simple but realistic analysis of their metabolism. It is easily understandable that, in economical terms, this type of tests should be promoted in order to ensure that undesirable candidates are earlier excluded.<sup>51, 55</sup>



A distinct aspect that has recently attracted the research community attention is related to the fact that several of the most worldwide prescribed drugs (and corresponding metabolites) have been referred as important emerging aquatic pollutants. The growing number of publications describing their occurrence in several ecosystems motivates the researchers concern about the environmental impact of such substances. Taking into account the low transformation rates of most of the drugs and the pharmacological activity of several of their metabolites, urges not only the development of efficient identification methodologies of this type of compounds in the several ecosystems, but also the promotion of ambient decontamination approaches.<sup>51, 55</sup>

### 1.3.1. METALLOPORPHYRINS BASED BIOMIMETIC MODELS

Mimicking all the steps and the distinct iron species involved in the catalytic cycle of CYP-450 is an arduous and almost utopic task. In this sense the identification of the “peroxide shunt” pathway has brought the necessary impetus to the development of new models for these monooxygenases.

Moreover, the recognized structural proximity of porphyrin complexes with the heme group triggered the interest of scientific community about metalloporphyrin-based oxidation catalytic systems. As already mentioned, in 1979 Groves and co-workers described for the first time the efficient use of the iron(III) complex of *meso*-tetraphenylporphyrin (TPP) in the oxidation of several substrates by iodosylbenzene.<sup>7</sup> Since this pioneering work, all the meanwhile disclosed reports decisively contribute to the recognition of the preponderant role of metalloporphyrins and analogues in biomimetic oxidative catalysis.

Over more than thirty years of research, as exemplified in Figure 1-6, many metalloporphyrin-based catalytic systems have emerged and were tested with different substrates and oxidants giving rise to important reviews.<sup>13, 35c, 47a, 56</sup> It is already established in the literature that the efficiency/selectivity of this bio-inspired systems is affected not only by the structure of the porphyrin catalyst or by the choice of the oxidant, but also by the addition of certain additives.

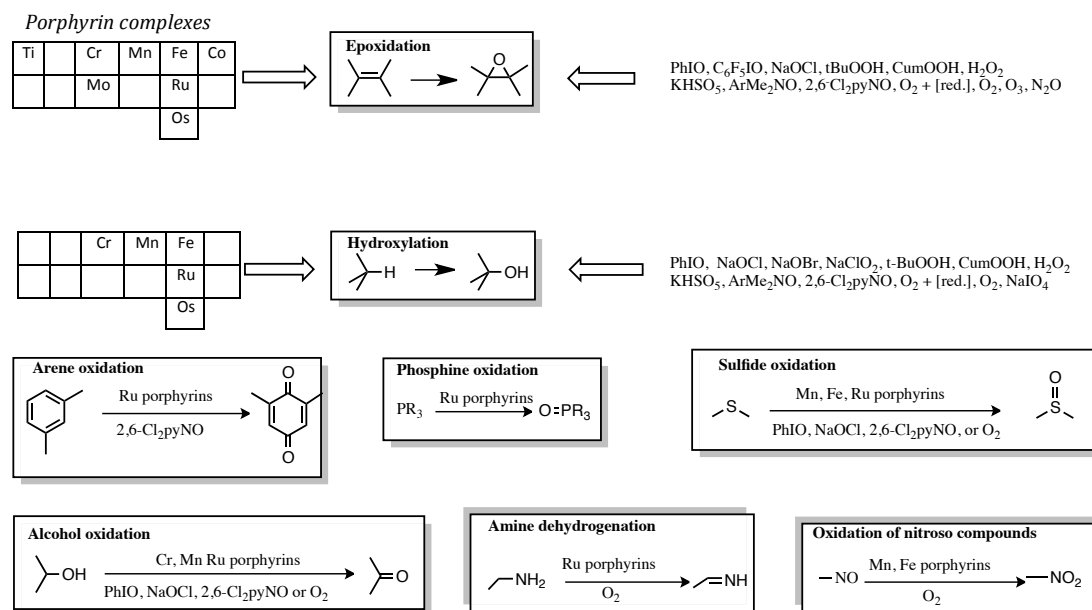


**Figure 1-6** Metalloporphyrin catalyzed oxidative transformations<sup>52</sup>

### 1.3.1.1. EFFECT OF THE PORPHYRIC LIGAND STRUCTURE

The first investigations related with this topic are mainly directed towards regioselective epoxydations and rely primarily on the use of simpler porphyrins such as *meso*-tetraphenylporphyrin or *meso*-tetratrimethylphenylporphyrin. However, this first generation of catalysts suffered from rapid deactivation, assigned to the oxidative degradation of the complex and to the formation of inactive  $\mu$ -oxo dimers.<sup>13, 57, 58</sup> In order to minimize this problem, more stable metalloporphyrin catalysts, known as the second and third generations, substituted with halogens, nitro or sulfonic groups at the *meso*-aryl and  $\beta$ -pyrrolic positions of the macrocycle, were developed.<sup>47a, 35c</sup>

The presence of electron-withdrawing substituents (EWS), namely in the *ortho* positions of *meso*-aryl groups, affects the general catalytic activity of metalloporphyrins by two main reasons: I) EWS increase the steric hindrance around the metallic center, avoiding the intermolecular interactions that can generate inactive catalytic species or promote the auto-oxidative destruction; II) EWS are also responsible for the higher electrophilic character of the catalytic intermediate species, which makes them more powerful oxidizing species.<sup>59</sup>

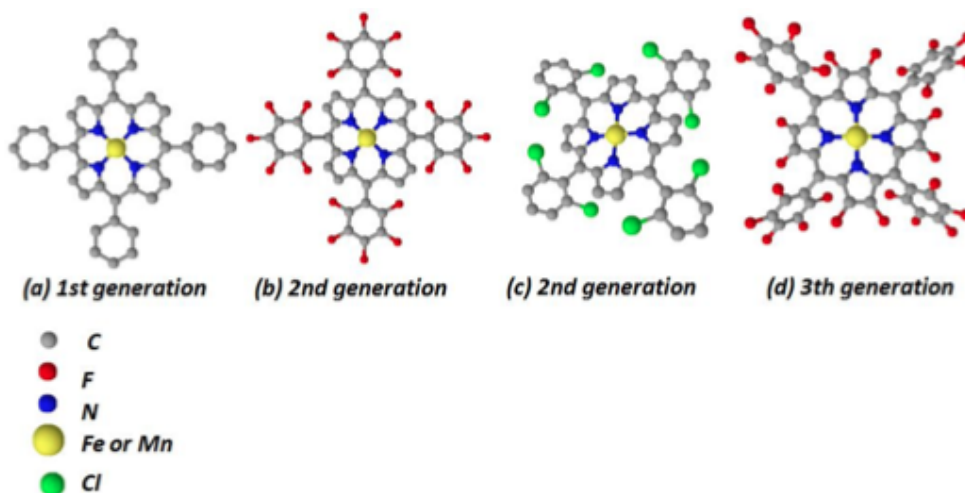


**Figure 1-7** Different metalloporphyrin based catalyst generations<sup>60</sup>

Notwithstanding the above mentioned, it is important to understand that, on the contrary of what was expectable, the use of the third generation catalysts is not synonymous of better catalytic performance in the majority of the cases. A possible reason for this behavior lays on the fact that such number of EWS can increase the steric hindrance to a point that may cause an obstruction in the approximation of the oxidant to the substrate. Thus, this generation does not give rise to the same catalytic results as the second-generation counterparts.<sup>57, 61, 62</sup>

Some of the most important and referred metalloporphyrin-based catalysts are presented in Figure 1-8. The examples involve 1<sup>st</sup> (**1.3**), 2<sup>nd</sup> (**1.4** and **1.5**) and 3<sup>rd</sup> (**1.6**) generation catalysts, and water-soluble metalloporphyrins (**1.7** and **1.8**) by the introduction of ionic functional groups. The synthesis of water-soluble complexes is essential to understand more about the catalyzed reactions of cytochromes and the metabolism *in vivo*.

Despite porphyrins' ability to complex with almost any of the transition metals, for catalysis application the majority of the reports involve Mn(III),<sup>56, 63</sup> Fe(III),<sup>64</sup> Ru(III)<sup>52</sup> and Cr(III) complexes.<sup>13, 65</sup> Nevertheless, the preferred in terms of efficiency and reaction rate are manganese and iron complexes.



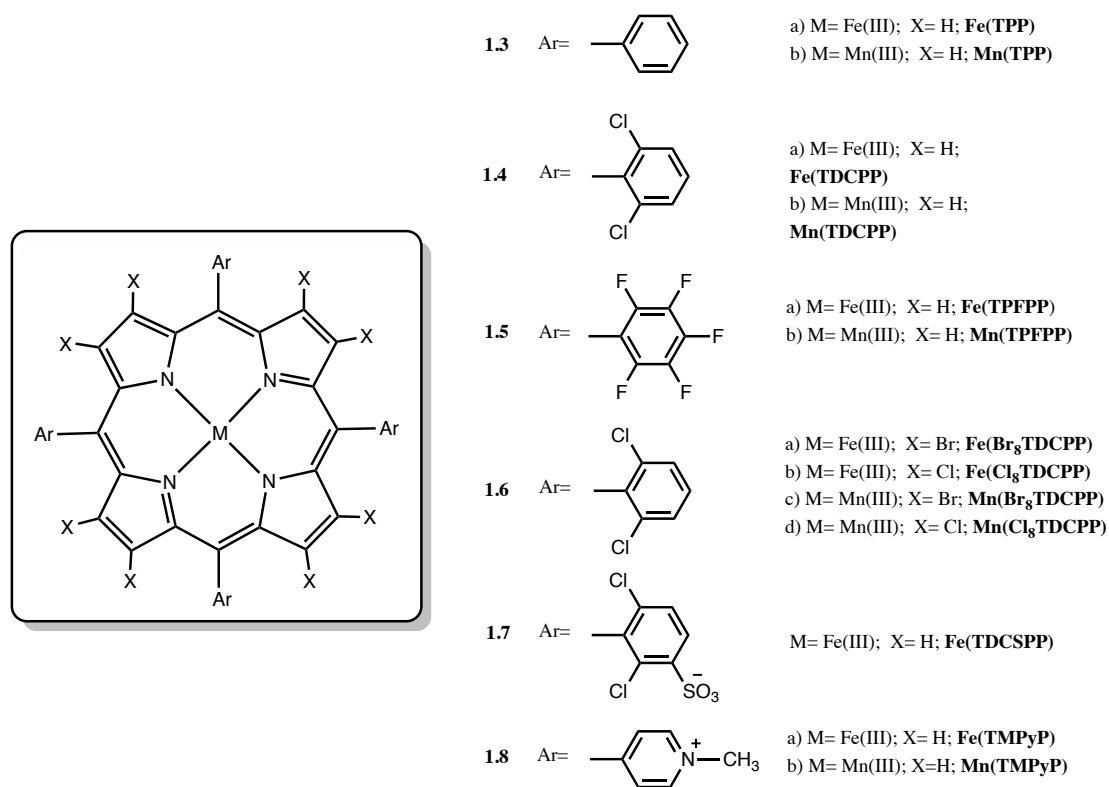


**Figure 1-8** Most relevant examples of metalloporphyrin based catalysts

In 2001 Mansuy and co-workers proved the positive effect induced in the catalytic activity of **1.4a** by the introduction of nitro groups in the  $\beta$ -pyrrolic positions. The iron complex functionalized with five nitro groups showed high efficiency in the oxidation of cyclooctene, adamantane and anisole by  $\text{H}_2\text{O}_2$ , using a mixture of  $\text{CH}_2\text{Cl}_2/\text{CH}_3\text{CN}$  (1:1) as solvent.<sup>66</sup> Besides the nature of the substituents present in the porphyrin macrocycle, and the coordinated metal affecting the electronic nature of the catalyst, Nam *et al.* placed in evidence, for the case of the electron deficient iron(III) complex (**1.5a**), the relevance of the ligand linked to the central metal ion in their catalytic efficiency.<sup>67</sup> Authors demonstrated that in epoxidation and hydroxylation reactions using  $\text{H}_2\text{O}_2$ , and aprotic solvents (e.g.,  $\text{CH}_3\text{CN}$ ) the efficiency of different  $[\text{Fe}(\text{TPFPP})\text{X}]$  complexes is markedly influenced by the nature of anionic axial ligands. The anionic axial ligand effect is due to the difference of the electron-donating ability of the anionic axial ligands, and the catalytic ability of  $[\text{Fe}(\text{TPFPP})\text{X}]$  decreases in the order:  $\text{X}^- = \text{NO}_3^- > \text{CF}_3\text{SO}_3^-, \text{ClO}_4^- \gg \text{OAc}^-, \text{Cl}^- \geq \text{OH}^-$ . Weaker electron donors (as  $\text{NO}_3^-$ ,  $\text{CF}_3\text{SO}_3^-$ ) generally allow better yields in epoxidation and hydroxylation transformations whereas stronger electron donors ( $\text{OAc}^-$  or  $\text{Cl}^-$ ) gave rise to poorer results. Moreover, under the same conditions but using *m*-CPBA as the



oxygen atom source, the formation of distinct catalytic active species is detected depending on the anionic ligand present. The results with *m*-CPBA indicate a different mechanism of  $-O-O-$  bond cleavage, depending on the ligand electron-donating ability.<sup>67</sup>

### 1.3.1.2. OXIDANT INFLUENCE

Several oxygen donors have already been tested with metalloporphyrin-based catalytic systems (Table 1-2). The first experiments were performed using oxygen donors with only one oxygen atom, but well adapted to the selective and clean formation of metal-oxo intermediates, as iodosylarenes, hypochlorites and pyridine *N*-oxides. Good results have also been reported with oxidants such as peracids or potassium monopersulfate, where the  $-O-O-$  bond is not symmetric, and its heterolytic cleavage is specially favored.

The choice of the oxidant is a crucial step in the development of oxidative biomimetic catalytic systems and it is important to understand that the objective always lays on the use of simpler, easy accessible and environmental safe oxidants.<sup>68,69</sup> On the other hand, the atomic efficiency is another aspect to consider and, at least for some of them, it can be very small, as can be observed in Table 1-2.

Thus, although dioxygen is usually considered an ideal oxidant (does not generate by-products and present an atomic efficiency of 100%), the inherent difficulty to its use, related to the high reactivity, associated to a hard control of the reaction selectivity, not to mention the security issues, make it less attractive than would be expected.<sup>70-72</sup> Nevertheless, several catalytic systems involving  $O_2$  and iron or manganese porphyrin complexes have been developed.<sup>73-75</sup> In most cases, it must be referred that the presence of a reducing agent such as,  $NaBH_4$ , ammonium borohydride, ascorbate, zinc amalgam, or aldehydes, just to mention a few examples, is essential.<sup>76</sup>

It is widely accepted that hydrogen peroxide is also an ideal oxidant due to its high active oxygen content, availability, and non-toxicity. Moreover, it is considered as non-polluting, producing only water as the by-product. Being a relatively cheap and easy accessible reagent, it has been the subject of innumerable studies concerning metalloporphyrin catalysts. On the contrary to what is referred to iodosylarenes or hypochlorites, in which the heterolytic cleavage is clearly favored, with  $H_2O_2$  the situation is much more complex. This is because manganese(III) or iron(III)porphyrin

complexes have the ability to favour both, an heterolytic cleavage, resulting in the formation of Mn(V)=O catalytic active species, or an homolytic cleavage, with the corresponding formation of •OH intermediates.<sup>77</sup>

**Table 1-2** Oxidants used in metalloporphyrin catalyzed oxidations and their corresponding atomic efficiency (adapted from reference 69)

Oxidant	Atomic efficiency (%)	Co-product
Oxygen (O <sub>2</sub> )	100	None
Oxygen (O <sub>2</sub> )/reductant	50	H <sub>2</sub> O
H <sub>2</sub> O <sub>2</sub>	47	H <sub>2</sub> O
NaOCl	21.6	NaCl
CH <sub>3</sub> CO <sub>3</sub> H	21.1	CH <sub>3</sub> CO <sub>2</sub> H
<i>t</i> -BuOOH	17.8	<i>t</i> -BuOH
KHSO <sub>5</sub>	10.5	KHSO <sub>4</sub>
BTSP <sup>(a)</sup>	9	hexamethyldisiloxane
PhIO	7.3	PhI

<sup>(a)</sup> bis(trimethylsilyl)peroxide

Besides the two above referred oxygen atom donors, several other oxidants have been tested for metalloporphyrins catalytic systems. Sodium hypochlorite (NaOCl), iodosylbenzene (PhIO), *tert*-butylhydroperoxide (*t*-BuOOH) or peroxycarboxylic acids like 3-chloroperoxybenzoic acid (*m*-CPBA)<sup>35c, 76, 78</sup> have also been employed in common methodologies. The different mechanistic pathways followed for each oxidant can lead to completely distinct regioselectivities in the oxidation reactions.

### 1.3.1.3. ROLE OF THE CO-CATALYST AND THE SOLVENT

When Mansuy and co-workers described for the first time the catalytic efficiency of manganese porphyrins in alkenes epoxidation by hydrogen peroxide, they noticed that the reaction can be significantly improved through the introduction of a co-catalyst, namely a nitrogen base such as imidazole.<sup>79</sup> Since then, the use of these additives was studied with different metalloporphyrin catalytic systems and, besides the improvement in catalytic efficiency, the variation of the co-catalyst also allows the control of reaction selectivity.<sup>80, 81</sup>

It is generally accepted that in Mn(III)porphyrin catalyzed alkenes epoxidation and alkanes hydroxylation by hydrogen peroxide the imidazole co-catalyst displays two important roles. First, as a Mn-ligand, imidazole enriches the metal center favoring the heterolytic cleavage of the peroxydic bond of the H<sub>2</sub>O<sub>2</sub> molecule; secondly, as a base, imidazole facilitates the proton abstraction from H<sub>2</sub>O<sub>2</sub> and the departure of H<sub>2</sub>O to generate a Mn(V)=O catalytic active species.<sup>82, 83</sup> The functions of the co-catalyst can be compared to those of the histidine residues present in the natural enzyme peroxidase, which is supposed to act through a “pull-push” effect.

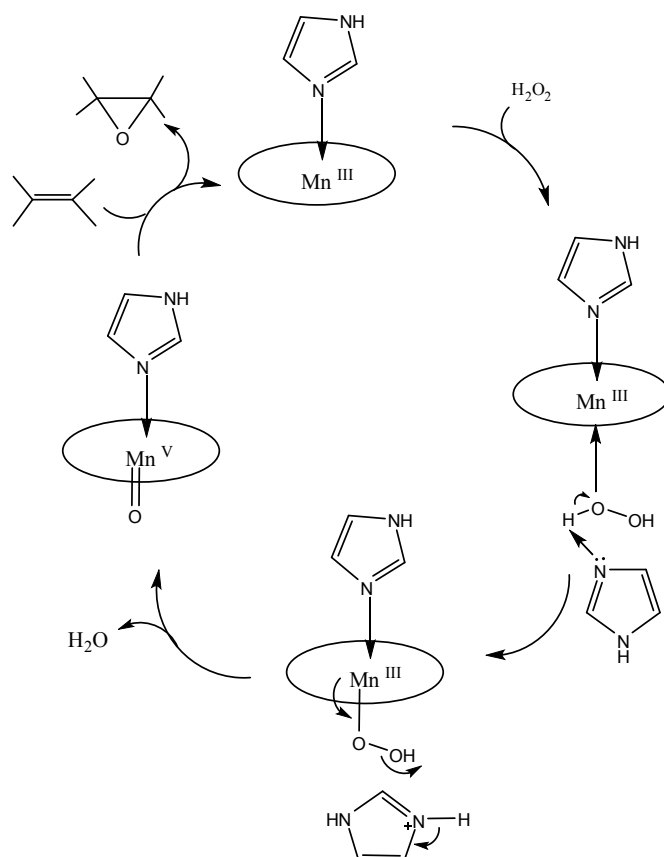


**Figure 1-9** Effect of the co-catalyst in Mn(III)porphyrin catalyzed oxidations (adapted from 13)

In fact, the Mn(III)porphyrin/H<sub>2</sub>O<sub>2</sub>/co-catalyst system proved to be particularly efficient in alkenes' epoxidation and alkanes or aromatic derivatives hydroxylation.<sup>84</sup> Several co-catalysts have been investigated, including ammonium acetate, amine *N*-oxides or sodium hydrogen carbonate and the effect compared to that of imidazole.<sup>85,86</sup> The role of the co-catalyst in this catalytic systems is absolutely vital, inclusively it has been noticed that the destructive oxidation of the co-catalyst is in fact a limiting factor of the reaction, and thus a considerable excess of the co-catalyst is needed. Significantly, the oxidative conditions applied to alkenes were not ideally

transposable to alkanes or alkyl groups. So, despite the appreciable catalyst regeneration observed, the achievement of good yields is limited in hydroxylation transformations.<sup>56b</sup> In this sense, in 2002 Segresta *et al.* reported the improvements brought by the addition of formic acid to the catalytic system (MnTDCPP)/Imidazole/H<sub>2</sub>O<sub>2</sub>) in different hydrocarbons' oxidation. Under acidic conditions, the co-catalyst appeared to be more stable thus contributing to a significant improvement on the hydroxylation yield.<sup>87</sup>

More recently, Elemans *et al.* developed a metalloporphyrin with a diphenylglycoluril-based cavity, **1.10**, which proved to be efficient for alkenes epoxidation, in the presence of several nitrogen-containing axial ligands (Figure 1-10).<sup>88</sup> A very strong binding of the axial ligands was detected, resulting in a quite remarkable activation of the catalyst in the presence of only one equivalent of the ligand, comparatively to the large excess normally employed. In this work the authors also conclude that the use of sterically demanding ligands as 4-*tert*-butylpyridine, besides inducing specific selectivity, also avoids catalyst decomposition through the formation of  $\mu$ -oxo dimers. This is observed in the systems with the substrate-binding cavity **1.10** and also for simple systems like **1.11** and **1.12**.

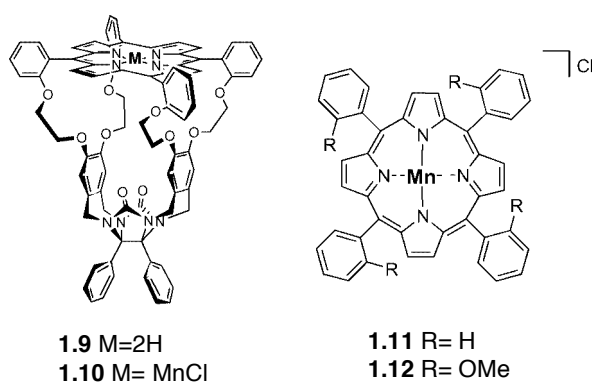


**Figure 1-10** Examples of metalloporphyrin catalysts tested with different axial ligands<sup>88</sup>

The situation with the iron(III)porphyrin complexes/H<sub>2</sub>O<sub>2</sub> catalytic systems, due to the different catalytic species involved (as discussed later) is completely different and, as demonstrated by our research group, the use of a co-catalyst can even lead to the inhibition of the catalyst activity, the active hydroperoxy oxidation species being not observed in this conditions.<sup>89</sup>

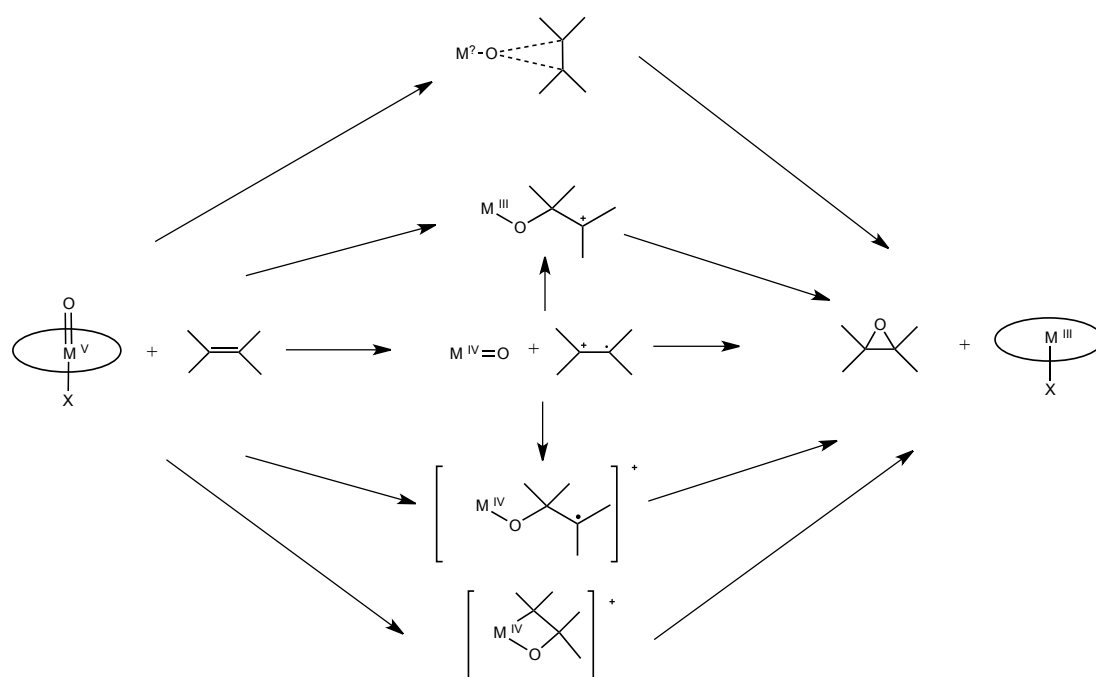
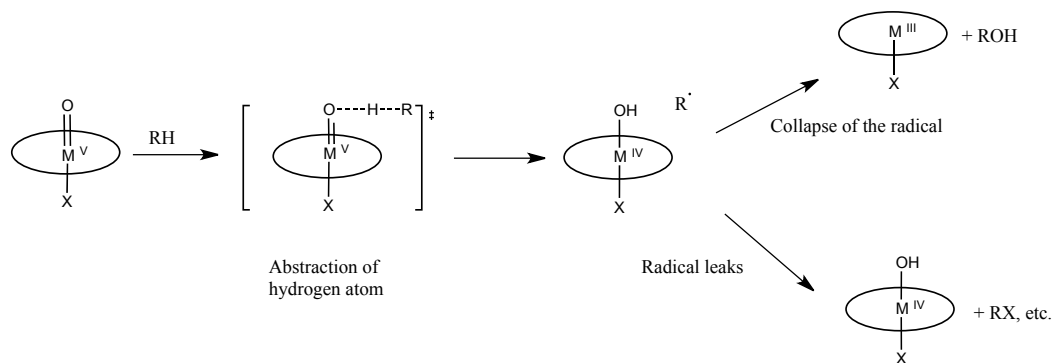


Another important aspect in the metalloporphyrin based catalytic systems is the choice of the solvent, which is not always simple since it is necessary to choose the most appropriate solvent to the reaction conditions and in parallel to be less polluting and less toxic as possible. Besides their protic nature and electronic parameters, polar protic solvents can coordinate to metal center promoting the catalyst inactivation or at least compete with the substrate in the oxidation process.<sup>90</sup> Here again a distinct behavior for Mn(III) or Fe(III) complexes is observed: if the catalytic performance of Mn(III)porphyrin complexes is favored in aprotic solvents (ex: CH<sub>3</sub>CN), the Fe(III) complexes give much better results in the presence of protic solvents (ex: methanol).<sup>89, 91</sup>

#### 1.3.1.4. MECHANISTIC CONSIDERATIONS

The development of metalloporphyrin synthetic models, able to mimic the catalytic activity of natural enzymes, decisively contributed to a better understanding of the mechanisms of action in biological systems. The reproduction of the “peroxide shunt” of the CYP-450 catalytic cycle associated to the spectroscopic characterization of several oxo-metalloporphyrin intermediates were essential for the elucidation of the mechanism proposed in Scheme 1-3. Both steps, the initial oxo-complex formation and the oxygen atom transfer from the oxidant to the substrate, have been the subject of intensive studies through the use of these synthetic analogues.<sup>35c</sup>

The most widely accepted mechanisms for epoxidation and hydroxylation transformations using metalloporphyrin-based models are described in Scheme 1-3. Independently of the nature of the oxidant, the main question lies on the chemical structure of the high valence oxo-metal species generated in the reaction of the oxygen donor with the M(III)-porphyrins and, of course, in the mechanism involved in the oxygen transfer from those species to the substrate.<sup>92</sup> It is generally accepted for Mn(III) and Fe(III) porphyrins that, depending on the reaction conditions, two intermediates, [(Por)M(V)=O] or [(Por•)M(IV)=O]<sup>+</sup>, can be formed. In the hydrocarbons oxidation with peroxide oxidants (ROOH) two different pathways have been reported for the formation of the oxo-metal species: the heterolytic and homolytic cleavage of the –O–O– bond in the intermediate (Por)Mn–OD, Scheme 1-4.<sup>93</sup>

Scheme 1-3<sup>25</sup>

The mechanism of this first step has been deeply investigated by Groves,<sup>94</sup> Morishima,<sup>95</sup> Traylor<sup>96</sup> and Bruice,<sup>92a, 97</sup> who independently recognized some of the most important features affecting the course of the reaction. Briefly, they can be pointed as: I) the heterolytic cleavage of **a** (Scheme 1-4) is favored in the presence of acid;<sup>94b, 95</sup> II) the homolytic cleavage occurs mainly in basic catalyzed conditions in the presence of electron-donor groups coordinated to the metal center;<sup>98</sup> III) The homolysis of (Por)M-OD intermediate affords the M(IV)-oxo complex **c** (Scheme 1-4), while the heterolysis of this same intermediate affords the M(V)-oxo species **b** (Scheme 1-4); IV) acylperoxides with electron-withdrawing groups increase the

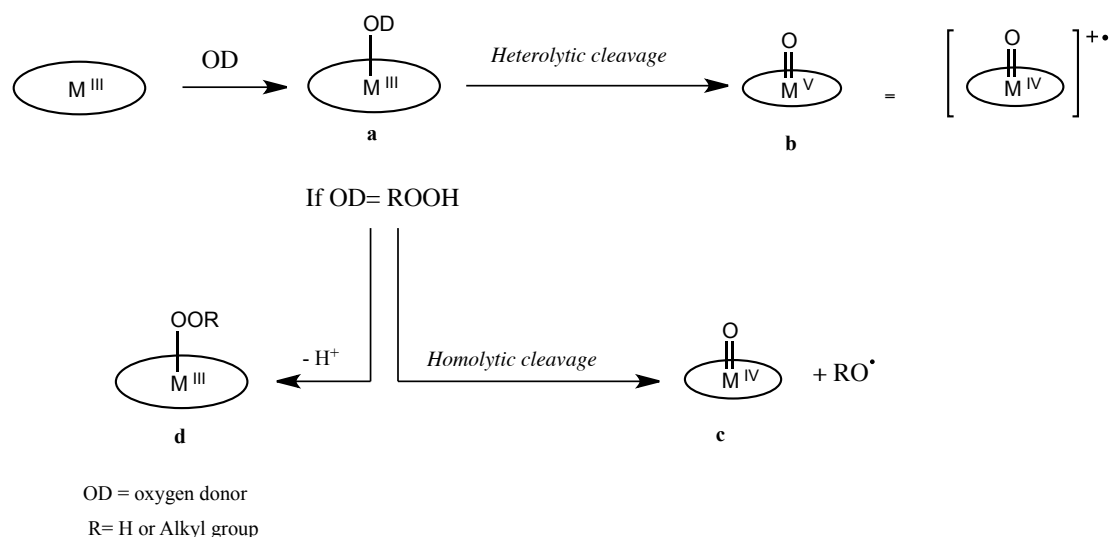


heterolytic cleavage; on the other hand, the presence of electron-donor groups favors the homolytic cleavage.<sup>98,99</sup>

It is important to refer here some other peculiar aspects that meanwhile have been disclosed concerning the formation and reactivity of high valence oxometalloporphyrin species. In 1987 Groves and co-workers reported an interesting result on Mn(V)=O reactivity, which revealed to be stereospecific in the epoxidation of *cis*-olefins, differing from the Mn(IV)=O that allows the formation of the two isomers of the epoxide product.<sup>98</sup>

If for the manganese porphyrin complexes it is well established that the main catalytic active species to consider are the oxo-species, for the iron metalloporphyrins several independent groups described that, depending on the reaction conditions, the hydroperoxo-species are preferentially involved. Thus, the use of protic solvents in addition to the absence of a co-catalyst, inhibit the oxo-intermediates formation, being only detected evidence of type **d** intermediates (Scheme 1-4).<sup>100, 101</sup>

The use of different catalytic systems (metalloporphyrin/oxidant) under the appropriate conditions allows a possible modulation of the reaction selectivity.



**Scheme 1-4** <sup>102</sup>

### 1.3.1.5. SUBSTRATE SCOPE

Over the last decades of research the great versatility of metalloporphyrin's biomimetic models has been extended to countless substrates. In order to produce



target components that cannot be easily obtained by conventional routes, much efforts have been directed towards substrates presenting significant reactivity features in one functional group. Good examples are alkenes epoxidation, alkanes hydroxylation, sulfides oxidation or phenolic derivatives obtention by the oxidation of aromatic compounds. Thus, the use of this kind of approach opens access to chemical transformations, which can potentially replace expensive processes and to whom the same product selectivity is not observed.<sup>52-56</sup>

However, much less effort has been made to reproduce the oxidation of more complex molecules, with a range of functionalities, such as pesticides, drugs, or other xenobiotics. Moreover, several natural products, largely of vegetal origin, due to their abundant occurrences, low extraction costs, structural functionalities, and putative applications, are excellent substrates to consider in catalytic oxidative studies. Natural products oxidation, despite constituting a relatively recent area, is a very interesting and promising field. The ability of metalloporphyrins to efficiently catalyze epoxidation, aliphatic and aromatic hydroxylation, dealkylation, decarboxylation processes and others, even for more complex molecules, led to an increasing interest in metalloporphyrins as biomimetic catalysts. In Figure 1-11 are summarized some relevant substrates successfully tested with metalloporphyrin catalytic systems: polycyclic aromatic compounds (**1.19-1.21**), natural occurring monoterpenes (**1.13-1.18**), steroids (**1.27-1.30**), and even more complex molecules such as drugs (or potential drugs) (**1.22-1.25**) and pesticides (**1.26**). It is well established that through the modification of reaction conditions (structure of the macrocycle, metal center, co-catalyst or the solvent) is possible to modulate the chemo and regioselectivity of the oxidation reactions, as evidenced for the next examples.

Starting with monoterpenes, the oxidation of derivatives **1.15-1.18** by hydrogen peroxide under mild conditions was evaluated with several manganese(III) porphyrin complexes with electron-withdrawing and electron-donating groups as catalysts (MnTDCPP **1.4b**, MnTPFPP **1.5b** and  $\beta$ -NO<sub>2</sub> substituted derivatives).<sup>84</sup> So, for all the oxidative transformations involving (+)-carene (**1.15**) high conversion levels were detected (81-100%) and the authors describe the formation of 4 products, namely two epoxides, the  $\alpha$ -3,4-epoxycarane (**1.31**) and the  $\beta$ -3,4-epoxycarane (**1.32**), and two other products resulting from allylic oxidation, **1.33** and **1.34**. Despite the  $\alpha$ -epoxide **1.31** was always the major oxidation product observed, the selectivity of the reaction seems to be affected by the nature of the porphyrin catalyst.

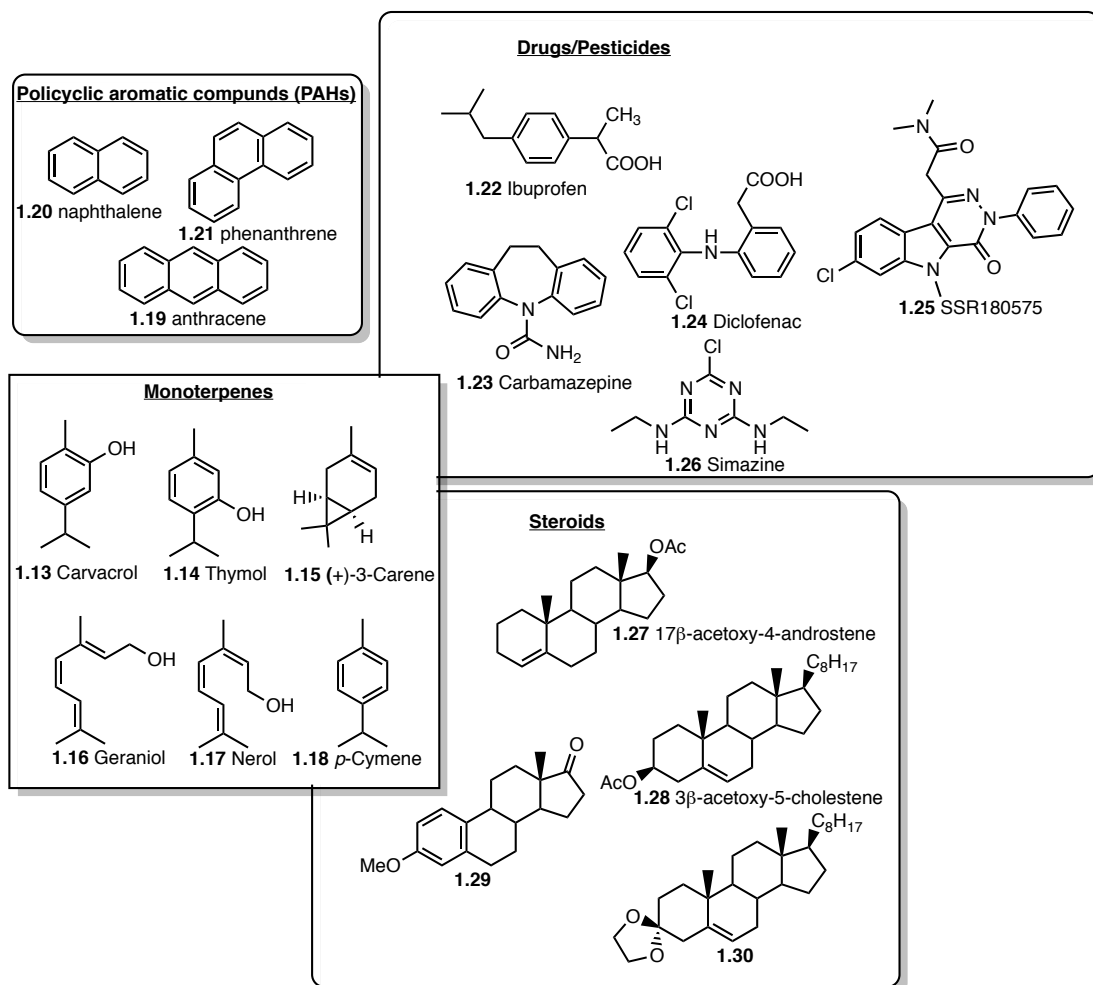


**Figure 1-11** Some representative examples of complex substrates studied using metalloporphyrins as catalysts.

The presence of electron-donor substituents in the *meso*-phenyl rings increases the catalyst performance but, on the other hand, decreases the  $\alpha$ -selectivity. In the same work the authors also evaluated the catalyzed oxidation of geraniol (**1.16**) and nerol (**1.17**), affording the corresponding epoxide products **1.35-1.37** (Figure 1-12). Despite in both cases the 2,3-epoxides, 6,7-epoxides and diepoxide mixtures were observed, it was ascertain that the epoxidation preferentially occurs at the 6,7 double bond. Alcohol moiety oxidation was only detected with geraniol, giving rise to the 6,7-epoxygeranial (**1.38**).

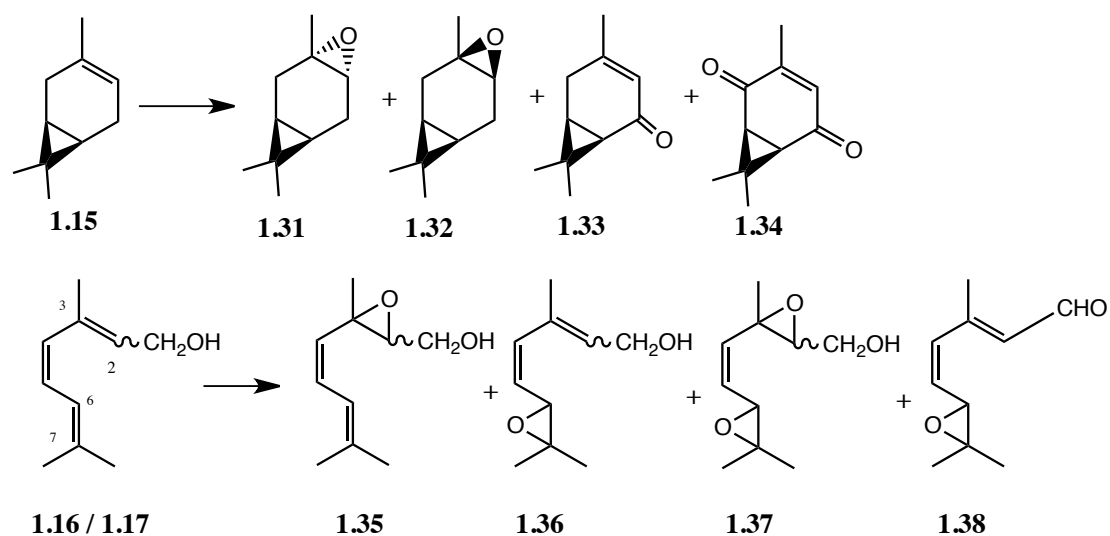
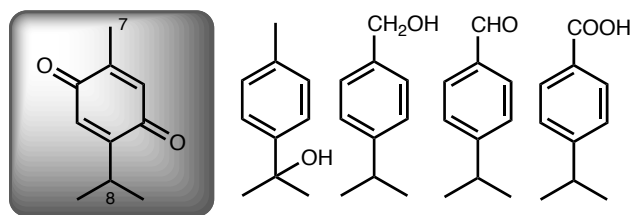


**Figure 1-12** Oxidation of monoterpenes using metalloporphyrin/H<sub>2</sub>O<sub>2</sub> catalytic systems

The same group has reported earlier a similar approach for the oxidation of the menthane-type aromatic monoterpenes, carvacrol (**1.13**), thymol (**1.14**), and *p*-cymene (**1.18**).<sup>103</sup> In the case of the high-activated derivatives **1.13** and **1.14** the catalyzed oxidative transformation selectively affords the thymoquinone **1.39**. The hydroxylation occurs selectively at the *para*-position, relatively to the hydroxyl group of the starting material, followed by the subsequent oxidation of the resulting hydroquinone to the quinone stage. Comparatively to the starting aromatic monoterpenes **1.13** and **1.14**, quinone **1.39**, due its anticancer, anti-inflammatory and hepatoprotective effect, is a much valuable compound. Milos *et. al.* in 2001 has also reported a good thymoquinone (**1.39**) production, through the direct oxidation of the essential oil of oregano isolated from dried plant material using the first generation iron(III) complex **1.3a** and oxone as oxidant.<sup>104</sup> Relatively to the *p*-cymene (**1.18**), the oxidation takes place mainly at the benzylic positions 7 and 8 and, in a lower extent, at the aromatic ring, being the principal oxidation products detected presented in Figure 1-13.

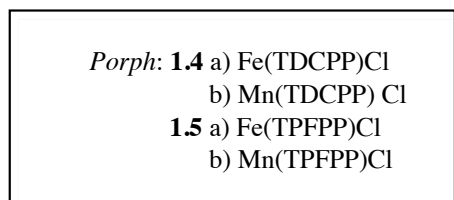
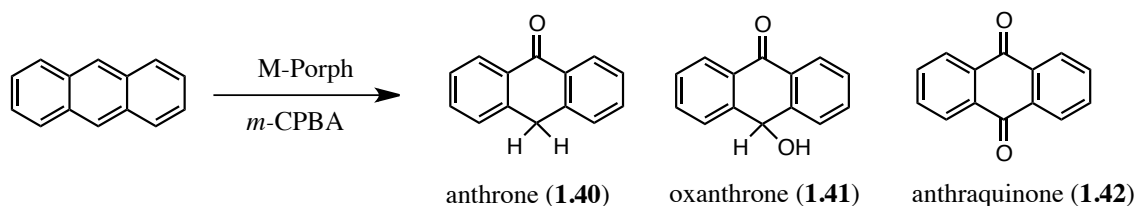
The polycyclic aromatic hydrocarbons (PAHs) introduced into the environment by incomplete combustion of fossil fuels, due their slow degradation rates and being precursors of carcinogenic species, have emerged as important environmental pollutants. Thus, the development of new environmental friendly catalytic systems able to promote their oxidation is of great interest.



1.39

**Figure 1-13** Representative oxidation products of substrates **1.13**, **1.14** and **1.18** using metalloporphyrin catalysts

Moreover, the oxidation products are also important precursors in the synthesis of antibiotics, tumour inhibitors and in several asymmetric routes leading to potentially active biological molecules. In 2005 Safari *et al.* described the successful oxidation of anthracene (**1.19**) to anthrone (**1.40**), oxanthrone (**1.41**), and anthraquinone (**1.42**) with *m*-CPBA using metalloporphyrin catalysts **1.4** and **1.5** (Scheme 1-5).<sup>78</sup>



Scheme 1-5

The yield and the selectivity of the products proved to be dependent on the catalyst and on the solvent used in the experiments. So, using **1.5a** and CH<sub>3</sub>CN as solvent, anthraquinone (**1.42**) is the only oxidation product observed (60% yield); however, changing the solvent to CH<sub>3</sub>CN:H<sub>2</sub>O (4:1) the formation of anthrone (**1.40**) and oxanthrone (**1.41**) predominated, with the latter being the major product (84.4% yield). In all the tested conditions, comparatively to the Mn(III) complexes, iron catalysts present better performances affording higher yields of oxidation products

and, in some cases, higher selectively, although Mn(III)porphyrins generally produce the better results for **1.40**.

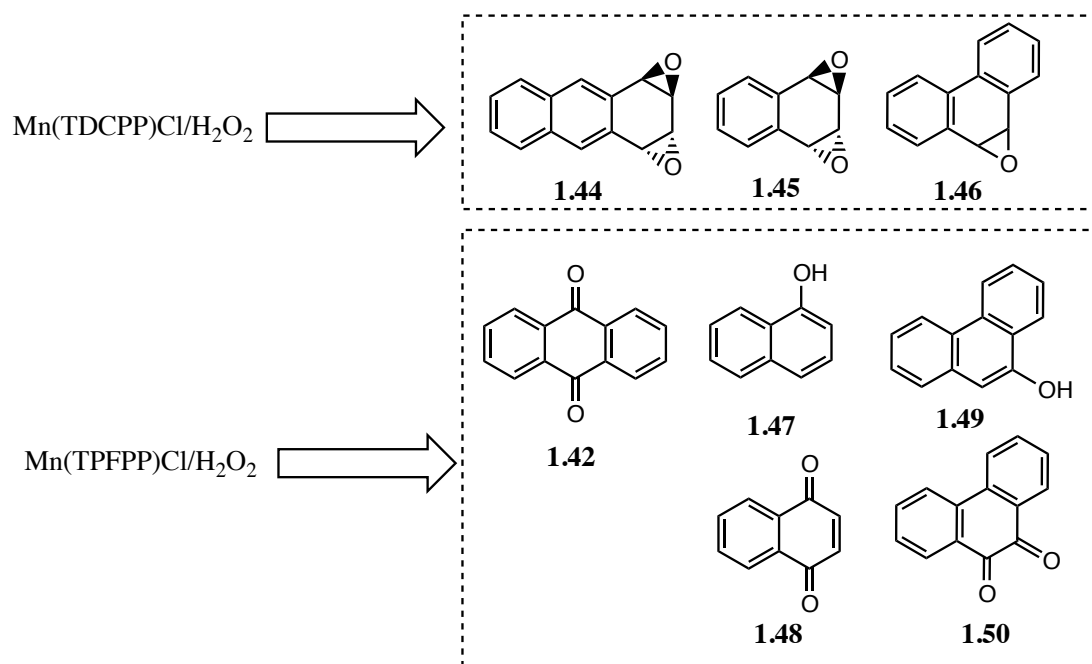


**Figure 1-14** Oxidation products of substrates **1.19-1.20** using different Mn(III) porphyrins and H<sub>2</sub>O<sub>2</sub> as oxidant.

Previously, the Aveiro group has demonstrated that the oxidation of PAHs **1.19-1.21** (Figure 1-11) with hydrogen peroxide and catalyzed by Mn(III)porphyrins may follow two distinct pathways: 1) direct epoxidation of the aromatic ring; 2) hydroxylation of the aromatic ring (Figure 1-14). Using the catalytic system **1.4b**/H<sub>2</sub>O<sub>2</sub> and ammonium acetate as co-catalyst at room temperature to perform the oxidation of PAHs **1.19-1.21**, the corresponding epoxides **1.44-1.46** were isolated as the major products.<sup>105</sup> Similarly to the oxidation with *m*-CPBA, with catalyst **1.5b** the aromatic hydroxylation and the transformation of the phenol products into the corresponding quinones were always the main transformations. The main products from the catalytic experiments with substrates **1.19-1.21** were **1.42**, **1.47-1.48** and **1.49-1.50**, respectively.

Extending the oxidation of **1.20** to Fe(III) porphyrin complexes using H<sub>2</sub>O<sub>2</sub> as oxidant under mild conditions, Rebelo *et al.* performed catalytic experiments using a protic solvent (CH<sub>3</sub>OH/CH<sub>2</sub>Cl<sub>2</sub>) and **1.4a** or **1.5a** as catalyst. These assays only allow the formation of the corresponding naphthol **1.47** and 1,4-naphthoquinone **1.48**.<sup>89</sup> More



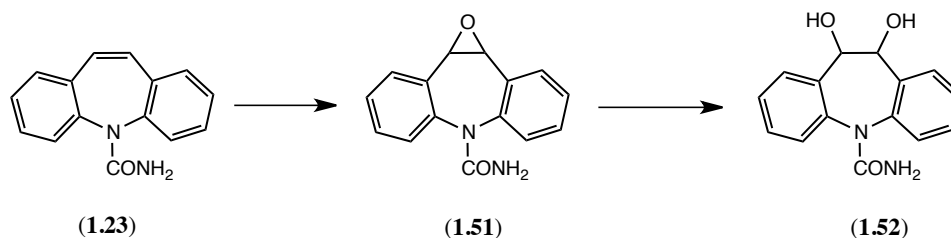
recently, this type of approach was extended to others PAHs, namely tetracene and pentacene.<sup>106</sup>

The use of synthetic models, as metalloporphyrins, is also advantageous to quickly predict the biotransformation of a drug or drug candidate,<sup>50</sup> giving access to important metabolites in reasonable quantities. This constitutes a synthetic strategy to obtain biological active molecules enabling the prediction of their toxic effect at the same time.<sup>35c</sup> Every day new chemical entities appear in the market making urgent the development of fast screening techniques that provide both reliable and easily accessible information about the biotransformation of a drug candidate. For economic reasons, it is important to perform these tests at an early stage to exclude unsuitable drug candidates, as soon as possible, from the development process.<sup>51, 55</sup> Another important feature related to the importance of the research in this area lies in the fact that pharmaceutical products, including drugs and their metabolites, are labeled as emerging aquatic and soil contaminants. An increasing number of reports referring their occurrence in a variety of ecosystems give rise to growing concerns about their potential environmental impacts. Due to drugs low transformation rates and the pharmacological activity of their metabolites, it is critical to determine the presence of parent compounds as well as their main metabolites in the environment.<sup>35c, 51, 107</sup>

So, several chemical and enzymatic model systems have been widely used throughout all the phases of drug design and development, mimicking the metabolic processes occurring *in vivo*.<sup>108</sup> Metalloporphyrins as surrogates of CYP-450 had been widely used in several drugs' oxidation and the accomplishments meanwhile achieved were already subject of reviewing.<sup>51, 55, 109</sup> In Figure 1-11 are represented some important examples of drugs and drug candidates, compounds **1.22-1.25**, already subject to catalytic experiments using metalloporphyrins as biomimetic models.

Carbamazepine (**1.23**), 5*H*-dibenz[*b,f*]azepine-5-carboxamide, is one of the most commonly prescribed antiepileptic drugs and is also used in the treatment of trigeminal neuralgia and psychiatric disorders.<sup>110</sup> Over the last two decades, 33 metabolites have been isolated and identified in the urine of patients after oral doses of **1.23**. Nevertheless, the most important pathway in **1.23** metabolism involves the formation of carbamazepine-10,11-epoxide (**1.51**) that is further converted into 10,11-dihydro-10,11-dihydroxycarbamazepine (**1.52**) by an epoxide hydrolase.<sup>111, 112</sup> Since the first catalytic experiments performed by Meunier and co-workers concerning the *in vitro* epoxidation studies with **1.23** using water soluble metalloporphyrins (**1.7** and

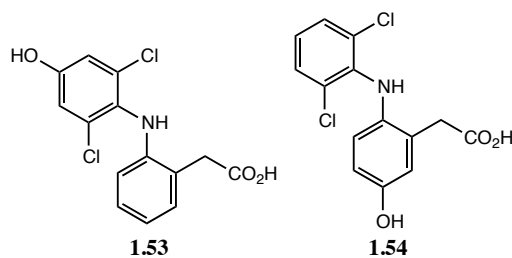
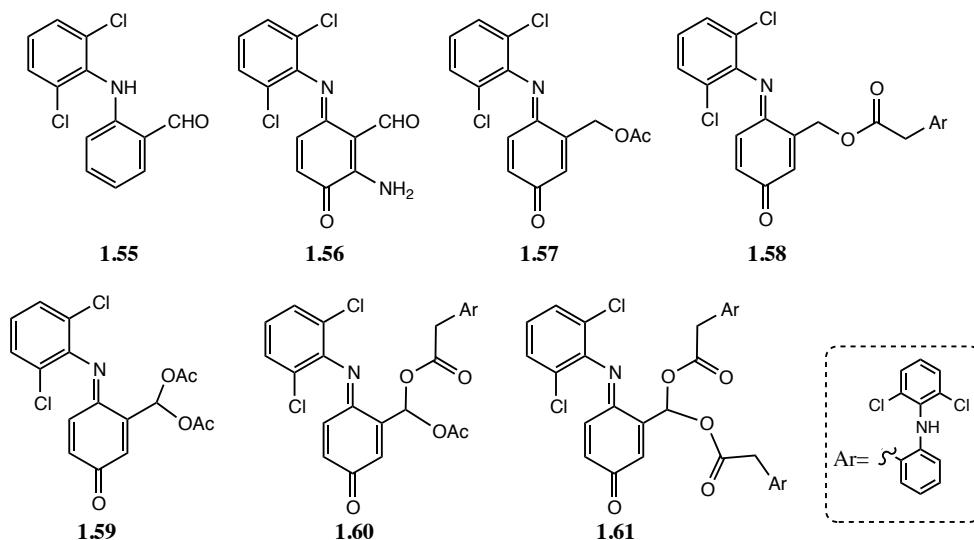
**1.8b)**<sup>113</sup> carbamazepine has been regarded as the CYP-450 based drug metabolism reaction model.



**Figure 1-15** Main metabolic pathway of carbamazepine (**1.23**)

Diclofenac (**1.24**, Figure 1-11) is one of the most prescribed anti-inflammatory drugs. It is metabolized in humans by CYP-450 enzymes to hydroxyl derivatives, among which 4'-hydroxydiclofenac (**1.53**), the major metabolite, and 5-hydroxydiclofenac (**1.54**) were isolated and characterized (Figure 1-16).<sup>114</sup> From the experiments already performed with metalloporphyrin catalysts using ammonium acetate as co-catalyst and  $\text{H}_2\text{O}_2$  or  $t\text{-BuOOH}$ , the hydroxylated derivatives of **1.24** were already reported.<sup>109, 115</sup> Despite that, metalloporphyrins already demonstrated ability to promote also the decarboxylation of carboxylic acids. Interestingly, some metabolites resulting from oxidative decarboxylation of diclofenac mediated by CYP-450 enzymes have also been reported.<sup>116</sup>

In a recent work, Cavaleiro and co-workers reported the oxidation of diclofenac (**1.24**) using Mn(III)porphyrins, Mn(TDCPP)Cl **1.4b** and Mn(TPFPP)Cl **1.5b**, and  $\text{H}_2\text{O}_2$  as oxidant.<sup>117</sup> In the procedure progressive additions of diluted oxidant, under normal atmosphere, in a mixture of acetonitrile/water at 30 °C were performed and several products, mainly resulting from an initial oxidative decarboxylation process, were detected. Besides the aromatic ring 5-hydroxylation (**1.54**) and subsequent quinone-imine formation (not isolated) the major products **1.55-1.61** (Figure 1-16) result from the oxidative decarboxylation of starting **1.24**, leading to the formation of esters **1.57** and **1.58** and geminal diesters **1.59-1.61**. The best conversions (59–78 %) of diclofenac were achieved in the presence of **1.4b**, and the products formed are also related with the co-catalyst used.

Hydroxylated productsDecarboxylation products

**Figure 1-16** Structures of diclofenac (**1.24**) derivatives

Simazine is an herbicide belonging to the class of *s*-triazines, usually used to control the annual grasses and broadleaf weeds; it degrades relatively slowly in soil and is moderately persistent. In the particular case of pesticides, the use of biomimetic models allows a deeper understanding of their degradation routes contributing to the elucidation of xenobiotics detoxification mechanisms.<sup>118</sup>

Despite the low toxicity to humans and mammals in general, simazine is associated with some endocrinal disorders, anorexia and is also a potential carcinogenic.<sup>119</sup> In order to ascertain the ability of metalloporphyrins to mimic the action of the natural enzymes, simazine **1.25** oxidation was evaluated under catalytic conditions with complexes **1.4**, **1.5** and **1.8** (Figure 1-8).<sup>120</sup> In this study different oxidants were tested, namely H<sub>2</sub>O<sub>2</sub>, PhIO and *m*-CPBA, and the best results were achieved with Fe(TDCPP)Cl **1.4a**/*m*-CPBA catalytic system (49 % total conversion). The authors demonstrate that porphyrin complexes can successfully mimic both *in vivo* and *in vitro* action of cytochrome P450 for **1.25** oxidation, forming mainly the dechlorinated



metabolites **1.62** and **1.63**, as well as two other unknown compounds, identified by HPLC/MS as **1.64** and **1.65**.

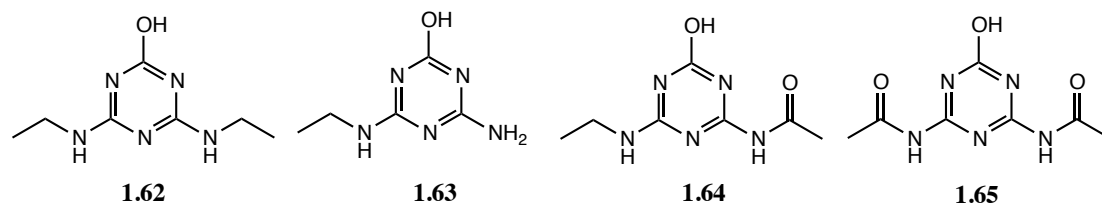


**Figure 1-17** Products of simazine (**1.25**) oxidation using metalloporphyrin catalysts

The functionalization of the steroid backbone is normally associated to novel and important biological properties. Giving access to potentially valuable therapeutic agents for the treatment of several diseases, including the treatment of breast cancer, this is a research area of major interest triggering the attention of scientific community. One of the most important possible modifications of these molecules is the epoxidation of unsaturated  $\Delta^4$ - and  $\Delta^5$ -steroids, which has been studied under catalytic and non-catalytic conditions. Interestingly, if the direct epoxidation using *m*-CPBA usually affords the respective  $\alpha$ -epoxides as major products,<sup>121</sup> the catalyzed processes using Ru or Mn porphyrins led mainly to the  $\beta$ -epoxidation.<sup>35b, 122, 123</sup>

Cavaleiro and co-workers reported the oxidation of  $\Delta^4$ - and  $\Delta^5$ -steroids of the androstane (**1.27**) and cholestane (**1.28**) series under catalytic mild conditions using hydrogen peroxide as oxidant.<sup>89, 124</sup> In this study different manganese and iron porphyrins were tested and it was noticed that the epoxidation is always the main pathway (Figure 1-18). The Mn(III) complexes afford preferentially the  $\beta$ -epoxides, being Mn(TDCPP)Cl **1.4b** the most efficient, allowing the obtention of the products **1.66** (49% yield and 71%  $\beta$ -selectivity) and **1.68** (73 % yield with 90%  $\beta$ -selectivity) in higher yields and better selectivity. With catalyst **1.5.b** [Mn(TPFPP)Cl], almost equal amounts of  $\beta$ -(**1.66** and **1.68**) and  $\alpha$ -epoxides (**1.67** and **1.69**) were obtained. However, by changing the core metal of the macrocycle to iron (**1.4a**), a different selectivity is observed, at total conversion, with 57 % yield for the  $\alpha$ -epoxide **1.67**. The authors also described for this catalytic system, Fe(TPFPP)Cl (**1.4a**)/H<sub>2</sub>O<sub>2</sub>, the influence of the substrate. Thus, if for  $\Delta^4$ -steroids (**1.27**) the main product observed is the  $\alpha$ -epoxide, for  $\Delta^5$ -steroids **1.28**, despite increasing the  $\alpha$ -selectivity, the main

product observed is still **1.68** (66% yield).<sup>124</sup>

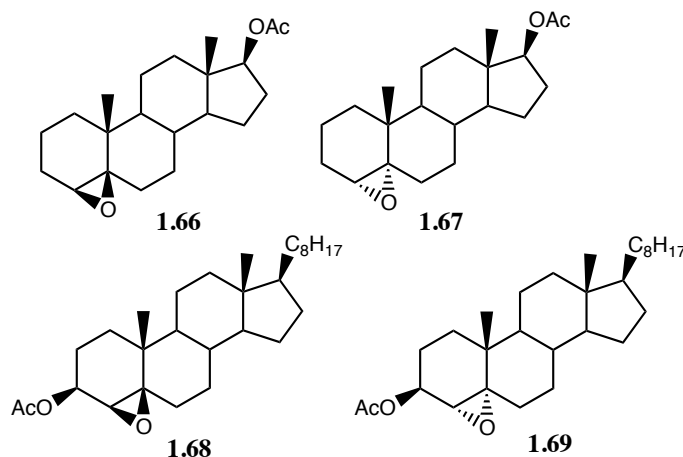


**Figure 1-18** Main oxidation products from steroids **1.27** and **1.28** using metalloporphyrin catalysts

#### 1.3.1.6. HETEROGENEOUS METALLOPORPHYRIN-BASED CATALYTIC SYSTEMS

As previously referred, the environmental and economical concerns associated with important industrial processes led to the development of catalytic process associated with a battery of new catalysts.<sup>69</sup> The strategy of immobilizing homogeneous catalysts on solid supports proved to be a good solution in order to take the main features of each type of catalyst, homogeneous and heterogeneous.<sup>35c</sup>

Concerning the use of heterogeneous synthetic models as biomimetic catalysts, a significant difference between CYP-450 model systems and the natural enzymes is the presence of the protein matrix in biological systems. This matrix is responsible to isolate the prosthetic group, thus playing many important roles in the metabolism of drugs or other xenobiotics.

In the case of metalloporphyrin-based models, all the known problems associated with their use, as homogeneous catalysts, turn that their potentiality had been fully recognized only through the heterogenization onto solid supports. Additionally, the local environment of the support can bring higher selectivity and prevent catalyst self-oxidation. This methodology not only responds to the growing environmental concerns but also allows the obtention of new bioinspired catalytic systems, which preserve the metalloporphyrin and the heterogeneous catalyst properties. Table 1-3

summarizes the principal advantages on the use of heterogeneous metalloporphyrins relatively to their homogeneous analogues.<sup>125</sup>

**Table 1-3** - Principal advantages on the use of heterogeneous metalloporphyrins<sup>125</sup>

Why to use heterogeneous metalloporphyrin-based catalysts:

- 1 Easy recovery of the catalyst from the reaction mixture
- 2 Possibility of reuse of the catalyst
- 3 Porphyrin solubility is not relevant
- 4 Possibility of interaction between the complex and the support
- 5 Decreased formation of porphyrin cluster,  $\mu$ -oxo dimers
- 6 Decreased ability for auto-oxidation of the porphyrin

There are several approaches available to prepare supported catalysts based on porphyrin metal complexes. In general, they should be simple and reproducible, adaptable to different supports, metal ions and porphyrins. Finally, they must allow also the control of the linkage to the support. Regarding the use of heterogeneous metalloporphyrins, the most important features they should present are listed on Table 1-4.<sup>4</sup>

The first report by Nolte and Drenth in 1983,<sup>126</sup> regarding the use of heterogeneous metalloporphyrins, involves a Mn-porphyrin linked to a polyisocyanide polymer tested in the epoxidation of alkenes by NaOCl. Since then, many reports have been disclosed referring different approaches to promote the immobilization of porphyrins in diverse supports.<sup>125, 127-132</sup> Concerning the success of this procedure, two important variables had been pointed out as crucial: the type of interactions established between the support and the metalloporphyrin and the choice of the support.

The interactions between the metalloporphyrin and the support can be discriminated as physical or chemical. Inside these two categories, the employed methodologies can be further divided according to the type of linkage established and according to the nature of the support. So, the chemical linkage of the porphyrin to the support can be subdivided in covalent or coordinative<sup>133, 134</sup> and the physical approach involves adsorption (electrostatic interactions),<sup>134</sup> intercalation<sup>135</sup> and encapsulation.<sup>136, 137</sup>

**Table 1-4** Principal characteristics that supported metalloporphyrin catalysts should present<sup>4</sup>

Supported metalloporphyrins should be:

- 
- 1 Oxidatively stable
  - 2 Tough and resistant to physical abrasion
  - 3 Reusable
  - 4 Resistant to metalloporphyrin leaching or removal
  - 5 Suitable for batch or continuous flow systems
  - 6 Suitable for use in a wide range of solvents and conditions
  - 7 Capable of being “tailor-made” for selective oxidation

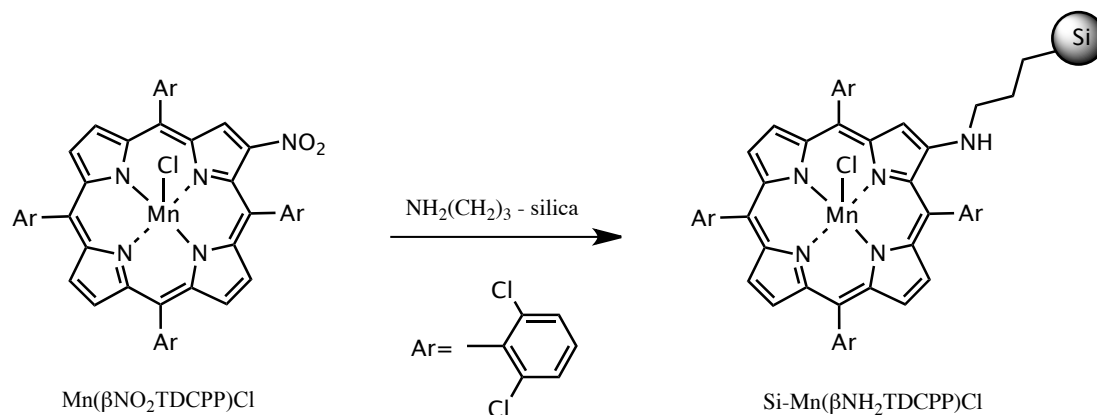
Relatively to the supports, inorganic and organic supports have been used in this heterogenization strategy. Silica gel, alumina, clays, zeolites, and solid metallophosphonates are amongst the most used inorganic supports. In respect to organic supports, the most commonly referred are polystyrene, ion-exchange resins, Merrifield resin, isocyanide polymer and polypeptides. Generally, the most common used approach to prepare heterogeneous metalloporphyrins is such that allows the formation of a covalent linkage between the support and the porphyrin derivative.<sup>35e,</sup>

<sup>131</sup> In this procedure one or more substituents of the porphyrin macrocycle react with a functional group of the support. The immobilization *via* coordinative interaction, despite being simple and more versatile than the previously one, establishes a weaker, reversible bond between the support and the porphyrin; thus, less robust catalysts are obtained and metalloporphyrin leaching from the support is often observed.<sup>125</sup>

Concerning the physical approach, in order to achieve metalloporphyrins heterogenization, a good strategy involves electrostatic interactions between ionic metalloporphyrins and contra-ionic groups on the surface of the support. Nevertheless being a restricted method to ionic metalloporphyrins, the electrostatic interactions are strong, thus avoiding or at least minimizing the leaching of the porphyrin macrocycle during the catalyzed reactions.<sup>138</sup>

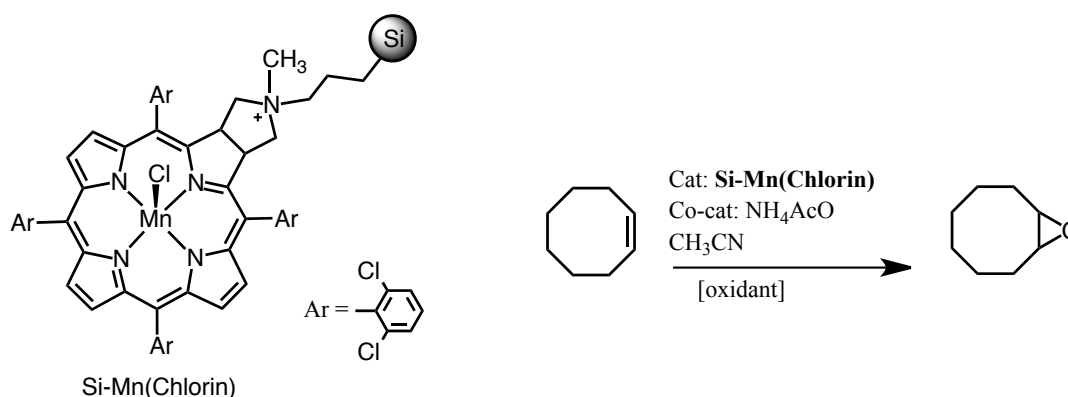
Taking into account the above cited advantages of the covalent immobilization procedure and the experiences of our group in the area, this was the chosen approach in order to obtain heterogeneous metalloporphyrin and metallochlorin catalysts. In 2006 Rebelo *et al.*, having into account a previous work concerning *ipso*-substitution of  $\beta$ -nitroporphyrins by amino groups, have successfully immobilized

Mn( $\beta$ NO<sub>2</sub>TDCPP)Cl on 3-aminopropylsilica (Scheme 1-6).<sup>139</sup> The heterogeneous catalyst Si-Mn( $\beta$ NH<sub>2</sub>TDCPP)Cl proved to be efficient in the oxidation of cyclootene and 3-carene by H<sub>2</sub>O<sub>2</sub>.



Scheme 1-6

Posteriorly, Pires *et al.* extended the covalent anchoring on functionalized silica gel to manganese chlorin complexes.<sup>140</sup> The new Si-Mn(Chlorin) has been conveniently prepared by immobilization onto 3-bromopropylsilica, *via* nucleophilic substitution reaction (Scheme 1-7). Si-Mn(Chlorin) was tested in cyclooctene epoxidation using *t*-BuOOH and H<sub>2</sub>O<sub>2</sub> as oxidants, giving the corresponding epoxide in high yields in both cases. With *t*-BuOOH, Si-Mn(Chlorin) also demonstrated a good recyclability, allowing to perform 5 reuses with good conversion values of the substrate.



Scheme 1-7

In this introductory chapter some important concepts for understanding the role of metalloporphyrin biomimetic models in oxidative catalysis have been addressed. The



main theme of these dissertation deals with the use of porphyrin catalysts on the development of catalytic and environmental sustainable methodologies to oxidize relevant substrates. Thus, in the next chapters will be presented and discussed the achieved results with metalloporphyrin/H<sub>2</sub>O<sub>2</sub> catalytic systems in the oxidation of organosulfur compounds, benzofuran and naphthoquinone derivatives.

Furthermore, with the same objective was also evaluated the performance of two non-porphyrinic catalysts, namely a manganese Keggin-type polyoxotungstate and graphene oxides in sulfoxidation processes.

## 1.4. BIBLIOGRAPHY

- <sup>1</sup> J.M. Thomas, R.J.P. Williams, *Phil. Trans. R. Soc. A* 363 (2005) 765.
- <sup>2</sup> R.A. Sheldon, in “*Biomimetic Oxidations Catalyzed by Transition Metal Complexes*”, B. Meunier (Ed.), Imperial College Press, London (2000) chapter 14.
- <sup>3</sup> G. Guillena, C. Nájera, D.J. Ramón, *Tetrahedron: Asymmetr.* 8 (2007) 2249.
- <sup>4</sup> R.A. Sheldon (Ed.), in “*Metalloporphyrins in Catalytic Oxidations*”, Marcel Dekker Inc., New York (1994) chapter 4.
- <sup>5</sup> J.T. Groves, in “*Cytochrome P-450: Structure, Mechanism, and Biochemistry*”, P.R. Ortiz de Montellano (Ed.), 3<sup>rd</sup> edition, Springer, New York (2005) chapter 1.
- <sup>6</sup> B. Meunier, A. Robert, G. Pratviel, J. Bernadou, in “*The Porphyrin Handbook*”, K.M. Kadish, K.M. Smith, R. Guilard (Eds.), vol. 4, Academic Press, New York (2000) chapter 31.
- <sup>7</sup> J.T. Groves, T.E. Nemo, R.S. Myers, *J. Am. Chem. Soc.* 101 (1979) 1032.
- <sup>8</sup> B. Lindstrom, L.J. Pettersson, *CATTECH* 7 (2003) 130.
- <sup>9</sup> D. Steinborn, A. Harmsenin, in “*Fundamentals of Organometallic Catalysis*”, Bergstr: Wiley-VCH (Ed.), Weinheim (2011).
- <sup>10</sup> M. Boudart, *Chem. Rev.* 95 (1995) 661.
- <sup>11</sup> S. A. Moya, in “*Fundamentos y Aplicaciones de la Catálisis Homogénea*” (CD-rom), Oro, L. A., Sola, E. (Eds.), CYTED, Ciencia y Tecnología para el Desarrollo, Zaragoza (2000) chapter 1.
- <sup>12</sup> A.H. Ahmed, *J. Appl. Sci. Research* 6 (2010) 1142.
- <sup>13</sup> B. Meunier, *Chem. Rev.* 92 (1992) 1411.
- <sup>14</sup> H. Gröger, Y. Asano, in “*Enzyme Catalysis in Organic Synthesis*”, K. Drauz, H Gröger, O. May (Ed.), 3<sup>rd</sup> Edition, Wiley-VCH Verlag GmbH & Co. KGaA (2012) Part I.
- <sup>15</sup> F.R.F Dias, V.F. Ferreira, A.C. Cunha, *Rev. Virtual Quim.* 4 (2012) 840.
- <sup>16</sup> L. Marchetti, M. Levine, *ACS Catal.* 1 (2011) 1090.
- <sup>17</sup> J. Rebilly, B. Colasson, O. Bistri, D. Over, O. Reinaud, *Chem. Soc. Rev.* (2014) DOI: 10.1039/C4CS00211C.
- <sup>18</sup> D.W.C. MacMillan, *Nature* 455 (2008) 304.
- <sup>19</sup> B. List, R.A. Lerner, C.F. Barbas, *J. Am. Chem. Soc.* 122 (2000) 2395.
- <sup>20</sup> K. A. Ahrendt, C.J. Borths, D.W.C. MacMillan, *J. Am. Chem. Soc.* 122 (2000) 4243.
- <sup>21</sup> I.R. Shaikh, *J. Catalysts* (2014) 1.
- <sup>22</sup> J.M Thomas, W.J. Thomas, in “*Principles and Practice of Heterogeneous Catalysis*”, VCH, Weinheim (1997) Chapter 1.



- <sup>23</sup> E. Farnetti, R. Di Monte, J. Kašpar in “*Inorganic and Bio-Inorganic Chemistry – Vol. II - Homogeneous and Heterogeneous Catalysis*”, Encyclopedia of Life Support Systems (EOLSS) (2005).
- <sup>24</sup> A.Z. Fadhel, P. Pollet, C.L. Liotta, C.A. Eckert, *Molecules* 15 (2010) 8400.
- <sup>25</sup> S.L.H. Rebelo, PhD Thesis (2004) University of Aveiro.
- <sup>26</sup> S.A. Moya, in “*Fundamentos y Aplicaciones de la Catálisis Homogénea*” (CD-rom), Oro, L. A., Sola, E. (Eds.), CYTED, Ciencia y Tecnología para el Desarrollo, Zaragoza (2000) chapter 2.
- <sup>27</sup> M. Sono, M.P. Roach, E.D. Coulter, J.H. Dawson, *Chem. Rev.* 96 (1996) 2841.
- <sup>28</sup> V.B. Urlacher, S. Eiben, *Trends Biotechnol.* 24 (2006) 324.
- <sup>29</sup> D. Mansuy, *Catal. Today* 138 (2008) 2.
- <sup>30</sup> D. Dolphin, in “*The Porphyrins, Biochemistry Part B*”, D. Dolphin (Ed.), Academic Press: New York, VII (1978) Chapter 6.
- <sup>31</sup> Y. Watanabe, S. Oae, T. Iyanagi, *Bull. Chem. Soc. Jpn.* 55 (1982) 188.
- <sup>32</sup> J.T. Groves, in “*Cytochrome P-450: Structure, Mechanism and Biochemistry*”, P.R. Ortiz de Montellano (Ed.), 3<sup>rd</sup> edition, Springer, New York (2005) chapter 1, p. 1-3.
- <sup>33</sup> L.R. Milgron, in “*The Colours of life: An Introduction to the Chemistry of Porphyrins and Related Compounds*”, Oxford University Press, New York (1997).
- <sup>34</sup> <http://www.nobel.se/chemistry/laureates/1930/fischer-lecture.pdf> accessed on November 2014
- <sup>35</sup> a) K.S. Suslick, in “*The Porphyrin Handbook*”, K. Kadish, K. Smith, R. Guillard (Eds.), Academic Press, New York (1999). b) C. Che, J. Huang, *Chem. Commun.* (2009) 3996. c) D. Mansuy, *C.R. Chimie* 10 (2007) 392. d) A. Rezaeifard, M. Jafarpour, P. Farshid, A. Naeimi, *Eur. J. Inorg. Chem.* (2012) 5515. e) E. Brulé, Y.R. de Miguel, *Org. Biomol. Chem.* 4 (2006) 599.
- <sup>36</sup> F. P. Guengerich, *Chem. Res. Toxicol.* 14 (2006) 611.
- <sup>37</sup> D.R. Nelson, *Hum. Genomics.* 4 (2009) 59.
- <sup>38</sup> J.T. Groves, in “*Cytochrome P-450: Structure, Mechanism and Biochemistry*” P.R. Ortiz de Montellano (Ed.), 3<sup>rd</sup> edition, Springer, New York (2005) p. 689.
- <sup>39</sup> K. Rückpaul, in “*Cytochrome P450*”, H. Akademie-Rein (Eds.), Verlag, Berlin (1984).
- <sup>40</sup> S.P. Visser, F. Ogliaro, P.K. Sharma, S. Shaik, *J. Am. Chem. Soc.* 124 (2002) 11809.
- <sup>41</sup> M. Klingenberg, *Arch. Biochem. Biophys.* 75 (1958) 376.
- <sup>42</sup> T. Omura, R. Sato, *J. Biol. Chem.* 239 (1964) 2370.
- <sup>43</sup> M. Katagiri, B.N. Ganduli, I.C. Gunsalus, *J. Biol. Chem.* 243 (1968) 3543.



- <sup>44</sup> R. Wang, S.P. de Visser, *J. Inorg. Biochem.* 101 (2007) 1464.
- <sup>45</sup> <http://www2.chem.uic.edu/newcomb/>, accessed on November 2014
- <sup>46</sup> F. Montanari, L. Casella, in “*Metalloporphyrins catalyzed oxidations*”, Kluwer Academic Publishers, Dordrecht (1994).
- <sup>47</sup> For a review concerning the mechanistic insights of cytochrome P450 catalyzed enzymes please see: a) B. Meunier, S.P. de Visser, S. Shaik, *Chem. Rev.* 104 (2004) 3947. b) Y. Watanabe, H. Nakajima, T. Ueno, *Acc. Chem. Res.* 40 (2007) 554.
- <sup>48</sup> B. Chiavarino, R. Cipollini, M.E. Crestoni, S. Fornarini, F. Lanucara, A. Lapi, *J. Am. Chem. Soc.*, 130 (2008) 3208.
- <sup>49</sup> E.M. Isin, F.P. Guengerich, *Biochim. Biophys. Acta* 1770 (2007) 314.
- <sup>50</sup> L.G. Yengi, L. Leung, J. Kao, *Pharm. Research* 24 (2007) 842.
- <sup>51</sup> J. Bernadou, B. Meunier, *Adv. Synth. Catal.* 346 (2004) 171.
- <sup>52</sup> C.-M. Che, J.-S. Huang, *Chem. Commun.* (2009) 3996.
- <sup>53</sup> K.P. Cusack, H.F. Koolman, U.E.W. Lange, H.M. Peltier, I. Piel, A. Vasudevan, *Bioorganic Med. Chem. Lett.* 23 (2013) 5471.
- <sup>54</sup> L. Que, W.B. Tolman, *Nature* 455 (2008) 333.
- <sup>55</sup> W. Lohmann, U. Karst, *Anal. Bioanal. Chem.* 391 (2008) 79.
- <sup>56</sup> For recent reviews on C-H functionalization using metalloporphyrin catalysts please see: a) H. Lu, X.P. Zhang, *Chem. Soc. Rev.* 40 (2011) 1899. b) C.-M. Che, V.K.-Y. Lo, C.-Y. Zhou, J.-S. Huang, *Chem. Soc. Rev.* 40 (2011) 1950. c) M. Costas, *Coord. Chem. Rev.* 255 (2011) 2912.
- <sup>57</sup> D. Dolphin, T.G. Traylor, L.Y. Xie, *Acc. Chem. Res.* 30 (1997) 251.
- <sup>58</sup> M. Benaglia, T. Danelli, G. Pozzi, *Org. Biomol. Chem.* 1 (2003) 454.
- <sup>59</sup> J. Połtowicz, K. Pamin, J. Haber, *J. Mol. Catal. A: Chem.* 257 (2006) 154.
- <sup>60</sup> E.H. Faria, G.P. Ricci, F.M. Lemos, M.L.A. Silva, A.A.S. Filho, P.S. Calefi, E.J. Nassar, K.J. Ciuffi, in “*Biomimetic Based Applications*”, M. Cavrak (Ed.), InTech, (2011) chapter 7.
- <sup>61</sup> S. Nakagaki, G.K.B. Ferreira, G.M. Ucoski, K.A.D.F. Castro, *Molecules* 18 (2013) 7279.
- <sup>62</sup> J. Leroy, A. Bondon, *Eur. J. Org. Chem.* (2008) 417.
- <sup>63</sup> W. Liu, J.T. Groves, *J. Am. Chem. Soc.* 132 (2010) 12847.
- <sup>64</sup> W. Nam, *Acc. Chem. Res.* 40 (2007) 522.
- <sup>65</sup> T. Takanami, M. Hayashi, K. Suda, *Tetrahedron Lett.* 46 (2005) 2893.
- <sup>66</sup> J.-F. Bartoli, K. Le Barch, M. Palacio, P. Battioni, D. Mansuy, *Chem. Commun.* (2001) 1718.



- <sup>67</sup> W. Nam, M.H. Lim, S. Oh, J.H. Lee, H.J. Lee, S.K. Woo, C. Kim, W. Shin, *Angew. Chem. Int. Ed.* 39 (2000) 3646.
- <sup>68</sup> G. Smith, F. Notheiz, in *"Heterogeneous Catalysis in Organic Chemistry"*, Elsevier (1999), Chapter 1.
- <sup>69</sup> J.E. Backval, in *"Modern Oxidation Methods"*, Wiley-VCH, Weinheim (2004)
- <sup>70</sup> I. Tabushi, *Coord. Chem. Rev.* 86 (1988) 1.
- <sup>71</sup> J. Piera, J. Bäckvall, *Angew. Chem. Int. Ed.* 47 (2008) 3506.
- <sup>72</sup> Z. Shi, C. Zhang, C. Tanga, N. Jiao, *Chem. Soc. Rev.* 41 (2012) 3381.
- <sup>73</sup> A.B. Solovieva, V.V. Borovkov, E.A. Lukashova, G.S. Grinenko, *Chem. Lett.* 24 (1995) 441.
- <sup>74</sup> C. Guo, M. Chu, Q. Liu, Y. Liu, D. Guo, X. Liu, *Appl. Catal. A: Gen.* 246 (2003) 303.
- <sup>75</sup> H. Ji, X. Zhou, In *"Biomimetics Learning from Nature- Biomimetic homogeneous oxidation catalyzed by metalloporphyrins with green oxidants"* A. Mukherjee (Ed.), InTech (2010) chapter 7.
- <sup>76</sup> B. Meunier, A. Robert, G. Pratviel, J. Bernadou, in *"The Porphyrin Handbook"*, K.M. Kadish, K. M., Smith, R. Guilard (Eds.), vol.4, Academic Press, New York (2000) chapter 31.
- <sup>77</sup> I.D. Cunningham, T.N. Danks, J.N. Hay, I. Hamerton, S. Gunathilagan, C. Janczak, *J. Mol. Catal. A: Chem.* 185 (2002) 25.
- <sup>78</sup> N. Safari, S.S. Naghavi, H.R. Khavasi, *Appl. Catal. A: Gen.* 285 (2005) 59
- <sup>79</sup> P. Battioni, J.P. Renaud, J.F. Bartoli, M. Reina-Artiles, M. Fort, D. Mansuy, *J. Am. Chem. Soc.* 110 (1988) 8462.
- <sup>80</sup> For a review on the effect of the co-catalyst in metalloporphyrin catalyzed oxidation please see: G.B. Shul'pin, *J. Mol. Catal. A: Chem.* 189 (2002) 39 and references cited therein.
- <sup>81</sup> T.-S. Lai, S.K.S Lee, L.-L. Yeung, H.-Y. Liu, I.D. Williams. C.K. Chang, *Chem. Commun.* (2003) 620.
- <sup>82</sup> N. Jin, J.T. Groves, *J. Am. Chem. Soc.* 121 (1999) 2923.
- <sup>83</sup> W. Nam, I. Kim, M.H. Lim, H.J. Choi, J.S. Lee, H.G. Jang, *Chem. Eur. J.* 8 (2002) 2067.
- <sup>84</sup> R.R.L. Martins, M.G.P.M.S. Neves, A.J.D. Silvestre, M.M.Q. Simões, A.M.S. Silva, A.C. Tomé, J.A.S. Cavaleiro, P. Tagliatesta, C. Crestini, *J. Mol. Catal. A: Chem.* 172 (2001) 33.
- <sup>85</sup> A. Thellend, P. Battioni, D. Mansuy, *J. Chem. Soc., Chem. Commun.* (1994) 1035.
- <sup>86</sup> A. Gonsalves, R.A.W. Johnstone, M.M. Pereira, *J. Chem. Soc., Perkin Trans. 1*, (1991) 645.

- <sup>87</sup> J. Segresta, P. Vérité, F. Estour, S. Ménager, O. Lafont, *Chem. Pharm. Bull.* 50 (2002) 744.
- <sup>88</sup> J.A.A.W. Elemans, E.J.A. Bijsterveld, A.E. Rowan, R.J.M. Nolte, *Eur. J. Org. Chem.* (2007) 751.
- <sup>89</sup> S.L.H. Rebelo, M.M. Pereira, M.M.Q. Simões, M.G.P.M.S. Neves, J.A.S. Cavaleiro, *J. Catal.* 234 (2005) 76.
- <sup>90</sup> Z. Gross, S. Ini, *J. Org. Chem.* 62 (1997) 5514.
- <sup>91</sup> N.A. Stephenson, A.T. Bell, *J. Mol. Catal. A: Chem.* 275 (2007) 54.
- <sup>92</sup> a) D. Ostovic, T. C. Bruice, *Acc. Chem. Res.* 25 (1992) 314. b) R. B. Brown, C.L. Hill, *J. Org. Chem.* 53 (1988) 5762. c) M.J. Nappa, R.J. McKinney, *Inorg. Chem.* 27 (1988) 3740. d) J.P. Collman, P.D. Hampton, J.I. Brauman, *J. Am. Chem. Soc.* 112 (1990) 2968.
- <sup>93</sup> S. Banfi, M. Cavazzini, F. Coppa, S.V. Barkanova, O.L. Kaliya *J. Chem. Soc., Perkin Trans. 2* (1997) 1577.
- <sup>94</sup> a) J.T. Groves, M.K. Stern, *J. Am. Chem. Soc.*, 109 (1987) 382. b) J.T. Groves, Y. Watanabe, *J. Am. Chem. Soc.* 110 (1988) 8443.
- <sup>95</sup> a) K. Yamaguchi, Y. Watanabe, I. Morishima, *Inorg. Chem.* 31 (1992) 156. b) K. Yamaguchi, Y. Watanabe, I. Morishima, *J. Am. Chem. Soc.* 115 (1993) 4058.
- <sup>96</sup> a) T.G. Traylor, T.Nakano, A.R. Miksztal, B.E. Dunlap, *J. Am. Chem. Soc.* 109 (1987) 3625  
b) T.G. Traylor, J.P. Ciccone, *J. Am. Chem. Soc.* 111. (1989) 8413.
- <sup>97</sup> R.D. Arasasingham, G.-X. Xe, T.C. Bruice, *J. Am. Chem. Soc.* 115 (1993) 7985.
- <sup>98</sup> J.T. Groves, M.K. Stern, *J. Am. Chem. Soc.* 109 (1987) 3812.
- <sup>99</sup> J.T. Groves, Y. Watanabe, *Inorg. Chem.* 25 (1986) 4808.
- <sup>100</sup> H. R. Khasavi, N. Safari, *J. Porphyr. Phthalocya.* 9 (2005) 75.
- <sup>101</sup> W. Nam, M.H. Lim, H.J. Lee, C. Kim, *J. Am. Chem. Soc.* 122 (2000) 6641.
- <sup>102</sup> S. Banfi, M. Cavazzini, F. Coppa, S.V. Barkanova, O.L. Kaliya, *J. Chem. Soc., Perkin Trans. 2* (1997) 1577.
- <sup>103</sup> R.R.L. Martins, M.G.P.M.S. Neves, A.J.D. Silvestre, A.M.S. Silva, J.A.S. Cavaleiro, *J. Mol. Catal. A: Chem.* 137 (1999) 41.
- <sup>104</sup> M. Milos, *Appl. Catal. A: Gen.* 216 (2001) 157.
- <sup>105</sup> S.L.H. Rebelo, M.M.Q. Simões, M.G.P.M.S. Neves, A.M.S. Silva, J.A.S. Cavaleiro, *Chem. Commun.* (2004) 608.
- <sup>106</sup> P. Costa, M. Linhares, S.L.H. Rebelo, M.G.P.M.S. Neves, C. Freire, *RSC Adv.* 3 (2013) 5350.
- <sup>107</sup> M.M.Q. Simões, M.G.P.M.S. Neves, J.A.S. Cavaleiro, *Jordan J. Chem.* 1 (2006) 1.



- <sup>108</sup> W. Nam, S.E. Park, I.K. Lim, M.H. Lim, J. Hong, J. Kim, *J. Am. Chem. Soc.* 125 (2003) 14674.
- <sup>109</sup> G.T. Balogh, G.M. Keserú, *Arkivoc* VII (2004) 124.
- <sup>110</sup> H. Breton, M. Cociglio, F. Bressolle, H. Peyriere, J.P. Blayac, D.H. Buys, *J. Chromatogr. B* 828 (2005) 80.
- <sup>111</sup> K. Lertratanangkoon, M.G. Horing, *Drug Metab. Dispos.* 10 (1982) 1.
- <sup>112</sup> a) Y. Zhu, H. Chiang, M.W. Radcliffe, R. Hilt, P. Wong, C.B. Kissinger, P.T. Kissinger, *J. Pharm. Biomed. Anal.* 38 (2005) 119. b) M. Hata, Y. Tanaka, N. Kyoda, T. Osakabe, H. Yuri, I. Ishii, M. Kitada, S. Neya, T. Hoshino, *Bioorg. Med. Chem.* 16 (2008) 5134.
- <sup>113</sup> J. Bernadou, A.S. Fabiano, A. Robert, B. Meunier, *J. Am. Chem. Soc.* 116 (1994) 9375.
- <sup>114</sup> a) I. Wiesenbergs-Boettcher, J. Pfeilschifter, A. Schweizer, A. Sallmann, P. Wenk, *Agents Actions* 34 (1991) 135. b) R.J. Sawchuk, J.A. Maloney, L.L. Cartier, R.J. Rackley, K.K.H. Chan, H.S.L. Lau, *Pharm. Res.* 12 (1995) 756. c) W. Blum, J.W. Faigle, U. Pfaar, A. Sallmann, *J. Chromatogr., Biomed. Appl.* 685 (1996) 251.
- <sup>115</sup> a) C. Bochet, J.-F. Bartoli, Y. Frapart, P. M. Dansette, D. Mansuy, P. Battioni. *J. Mol. Catal. A: Chem.* 263 (2007) 200. b) S. Othman, V. Mansuy-Mouries, C. Bensoussan, P. Battioni, D. Mansuy. *C. R. Acad. Sci. II C* 3 (2000) 751.
- <sup>116</sup> M.P. Grillo, J. Ma, Y. Teffera, D.J. Waldon, *Drug Metab. Dispos.* 36 (2008) 1740.
- <sup>117</sup> C.M.B. Neves, M.M.Q. Simões, M.R.M. Domingues, I.C.M.S. Santos, M.G.P.M.S. Neves, F.A.A. Paz, A.M.S. Silva, J.A.S. Cavaleiro, *RSC Adv.* 2 (2012) 7427.
- <sup>118</sup> A.E. Berns, M. Bertmer, A. Schaffer, R.J. Meier, H. Vereecken, H. Lewandowski, *Eur. J. Soil Sci.* 58 (2007) 882.
- <sup>119</sup> a) E.C. Catalkaya, F. Kargi, *J. Hazard. Mater.* 168 (2009) 688. b) E. Nelkenbaum, I. Dror, B. Berkowitz, *Chemosphere* 75 (2009) 48. b) S. Jain, R. Yamgar, R.V. Jayaram, *Chem. Eng. J.* 148 (2009) 342.
- <sup>120</sup> J.S. dos Santos, V. Palaretti, A.L. de Faria, E.J. Crevelin, L.A.B. de Moraes, M.D. Assis, *Appl. Catal. A: Gen.* 408 (2011) 163.
- <sup>121</sup> Y. Houminer. *J. Chem. Soc., Perkin Trans. 1* (1975) 1663.
- <sup>122</sup> a) J.C. Marchon, R. Ramasseul. *J. Chem. Soc., Chem. Commun.* (1988) 298. b) J.C. Marchon, R. Ramasseul. *Synthesis* (1989) 389. c) M. Tavarès, R. Ramasseul, J.C. Marchon, B. Bachet, C. Brassy, J.P. Mornon. *J. Chem. Soc., Perkin Trans. 2* (1992) 1321.
- <sup>123</sup> a) Z.L. Zhang, H.B. Zhou, J.S. Huang, C.M. Che., *Chem.-Eur. J.* 8 (2002) 1554. b) J. L. Zhang, C.M. Che, *Chem.-Eur. J.* 11 (2005) 3899.

- <sup>124</sup> S.L.H. Rebelo, M.M.Q. Simões, M.G.P.M.S. Neves, A.M.S. Silva, J.A.S. Cavaleiro, A.F. Peixoto, M.M. Pereira, M.R. Silva, J.A. Paixão, A.M. Beja, *Eur. J. Org. Chem.* (2004) 4778.
- <sup>125</sup> R.A. Sheldon, in "Metalloporphyrins in Catalytic Oxidations." Marcel Dekker Inc., New York (1994) Chapter 11.
- <sup>126</sup> A.W. Van-der-Made, J.W.H. Smeets, R.J.M. Nolte, W. Drenth, *J. Chem. Soc., Chem. Commun.* (1983) 1204.
- <sup>127</sup> D.W. Smithenry, K.S. Suslick, *J. Porphyr. Phthalocya.* 8 (2004) 182.
- <sup>128</sup> M. Benaglia, T. Danelli, G. Pozzi, *Org. Biomol. Chem.* 1 (2003) 454.
- <sup>129</sup> R. Rahimi, S.Z. Ghoreishi, M.G. Dekamin, *Monatsh Chem* 143 (2012) 1031.
- <sup>130</sup> X.-L. Yang, M.-H. Xie, C. Zou, Y. He, B. Chen, M. Keeffe, C.-D. Wu, *J. Am. Chem. Soc.* 134 (2012) 10638.
- <sup>131</sup> M.J.F. Calvete, M. Silva, M.M. Pereira, H.D. Burrows, *RSC Adv.* 3 (2013) 2277.
- <sup>132</sup> B. Gao, Z. Qiao, N. Shi, *J. Incl. Phenom. Macrocycl. Chem.* 79 (2014) 247.
- <sup>133</sup> A.L. de Faria, C. Airoidi, F.G. Doro, M.G. Fonseca, M.D. Assis, *Appl. Catal. A: Gen.* 268 (2004) 217.
- <sup>134</sup> O.A. Serra, C.R. Neri, Y. Yamamoto, E.J. Nassar, P.S. Calefi, S.A. Cicillini, C.M.C.P. Manso, *J. Incl. Phenom.* 35 (1999) 271.
- <sup>135</sup> L. Barloy, J.P. Lallier, P. Battioni, D. Mansuy, Y. Piffard, M. Tournoux, J.B. Valim, W. Jones, *New J. Chem.* 16 (1992) 71.
- <sup>136</sup> F.C. Skrobot, I.L.V. Rosa, A.P. Marques, P.R. Martins, J. Rocha, A.A. Valente, Y. Yamamoto, *J. Mol. Catal. A: Chem.* 237 (2005) 86.
- <sup>137</sup> O.A. Serra, E.J. Nassar, C.A. Kodaira, C.R. Néri, P.S. Calefi, I.L.V. Rosa, *Spectrochem. Acta A* 54 (1998) 2077.
- <sup>138</sup> F.S. Vinhado, P.R. Martins, Y. Yamamoto, *Curr. Topics Catal.* 3 (2002) 199.
- <sup>139</sup> S.L.H. Rebelo, A.R. Gonçalves, M.M. Pereira, M.M.Q. Simões, M.G.P.M.S. Neves, J.A.S. Cavaleiro, *J. Mol. Catal. A: Chem.* 256 (2006) 321.
- <sup>140</sup> S.M.G. Pires, R. De Paula, M.M.Q. Simões, M.G.P.M.S. Neves, I.C.M.S. Santos, A.C. Tomé, J.A.S. Cavaleiro, *Catal. Commun.* 11 (2009) 24.



## **Chapter 2 SYNTHESIS OF METALLOPORPHYRIN BASED CATALYSTS**





## 2. SYNTHESIS OF METALLOPORPHYRIN BASED CATALYSTS

Tetrapyrrolic macrocycles, due to their aromatic character, intrinsic chelating strength and variety of peripheral carbons, enabled the discovery of new and unique chemical reactions. Furthermore, the diversity and relevance of this family of compounds motivated the interest of distinct research areas ranging from medicine, biology, engineering, materials science and catalysis.

This chapter, concerning the synthesis of metalloporphyrinic based catalysts, starts with an overview on the chemical and physical properties of tetrapyrrolic macrocycles. Moreover, the most relevant synthetic methodologies already described in the literature as well as the peculiar reactivity of porphyrins and analogues, will be also emphasized, always in the perspective of their use as catalysts.

After the initial overview, all the synthetic routes outlined for the metalloporphyrins and analogues to be used in the catalytic experiments described in this dissertation are presented, as well as the experimental details and structural characterization.

### 2.1. PORPHYRINS AND ANALOGUES: GENERAL ASPECTS

#### 2.1.1. NOMENCLATURE AND STRUCTURAL DEFINITIONS

Structurally, tetrapyrrolic macrocycles are highly conjugated aromatic compounds constituted by four pyrrole units linked by methinic bridges, being denominated as porphyrins in their total unsaturated form.

These compounds are normally identified by two distinct nomenclatures: in the first, introduced by Fischer, the four pyrrole rings are designed as A, B, C, D and the methinic bridges by the Greek letters  $\alpha$ ,  $\beta$ ,  $\gamma$  and  $\delta$ ; in the second, recommended by IUPAC, all the carbon and nitrogen atoms forming the macrocycle are numbered from 1 to 24 (Figure 2-1).<sup>1</sup> In this dissertation the IUPAC nomenclature will be adopted, however references to positions 5,10,15,20 as *meso*-positions and carbons 2,3,7,8,12,13,17,18 as  $\beta$ -pyrrolic carbons can be found.

Depending on the type of substituent, aryl or alkyl, it is also common to distinguish between alkyl and arylporphyrins. Included in these two vast groups, if the macrocycle is substituted at the four *meso*-positions, it receives the designation of

*meso*-tetra-porphyrin, and if the four substituents are identical it can also be used the prefix tetrakis to designate these particular symmetrical porphyrins.<sup>2</sup>

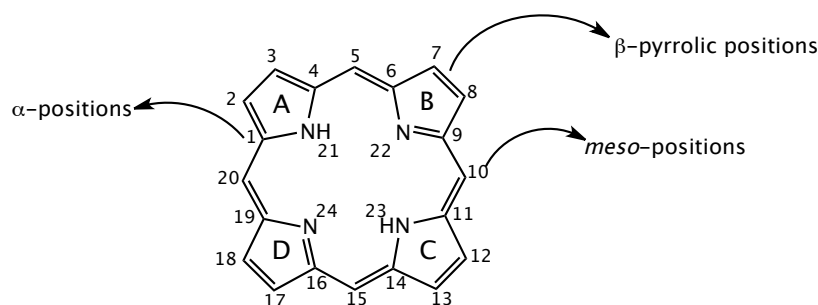


**Figure 2-1** IUPAC adopted numbering system

### 2.1.2. AROMATICITY AND PRINCIPAL PHYSICO-CHEMICAL PROPERTIES

The porphyrin macrocycle, being totally unsaturated, is highly conjugated and can be represented by the two resonance structures described in Figure 2-2.<sup>3</sup> As can be easily verified, the aromatic system is constituted by 22  $\pi$  electrons, but only 18 can be effectively delocalized, which is in accordance with the Hückel's law for aromaticity ( $4n + 2 \pi$  electrons).

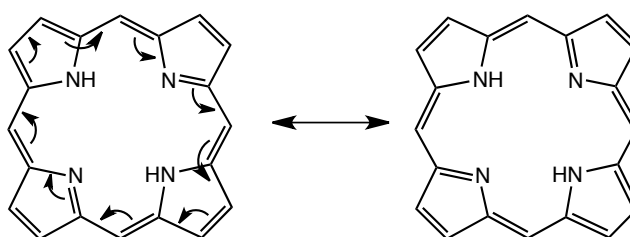


**Figure 2-2** Example of the electronic delocalization in the porphyrin macrocycles

As a result, the porphyrin ring may lose up to two double bonds and maintain the aromaticity. When the porphyrin ring loses one double bond gives rise to a new tetrapyrrolic macrocycle named chlorin. On the other hand, when the porphyrin loses two double bonds the new macrocycle, depending on the positions of the saturated carbon-carbon bonds, can be designated as bacteriochlorin or isobacteriochlorin (Figure 2-3).<sup>4</sup>

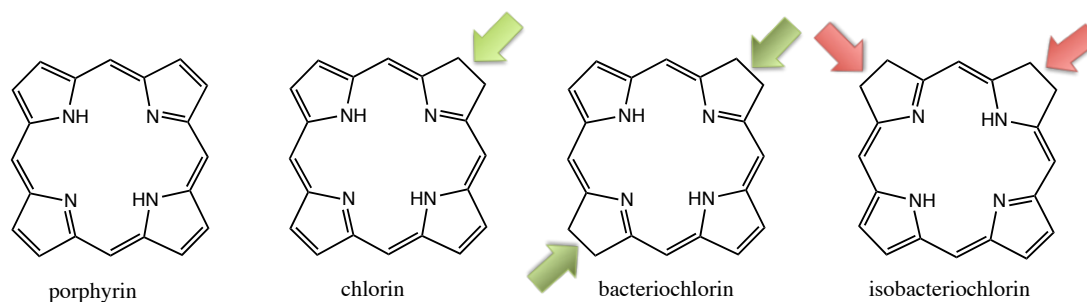


**Figure 2-3** Porphyrin macrocycle and its reduced derivatives

### 2.1.3. PROTON NMR SPECTROSCOPY

As already stated above, chlorins, bacteriochlorins and isobacteriochlorins are also aromatic macrocycles since the 18  $\pi$  conjugated electrons persist.

The aromatic character of this type of derivatives is clearly demonstrated in their  $^1\text{H}$  NMR spectra, as a consequence of the high magnetic anisotropic effect, resulting from the flow of the electronic current around the ring. Thus, there is a huge difference between the chemical shift of the inner NH's ( $\delta$  around -2 and -3 ppm) and the chemical shift of the  $\beta$ -pyrrolic and *meso* peripheral protons ( $\delta$  around 8 - 9 and 10-11 ppm, respectively). This anisotropic effect is less pronounced for chlorins and bacteriochlorins since the electronic delocalization is minor; in these cases the internal NH's appear at slightly higher chemical shifts and the peripheral protons appear at smaller chemical shifts comparatively to porphyrins. This flow decrease is even more pronounced for isobacteriochlorin counterparts.<sup>5</sup>

### 2.1.4. UV-VIS ABSORPTION SPECTROSCOPY

One of the main characteristics of tetrapyrrolic macrocycles is the usually intense and distinctive colors they present, ranging from purple to green or pink, depending on the substituents present and on the degree of saturation of the compound.<sup>3, 5, 6</sup> So, one of the most used characterization techniques concerning tetrapyrrolic macrocycles is UV-Vis spectroscopy, which quickly allows to distinguish between the different members of this family of compounds.

Beginning with porphyrins, they normally present a characteristic purple color and the typical absorption spectrum presents one band of great intensity around 400 nm assigned as the Soret band, and a set of four other bands of lower intensity between

500-650 nm, denominated as Q bands (I, II, III, IV) (Figure 2-4). The Soret band is common to all tetrapyrrolic macrocycles, being its origin in transitions  $\pi \rightarrow \pi^*$ ; its absence can be only justified by the interruption of the conjugation or by ring opening.

Relatively to the Q bands, their position and intensity allow an easy identification of the type of tetrapyrrolic derivative involved. For example, the reduced derivatives of the chlorin type present a Q band at *ca* 650 nm (I) of increased intensity comparatively to the others. This is explained through the modification of the molecule symmetry, caused by the reduction of a double bond.

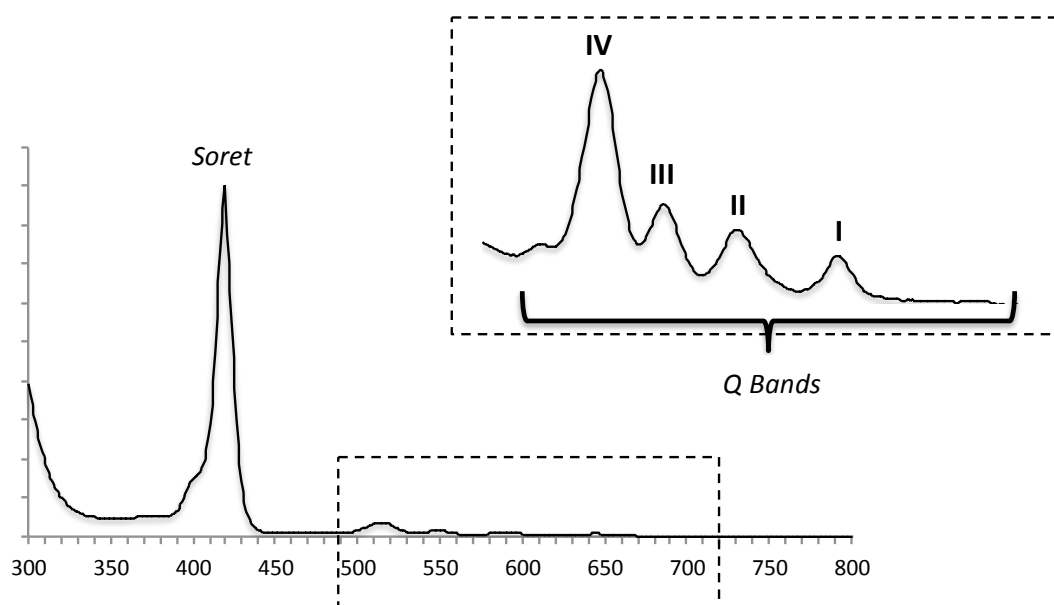


**Figure 2-4** Typical UV-Vis absorption spectrum of a porphyrinic macrocycle

Bacteriochlorins possess a strong absorption band in the 700-750 nm region, while isobacteriochlorins, usually pink, have a typical absorption spectrum with a Q band of weak intensity at 650 nm and a set of 3 Q bands between 500 and 600 nm.<sup>3, 5, 6</sup>

It is noteworthy that the relative intensity of the Q bands can also reflect the nature of the macrocycle and of its substituents. The natural occurring porphyrins usually present absorption spectra of the “etio” type (IV>III>II>I). However, “rhodo” (III>IV>II>I), “oxo-rhodo” (III>II>IV>I) and “phylo” (IV>II>III>I) type spectra are also described for synthetic derivatives.<sup>4</sup>

Additionally, the UV-Vis spectroscopy can give important and determinant information relatively to the coordination of a metal ion in the core of the macrocycle.

Depending on the structure of the macrocycle and on the coordinated metal ion, striking differences in the spectrum are observed involving the Soret band wavelength and the intensity and number of the Q bands. Generally, the complexation with different metals increases the ring symmetry (from  $D_{2h}$  to  $D_{4h}$ ) resulting in an intensity increment of the Soret band accompanied by a decrease of the number of Q bands.<sup>4,7</sup>

#### 2.1.5. SYNTHETIC METHODOLOGIES

Since 1929, when Fischer and his collaborators<sup>8</sup> described for the first time the synthesis of protoporphyrin IX, several reports were disclosed in the literature trying to solve the main problems detected in that pioneering work.

The reason for the enormous number of synthetic procedures reported until today can be easily understood analyzing the porphyrin skeleton. Many chemical strategies, involving a wide range of different building blocks like pyrroles, aldehydes, dipyrromethanes, dipyrromethenes, tripyrranes and linear tetrapyrroles, can be envisaged in order to synthetically obtain a porphyrin macrocycle. In general, the referred procedures are carried out in acidic conditions followed by the oxidation step of the porphyrinogen.<sup>5</sup>

Such a high number of synthetic methodologies to prepare porphyrin derivatives do not allow, within the scope of this dissertation, a particular reference to all of them. Probably the most studied and synthesized porphyrins are *meso*-tetraarylporphyrins, not only because they are easier to be obtained but also due to their proven efficiency as catalysts. Depending on the chosen synthetic route, the substituents introduced on the *meso*-positions can be all equal, resulting in symmetric porphyrins, or different originating asymmetric derivatives.

The role of *meso*-tetraarylporphyrins in the field of catalysis turns very relevant to summarize here the main synthetic routes meanwhile disclosed since the first report by Rothmund and co-workers in 1935.<sup>9</sup> Since then, several modifications were introduced to the original described procedure comprising the use of more advantageous conditions either by the introduction of an acid catalyst or by the use of a more adequate oxidant.<sup>10</sup> These improved approaches, allowing an efficient oxidation of the porphyrinogen, avoid an arduous purification step and contribute to increase the low yields usually observed.



#### 2.1.5.1. MESO-TETRAARYLPORPHYRINS

The two most common methods referred for symmetric porphyrin synthesis are the Adler-Longo, developed in the 1960's,<sup>11</sup> and the Lindsey procedure,<sup>12</sup> which appeared already in the 80's decade. The reaction conditions reported by Adler-Longo, less aggressive comparatively to those described by Rothmund, despite contributing to a significant improvement of the overall reaction yields, still afford the same chlorin contaminant (5-10% yield). A fundamental problem concerning the synthesis of porphyrin derivatives presenting substituents at the 2,6 positions of the phenyl groups, is the low yields obtained (around 10 % or less).

With the purpose to give answer to the persisting problems in the Adler-Longo procedure, various approaches have followed, as for example the oxidation of the reaction mixture with quinone in order to oxidize the chlorin secondary product to the corresponding porphyrin, thus avoiding the purification step. The procedure developed by Lindsey tried to minimize the occurrence of side reactions and thus the condensation is carried out under moderate conditions.<sup>13</sup> Despite being more expensive since involves two steps, the formation of the porphyrinogen followed by its oxidation with DDQ or *p*-chloranil, this procedure allowed the enlargement of the scope of aldehydes used in the porphyrin synthesis and the improvement of some of the results previously accomplished. For example, in the case of 5,10,15,20-tetrakis(2,6-dichlorophenyl)porphyrin (H<sub>2</sub>TDCPP) it is possible to reach with Lindsey's method 19% yield while yields of 2-5% are obtained using the Adler-Longo approach. Table 2-1 summarizes and compares the experimental conditions used for each one of the methodologies referred.<sup>14</sup>

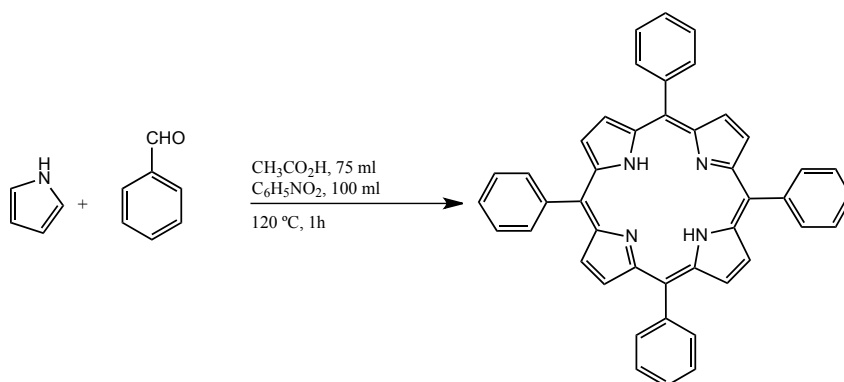
It is worth to refer that before Lindsey, Gonsalves and Pereira reported a similar two step methodology involving the condensation of pyrrol with aliphatic aldehydes in carbon tetrachloride, in the presence of an acid catalyst, followed by the oxidation of the porphyrinogen.<sup>15</sup>

In 1991 Gonsalves and co-workers reported another important data concerning the synthesis of *meso*-tetrarylporphyrins. The authors verified that the condensation of pyrrole and an aldehyde in a mixture of nitrobenzene/acetic acid allows the obtainment of the porphyrinic macrocycle, in one step, free of the chlorin contaminant. The use of nitrobenzene is responsible for the oxidation of the

porphyrinogen and minimizes also the formation of the chlorin contaminant (Scheme 2-1).<sup>16</sup> This approach was selected to synthesize the porphyrins used as catalysts in this work.

**Table 2-1** Experimental conditions referring to the most common *meso*-substituted porphyrins synthetic procedures. (adapted from 14)

METHOD	<i>Rothmund</i>	<i>Adler-Longo</i>	<i>Lindsey</i>
Solvent	Pyridine	I) Propionic acid II) Acetic acid	CH <sub>2</sub> Cl <sub>2</sub> /CHCl <sub>3</sub>
Temperature (°C)	220	I) 141 II) 120	25
Catalyst	-	The solvent	TFA BF <sub>3</sub> .Et <sub>2</sub> O BF <sub>3</sub> .Et <sub>2</sub> O/EtOH
Oxidant	-	O <sub>2</sub>	DDQ or <i>p</i> -Chloranil
Reagents concentration	3.6 M	0.3-1.0 M	0.001-0.1 M
Reaction time	48 h	0.5-1.0 h	1 h
Procedure	One step	One step	Two steps
Purification ("work up")	Crystallization	Filtration	Chromatography
Yield (%)	< 10	~ 20	Above 40
Scope of the method	Restricted	Median	High



**Scheme 2-1**

More recently, based on the Adler approach, several groups including ours successfully applied microwave irradiation to porphyrin synthesis.<sup>17, 18</sup> The time saving and a good yield for TPP (35%) indicate that MW can be used as an efficient



alternative energy source. MW irradiation, besides allowing a faster achievement of the desired temperature, affects also several physico-chemical parameters.<sup>19</sup>

#### 2.1.6. PORPHYRINIC MACROCYCLE REACTIVITY

Porphyrins and their analogue derivatives, being aromatic compounds, present their typical reactivity. Therefore, they are susceptible to nitration, halogenation, sulfonation, formylation or acylation processes. The chemical transformations can occur in the inner core or in the periphery of the ring as already mentioned.<sup>20</sup>

Beginning by the transformations observed in the internal cavity of the ring, the nitrogen atoms of the pyrrolic units can be involved in acid-base reactions and in metal coordination processes. In the first case, the easy formation of dicationic species, in the presence of acids, or dianionic species in the presence of bases, is influenced by the substituent groups in the periphery of the ring. Furthermore, the internal cavity of porphyrins, with a radius of approximately 70 pm, presents the ideal size to coordinate several metal ions by exchange with the aminic protons. The relative stability of the common metalloporphyrins is: Fe > Pd > Ni > Cu > Co > Zn > Mg > Cd > Hg > Ca. In fact, it is in the form of complexes that tetrapyrrolic macrocycles play the most notable biological activities as mentioned in the first chapter. This transformation, besides inducing significative alterations in molecule symmetry, leads also to the activation of the peripheral positions of the macrocycle for further transformations. For example, Mg(II), Zn(II), Cu(II) and Ni(II) complexes, in other words complexes involving lower electronegative metal ions, induce a negative charge in the periphery of the macrocycle smoothing the reactions with oxidants and electrophiles. On the contrary, the highly electronegative Fe(III) and Pd(II) complexes are prone to nucleophile attack and reduction processes.<sup>4, 21</sup>

Relatively to the characteristic transformations on the periphery of the porphyrinic ring, besides the already mentioned aromatic electrophilic substitutions, it can participate in nucleophilic addition, cycloaddition, oxidation and reduction processes.<sup>4, 18, 21-23</sup> One of the great advantages of this type of compounds is concerned precisely with their synthetic versatility, which can be achieved by two different ways. The first one is based on the use of different aldehydes and pyrrole units to obtain the required macrocycle; the second implies the post-functionalization of a previous synthesized macrocycle.



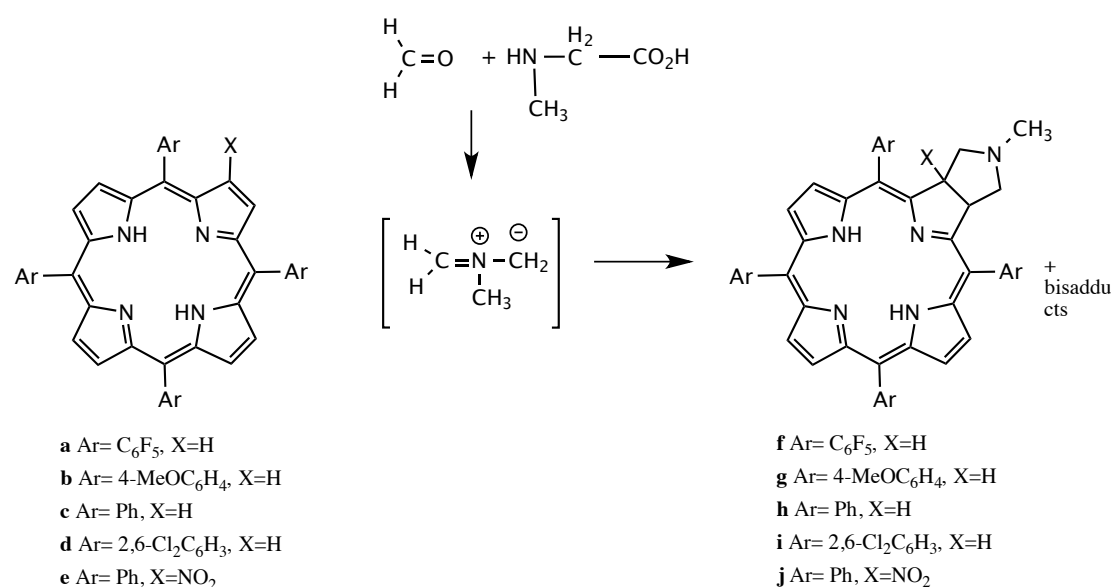
Focusing only on the *meso*-tetraarylporphyrins reactions, in order to achieve chlorin derivatives, one of the objectives proposed to this PhD project, the procedures cited in the literature involve chemical transformations on the  $\beta$ -pyrrolic positions of the macrocycle. This can be attained either by the introduction of certain functional groups in the  $\beta$ -pyrrolic positions and subsequent derivatization or by the direct modification on adjacent  $\beta,\beta'$ -pyrrolic positions.<sup>24,25</sup> The chlorin derivatives to be synthesized should be structurally based on robust porphyrin macrocycles; in this sense, our research group has developed a viable synthetic route involving 1,3-dipolar cycloaddition reactions, as described below.<sup>3</sup>

Envisage new procedures to obtain dihydroporphyrins (chlorins) is a research area of great significance, mainly due to the potential application of these compounds in distinct and comprehensive fields such as medicine or catalysis. Cavaleiro and co-workers, among others, have already demonstrated that Diels-Alder and 1,3-dipolar cycloaddition reactions constitute excellent synthetic routes to prepare novel reduced porphyrin derivatives.<sup>26-29</sup> One interesting procedure involves the synthesis of chlorins functionalized with a pyrrolidine group by 1,3-dipolar cycloaddition reactions.

In fact, *meso*-tetraarylporphyrins can participate as  $2\pi$  components in cycloaddition reactions with 1,3-dipoles, as azomethine ylides, to afford mono- and bis-addition products, according to the reaction conditions. The azomethine ylide is formed *in situ* (due to its extreme instability) through a decarboxylation process of the imine formed by the reaction of sarcosine with paraformaldehyde (Scheme 2-2).<sup>30</sup> In addition, the high versatility, the regio- and stereoselectivity found in those reactions can be used to prepare new porphyrinic compounds with well defined stereochemistry. Steric and electronic effects control the reaction regioselectivity, whereas the stereoselectivity observed in the cycloadducts formed preserve the dipolarophile stereochemistry.

Besides azomethine ylides, other 1,3-dipoles, such as nitrones, diazoalkanes and carbonic ylides, have already been successfully tested in cycloaddition transformations.<sup>18</sup> Recently, a work from Jiménez-Osés *et al.*<sup>31</sup> put in evidence the different behavior of azomethine ylides and nitrones in 1,3-dipolar cycloadditions. In terms of bis-addition stereoselectivity, the use of azomethine ylides favors the isobacteriochlorin product, resulting from a kinetic control of the process, whereas with nitrones the bacteriochlorins, being kinetic and thermodynamic favored, are

preferentially formed. Besides, the important role of the solvent fostering the thermodynamically less stable bacteriochlorins is also described. The simple modification of the solvent can lead, in the case of azomethine ylides, to the exclusive obtention of isobacteriochlorins or to a 1:1 mixture of bacteriochlorins/isobacteriochlorins instead.<sup>31</sup>



Scheme 2-2

## 2.2. SYNTHETIC ROUTES TO PORPHYRINS AND ANALOGUES

Using well-known and established procedures, distinct metalloporphyrin and metallochlorin complexes were prepared including meso-aryl and meso-imidazole substituted ones. In the next sections all the synthetic procedures used to prepare the metalloporphyrin-based catalysts evaluated in the oxidation of organic compounds under homogeneous conditions will be described. The general synthetic routes to the synthesized metalloporphyrins are summarized in Scheme 2-3. First, the synthesis of the meso-aryl substituted free-base porphyrins **2.1-2.2** will be described, followed by the procedure to obtain the meso-imidazole **2.3** and chlorin derivatives **2.4** and **2.5**. The description of the metallation approach followed to synthesize complexes **I-VII** will be then presented.

2.2.1. *MESO-ARYLPORPHYRINS (2.1 AND 2.2)*

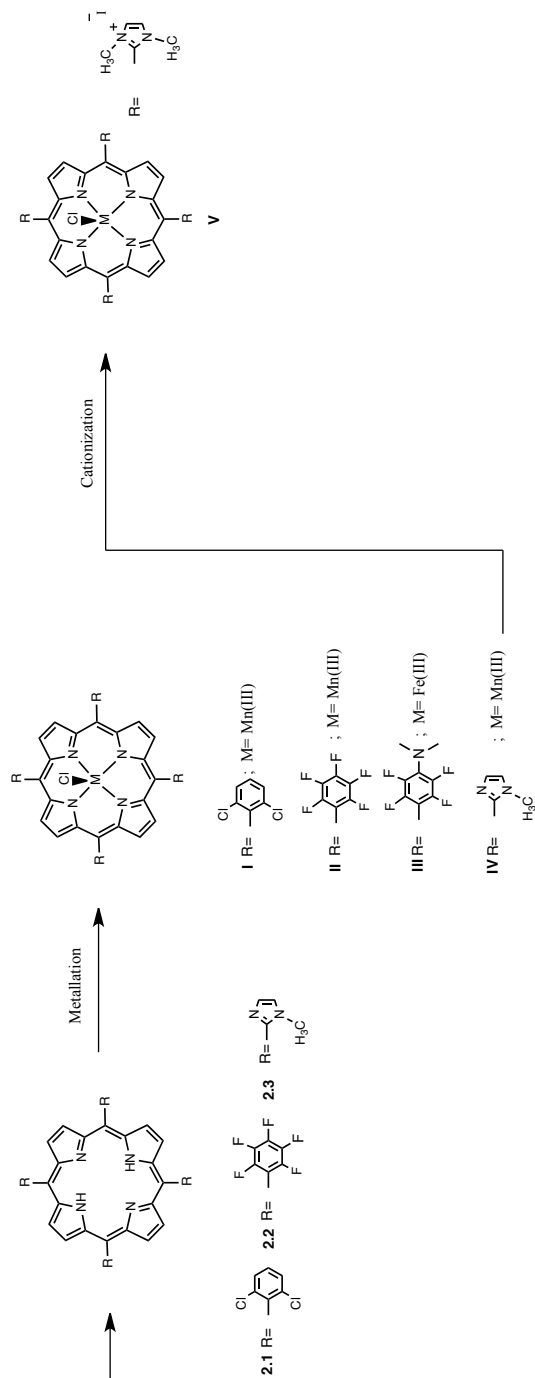
The free-bases **2.1** and **2.2** were obtained through the so-called nitrobenzene methodology, developed by Gonsalves and collaborators.<sup>16</sup> In this approach the condensation of the pyrrole with the corresponding aldehyde in a mixture of acetic acid and nitrobenzene is carried out at 120 °C for 45 minutes.

These two derivatives, **2.1** and **2.2**, besides being symmetrical porphyrins thus presenting simple synthetic routes and purification steps are also considered good dipolarophiles in 1,3-cycloaddition reactions.<sup>30</sup> As mentioned above, this type of transformation constitutes an efficient methodology to prepare the corresponding dihydrogenated derivatives. Moreover, in the particular case of derivative **2.2**, this can easily suffer further derivatization by nucleophilic substitution of the *p*-fluorines, which turns it an optimal model for new catalysts synthesis, both homogeneous or heterogeneous.<sup>32, 33</sup>

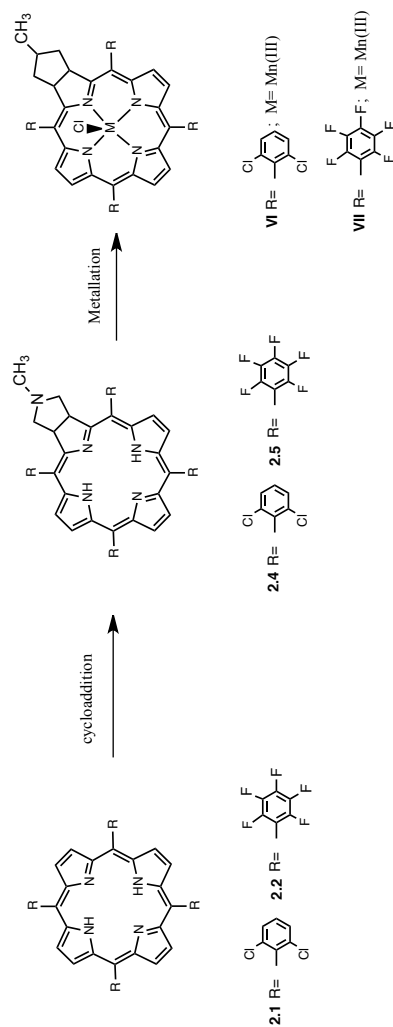
Derivative **2.1** was obtained pure directly from the reaction medium after addition of methanol, in a 5.3% yield. With the pentafluoroporphyrin **2.2**, after the terminus of the reaction, the solvents needed to be distilled under reduced pressure and the reaction crude purified by column chromatography. After the purification and recrystallization processes the product **2.2** was isolated in 16.8% yield. It is important to mention that the higher yield obtained, comparatively to those normally referred in the literature ( $\approx 11\%$ ), results from a modification of the original procedure implying a higher dilution of the reagents.

In both cases the reactions were followed by TLC and UV-Vis spectroscopy and the respective structures confirmed by different spectroscopic techniques, namely <sup>1</sup>H NMR, UV-Vis and mass spectrometry.

SYNTHESIS OF PORPHYRIN CATALYSTS



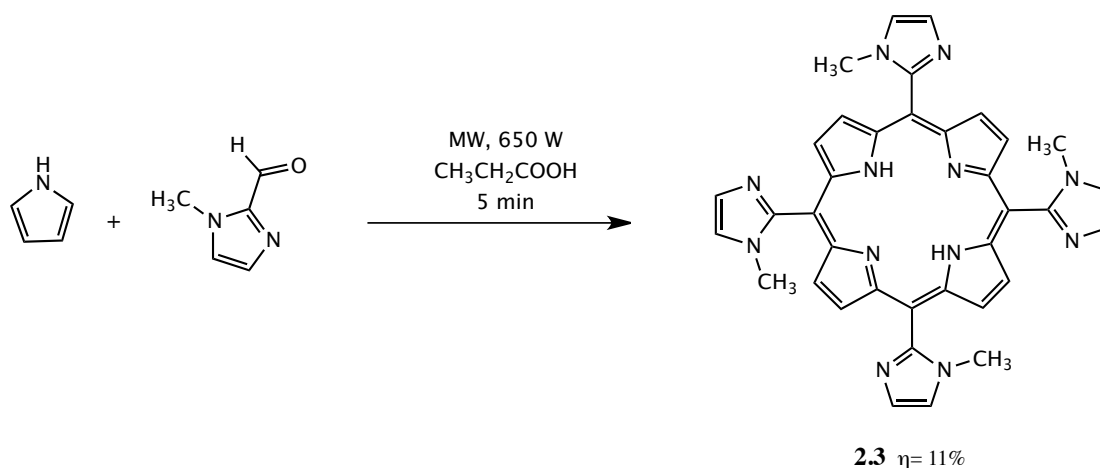
SYNTHESIS OF CHLORIN CATALYSTS



Scheme 2-3

2.2.2. *MESO-IMIDAZOL PORPHYRIN DERIVATIVE (2.3)*

The synthesis of the symmetric imidazole porphyrin **2.3** was accomplished using a different methodology which involves the adaptation of the Adler methodology using propionic acid and microwave irradiation, accordingly to a developed procedure by the Aveiro research group (Scheme 2-4).<sup>14, 34</sup>



Scheme 2-4

Noteworthy, with this type of porphyrins (imidazol-2-yl-porphyrin derivatives) the formation of an atropisomeric mixture is observed. Despite that, this peculiar characteristic is not evident in the porphyrin electronic spectrum, it is clearly evident by TLC, where four brown spots are observed, and in the extremely complex <sup>1</sup>H and <sup>13</sup>C NMR spectra. The observations are in accordance to the expected four atropisomeric forms of **2.3**, as elucidated in Figure 2-5.

Taking into account that the purification of the atropisomers goes beyond the objectives traced for the present experimental work, since in the catalytic assays only the metallocomplexes will be used, the quantification of the mixture allowed the determination of an 11% yield, in accordance with the literature.<sup>14, 35</sup>

2.2.1. *SYNTHETIC ROUTES TO FREE BASE CHLORIN DERIVATIVES (2.4 AND 2.5)*

As referred previously, metalloporphyrin biomimetic models have been extensively used as efficient oxidation catalysts; however, much less effort has been put in the study of the analogue reduced chlorins. The use of chlorin-based catalysts in oxidative

transformations, behind its novelty, can allow the functionalization of a robust macrocycle permitting the linkage to a solid support, otherwise impossible.

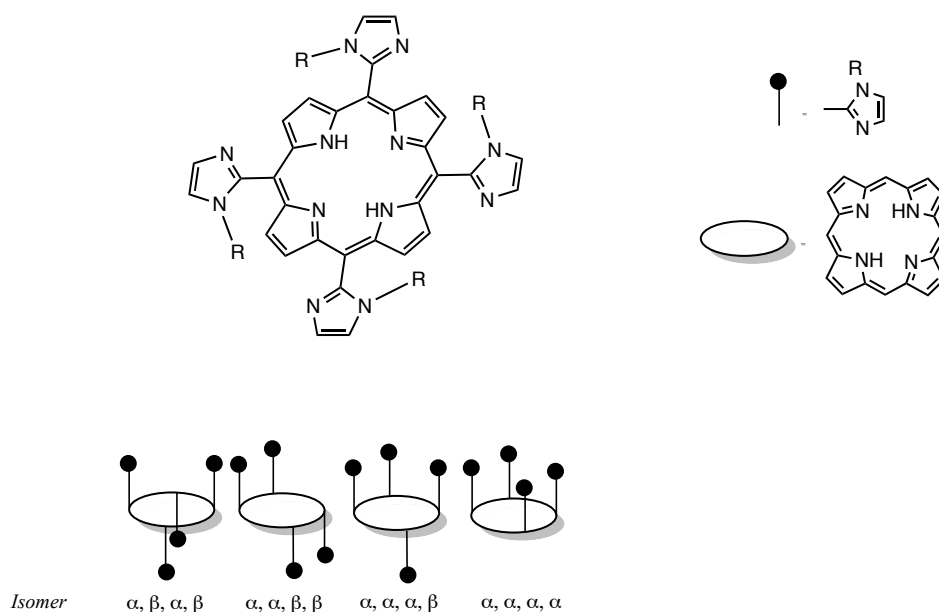
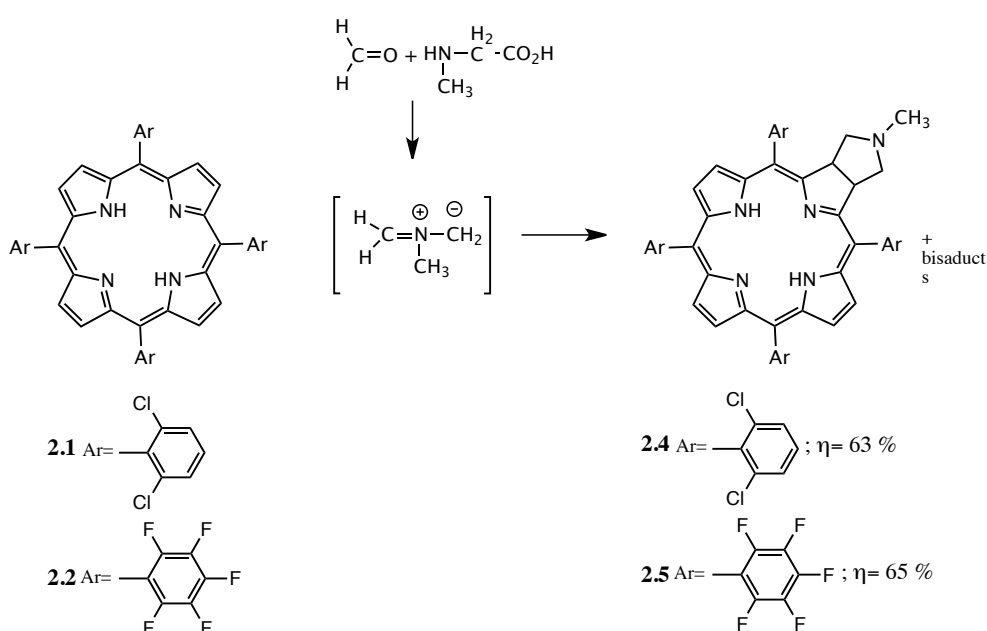


**Figure 2-5** Atropisomeric forms of (imidazol-2-yl)porphyrinic derivatives

Based on the approach developed by our group to synthesize chlorin derivatives using the azomethine ylide generated from formaldehyde and glycine as 1,3-dipole and porphyrins **2.1** and **2.2** as the  $2\pi$  component, the corresponding chlorins **2.4** and **2.5** were obtained as illustrated in Scheme 2-5.<sup>30</sup>



**Scheme 2-5**<sup>30</sup>

In this type of transformations, the monitoring of the reaction evolution by TLC and by UV-Vis is very important in order to properly control the bis-adducts formation. By UV-Vis the chlorin formation is evidenced by the increase of the Q band around the 650 nm; by TLC the appearance of a green/brown spot below the starting porphyrin (eluted with a smaller  $R_f$ ) is indicative of chlorin formation. As an example, the UV-Vis reaction profile for the synthesis of **2.4** is illustrated in Figure 2-6.

In the referred 1,3-dipolar cycloaddition transformations, successive additions of the ylide precursors were made each 5 hours to force the reaction. However, it is important to realize that a compromise between the number of additions and the conversion of the starting porphyrin must be found, since at the same time the bis-adducts formation is also promoted (bacteriochlorins and isobacteriochlorins). In terms of the reactivity observed for both dipolarophiles (**2.1** and **2.2**), the superior electrophilic character of H<sub>2</sub>TPFPP (**2.2**), presenting more electron-withdrawing substituents, turns it more reactive thus affording higher yields, in lower reaction times and less ylide precursor additions. Thereby with **2.1** five sarcosine/paraformaldehyde additions are necessary in a total of 25 h of reaction to obtain the corresponding chlorin **2.4** in 62% yield. For the derivative **2.2** only two additions in 10 hours of reaction are necessary and chlorin **2.5** is obtained in 65% yield.

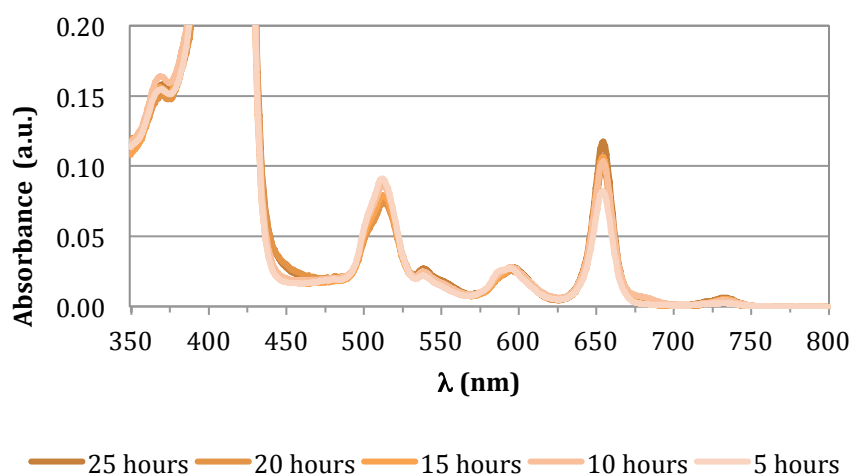
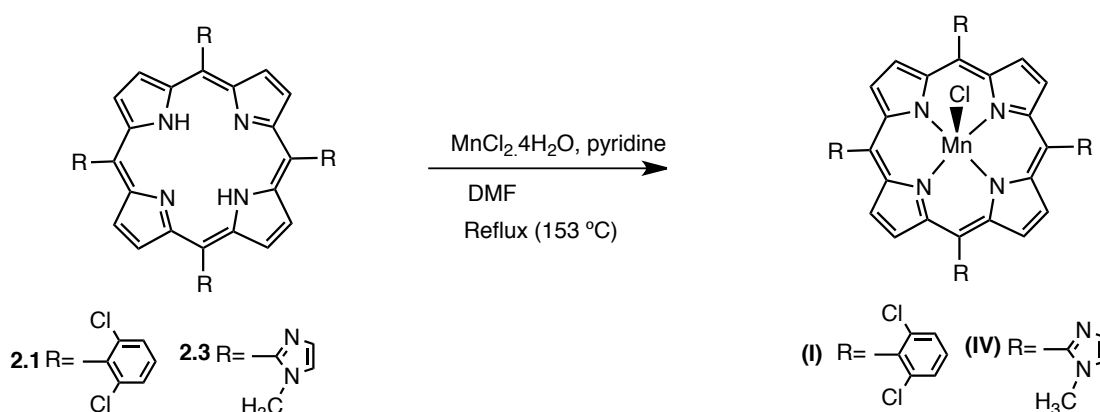


Figure 2-6 UV-Vis reaction profile for chlorin **2.4** synthesis

### 2.3. SYNTHESIS OF PORPHYRIN AND CHLORIN COMPLEXES (I-VII)

The preparation of the manganese and iron complexes was accomplished based on the Adler procedure<sup>36</sup> and involved the reaction of the free-bases with the corresponding salt,  $\text{MnCl}_2 \cdot 4\text{H}_2\text{O}$  or  $\text{FeCl}_2 \cdot 4\text{H}_2\text{O}$ . The complexation was performed in DMF at reflux as exemplified in (Scheme 2-5) for the synthesis of manganese(III) complexes of porphyrins **2.1** and **2.3**.



Scheme 2-6

The insertion of the manganese ion in the porphyrin/chlorin core is easily monitored by UV-Vis since the bathochromic shift (to higher wavelengths) of the Soret band as well as the disappearance of two of the Q bands is clearly evident. In the complexes obtained the appearance of the metal transition band just before the Soret band (350-370 nm) is also characteristic. To highlight the referred transformations in the UV-Vis spectrum with the complexation, the typical UV-Vis absorption spectrum before and after the metal insertion are represented in Figure 2-7 for complex **I**.

In the particular case of the synthesis of the Fe(III) complex **III** the shift of the Soret band was not evident, and the reaction was followed mainly by TLC. The performed metallations were considered complete when no shift of the Soret band was observed and/or no more starting material was detected by TLC. Since the purifications of Mn(III) and Fe(III) complexes are not a simple task and the complexations are usually quantitative transformations, in some cases it was necessary to force the transformation by adding more salt.



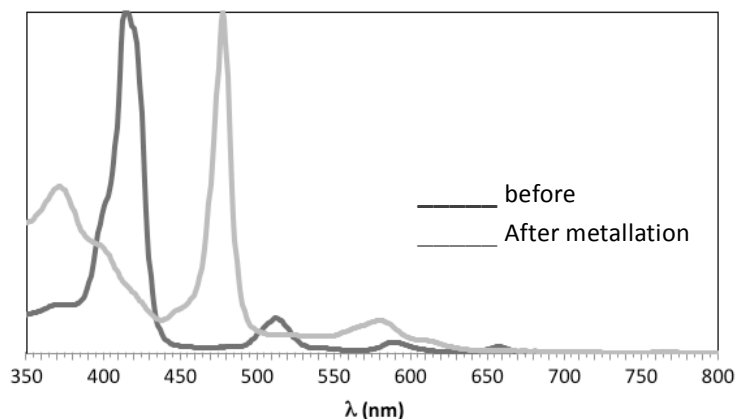


**Figure 2-7** Monitoring the metallation reaction by UV-Vis (synthesis of complex I)

The preparation of the complex **IV**, despite based in the same procedure, implies a different reaction work-up due its solubility in water.<sup>34</sup> In this case, a reverse-phase chromatography was performed instead. Thus the complex is retained in the top of the column, while the water used as solvent removes the unreacted salt. The four atropisomeric forms of manganese complex **IV** [Mn(TMImP)Cl], were recovered from the column as verified by TLC. However, differently from the corresponding free-base **2.3** with the insertion of the metal the intermolecular interactions led to a strong aggregation of the molecules.

It is noteworthy to mention that, in certain cases, the UV-Vis spectra of the complexes formed can present two Soret bands, resulting either from the possibility of the metal to be in different oxidation states, (II) or (III), or due to the interaction of the metal with the pyridine. To solve the problem the reaction mixture was exposed to the ambient atmosphere overnight, and the organic phase was washed with an aqueous solution of HCl (11%).

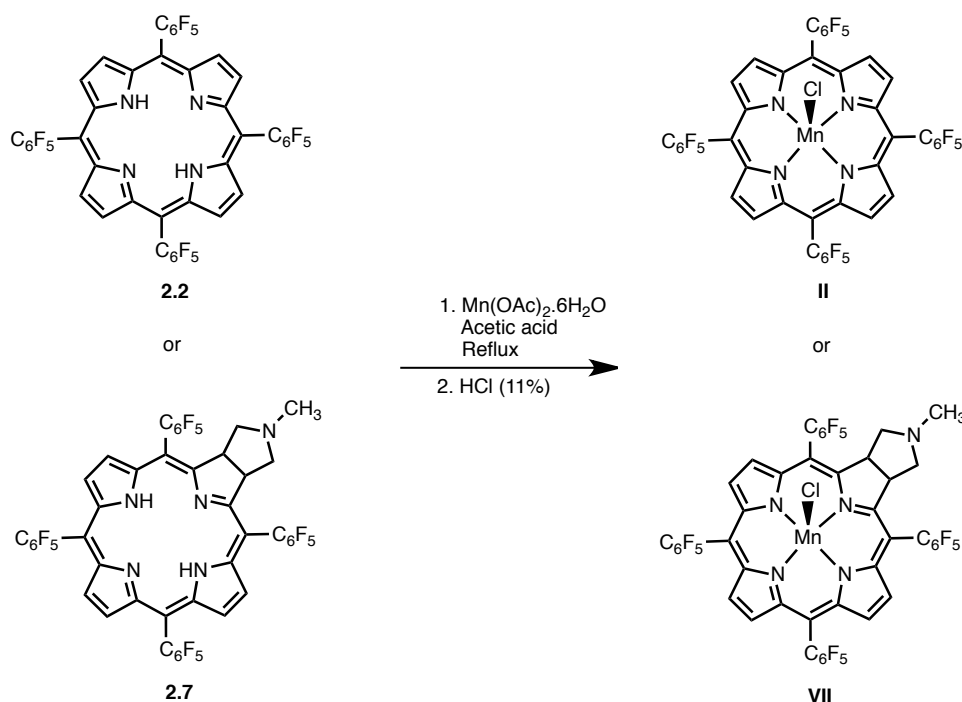
The characterization of all the synthesized complexes was carried out based on UV-Vis spectroscopy and mass spectrometry.

### 2.3.1. SYNTHESIS OF THE MANGANESE COMPLEXES BASED ON THE STRUCTURE OF H<sub>2</sub>TPFPP (II E VII)

In the particular case of the H<sub>2</sub>TPFPP (**2.2**) metallation, the above mentioned general procedure, besides efficiently affording the manganese(III) porphyrin derivatives also promotes a secondary reaction in which the *meso*-pentafluorophenyl substituents

suffer substitution in the *para* positions.<sup>37</sup> Thus, a distinct approach was used, and the derivatives **2.2** and **2.7** were reacted with manganese(II) acetate tetrahydrate under reflux of acetic acid.<sup>38</sup> The transformation was also monitored by UV-Vis and by TLC and the mass spectrometry analysis confirmed the formation of complexes **II** and **VII**.

To promote the exchange of acetate as the metal ligand by chloride, during the washing extraction procedure the obtained residue was also washed with a HCl (11%) aqueous solution.



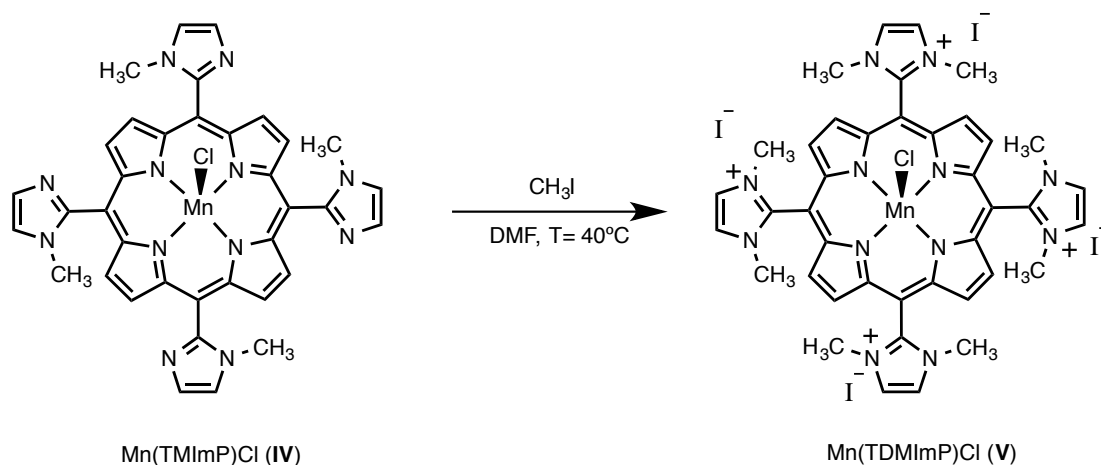
**Scheme 2-7**

### 2.3.2. SYNTHESIS OF THE CATIONIC CATALYST V

The *N*-methylation of the complex **IV** was accomplished using methyl iodide as the alkylating agent, accordingly to an already reported methodology,<sup>34, 39</sup> represented in Scheme 2-8, and observing all the Chemistry Department security regulations relatively to the manipulation of hazardous reagents.<sup>40</sup>

With this tetracationization step, it was obtained the water soluble catalyst Mn(TDMImP)Cl (**V**) and due to its symmetry it was isolated as a single compound and not as an atropisomeric mixture. Furthermore, the self-aggregation previously detected in complex **IV** was minimized due to the repulsive forces between

porphyrinic cations. This transformation allowed the quantitative production of catalyst **V** from **IV** and the structure was confirmed by UV-Vis and MS.



Scheme 2-8

## 2.4. EXPERIMENTAL

The synthesis of all the compounds described in this chapter were accomplished using high purity reagents. So, with the exception of pyrrole, acquired from Sigma-Aldrich, which was first distilled, other solvents and reagents were used as received without further purification. The aldehydes 2,6-dichlorobenzaldehyde and 1-methyl-2-imidazolecarboxaldehyde were purchased also from Sigma-Aldrich and 2,3,4,5,6-pentafluorobenzaldehyde from Fluka. The salts used in the metallations, namely manganese(II) chloride.4H<sub>2</sub>O, iron(II) chloride.4H<sub>2</sub>O and manganese(II) acetate.6H<sub>2</sub>O, were purchased from Merck, Sigma-Aldrich, and Panreac, respectively. To monitor the reactions by TLC plastic sheets coated with silica gel 60 without indicator, from Merck, were used.

In the chromatographic column purifications the stationary phase was always silica gel 60, with 0.063-0.200 mm of porosity, from Merck. When preparative thin layer chromatography was required to purify the compounds, glass plates (20 x 20 cm) were degreased and then coated with a 0.5 mm layer of silica gel G60 (without indicator) from Merck; they were activated in the oven at 100 °C for twelve hours before use.

The microwave apparatus was a Milestone MycroSynth, which operates at a fixed frequency (2.45 GHz) in a multimode system (enabling the use of 12 reactional vials



simultaneously). The equipment possesses two devices to control the temperature: one directly introduced in the reaction mixture and the other in the basis of the apparatus, operating through an infrared radiation system. The maximum work temperature is 250 °C. Pressure is another parameter that the microwave apparatus can control, by varying the potency between 0 and 1000 W (being fractionated at each 10 W).

The  $^1\text{H}$  and  $^{19}\text{F}$  NMR spectra were recorded on a Bruker Avance 300 equipment at 300.13 and 282.38 MHz, respectively, using  $\text{CDCl}_3$  as solvent and TMS ( $\delta = 0$  ppm) as internal reference. The mass spectrometry analyses were carried out on a 4800 mass spectrometer Maldi TOF/TOF, Applied Biosystems 4700 Proteomics Analyser 66, without matrix. The UV/Visible spectra were recorded in a dual beam spectrophotometer Shimadzu UV-2501 PC, in 1 cm glass cells.

The characterization of all the synthesized tetrapyrrolic macrocycles is in accordance with the reported in literature.

#### 2.4.1. SYNTHESIS OF PORPHYRINS 2.1 AND 2.2

In a 1L two necked round bottom flask, the glacial acetic acid and the nitrobenzene were mixed. The mixture was kept under magnetic stirring and heated until reflux in an oil bath. Then the aldehyde was added, followed by the dropwise addition of pyrrole. The black mixture formed was then reacted for 45 minutes properly protected from light by aluminum foil.

##### ✓ 5,10,15,20-tetrakis(2,6-dichlorophenyl)porphyrin 2.1

The quantities of reactants used were 105 mL of glacial acetic acid and 75 mL of nitrobenzene for 6.3 g of 2,6-dichlorobenzaldehyde (28.8 mmol) and 2.0 mL of pyrrole (28.8 mmol).

After cooling, porphyrin **2.1** was crystallized directly from the reaction medium through the addition of 200 mL of methanol. After seven days, the purple solid obtained was filtered through a normal glass funnel with cotton wool. The crystals were thoroughly washed with methanol and recovered from the cotton wool with  $\text{CHCl}_3$ . Next, the solvent was evaporated under reduced pressure and the residue was recrystallized using a mixture of chloroform/methanol. Finally, the precipitate obtained was filtered under vacuum and the brilliant purple crystals of **2.1** recovered

and dried in an oven at 60 °C, overnight. Porphyrin **2.1** was obtained in 5.3% yield (0.22 g).

**<sup>1</sup>H NMR** (300 MHz; CDCl<sub>3</sub>, TMS as the internal standard) δ<sub>H</sub>/ppm: -2.54 (*s*-broad, 2H, NH); 7.67-7.81 (*m*, 12H; H-Ar); 8.67 (*s*, 8H, H-β). **UV-Vis** (CH<sub>2</sub>Cl<sub>2</sub>) λ<sub>max</sub>, nm (%): 417 (100); 512 (7); 588 (2); 657 (0.8). MALDI(TOF/TOF)-MS (*m/z*): 889.9 [M]<sup>++</sup>, in accordance with the expected chemical formula [C<sub>44</sub>H<sub>22</sub>Cl<sub>8</sub>N<sub>4</sub>] of MW=890.3 (in agreement with reference 16).

✓ 5,10,15,20-tetrakis(pentafluorophenyl)porphyrin 2.2

In this case, and in order to increase the yield, a different dilution factor of the reactants was used; the condensation was performed using 400 mL of glacial acetic acid and 300 mL of nitrobenzene for 8 mL of pentafluorobenzaldehyde (0.065 mol) and 5 mL of pyrrol (0.072 mol). After the end of the reaction the solvents were distilled under reduce pressure and the black residue obtained washed with petroleum ether and purified by silica gel column chromatography using a mixture of petroleum ether/CH<sub>2</sub>Cl<sub>2</sub> (3:1) as eluent. The first fraction eluted from the column, containing porphyrin **2.2**, presented a red/brown color. Then, the solvents were removed under reduced pressure and the residue was crystalized in a CH<sub>2</sub>Cl<sub>2</sub>/methanol (1:1) mixture. The brilliant purple solid was finally filtered and dried in the oven (T= 60°C) overnight. The spectroscopic data <sup>1</sup>H, <sup>19</sup>F NMR and MS confirmed the structure of porphyrin **2.2** (1.6 g, 16 % yield).

**<sup>1</sup>H NMR** (300 MHz; CDCl<sub>3</sub>, TMS as the internal standard) δ<sub>H</sub>/ppm: -2.93 (*s*-broad, 2H, NH); 8.92 (*s*, 8H, H-β). **<sup>19</sup>F NMR** (ppm): -160.02 (*dd*, 8F, *J* = 25.4 and 8.5 Hz, Ar *o*-F); -174.67 (*t*, 4F, *J* = 21.2 Hz, Ar *p*-F); from -184.84 to -184.68 (*m*, 8F, Ar *m*-F). **UV-Vis** (CH<sub>2</sub>Cl<sub>2</sub>) λ<sub>max</sub>, nm (%): 411 (100); 506 (7); 583 (2); 537 (0.4). MALDI(TOF/TOF)-MS (*m/z*): 974.1 [M]<sup>++</sup>, in accordance with the expected chemical formula [C<sub>44</sub>H<sub>10</sub>F<sub>20</sub>N<sub>4</sub>] of MW=974.6 (in agreement with reference 16).



#### 2.4.2. SYNTHESIS OF 5,10,15,20-TETRAKIS-(1-METHYLIMIDAZOLIUM-2-YL) PORPHYRIN 2.3

The synthesis of the porphyrin **2.3** was performed under microwave (MW) irradiation. For each reactor, in a total of six, the pyrrole (0.280 mL;  $4 \times 10^{-3}$  mol) and the 1-methyl-2-imidazolecarboxaldehyde (0.45 g;  $4 \times 10^{-3}$  mol) were dissolved in 20 mL of propionic acid and irradiated for 5 minutes, at 8 bar and 650 W. After cooling to room temperature, the content of the reactors was transferred to a round bottom flask and the solvent evaporated to dryness under reduced pressure. The residue obtained was purified by column chromatography, using alumina (grade III) and  $\text{CHCl}_3$  to elute the atropoisomeric mixture with some impurities. The red/brown fraction containing **2.3**, after the solvent evaporation, suffered another alumina column purification step, but this time using a mixture of  $\text{CHCl}_3$ /methanol (98:2). The four atropoisomers **2.3** were recovered and then precipitated in a  $\text{CHCl}_3$ /hexane (2:1) mixture. The precipitate was then filtered and the solid obtained in 11% yield.

$^1\text{H NMR}$  (300 MHz;  $\text{CDCl}_3$ , TMS as the internal standard)  $\delta_{\text{H}}$ /ppm: -2.95 to -2.85 (*s*, 2H, internal NH), 3.37 - 3.55 (*s*, 12H, N- $\text{CH}_3$ ), 7.49-7.51(*m*, 4H, imidazol- $\text{H}^4$ ), 7.68-7.70 (*m*, 4H, imidazol- $\text{H}^5$ ), 8.86-8.95 (*s*-broad, 8H, H- $\beta$ ). MALDI(TOF/TOF)-MS (*m/z*): 631.3  $[\text{M}+\text{H}]^+$  in accordance with the expected chemical formula  $[\text{C}_{36}\text{H}_{30}\text{N}_{12}]$  of  $\text{Mw} = 630.7$  (in agreement with reference 34).

#### 2.4.3. SYNTHESIS OF FREE BASE CHLORIN DERIVATIVES 2.4 AND 2.5

A solution of the corresponding porphyrin macrocycle (25 mg) in the appropriate solvent, toluene or *o*-DCB, and under nitrogen atmosphere, was heated at reflux temperature. Then, sarcosine and paraformaldehyde were added and the reaction mixture was left to react under stirring and protected from light for a 5 hour period. Depending on the reactivity of the substrate, additional portions of sarcosine and paraformaldehyde were added and the reaction mixture was maintained under reflux for another 5 hours.

After finding the compromise between the consumption of the starting porphyrin and the formation of bis-adducts, and after cooling to room temperature, the adducts

formed were purified by column silica chromatography using the suitable mixture of solvents. Both chlorins were precipitated using a CH<sub>2</sub>Cl<sub>2</sub>/ hexane mixture.

✓ *N-methyl-5,10,15,20-tetrakis(2,6-dichlorophenyl)-tetrahydropyrrole[3,4:b] porphyrin 2.4*

Accordingly to the general procedure, to a solution of porphyrin **2.1** (25 mg, 25.5 μmol) in *o*-DCB (7.0 mL) in a pear-shaped flask successive additions of sarcosine (51.0 mg, 0.573 mmol) and paraformaldehyde (21.5 mg, 0.716 mmol) were added at each 5 hours, in a total of 25 hours. The purification step, performed by silica column chromatography, and after the elution of *o*-DCB with petroleum ether, allowed the recovery of the unreacted porphyrin (11.8 mg, 47.2%) using CH<sub>2</sub>Cl<sub>2</sub>, the isolation of the mono-adduct **2.4** (17.2 mg, 62%) with a mixture of CH<sub>2</sub>Cl<sub>2</sub>/acetone, followed by a minor fraction containing the mixture of bis-adducts.

<sup>1</sup>H NMR (300 MHz; CDCl<sub>3</sub>, TMS as the internal standard) δ<sub>H</sub>/ppm: -1.59 (*s*, 2H, NH); 2.20 (*s*, 3H, CH<sub>3</sub>); 2.62-2.64 and 2.96-3.05 (2 *m*, 4H; H-pyrrolidine), 5.19-5.23 (*m*, 2H, H-2,3); 7.58-7.66 and 7.71-7.77 (2 *m*, 12H, H-Ar); 8.16 (*d*, 2H, *J* = 4.9 Hz, H-β); 8.29 (*s*, 2H, H-12,13); 8.48 (*d*, 2H, *J* = 4.9 Hz, H-β), UV-vis (CH<sub>2</sub>Cl<sub>2</sub>) λ<sub>max</sub>, nm (%): 418 (100); 513 (9); 539 (3.4); 600 (2.9) 654 (23). MALDI(TOF/TOF)-MS (*m/z*): 944.0 [M+H]<sup>+</sup> in accordance with the expected chemical formula [C<sub>47</sub>H<sub>29</sub>Cl<sub>8</sub>N<sub>5</sub>] with Exact mass=943.0 (in agreement with reference 30).

✓ *N-methyl-5,10,15,20-tetrakis(pentafluorophenyl)-tetrahydropyrrole[3,4:b] porphyrin 2.5*

Accordingly to the general procedure, to a solution of **2.2** (25 mg, 25.5 μmol) in toluene (5.0 mL) two additions of sarcosine (4.0 mg, 45.4 μmol) and paraformaldehyde (3.4 mg, 0.114 mmol) were carried out during a total of 10 hours of reaction. The mixture obtained was then purified by chromatography in a silica column, using a mixture of CH<sub>2</sub>Cl<sub>2</sub>/petroleum ether (4:1) to recover first the starting



porphyrin (4.7 mg, 20%), and then the green fraction corresponding to chlorin **2.5** (17.7 mg, 65%).

$^1\text{H NMR}$  (300 MHz;  $\text{CDCl}_3$ , TMS as internal standard)  $\delta_{\text{H}}/\text{ppm}$ : -1.82 (*s*, 2H, NH) 2.21 (*s*, 3H, N- $\text{CH}_3$ ), 2.52-2.56 (*m*, 2H, H-pyrrolidine), 3.11-3.16 (*m*, 2H, H-pyrrolidine), 5.24-5.29 (*m*, 2H,  $\beta$ -H), 8.40 (*d*, 2H,  $J = 4.9$  Hz,  $\beta$ -H), 8.71 (*d*, 2H,  $J = 4.9$  Hz, H- $\beta$ ), 8.48 (*s*, 2H, H- $\beta$ ).  $^{19}\text{F NMR}$  ( $\text{CDCl}_3$ )  $\delta_{\text{F}}/\text{ppm}$ : -158.89 (*dd*,  $J = 8.5$  and 25.4 Hz, 2F, Ar-*o*-F), from -160.29 to -160.44 (*m*, 4F, Ar-*o*-F), -160.81 (*dd*, 2F,  $J = 8.5$  and 25.4 Hz, Ar-*o*-F), 174.93 (*t*, 2F,  $J = 20.6$  Hz, Ar-*p*-F), -175.31 (*t*, 2F,  $J = 20.6$  Hz, Ar-*p*-F), -183.62 (*ddd*, 2F,  $J = 8.5$ , 22.8 and 25.4 Hz, Ar-*m*-F-), -184.02 (*ddd*, 2F,  $J = 8.5$ , 22.8 and 25.4 Hz, Ar-*m*-F) -184.99 (*ddd*,  $J = 8.5$ , 22.8 and 25.4 Hz, 4F, Ar-*m*-F, **UV-Vis** ( $\text{CH}_2\text{Cl}_2$ )  $\lambda_{\text{max}}$ , nm (%): 410 (100); 504 (12); 595 (4); 609 (4); 653 (29) nm. MALDI(TOF/TOF)-MS ( $m/z$ ): 1032.1  $[\text{M}+\text{H}]^+$  in accordance with the expected chemical formula  $[\text{C}_{47}\text{H}_{17}\text{F}_{20}\text{N}_5]$  of MW= 1031.6 (in agreement with reference 30).

#### 2.4.4. SYNTHESIS OF THE MANGANESE AND IRON PORPHYRIN-BASED CATALYSTS

##### 2.4.4.1. GENERAL PROCEDURE FOR COMPLEXES **I**, **III**, **IV** AND **VI**

In a 25 mL round bottom flask equipped with a magnetic stirring bar it was added the free-base porphyrin was added properly dissolved in DMF (5.0 mL). This solution, protected from light and under nitrogen atmosphere, was heated at 154 °C and then pyridine (0.5 mL) and the Fe(II) or Mn(II) chloride (10 equiv.) were added. The mixture was left to react, being the reaction evolution monitored by UV-Vis/TLC (when necessary, more metal salt or pyridine were added to the reaction). When the UV-Vis and TLC confirmed the total consumption of the starting material, the reaction was terminated and, after cooling, exposed to air overnight although maintaining the system under stirring. The solvents were then evaporated to dryness in the rotary evaporator. The obtained residue, dissolved in  $\text{CH}_2\text{Cl}_2$ , was washed several times in a separating funnel with distilled water, to remove all the salt excess. The recovered organic phase, extracted with  $\text{CH}_2\text{Cl}_2$ , was finally dried by filtration through sodium sulfate anhydrous. After evaporating the solvent, the obtained complex was precipitated with a  $\text{CH}_2\text{Cl}_2$ /petroleum ether mixture (1:1).



✓ *Chloro[5,10,15,20-tetrakis(2,6-dichlorophenyl)porphyrinate]manganese(III) - I*

The synthesis of complex **I** was performed according to the general procedure, using 50 mg of porphyrin **2.1** and the reaction was terminated after two hours at reflux.

**UV-vis** (CH<sub>2</sub>Cl<sub>2</sub>)  $\lambda_{\text{max}}$ , nm (%): 371 (43), 478 (100); 581 (4). **MALDI(TOF/TOF)-MS** ( $m/z$ ): 942.9 [M]<sup>++</sup> in accordance with the expected chemical formula [C<sub>44</sub>H<sub>20</sub>Cl<sub>8</sub>MnN<sub>4</sub>] with Exact Mass = 943.2 (in agreement with reference 11).

✓ *Chloro[5,10,15,20-tetrakis(4-N,N-dimethylamine-2,3,5,6-tetrafluoro)porphyrinate]iron(III) - III*

The synthesis of complex **III** was performed according to the general procedure, using 50 mg of porphyrin **2.2**. In this case, for the success of the complexation, the oxidation state of the iron(II) salt is determinant and it should be a green solid. Before the addition of pyridine and of the metal salt, the solution of **2.2** in DMF was degassed with N<sub>2</sub> for 10 minutes. After 4 hours, the reaction was finished according to the general work up.

**UV-vis** (CH<sub>2</sub>Cl<sub>2</sub>)  $\lambda_{\text{max}}$ , nm (%): 350 (20), 410 (100), 492 (7), 608 (6). **MALDI(TOF/TOF)-MS** ( $m/z$ ): 1128.1 [M]<sup>++</sup> in accordance with the expected chemical formula [C<sub>52</sub>H<sub>32</sub>F<sub>16</sub>FeN<sub>8</sub>] of MW= 1128.68 (in agreement with reference 11).

✓ *Chloro[5,10,15,20-tetrakis(1-methylimidazolium-2-yl)porphyrinate]manganese(III)-IV*

The synthesis of complex **IV** was performed using 100 mg of H<sub>2</sub>TMImP **2.3** (1.0x10<sup>-4</sup> mol) and approximately 15 equiv. (0.50 g) of the manganese salt and the reflux was performed in 5.0 mL of DMF. Since derivative **IV** is water-soluble, the usual work up was modified. After the evaporation of DMF and pyridine, the obtained residue was dissolved in 500 mL of distilled water and chromatographed in a silica reversed-phase column (C18-Waters Sep-Pak Vac 35 cc, 10g). First, the excess of salt was removed by using water as eluent. Then, the desired manganese(III) complex **IV**



retained on the top of the column was recovered by using methanol as eluent. Complex **IV**, after being precipitated in a CHCl<sub>3</sub>/methanol (9:1) mixture, was filtered and its structure confirmed by the adequate spectroscopic techniques.

**UV-Vis** (CH<sub>3</sub>CN) 364 (4.46), 473 (4.50), 579 (3.88). MALDI(TOF/TOF)-MS (*m/z*): 683.2 [M]<sup>+</sup> in accordance with the expected chemical formula [C<sub>36</sub>H<sub>28</sub>MnN<sub>12</sub>] of MW= 683.6 (in agreement with reference 34).

✓ *Chloro[N-methyl-5,10,15,20-tetrakis(2,6-dichlorophenyl)-tetrahydropyrrole[3,4:b]]porphyrinate] manganese (III)-VI*

The synthesis of complex **VI** was performed according to the general procedure, using 25 mg of chlorin **2.4** and the reaction was terminated after approximately 3 hours.

**UV-Vis** (CH<sub>2</sub>Cl<sub>2</sub>) λ<sub>max</sub>, nm (%): 477 (100), 573 (25.1), 651 (43.2). MALDI(TOF/TOF)-MS (*m/z*): 996 [M]<sup>+</sup> in accordance with the expected chemical formula [C<sub>47</sub>H<sub>27</sub>Cl<sub>8</sub>MnN<sub>5</sub>] with Exact mass = 995.9 (in agreement with reference 41)

#### 2.4.4.2. GENERAL PROCEDURE FOR COMPLEXES **II** AND **VII**

In a 250 mL round bottom flask equipped with a magnetic stirring bar the free-base porphyrin **2.2** (50 mg) was added and properly dissolved in 100 mL of acetic acid. This solution, protected from light and under nitrogen atmosphere, was heated at 120 °C and then the manganese salt Mn(OAc)<sub>2</sub>·6H<sub>2</sub>O (10 equiv.) was added. Similarly to the procedure described in section 2.4.4.1 the evolution of the process was followed by UV-Vis and TLC. At the end of the reaction, and after cooling overnight at room temperature and exposed to air, the obtained manganese(III) complex suffered the normal work-up procedure. In order to promote the change of the counter-ion (acetate by chloride) besides being washed with water, the synthesized metalloporphyrin derivatives were also washed with an HCl solution (11%).

All the compounds were precipitated in a mixture of CH<sub>2</sub>Cl<sub>2</sub>/hexane (1:1) and isolated in quantitative yields by filtration.

✓ Chloro[5,10,15,20-tetrakis(pentafluorophenyl)porphyrinate]manganese (III)-II

The synthesis of complex **II** was performed according to the general procedure, and the reaction was terminated after approximately 3 hours.

**UV-Vis** (CH<sub>2</sub>Cl<sub>2</sub>)  $\lambda_{\text{max}}$ , nm (%): 364 (66), 474 (100); 573 (12). **MALDI(TOF/TOF)-MS** ( $m/z$ ): 1027.0 [M]<sup>+</sup> in accordance with the expected chemical formula [C<sub>44</sub>H<sub>8</sub>F<sub>20</sub>MnN<sub>4</sub>] of MW=1027.5 (in agreement with reference 38)

✓ Chloro[N-methyl-5,10,15,20-tetrakis(pentafluorophenyl-tetrahydropyrrole[3,4:b])porphyrinate]manganese-VII

The synthesis of complex **VII** was performed according to the general procedure, and the addition of more 5 equiv. of Mn(OAc)<sub>2</sub>·6H<sub>2</sub>O was necessary. The reaction was terminated after approximately six hours.

**UV-Vis** (CH<sub>2</sub>Cl<sub>2</sub>)  $\lambda_{\text{max}}$ , nm (%): 371 (54), 477 (100), 573 (23), 652 (43). **MALDI(TOF/TOF)-MS** ( $m/z$ ): 1084.0 [M]<sup>+</sup> in accordance with the expected chemical formula [C<sub>48</sub>H<sub>18</sub>F<sub>19</sub>MnN<sub>5</sub>] of MW= 1084.6 (in agreement with reference 42).

2.4.4.3. CATIONIC CATALYST COMPLEX-V

A mixture containing 50 mg of **2.3** dissolved in DMF (5.0 mL) and a large excess of methyl iodide (100 equiv.) was maintained in a sealed tube protected from light, at 40 °C overnight.

The reaction was finished by carefully adding 15 mL of diethyl ether to the reaction mixture. Then, the precipitate was filtered through a normal glass funnel with cotton wool to an erlenmeyer containing diethylamine to neutralize the excess of CH<sub>3</sub>I. The solid retained in the cotton was extensively washed with diethyl ether and redissolved with methanol to a different flask. The final step, concerning the precipitation of **V**, was performed with a CHCl<sub>3</sub>/methanol (3:1) mixture. This quantitative transformation afforded the desired cationic porphyrin **V**.



- ✓ Chloro[5,10,15,20-(1,3-dimethylimidazolium-2-yl)porphyrinato manganese(III)] tetraiodide (V)

**UV-Vis** (H<sub>2</sub>O)  $\lambda_{\max}$ , nm (%): 346 (46), 445 (100), 551 (9), 586 (6)

**MALDI(TOF/TOF)-MS** ( $m/z$ ): 698.1 [M-3CH<sub>3</sub>]<sup>+</sup> in accordance with the chemical formula [C<sub>40</sub>H<sub>40</sub>MnN<sub>12</sub>]<sup>4+</sup> of MW= 743.8 (in agreement with reference 34)

## 2.5. BIBLIOGRAPHY

- <sup>1</sup> J.T. Groves, *J. Porphyr. Phthalocya.* 4 (2000) 350.
- <sup>2</sup> J.E. Merritt, K.L. Loening, *Pure Appl. Chem.* 51 (1979) 2251
- <sup>3</sup> A.M.G. Silva, PhD Thesis, University of Aveiro (2002).
- <sup>4</sup> L.R. Milgrom, in *"The Colors of Life: An Introduction to the Chemistry of Porphyrins and Related Compounds"*, Oxford University Press, United Kingdom (1997).
- <sup>5</sup> K.M. Kadish, K.M. Smith, R. Guilard (Eds.), in *"The porphyrin handbook- Applications, Past, Present and Future"* vol.1, Academic Press, New York (2000).
- <sup>6</sup> S.L.H. Rebelo, PhD Thesis, University of Aveiro (2004).
- <sup>7</sup> K.S. Suslick, R.A. Watson, *New J. Chem.* 16 (1992) 633.
- <sup>8</sup> H. Fischer, K. Zeile, *Liebigs Ann. Chem.* 468 (1929) 98.
- <sup>9</sup> P. Rothmund, *J. Am. Chem. Soc.* 57 (1935) 2010.
- <sup>10</sup> a) P. Rothmund, *J. Am. Chem. Soc.* 58 (1936) 625. b) P. Rothmund, *J. Am. Chem. Soc.* 61 (1939) 2912. c) P. Rothmund, A.R. Menotti, *J. Am. Chem. Soc.* 4 (2000) 139.
- <sup>11</sup> A.D. Adler, F.R. Longo, J.D. Finarelli, J. Goldmacher, J. Assour, L. Korsakoff, *J. Org. Chem.* 32 (1967) 476.
- <sup>12</sup> J.S. Lindsey, H.C. Hsu, I.C. Schreiman, *Tetrahedron Lett.* 27 (1986) 4969.
- <sup>13</sup> J.S. Lindsey, I.C. Schreiman, H.C. Hsu, P.C. Kearney, A.M. Marguerettaz, *J. Org. Chem.* 52 (1987) 827.
- <sup>14</sup> J.S. Lindsey, in: *"The Porphyrin Handbook- Synthesis and Organic Chemistry"* K.M. Kadish, K.M. Smith, R. Guilard (Eds.), vol. 1, Academic Press, San Diego (2000) chapter 2.
- <sup>15</sup> A.M.A.R. Gonsalves, M.M. Pereira, *J. Heterocycl. Chem.* 22 (1985) 931.
- <sup>16</sup> A.M.A.R. Gonsalves, J.M.T.B. Varejão, M.M. Pereira, *J. Heterocycl. Chem.* 28 (1991) 635.
- <sup>17</sup> R. De Paula, M.A.F. Faustino, D.C.G.A. Pinto, M.G.P.M.S. Neves, J.A.S. Cavaleiro, *J. Heterocycl. Chem.* 45 (2008) 453.
- <sup>18</sup> J.A.S. Cavaleiro, A.C. Tomé, M.G.P.M.S. Neves in *"Handbook of porphyrin Science"*, K.M. Kadish, K.M. Smith, R. Guilard (Eds.), World Scientific Publishing Company Co., Singapura, Vol.2 (2010) p. 193-294.
- <sup>19</sup> a) M.R. Kishan, V.R. Rani, M.R.V.S. Murty, P.S. Devi, S. J. Kulkarni, K.V. Raghavan, *J. Mol. Catal. A: Chem.* 223 (2004) 263. b) F. Langa, P. de la Cruz, *Comb. Chem. High Throughput Screen* 10 (2007) 766. c) D. Samaroo, C.E. Soll, L.J. Todaro, C.M. Drain, *Org. Lett.* 8 (2006) 4985. d) A. Petit, A. Loupy, P. Maillard, M. Momenteau, *Synth. Commun.* 22 (1992) 1137.
- <sup>20</sup> S. Horn, K. Dahms, M.O. Senge, *J. Porphyr. Phthalocya.* 12 (2008) 1053.
- <sup>21</sup> a) M.G.H. Vicente, in *"The Porphyrin Handbook-Synthesis and Organic Chemistry"* K.M.

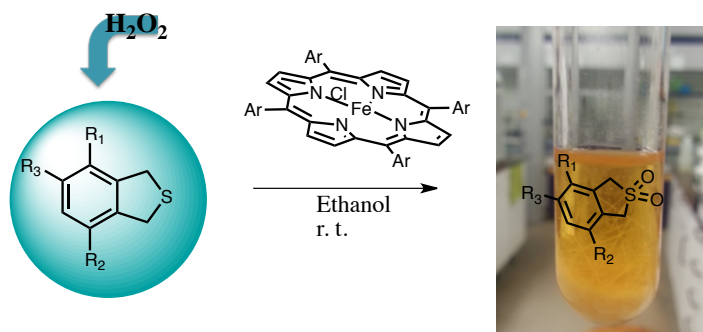
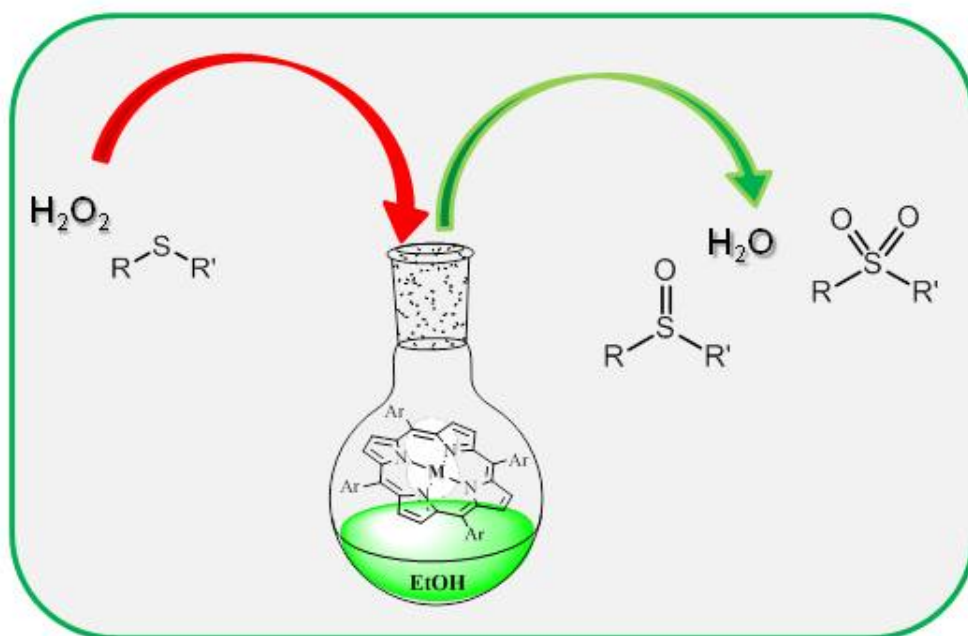


- Kadish, K.M. Smith, R. Guilard (Eds.) Academic Press, San Diego, vol. 1, chapter4 (2000) p. 150- 193. b) L. Jaquinod, in *The Porphyrin Handbook-Synthesis and Organic Chemistry* K.M. Kadish, K.M. Smith, R. Guilard (Eds.) Academic Press, San Diego, vol.1, chapter5, (2000) p. 202- 232.
- <sup>22</sup> T.R. Janson, J.J. Katz, in: D. Dolphin (Ed.) *"The Porphyrins: Physical Chemistry – Part B"*, Academic Press, New York (1978).
- <sup>23</sup> V.I.V. Serra, S.M.G. Pires, C.M.A. Alonso, M.G.P.M.S. Neves, A.C. Tomé, J.A.S. Cavaleiro, in *"Topics in Heterocycle Chemistry"* Springer-Verlag, Berlin Heidelberg 33 (2014) p. 35–78.
- <sup>24</sup> a) M.A. Faustino, M.G.P.M.S Neves, M.G.H. Vicente, A.M.S. Silva, J.A.S. Cavaleiro, *Tetrahedron Lett.* 36 (1995) 5977. b) M.A. Faustino, M.G.P.M.S Neves, M.G.H. Vicente, A.M.S. Silva, J.A.S. Cavaleiro, *Tetrahedron Lett.* 37 (1996) 3569.
- <sup>25</sup> a) K.M. Shea, L. Jaquinod, K.M. Smith, *J. Org. Chem.* 63 (1998) 7013. b) K.M. Shea, L. Jaquinod, R.G. Khoury, K.M. Smith, *Tetrahedron* 56 (2000) 3139.
- <sup>26</sup> J.A.S. Cavaleiro, M.G.P.M.S. Neves, A. C. Tomé, *Arkivoc* XIV (2003) 107.
- <sup>27</sup> a) A.C. Tomé, P.S.S. Lacerda, M.G.P.M.S. Neves, J.A.S. Cavaleiro, *Chem. Commun.* (1999) 1767. b) A.M.G. Silva, A.C. Tomé, M.G.P.M.S. Neves, J.A.S. Cavaleiro, *Tetrahedron Lett.* 41 (2002) 3065.
- <sup>28</sup> a) A.M.G. Silva, A.C. Tomé, M.G.P.M.S. Neves, A.M.S. Silva, J.A.S. Cavaleiro, *Chem. Commun.* (1999) 1767. b) A.M.G. Silva, A.C. Tomé, M.G.P.M.S. Neves, A.M.S. Silva, J.A.S. Cavaleiro, D. Perrone, A. Dondoni, *Tetrahedron Lett.* 43 (2002) 603. c) A.M.G. Silva, A.C. Tomé, M.G.P.M.S. Neves, J.A.S. Cavaleiro, *Synlett* (2002) 1155. d) A.M.G. Silva, A.C. Tomé, M.G.P.M.S. Neves, A.M.S. Silva, J.A.S. Cavaleiro, *J. Org. Chem.* 67 (2002) 726.
- <sup>29</sup> a) A. Desjardins, J. Flemming, E.D. Sternberg, D. Dolphin, *Chem. Commun.* (2002) 2622. b) J. Flemming, D. Dolphin, *Tetrahedron Lett.* 43 (2002) 7281.
- <sup>30</sup> A.M.G. Silva, A. C. Tomé, M.G.P.M.S. Neves, A.M.S. Silva, J.A.S. Cavaleiro, *J. Org. Chem.* 70 (2005) 2306.
- <sup>31</sup> G. Jiménez-Osés, J.I. García, A.M.G. Silva, A.R.N. Santos, A.C. Tomé, M.G.P.M.S. Neves, J.A.S. Cavaleiro, *Tetrahedron* 64 (2008) 7937.
- <sup>32</sup> J.I.T. Costa, A.C. Tomé, M.G.P.M.S. Neves, J.A.S. Cavaleiro, *J. Porphyrins and Phthalocyanines*, 15 (2011) 1116.
- <sup>33</sup> M.A. Hyland, M.D. Morton, C. Brückner, *J. Org. Chem.* 77 (2012) 3038.
- <sup>34</sup> R. De Paula, M.M.Q. Simões, M.G.P.M.S. Neves, J.A.S. Cavaleiro, *Catal. Commun.* 10 (2008) 57.

- <sup>35</sup> D.H. Tjahjono, T. Akutsu, N. Yoshioka, H. Inoue, *Biochim. Biophys. Acta-Gen. Subj.*, 1472 (1999) 333.
- <sup>36</sup> A.D. Adler, F.R. Longo, F.L. Kampas, *J. Inorg. Nucl. Chem.* 32 (1970) 2443.
- <sup>37</sup> J.I.T. Costa, A.C. Tomé, M.G.P.M.S. Neves, J.A.S. Cavaleiro, *J. Porphyr. Phthalocya.* 15 (2011) 1117.
- <sup>38</sup> Y. Liu, H.J. Zhang, Y.Q. Cai, H.H. Wu, X.L. Liu, Y. Lu, *Chem. Lett.* 36 (2007) 848.
- <sup>39</sup> J.P.C. Tomé, M.G.P.M.S. Neves, A.C. Tomé, J.A.S. Cavaleiro, M. Soncin, M. Magaraggia, S. Ferro, G. Jori, *J. Med. Chem.* 47 (2004) 6649.
- <sup>40</sup> P. Domingues, M.M.Q. Simões, *Safety First! Booklet* (2010) 7.
- <sup>41</sup> S.M.G. Pires, R. De Paula, M.M.Q. Simões, M.G.P.M.S. Neves, I.C.M.S. Santos, A.C. Tomé, J.A.S. Cavaleiro, *Catal. Commun.* 11 (2009) 24.
- <sup>42</sup> M.C.R. Castro, Master Thesis (2009) University of Aveiro







## Chapter 3 HOMOGENEOUS BIOMIMETIC OXIDATION OF ORGANOSULFUR COMPOUNDS WITH $\text{H}_2\text{O}_2$ CATALYZED BY METALLOPORPHYRINS



Chapter based on the following publications:

- "*Biomimetic oxidation of organosulfur compounds with hydrogen peroxide catalyzed by manganese porphyrins*", S.M.G. Pires, M.M.Q. Simões, I.C.M.S. Santos, S.L.H. Rebelo, M.M. Pereira, M.G.P.M.S. Neves, J.A.S. Cavaleiro., *Appl. Catal. A: Gen.* 439-440 (2012) 51.

- "*Oxidation of organosulfur compounds using an iron(III) porphyrin complex: an environmentally safe and efficient approach*", S.M.G. Pires, M.M.Q. Simões, I.C.M.S. Santos, S.L.H. Rebelo, F.A.A. Paz, M.G.P.M.S. Neves, J.A.S. Cavaleiro, *Appl. Catal. B: Environ.*" 160–161 (2014) 80.

- "*A green and sustainable method for the oxidation of 1,3-dihydrobenzo[c]thiophenes to sulfones using metalloporphyrin complexes*", G. da Silva, S. M.G. Pires, V.L.M. Silva, M.M.Q. Simões, M.G.P.M.S. Neves, S.L.H. Rebelo , A.M.S. Silva, J.A.S. Cavaleiro, *Catal. Commun.* 56 (2014) 68.

### **3. HOMOGENEOUS BIOMIMETIC OXIDATION OF ORGANOSULFUR COMPOUNDS WITH H<sub>2</sub>O<sub>2</sub> CATALYZED BY METALLOPORPHYRINS**

#### **3.1. OXIDATION OF SULFIDES, BENZOTHIOPHENES AND DIBENZOTHIOPHENES**

The negative impact induced by the presence of the most recalcitrant organosulfur derivatives, as dibenzothiophenes, in petroleum products is well established, both from environmental and industrial reasons. Firstly, beyond the SO<sub>x</sub> emissions resulting from their combustion being normally associated with the formation of acid rains, they are also important pollutants to air, water, and soil, putting in danger the public health. Secondly, they are also responsible for the poisoning of catalysts and corrosion of internal parts of combustion engines of most refineries.<sup>1-3</sup>

Furthermore, the very restrictive regulations recently approved, limiting the sulfur content on petroleum products, allied to the technical limitations of the common hydrodesulfurization procedures (HDS), definitely made the deep desulfurization of liquid fuels a worldwide challenge.<sup>3,4</sup> The recent intense research in the area led to the appearance of very promising and much more environmentally sustainable alternatives such as the oxidative desulfurization (ODS) or the biodesulfurization (BDS) methodologies.<sup>4-7</sup> Besides, these alternatives can answer to other important drawbacks of HDS technology application in most refineries, as the significative economical impact and safety issues associated to the use of hydrogen and to the high temperatures/pressures required. It is important to understand that, contrasting with ODS and BDS, HDS cannot readily achieve the very low sulfur levels envisaged for future “zero sulfur” contents.<sup>8,9</sup> Moreover, it has already been proved that from an economical point of view, BDS is hardly viable at an industrial scale, whereas ODS presents recognized advantages such as the lower capital and operating costs needed to be integrated in the already existing hydrotreating units.<sup>1,5</sup>

The oxidation of the refractory organosulfur derivatives, benzothiophenes (BTs) and dibenzothiophenes (DBTs), into the corresponding sulfoxides and sulfones (more polar comparatively to the starting material) assists their easy removal from fuels. Extraction, distillation, decomposition or adsorption into activated silica/alumina are good examples of the most employed extraction procedures.<sup>1,10-14</sup> Besides, sulfoxide or sulfone derivatives have attracted also the attention of the scientific community by



their recognized biological activity, or through their efficient use as ligands in asymmetric catalysis and as oxygen transfer agents.<sup>15-17</sup>

Thus, the growing interest in the development of new and more efficient ODS processes already gave origin to several reports in the literature describing the good results obtained with several oxidants: peroxyacids, NaIO<sub>4</sub>, MnO<sub>2</sub>, CrO<sub>3</sub>, SeO<sub>2</sub>, *t*-BuOOH, cumene hydroperoxide, PhIO, O<sub>3</sub> and O<sub>2</sub>, being H<sub>2</sub>O<sub>2</sub> the most commonly used, by efficiency and environment protection reasons.<sup>18, 19</sup> Several catalytic systems have been tested with this oxidant, including homogeneous and heterogeneous catalysts,<sup>19-32</sup> organic acid catalysts<sup>33-35</sup> and polyoxometalates.<sup>36-40</sup> Nevertheless, despite the diversity of catalytic systems there are still important gaps to overcome like the narrow applicability of ODS to BTs and DBTs. Until now, ODS efficiency only have been proved to a limited number of BTs and DBTs and much work is still to be done, different catalysts to be evaluated and new methodologies to be addressed. One possible solution to this challenge passes through the use of bio-inspired catalysts mimicking the activity of CYP-450 enzymes. The application of tetrapyrrolic macrocycles such as porphyrins,<sup>41-47</sup> phthalocyanines<sup>48</sup> or corroles<sup>49</sup> as catalysts in sulfoxidation reactions, thinking about a possible future application on oxidative desulfurization is not new. However, as far as we know, until now Fe(III), Mn(III) or Ru(III) complexes have been tested mainly with sulfide derivatives, considered as the easier to be oxidized. Thus, the development of metalloporphyrin-based catalytic systems seems relevant, if under environmental safe conditions they are able to promote the sulfoxidation of BTs and DBTs.

### 3.1.1. PRESENTATION OF THE WORK DEVELOPED

The amount of work performed in our laboratory in the field of oxidative catalysis with metalloporphyrins,<sup>50-60</sup> and the interest on the development of new, efficient and environmental benign sulfoxidation methodologies, led to the evaluation of this catalysts' efficiency in the oxidation of several organosulfur derivatives by hydrogen peroxide, as one of the main goals of this dissertation.

In order to study the influence of porphyrinic catalysts' structure induced by the presence of different substituents on the *meso*-positions, or by the central metal ion, the homogeneous catalytic assays involved the use of different second generation metalloporphyrins: two manganese(III) complexes, **(I)** and **(II)**, and the iron complex

(III) (Figure 3-1). It is important to refer here, relatively to the substrates used in this study, that this is the first time that such biomimetic approach is applied not only to sulfides (**3.1** and **3.2**) but also to a wide range of recalcitrant BTs (**3.3-3.6**) and DBTs (**3.7-3.10**) (Figure 3-2).

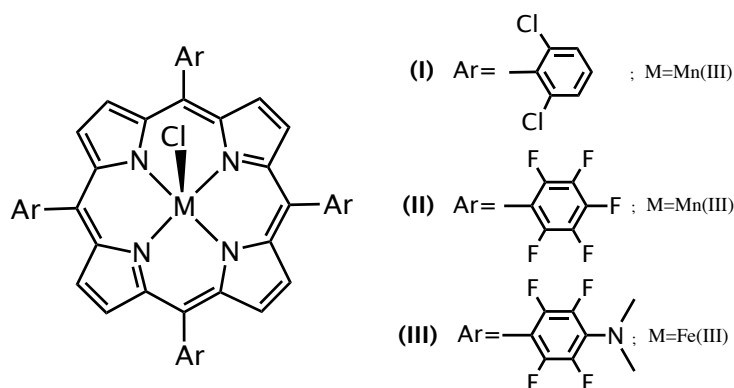


**Figure 3-1** Metalloporphyrins studied as catalysts

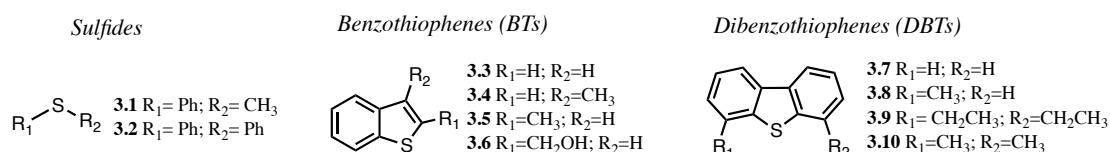
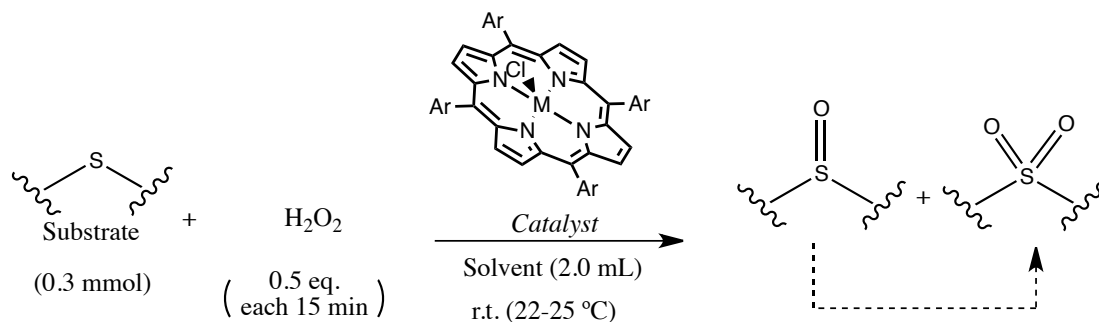


**Figure 3-2** Organosulfur compounds studied for sulfoxidation with  $H_2O_2$  (30%) using metalloporphyrin catalysts

Typically, the experiments were performed under very mild conditions, thus using room temperature and hydrogen peroxide as oxidant, and in the absence of light. In order to prevent the premature destruction of the catalyst in the highly oxidative medium,  $H_2O_2$  (30%) was used diluted in an appropriate solvent, being progressively added to the reaction, in small aliquots of 0.5 equiv. in regular intervals of 15 minutes. The general approach followed in the catalytic assays is summarized in Scheme 3-1. The evolution of the catalytic experiments was monitored by GC (as discussed below; the only exception was DBT **3.10**), using chlorobenzene as the internal standard. The typical GC analysis chromatograms of the sulfur derivatives studied is represented in Figure 3-3. Generally, it is possible to observe the conversion of the substrate into the corresponding sulfoxide (S=O) and sulfone ( $SO_2$ ) products, only the corresponding  $SO_2$  being detected at the end of the reactions.



Scheme 3-1

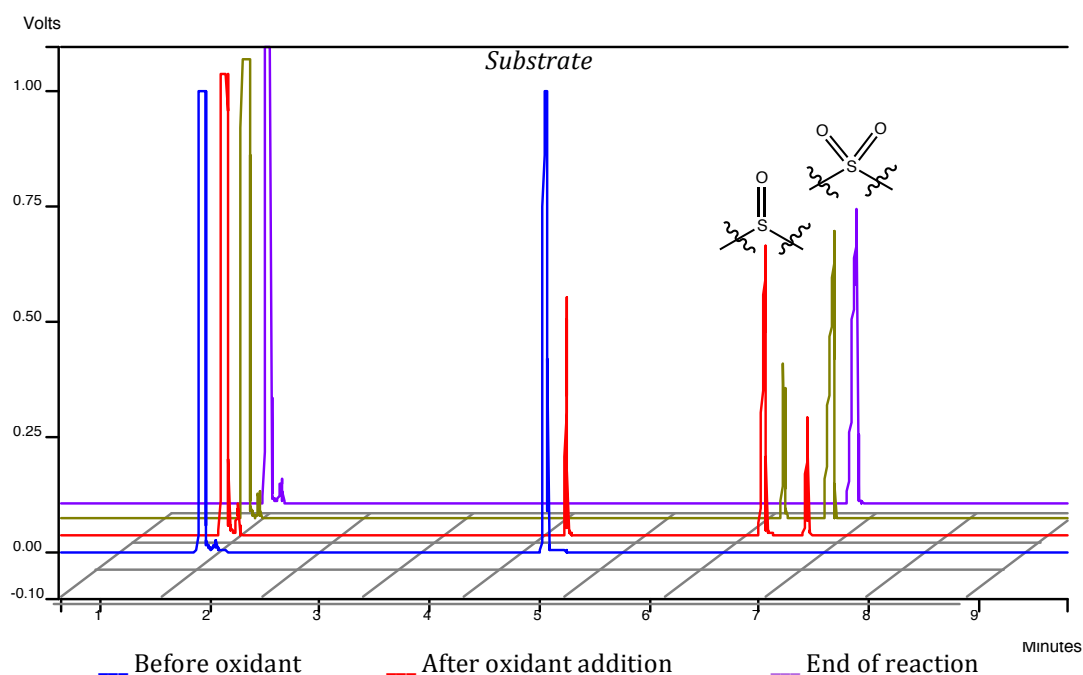


Figure 3-3 Typical GC-FID chromatograms profile

From the research carried out so far, two papers have already been published, one concerning the assays with the manganese(III) complexes and substrates **3.1-3.7** (Part A),<sup>61</sup> and the other related to the results obtained with the iron(III) complex (**III**) where the list of substrates was also extended to include substrates **3.1-3.10** (Part B).<sup>62</sup> The results achieved with both catalytic systems are also compared.

### 3.1.2. PART A- CATALYTIC EXPERIMENTS WITH MANGANESE(III) COMPLEXES

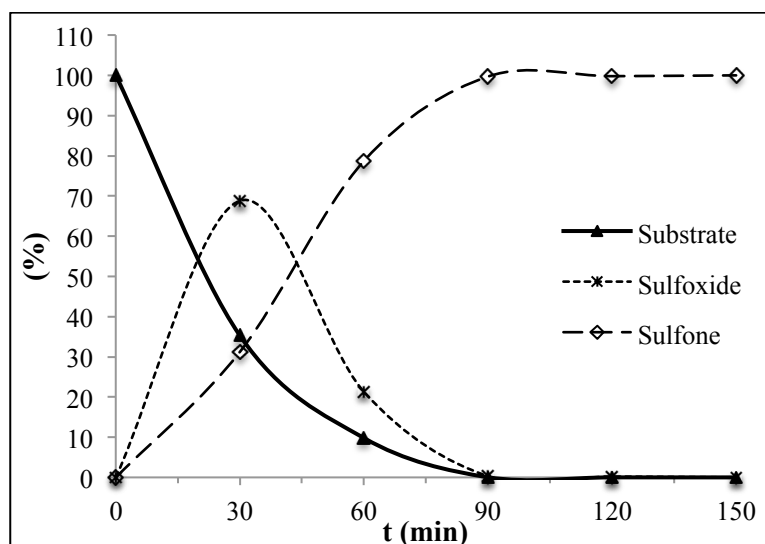
Two well-known and extensively studied manganese(III) porphyrins, namely catalyst **I** [Mn(TDCPP)Cl] and catalyst **II** [Mn(TPFPP)Cl], were evaluated for the

sulfoxidation of organosulfur compounds (**3.1-3.7**) by H<sub>2</sub>O<sub>2</sub>. In the specific case of manganese (III) porphyrin complexes, the solvent of reaction was the aprotic CH<sub>3</sub>CN, aprotic able to properly dissolve all the components of the reaction (catalyst, substrate and H<sub>2</sub>O<sub>2</sub>), and ammonium acetate was used as co-catalyst. The results achieved with both complexes, **I** and **II**, for two S/C molar ratios, 150 and 300, are summarized in Table 3-1; the values presented were determined based on the GC-FID analysis.

The results obtained for the oxidation of substrates (**3.1-3.7**) (Figure 3-2) with H<sub>2</sub>O<sub>2</sub> using porphyrin catalysts [Mn(TDCPP)Cl] (**I**) and [Mn(TPFPP)Cl] (**II**) (Figure 3-1) show that the approach is an easy, high efficient, green, and sustainable procedure to oxidize sulfides (**3.1-3.2**), benzothiophenes (**3.3-3.6**), and dibenzothiophene (**3.7**).

For both catalysts, (**I**) and (**II**), and for all the substrates tested, the resulting sulfones (**3.11-3.17**) were obtained as the only products at the end of the oxidation reactions, corresponding to moderate to high substrate conversion values, depending on the catalyst and on the substrate/catalyst molar ratio. At the end of reaction, for each substrate, the reaction mixture was directly applied in preparative TLC plates and the sulfones properly purified and characterized by <sup>1</sup>H NMR and GC-MS.

To confirm that metalloporphyrins are in fact catalyzing the oxidation of substrates (**3.1-3.7**), blank experiments were performed, without catalyst, for all the substrates, and no significant conversions were registered (always <5%). In the GC-FID and GC-MS analyses for all the substrates, two products were detected at the beginning of the reactions. The peaks with lower retention times were identified by GC-MS as the resulting sulfoxides, whereas the peaks with higher retention times were attributed to the corresponding sulfones. As exemplified for 3-methylbenzothiophene (Figure 3-4), after the initial 30 min of reaction the sulfoxide decreases until its total disappearance whereas the sulfone increases until the end of the reaction. So, the manganese(III) porphyrin catalyzed oxidation reactions seem to involve a two-step process: first the oxidation to the sulfoxide, followed by its oxidation to the respective sulfone.

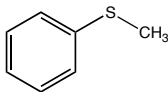
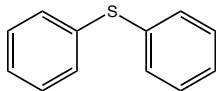
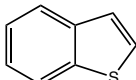
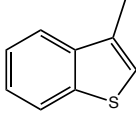
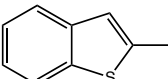
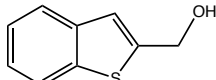
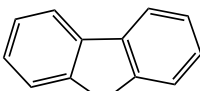


**Figure 3-4** 3-Methylbenzothiophene (**3.4**) oxidation reaction profile with  $\text{H}_2\text{O}_2$  in the presence of catalyst (**I**) for a sub/cat molar ratio of 150

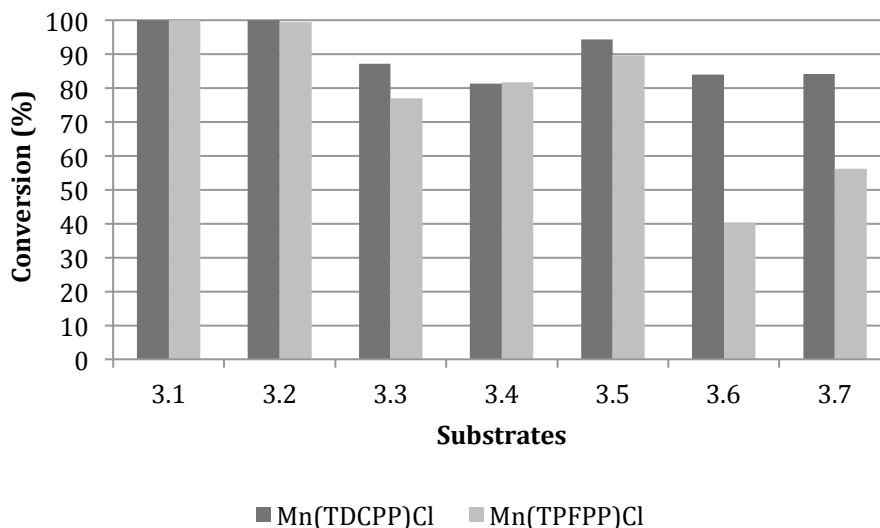
As clearly evidenced by the results presented in Table 3-1 and in Figure 3-5, generally  $[\text{Mn}(\text{TDCPP})\text{Cl}]$  affords the best results, giving higher conversions in lower reaction times, under similar conditions. The conversion values obtained after 90 min of reaction using a substrate/catalyst molar ratio of 300 [Figure 3-5 (i)] or of 150 [Figure 3-5 (ii)], also put in evidence the better performance of both catalysts in the oxidation of sulfides (**3.1**) and (**3.2**), comparatively to the so-called refractory substrate **3.7**, probably due to the sulfur unshared electrons involvement in the aromatic system of **3.7**. Besides that, in the presence of catalyst (**I**), a substituent at positions 2 or 3 of benzothiophene does not seem to affect the efficiency of the reaction (substrates **3.4-3.6**). In general, the substrates tested give rise to lower conversions in the presence of catalyst (**II**), with special emphasis on **3.6** and **3.7**. As referred previously, in the introduction of this dissertation, this behavior can be understood by considering the electron-withdrawing capabilities of  $[\text{Mn}(\text{TPFPP})\text{Cl}]$  relatively to  $[\text{Mn}(\text{TDCPP})\text{Cl}]$ , thus suggesting a more difficult formation of the active oxo-species for  $[\text{Mn}(\text{TPFPP})\text{Cl}]$ .<sup>55</sup>



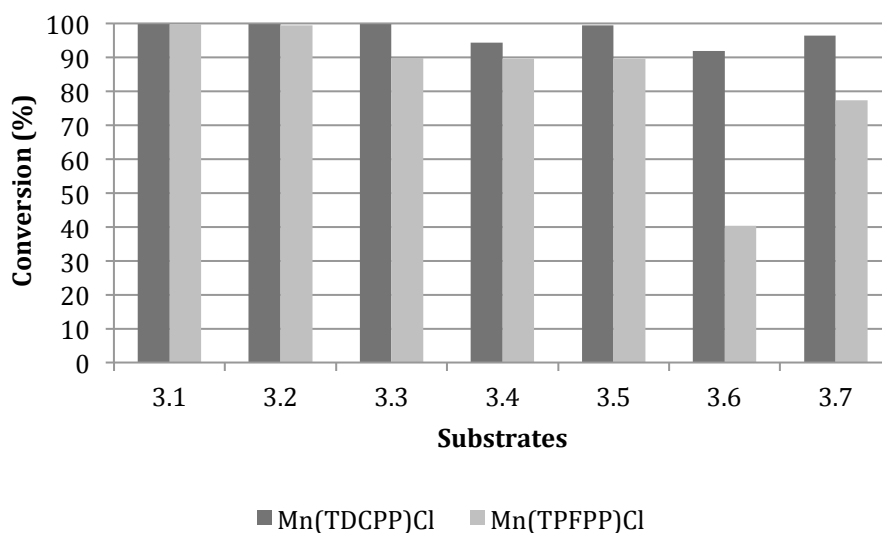
**Table 3-1** Results obtained for the oxidation of substrates (3.1-3.7) with H<sub>2</sub>O<sub>2</sub> catalyzed by manganese porphyrins (I) and (II).<sup>a</sup>

Substrate	Catalyst	H <sub>2</sub> O <sub>2</sub> (mmol)	S/C molar ratio	Conversion (%)	Products selectivity (%)		Time (min)
					S=O	SO <sub>2</sub>	
 (3.1)	I	0.6	150	99.9	-	100	60
		0.9	300	99.9	-	100	90
	II	1.2	150	99.9	-	100	120
		1.8	300	92.1	-	100	180
 (3.2)	I	0.9	150	99.9	-	100	90
		1.2	300	99.7	-	100	120
	II	1.5	150	99.9	-	100	150
		2.4	300	92.5	-	100	240
 (3.3)	I	0.9	150	99.9	-	100	90
		1.8	300	97.0	-	100	180
	II	1.5	150	97.8	-	100	150
		1.8	300	87.4	-	100	180
 (3.4)	I	0.9	150	99.7	-	100	90
		1.2	300	95.1	-	100	120
	II	1.2	150	98.8	-	100	120
		1.8	300	85.9	-	100	180
 (3.5)	I	1.2	150	99.8	-	100	120
		1.5	300	96.1	-	100	150
	II	1.8	150	96.5	-	100	180
		1.8	300	81.9	-	100	180
 (3.6)	I	1.2	150	99.7	-	100	120
		1.8	300	99.4	-	100	180
	II	1.5	150	95.9	-	100	150
		1.5	300	66.1	*	*	150
 (3.7)	I	1.2	150	99.9	-	100	120
		1.8	300	90.9	-	100	180
	II	1.2	150	92.4	-	100	120
		1.2	300	50.9	*	*	120

<sup>(a)</sup>The substrate (0.3 mmol) was dissolved in 2.0 mL of CH<sub>3</sub>CN and kept under magnetic stirring at 22-25 °C in the presence of manganese(III) porphyrins I and II (for S/C molar ratio of 150, the catalyst amount was 2.0 x 10<sup>-3</sup> mmol; for S/C molar ratio of 300, the catalyst amount was 1.0 x 10<sup>-3</sup> mmol). The co-catalyst used was NH<sub>4</sub>CH<sub>3</sub>CO<sub>2</sub> (0.12 mmol). The oxidant, diluted 1:10 in CH<sub>3</sub>CN, was progressively added at regular intervals of 15 min in small aliquots, each corresponding to a half-substrate amount. The conversion and selectivity values are the result of at least two assays. \*The chromatograms do not allow the determination of the corresponding selectivities.



(i)



(ii)

**Figure 3-5** Conversion values obtained for substrates (3.1-3.7) after 90 min of oxidation reaction with H<sub>2</sub>O<sub>2</sub>, using (i) a sub/cat molar ratio of 300 and (ii) a sub/cat molar ratio of 150.

The catalytic system was evaluated for the removal of refractory *S*-containing compounds in a model fuel, consisting on a mixture of benzothiophene (3.3), 3-methylbenzothiophene (3.4), 2-methylbenzothiophene (3.5), and dibenzothiophene (3.7) in hexane, using the more efficient catalyst, [Mn(TDCPP)Cl], as demonstrated above. GC-MS analyses were used to follow the oxidation reactions of the model fuel. The chromatograms obtained before [Figure 3-6 (A)] and after [Figure 3-6 (D)] the catalytic oxidation of the model fuel were used to confirm that all the *S*-containing

compounds had been completely oxidized to the corresponding sulfones **3.13** ( $R_t = 10.23$ ), **3.14** ( $R_t = 10.84$ ), **3.15** ( $R_t = 11.93$ ), and **3.17** ( $R_t = 15.68$ ). After 60 min of reaction [Figure 3-6 (B)] is possible to observe the four chromatographic peaks corresponding to the substrates, four new peaks corresponding to the sulfones and two additional peaks identified by GC-MS as the sulfoxides ( $R_t = 10.04$  for the benzothiophene oxide and  $R_t = 11.68$  for the 2-methylbenzothiophene oxide). After 120 min of reaction almost complete conversion of the model fuel is achieved, as can be observed in Figure 3-6 (C).

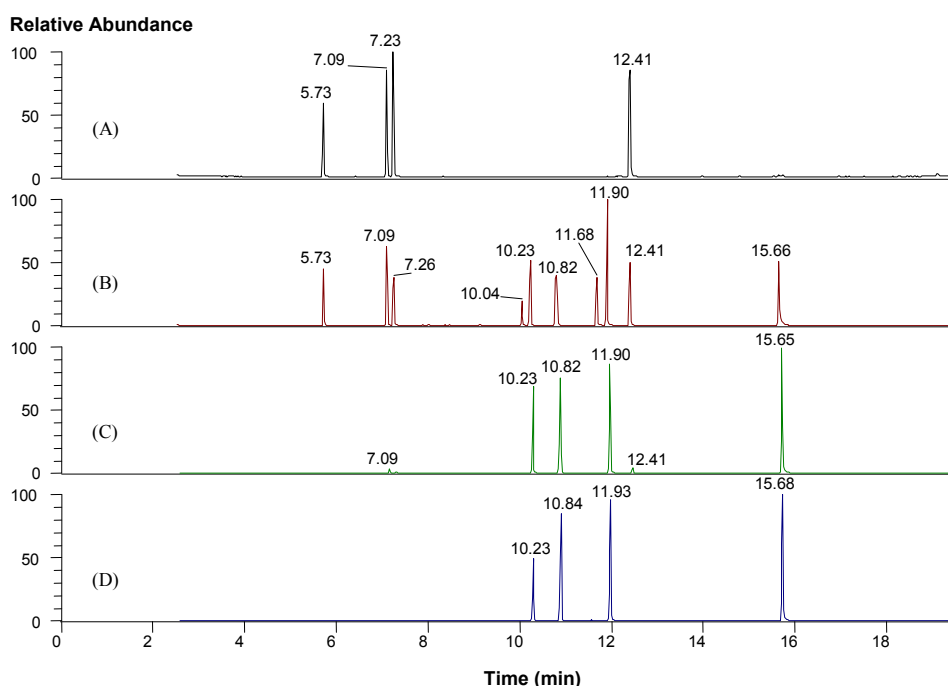


**Figure 3-6** Typical GC-MS chromatograms illustrating the model fuel oxidation reaction profile with  $H_2O_2$  in the presence of catalyst (**I**) for a sub/cat molar ratio of 150. (A) Initial reaction mixture before the addition of  $H_2O_2$ ; (B) after 60 min of reaction; (C) after 120 min of reaction; (D) after 180 min of reaction. The model fuel is a solution of **3.3** ( $R_t = 5.73$ ), **3.4** ( $R_t = 7.09$ ), **3.5** ( $R_t = 7.23$ ), and **3.7** ( $R_t = 12.41$ ) in hexane (with 0.03 mmol each).

### 3.1.3. PART B- CATALYTIC EXPERIMENTS WITH IRON(III) COMPLEXES

Encouraged by the promising results achieved for the oxidation of several organosulfur compounds using the manganese(III)/ $H_2O_2$  catalytic system (Part A, chapter 3), we decided to extend this type of approach to a different metalloporphyrin catalytic system and increase the number of evaluated DBTs. We thus propose to investigate the performance of the iron(III) porphyrin **III**, and the necessary



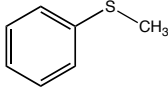
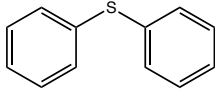
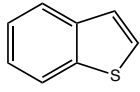
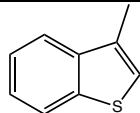
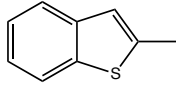
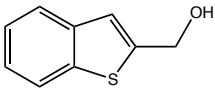
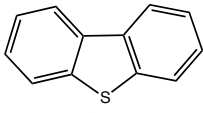
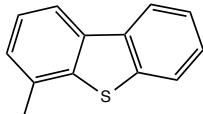
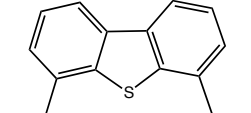
readjustments on the protocol were designed. So, under the new conditions the catalytic sulfoxidation of substrates **3.1-3.10** (Figure 3-2) by  $\text{H}_2\text{O}_2$  was performed in the presence of  $\text{FeTNMe}_2\text{F}_4\text{PPCl}$  (**III**, Figure 3-1) using ethanol as solvent, accordingly to Scheme 3-1. Due to the insolubility of substrate **3.10** its oxidation required slightly different experimental conditions; in order to facilitate the discussion, the analysis of the results obtained with this substrate will be separated from those obtained with substrates **3.1-3.9**.

Although the experimental procedure seems similar to that described for manganese catalysts,<sup>61</sup> there are two important differences that must be highlighted: the solvent used in the reaction and in the dilution of the aqueous hydrogen peroxide, and the presence or the absence of a co-catalyst. As explained in chapter 1, for a Fe-Porph/ $\text{H}_2\text{O}_2$  catalytic system the formation of the hydroperoxy active species is favored by the use of a protic solvent and does not require the presence of a co-catalyst.<sup>55, 63</sup> On the other hand, in the case of the Mn-Porph/ $\text{H}_2\text{O}_2$  catalytic system, where the oxo-species is considered the main active catalytic species, its formation is favored in the presence of an aprotic solvent and of a buffering substance as the co-catalyst.<sup>55, 63</sup> Thus, in the catalytic experiments using catalyst **III** ethanol was the solvent of choice, and no co-catalyst was used, differently from catalysts **I** and **II** where  $\text{CH}_3\text{CN}$  was the reaction solvent and a co-catalyst, ammonium acetate, was obligatory employed.<sup>64</sup>

The results achieved in the catalytic assays using the iron catalyst **III** are summarized in Table 3-2. In Table 3-3, resulting from the extension of the range of DBTs, are summarized those obtained in the oxidation of substrates **3.8** and **3.9** with manganese complexes **I** and **II**. Before starting the results analysis, as already referred for the manganese complexes, blank experiments (without catalyst) were performed for all the organosulfur compounds **3.1-3.9**, in the new reaction conditions. No significant conversions were observed, being lower than 5% for all cases.

Iron(III) catalyst **III** behaves as the most efficient in the sulfoxidation of substrates **3.1-3.9**. Besides achieving more rapidly almost total conversion for all the organosulfur compounds studied, including the most recalcitrant DBTs (**3.7-3.9**), permits also the use of lower amounts of catalyst, without significant decrease in the efficiency.

**Table 3-2** Results obtained for the oxidation of substrates **(3.1-3.9)** with H<sub>2</sub>O<sub>2</sub> catalyzed by the iron(III) porphyrin complex **(III)**<sup>(a)</sup>

Substrates	S/C molar ratio	H <sub>2</sub> O <sub>2</sub> (mmol)	Conversion (%)	Products selectivity (%)		Time (min)
				S=O	SO <sub>2</sub>	
 <b>(3.1)</b>	300	0.6	99.9	-	100	60
	600	0.6	99.9	-	100	60
	1200	1.2	97.2	-	100	120
 <b>(3.2)</b>	300	0.9	99.9	-	100	90
	600	0.9	99.9	-	100	90
	1200	0.9	99.9	6.9	93.1	90
 <b>(3.3)</b>	300	1.2	99.9	-	100	120
	600	1.2	99.9	-	100	120
	1200	1.5	92.4	3.2	96.8	150
 <b>(3.4)</b>	300	0.9	99.9	-	100	90
	600	1.2	98.4	-	100	120
	1200	1.2	44.6	100	0	120
 <b>(3.5)</b>	300	1.5	99.9	-	100	150
	600	1.5	99.9	-	100	150
	1200	1.5	90.1	54.8	45.2	150
 <b>(3.6)</b>	300	1.8	99.5	-	100	180
	600	1.8	96.1	-	100	180
	1200	1.8	73.8	*	*	180
 <b>(3.7)</b>	300	0.9	99.9	-	100	90
	600	1.5	98.7	-	100	150
	1200	1.8	71.3	*	*	180
 <b>(3.8)</b>	300	1.5	99.7	-	100	150
	600	1.8	98.2	2.1	97.9	180
	1200	1.8	84.4	10	90	180
 <b>(3.9)</b>	300	1.8	96.3	88.5	22.9	180
	600	1.8	88.6	59.8	40.2	180
	1200	1.2	43.7	80.9	19.1	120

<sup>(a)</sup>The substrate (0.3 mmol) was dissolved in 2.0 mL of ethanol and kept under magnetic stirring at 22-25 °C in the presence of the iron(III) catalyst **III** (for the S/C molar ratio of 300, the catalyst amount was  $1.0 \times 10^{-3}$  mmol; for the S/C molar of 600, the catalyst amount was  $0.5 \times 10^{-3}$  mmol; for the S/C molar of 1200, the catalyst amount was  $0.25 \times 10^{-3}$  mmol). The oxidant, diluted 1:10 in ethanol, was progressively added at regular intervals of 15 min in small aliquots, each corresponding to a half-substrate amount. The conversion and selectivity values are the result of at least two assays. \*The chromatograms do not allow the determination of the corresponding selectivity



It is notable that, comparatively to the manganese porphyrin complexes, and even using a substrate/catalyst (S/C) molar ratio of 600, catalyst **III** allows conversions ranging from 88.6 to 99.9 %. Figure 3-7, which compares the activity of catalysts **I-III** after 90 min of reaction for substrates **3.1-3.9**, using a S/C molar ratio of 300, puts in evidence the greater efficiency of the iron porphyrin (**III**) in the performed sulfoxidations. In opposition to catalysts **I** and **II**, after 90 min of reaction with catalyst **III** the conversions are already higher than 90% for all cases, even for the more recalcitrant DBTs (**3.7-3.9**).

**Table 3-3** Results obtained for the oxidation of substrates **3.8** and **3.9** with H<sub>2</sub>O<sub>2</sub> catalyzed by the manganese(III) porphyrins (**I**) and (**II**)<sup>(a)</sup>

Substrates	Catalyst	H <sub>2</sub> O <sub>2</sub> (mmol)	S/C molar ratio	Conversion (%)	Products selectivity (%)		Time (min)
					S=O	SO <sub>2</sub>	
 ( <b>3.8</b> )	<b>I</b>	1.8	150	99.7	4.88	95.1	180
		1.8	300	89.3	3.95	96.0	180
	<b>II</b>	1.8	150	96.2	22.1	77.9	180
		1.8	300	72.3	19.9	80.1	180
 ( <b>3.9</b> )	<b>I</b>	1.8	150	96.6	73.4	26.6	180
		1.8	300	79.2	80.2	19.8	180
	<b>II</b>	1.8	150	94.1	64.8	35.2	180
		1.8	300	52.7	71.7	28.3	180

<sup>(a)</sup>The substrate (0.3 mmol) was dissolved in 2.0 mL of CH<sub>3</sub>CN and kept under magnetic stirring at 22-25 °C in the presence of **Mn-Porph** (for S/C molar ratio of 150, the catalyst amount was 2.0 x 10<sup>-3</sup> mmol; for S/C molar ratio of 300, the catalyst amount was 1.0 x 10<sup>-3</sup> mmol). The co-catalyst used was NH<sub>4</sub>CH<sub>3</sub>CO<sub>2</sub> (0.12 mmol). The oxidant, diluted 1:10 in CH<sub>3</sub>CN, was progressively added at regular intervals of 15 min in small aliquots, each corresponding to a half-substrate amount. The conversion and selectivity values are the result of at least two assays.

Sulfides **3.1** and **3.2** are easily oxidized by H<sub>2</sub>O<sub>2</sub> in the presence of all the porphyrin catalysts (**I-III**), probably due to the fact that the sulfur unshared electrons are not involved in the aromatic system (as for BTs and DBTs). However, the extraordinary catalytic activity of the iron complex (**III**) in the oxidation of this kind of substrates deserves to be highlighted. For example, for thioanisole (**3.1**) it was necessary to work with at S/C molar ratio of 5000 to observe a significant decrease on catalyst **III** activity (Table 3-4 and Figure 3-8).

At the S/C molar ratio of 3000 and despite the excellent conversion, still above 95 %, the corresponding sulfone is no longer the only product observed at the end of the reaction. The sulfoxide/sulfone ratio is around 5.0 for selectivity values around 83.5% for the S=O and 16.5% for the SO<sub>2</sub>.

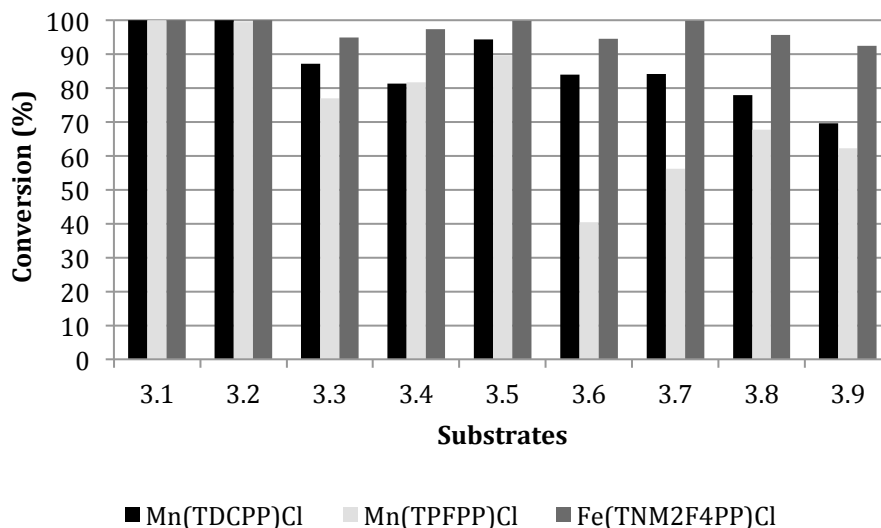


**Figure 3-7** Conversion values obtained for substrates 3.1-3.9 after 90 min of reaction in the presence of H<sub>2</sub>O<sub>2</sub>, using a S/C molar ratio of 300.

**Table 3-4** The influence of the S/C molar ratio in the oxidation of thioanisole (3.1) with H<sub>2</sub>O<sub>2</sub> catalyzed by (III)<sup>(a)</sup>

S/C molar ratio	H <sub>2</sub> O <sub>2</sub> (mmol)	Conversion (%)	Products selectivity (%)		Time (min)
			S=O	SO <sub>2</sub>	
300	0.9	99.9	-	100	90
600	0.6	99.9	-	100	60
900	1.8	98.2	-	100	180
1200	1.2	97.2	-	100	120
3000	1.2	96.6	83.5	16.5	120
5000	1.8	86.7	91.3	8.69	180
6000	1.8	62.3	83.0	17.0	180

<sup>(a)</sup>The substrate (0.3 mmol) was dissolved in 2.0 mL of ethanol and kept under magnetic stirring at 22-25 °C in the presence of the iron(III) catalyst **III**. The oxidant, diluted 1:10 in ethanol, was progressively added at regular intervals of 15 min in small aliquots, each corresponding to a half-substrate amount.

In the case of BTs (3.3-3.6), the reactivity seems to be affected not only by the presence of different substituents in the thiophene ring, but also by their position. For catalyst (III), and using a S/C molar ratio of 1200, the negative impact induced by the methyl substituent is evident in the conversion obtained (44.6%) for compound 3.4; furthermore, the sulfone is no longer obtained. Nevertheless, this is not observed when the same substituent is in a different position (at position 2), and for compound 3.5 conversions above 90% are achieved. It is interesting to note that and comparatively to the iron complex (III), for manganese catalysts (I, II) this effect is not so evident (Figure 3-7). Concerning compound 3.6, both the manganese and the



iron catalysts give rise to lower conversions if compared to the similar substituted compound **3.5**.

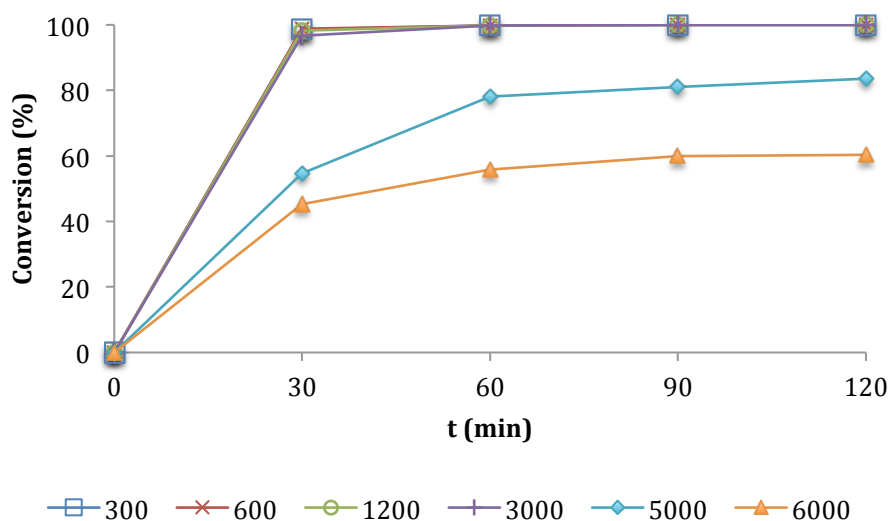


**Figure 3-8** Thioanisole (**3.1**) oxidation reaction profile in the presence of catalyst (**III**) using different S/C molar ratios.

From the experiments with the DBTs (**3.7-3.9**), it seems relevant that the alkyl monosubstitution of one of the benzene rings, for both catalytic systems, led to similar or slightly higher conversions; thus, the increased steric hindrance does not seem to affect much the oxidation results. This is not the case of the alkyl disubstituted DBT (**3.9**), for which the poorer results can be attributed to the higher steric hindrance induced by the two ethyl groups near the heteroatom. In fact, for the S/C molar ratio of 1200 the conversion reaches only 43.7 % and it is the only substrate that, in all assays, does not give the corresponding sulfone as the main product.

In summary, for the catalytic assays with substrates (**3.1-3.9**) and Fe(TNMe<sub>2</sub>F<sub>4</sub>PP)Cl (**III**), using H<sub>2</sub>O<sub>2</sub>, a more efficient and environmentally friendly approach was settled, as it uses ethanol as solvent and does not require the use of a co-catalyst. The superior performance of the iron catalyst can be understood through the different catalytic species involved in the two systems tested (iron and manganese) under the optimal reaction conditions. The structure/reactivity of the substrate has also an important role on the catalytic sulfoxidation reactions performed with the metalloporphyrin complexes. In the case of the iron catalyst **III**, and from the obtained results, the position and the type of substitution on the starting BT or DBT seems to have a



significant effect on its reactivity towards the oxidation using hydrogen peroxide.

Considering substrate **3.10**, it was necessary to modify the catalytic assays for manganese and iron complexes, due to its poor solubility either in CH<sub>3</sub>CN or ethanol at room temperature. Based on the aforementioned protocol, the initial catalytic studies were performed with catalyst **I**, and the modification of some parameters such as solvent, temperature and stirring method (magnetic or by sonication) have been tested. The results from these preliminary assays are summarized in Table 3-5, entries 1-9). All the results have been determined after three hours of reaction and after purification by preparative TLC. The best reaction conditions for catalyst (**I**) are shown in entry 8, when the temperature was set to 60 °C and CH<sub>3</sub>CN was the solvent of choice; with these conditions it was possible to achieve 90.5% of conversion into the corresponding oxidation products, sulfoxide **3.20** (40.3%) and sulfone **3.21** (24.4%). The possibility of using solvent mixtures (CH<sub>3</sub>CN/CH<sub>2</sub>Cl<sub>2</sub>, CH<sub>3</sub>CN/toluene or CH<sub>3</sub>CN/EtOAc), although presenting fair to good conversion values even at room temperature as exemplified on entry 3, are undoubtedly less attractive in terms of the development of a green and sustainable approach. In this sense, the use of CH<sub>2</sub>Cl<sub>2</sub> is not tolerable nowadays, and it has been detected here that mixtures including toluene or EtOAc give rise to the formation of side products.

The optimal approach (Table 3-5, entry 8) was extrapolated to the manganese porphyrin catalyst **II** (63.1% of conversion, Table 3-5, entry 10) and the use of heat was added to conditions previously reported for complex **III** (Table 3-5, entry 11). Results gathered for compound **3.10** when the oxidation in ethanol was performed at 60 °C put in evidence the greater efficiency of Fe(TNMe<sub>2</sub>F<sub>4</sub>PP)Cl (**III**), achieving total conversion (99.9%) and the corresponding sulfone **3.21** (60.1 %) being the major isolated product. It should be mentioned that the blank experiments for compound **3.10** give rise to conversions lower than 3%.

The structures of the sulfoxides and sulfones were confirmed by GC-MS and by <sup>1</sup>H NMR (experimental part). Because these derivatives afforded suitable single-crystals from crystallization using mixtures of CH<sub>2</sub>Cl<sub>2</sub>/hexane, the crystal structures of sulfoxides and sulfones **3.18-3.23**, not yet reported in the literature, were also fully elucidated by single-crystal X-ray diffraction studies.<sup>1</sup> The crystal structures of compounds **3.18** to **3.23** have been fully elucidated at 150 K using single-crystal X-

<sup>1</sup> The X-ray diffraction studies were performed by Dr. Filipe Paz.



ray diffraction studies (Figure 3-9).

**Table 3-5** Results obtained in the optimization of the reaction conditions for 4,6-dimethyldibenzothiophene (**3.10**) oxidation tests<sup>(a)</sup>

Entry	Catalyst	S/C Molar ratio	Solvent(s)	m (recovered fractions) (mg)			Conv. (%)
				S.M.	S=O	SO <sub>2</sub>	
1 <sup>(b)</sup>	<b>I</b>	150	CH <sub>3</sub> CN	31.2	27.8	2.7	56.0
2 <sup>(b)</sup>	<b>I</b>	150	CH <sub>3</sub> CN/CH <sub>2</sub> Cl <sub>2</sub> (2:1)	41	21.5	17.9	38.0
3 <sup>(b)</sup>	<b>I</b>	300	CH <sub>3</sub> CN/CH <sub>2</sub> Cl <sub>2</sub> (1:2)	6.6	43.5	16.7	90.0
4 <sup>(b)</sup>	<b>I</b>	300	CH <sub>3</sub> CN/Toluene (1:2)	22.1	35.8	8.3	66.4
5 <sup>(b)</sup>	<b>I</b>	300	CH <sub>3</sub> CN/ EtOAc (1:2)	20.3	18.4	24.1	68.6
6 <sup>(c)</sup>	<b>I</b>	150	CH <sub>3</sub> CN	13.9	22.2	19.5	78.9
7 <sup>(d)</sup>	<b>I</b>	150	CH <sub>3</sub> CN	10.7	17.3	18.0	83.7
8 <sup>(e)</sup>	<b>I</b>	150	CH <sub>3</sub> CN	6.3	40.3	24.4	90.5
9 <sup>(f)</sup>	<b>I</b>	150	CH <sub>3</sub> CN	7.0	14.4	2.0	89.4
10 <sup>(e)</sup>	<b>II</b>	150	CH <sub>3</sub> CN	2.8	13.7	25.2	63.1
11 <sup>(e)</sup>	<b>III</b>	150	EtOH	1.4	4.7	60.1	99.9

<sup>(a)</sup>Reaction conditions: the catalyst is added (for S/C molar ratio of 150, the catalyst amount was  $2.0 \times 10^{-3}$  mmol; for S/C molar ratio of 300, the catalyst amount was  $1.0 \times 10^{-3}$  mmol) to 0.3 mmol of **3.10** (64 mg), 0.3 mmol of internal standard (chlorobenzene), and the appropriate volume of solvent until 2.0 mL. With the experiments involving catalysts **I** and **II** it was also necessary to use a co-catalyst, NH<sub>4</sub>CH<sub>3</sub>CO<sub>2</sub> (0.12 mmol). The oxidant (diluted 1:10) was progressively added at regular intervals of 15 min in small aliquots, each corresponding to a half-substrate amount (total amount 1.8 mmol). After 3 h of reaction, with no evolution by TLC, the assays were finished and the reaction mixture purified by preparative TLC. <sup>(b)</sup>At r.t. (22-25 °C). <sup>(c)</sup>Under sonication. <sup>(d)</sup>At 40 °C. <sup>(e)</sup>At 60 °C. <sup>(f)</sup>At 80 °C. Abbreviations: S.M. (Starting Material); S=O (Sulfoxide); SO<sub>2</sub> (Sulfone).

All compounds, with the exception of compound **3.21**, crystallize in either triclinic or monoclinic centrosymmetric space groups with the latter crystallizing instead in the non-centrosymmetric orthorhombic *Pca*2<sub>1</sub> space group. The asymmetric unit of compounds **3.18** and **3.19** is composed of two crystallographically independent molecular units ( $Z' = 2$ ), which result from a combined effect of distinct structural conformations (see Figure 3-10 for maximum distances and root mean square distances for the overlay of the two molecules in each compound) and the crystal symmetry of the compound. Noteworthy, in compound **3.23** the asymmetric unit is solely composed of half of the molecule with the molecular unit depicted in Figure 3-9 being, thus, formed by a two-fold crystallographic axis. Individual molecules close pack in the solid state with the aim to effectively fill the available space (not shown). This process is also driven by the presence of a handful of supramolecular interaction, namely weak hydrogen bonding interactions (C–H···O, C–H···S and C–H··· $\pi$ ) and  $\pi$ - $\pi$  contacts.

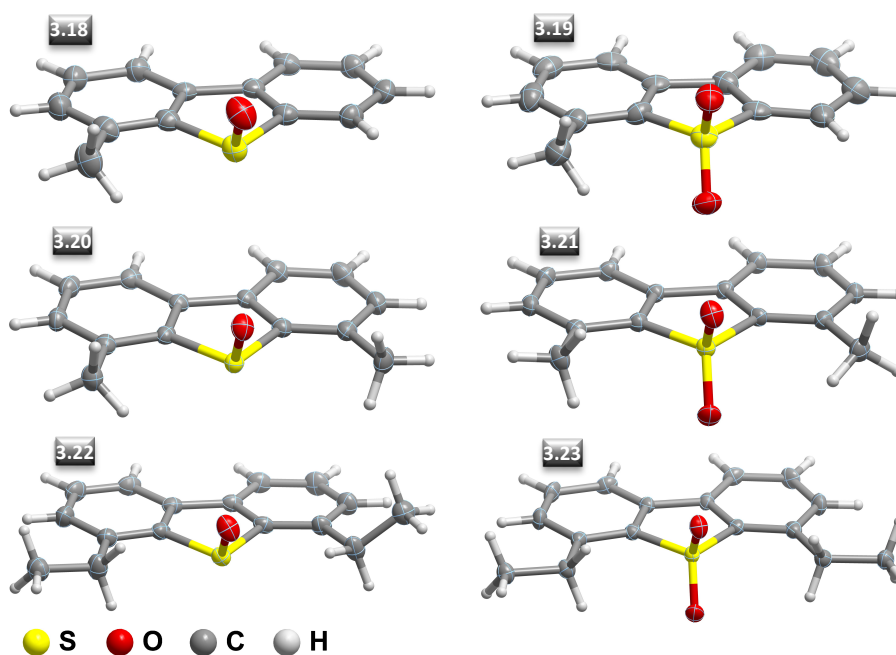
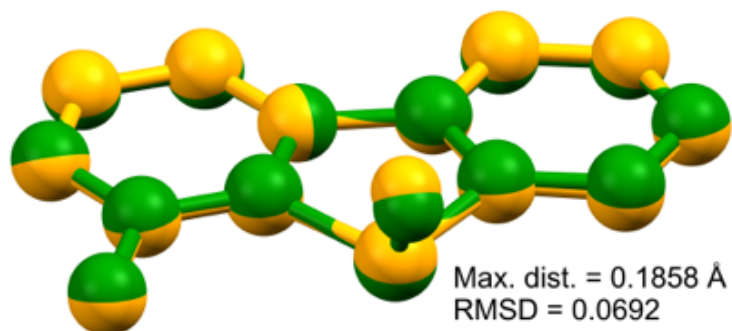


**Figure 3-9** Schematic representation of the molecular units present in the crystal structures of compounds **3.18** to **3.23**. Non-hydrogen atoms are represented as thermal ellipsoids drawn at the 50% probability level and hydrogen atoms as spheres with arbitrary radii.

**Compound 3.18**



**Compound 3.19**

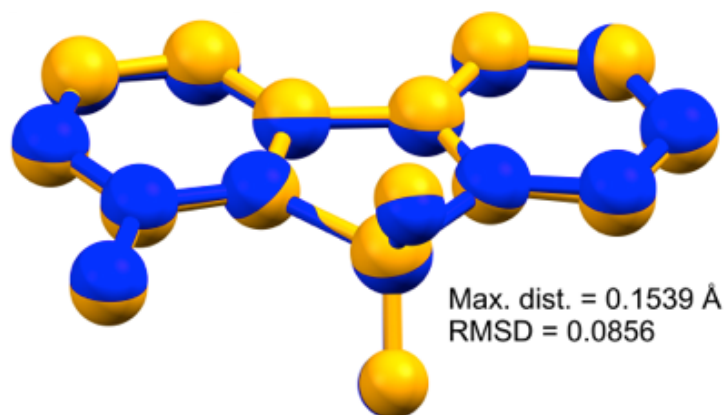


**Figure 3-10** Overlay of the two crystallographically independent molecular units composing the asymmetric unit of compounds **3.18** and **3.19** ( $Z' = 2$ ). For clarity, hydrogen atoms have been omitted and each molecule is represented in a different color. Molecular overlay performed using the software package Mercury.<sup>65</sup>



The excellent catalytic performance of **III** for the sulfoxidation of organosulfur compounds **3.1-3.10** prompted us to also evaluate its efficiency in the treatment of refractory *S*-containing compounds on an envisaged model fuel. In this study the model fuel consists of a mixture of benzothiophene (**3.3**), 3-methylbenzothiophene (**3.4**), 4-methyldibenzothiophene (**3.8**) and 4,6-diethyldibenzothiophene (**3.9**) in hexane and the evolution of the reaction was monitored by GC-FID, being the respective chromatograms at  $t_0$ ,  $t_{60}$ ,  $t_{120}$ , and  $t_{180}$  presented on Figure 3-11. After the first oxidant addition the peaks corresponding to substrates **3.3** ( $R_t = 5.92$ ), **3.4** ( $R_t = 6.76$ ), **3.8** ( $R_t = 10.05$ ) and **3.9** ( $R_t = 11.36$ ) start to reduce its intensity and the peaks matching the respective oxidation products (namely  $R_t = 8.57$ ;  $R_t = 9.42$ ;  $R_t = 11.70$ ;  $R_t = 12.72$ ;  $R_t = 12.78$ ) appear. After three hours of reaction, more than 80 % (84.4 %) of the model fuel is converted into the resulting sulfoxides/sulfones. Only the disubstituted DBT **3.9** ( $R_t = 11.36$ ) remains in solution.

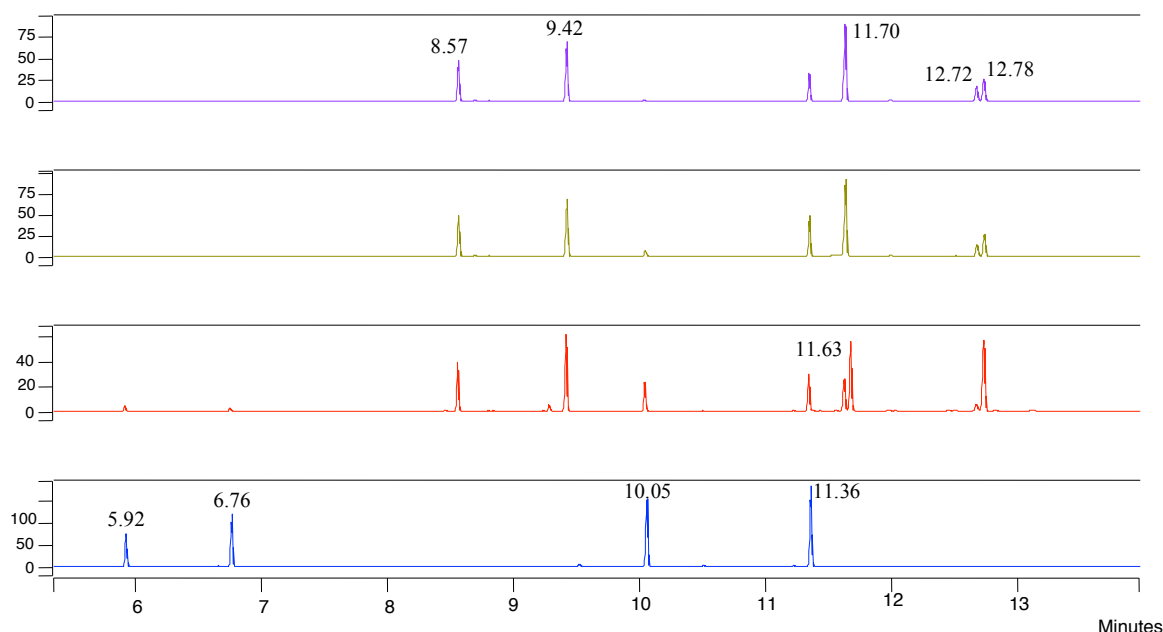


**Figure 3-11** GC-FID follow-up chromatograms of a model fuel oxidation reaction with  $H_2O_2$  in the presence of catalyst **III** for a *S/C* molar ratio of 150, at room temperature;  $t_0$  initial reaction mixture before the addition of  $H_2O_2$ ;  $t_{60}$  after 60 min of reaction;  $t_{120}$  after 120 min of reaction;  $t_{180}$  after 180 min of reaction. The model fuel is a solution of **3.3** ( $R_t = 5.92$ ), **3.4** ( $R_t = 6.76$ ), **3.8** ( $R_t = 10.05$ ), and **3.9** ( $R_t = 11.36$ ) in hexane (0.03 mmol each). The sulfones **3.13** ( $R_t = 8.57$ ), **3.14** ( $R_t = 9.42$ ), **3.19** ( $R_t = 11.70$ ), **3.23** ( $R_t = 12.72$ ) and the sulfoxide **3.22** ( $R_t = 12.78$ ) are identified in the chromatogram after 180 min of reaction.

#### 3.1.4. CONCLUSIONS

Herein we describe two promising, efficient and environmentally friendly approaches, involving metalloporphyrin catalysts and aqueous hydrogen peroxide as oxidant. This approach is able to promote the oxidation of several organosulfur compounds (**3.1-3.10**), including the so-called *S*-refractory compounds (BTs and DBTs). In general both types of catalyst gave rise to results directly dependent on the degree of complexity and substitution of the substrates, being the decreasing oxidation easiness in the following order: sulfides > BTs > DBTs.

The results from Part A, involving the catalytic experiments with Mn(III) porphyrins demonstrate that with both catalysts, [Mn(TDCPP)Cl] (**I**) and [Mn(TPFPP)Cl] (**II**), the corresponding sulfones are obtained in good to excellent yields at the end of the oxidation reactions. Nevertheless, [Mn(TDCPP)Cl] give rise to the best results, affording higher conversions in lower reaction times. In fact, the conversion of benzothiophene (**3.3**) reaches 99.9% in 90 min, whereas the conversion of dibenzothiophene (**3.7**) attains 99.9% after 120 min of reaction, both for catalyst (**I**)/substrate molar ratio of 150. The substituted benzothiophenes (**3.4-3.6**) give rise to similar results, conversions being always higher for a catalyst (**I**)/substrate molar ratio of 150 instead of 300. The best catalytic performance of **I** led to its evaluation in the oxidation of an envisaged model fuel, a solution of benzothiophene, 3-methylbenzothiophene, 2-methylbenzothiophene, and dibenzothiophene in hexane. The procedure using Mn(TDCPP)Cl, ammonium acetate as co-catalyst and CH<sub>3</sub>CN as solvent successfully affords total conversion of the model fuel into the corresponding sulfones after 3 hours of reaction.

Comparatively to the manganese(III) catalysts **I** and **II**, in Part B is possible to conclude that catalyst **III** demonstrates higher efficiency, allowing excellent conversions, faster reactions, and the use of smaller amounts of catalyst. When using a S/C molar ratio of 1200, it was possible to observe a major drop on the conversion values, mainly for substrates **3.4**, **3.6** and **3.9**; even when using a S/C molar ratio of 600, conversions remain between the 88.6% and 99.9%. Furthermore, catalyst **III** is the only one able to promote the total conversion of substrate **3.10**, mainly to the corresponding sulfone **3.21** (92.7 % selectivity). Not less important, the use of ethanol and the absence of other additives (as co-catalyst) in the catalytic assays with porphyrin **III**, as a green solvent, also meet the present policies of sustainable



chemistry promoting the development of increasingly cleaner procedures. Similarly to catalyst **I** the iron complex **III** was also successfully evaluated in the oxidation of a model fuel (in the case a mixture of substrates **3.3**, **3.4**, **3.8**, and **3.9** in hexane). After 3 h of reaction the major part of the model fuel was oxidized, remaining in solution only a small amount of substrate **3.9**.

This work clearly contributes to put in evidence the high potential of porphyrin complexes as catalysts for the sulfoxidation of the *S*-refractory benzothiophenes and dibenzothiophenes by H<sub>2</sub>O<sub>2</sub>.

### 3.2. OXIDATION OF 1,3-DIHYDROBENZO[*C*]THIOPHENES

1,3-Dihydrobenzo[*c*]thiophene 2,2-dioxides, also named sulfones, are well-known cyclic diene precursors in Diels-Alder cycloaddition reactions.<sup>67</sup> These compounds are stable intermediates for the generation of *ortho*-benzoquinodimethanes (*o*-xylylenes) or benzocyclobutenes, which can be trapped *in situ* by several dienophiles, yielding the corresponding cycloadducts.<sup>68</sup> *Ortho*-benzoquinodimethanes are particularly useful in organic synthesis as transient and highly reactive dienes, generated via chelotropic loss (thermal extrusion) of sulfur dioxide.<sup>68</sup> These compounds have a wide variety of applications, namely in the synthesis of several natural products and heterocyclic compounds.<sup>69</sup> In our group, they have been used in Diels-Alder cycloaddition reactions with several dienophiles such as porphyrin,<sup>70,71</sup> fullerene,<sup>72</sup> pyrazole,<sup>73</sup> chromone,<sup>74-76</sup> chalcone<sup>77</sup> and quinolone<sup>78</sup> derivatives. Therefore, the development of new, sustainable methods to perform the oxidation of 1,3-dihydrobenzo[*c*]thiophenes to the corresponding sulfones is of great interest.

Several methods involving different oxidation agents have already been reported to obtain sulfones from the adequate dihydrobenzo[*c*]thiophenes. However, these methods usually require the use of stoichiometric amounts of hazardous oxidants, such as *m*-chloroperbenzoic acid (*m*-CPBA) and solvents (e.g. chloroform, methylene chloride), which generate a large amount of dangerous wastes. The research and application of “Green Chemistry” principles has led to the development of other methods such as the use of hydrogen peroxide (in non-chlorinated solvents), as eco-friendly alternative oxidation systems, both environmentally and economically desirable.<sup>79,80</sup>

As discussed in the beginning of this chapter, a wide range of catalytic systems and oxidants have been reported for the oxidation of sulfides, thiophenes and benzothiophenes. However few works have been reported concerning the oxidation of 1,3-dihydrobenzo[*c*]thiophenes counterparts. The relevance of the resulting oxidized sulfones and driven by the excellent results obtained with metalloporphyrin catalyst, in the oxidation by H<sub>2</sub>O<sub>2</sub> of several sulfur derivatives, prompted us to applied the same methodology to the 1,3- dihydrobenzothiophenes.

Aiming to develop a facile and eco-friendly approach for important diene precursor sulfones, the catalytic efficiency of Mn(TDCPP)Cl (**I**) and Fe(TF<sub>4</sub>NMe<sub>2</sub>PP)Cl (**III**) was tested in the oxidation of dehydrobenzothiophenes **3.24-3.27** (Figure 3-12).

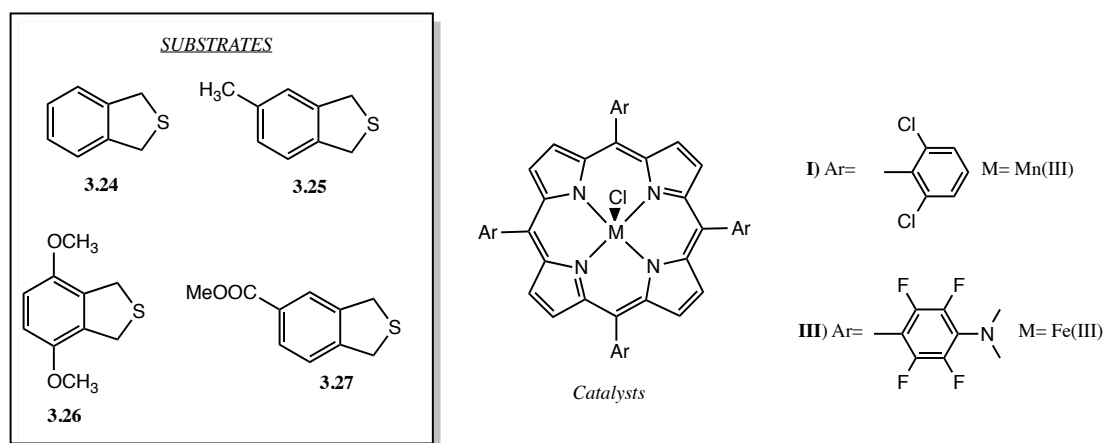


**Figure 3-12** 1,3-dihydrobenzothiophenes and porphyrins catalysts used in the catalytic experiments

### 3.2.1. *RESULTS AND DISCUSSION*

The commonly used synthetic procedure to oxidize the 1,3-dihydrobenzo[*c*]thiophenes to the corresponding 1,3-dihydrobenzo[*c*]thiophene 2,2-dioxides or sulfones requires a mixture of oxone and aluminium oxide in refluxing chloroform for 4-6 hours, which besides being time consuming is not an environmental safe strategy at all. Alternatively, in some cases, the oxidation can be performed using *m*-chloroperbenzoic acid (2.2 equiv) in dichloromethane at room temperature, which are hazardous oxidant and solvent, respectively. Encouraged by the achieved results on the oxidation of organosulfur compounds by H<sub>2</sub>O<sub>2</sub> using metalloporphyrin catalysts (Part A and B of this chapter) we decided to apply a similar approach to the oxidation of 1,3-dihydrobenzo[*c*]thiophene derivatives **3.24-**



**3.27.** The catalytic assays were performed with the most efficient metalloporphyrins in the sulfoxidation of benzo and dibenzothiophene derivatives, catalysts **I** and **III**, and the results are summarized on Table 3-6.

**Table 3-6** Results obtained in the oxidation of substrates (**3.24-3.27**) with H<sub>2</sub>O<sub>2</sub> catalyzed by the metalloporphyrins (**I** and **III**)<sup>a</sup>

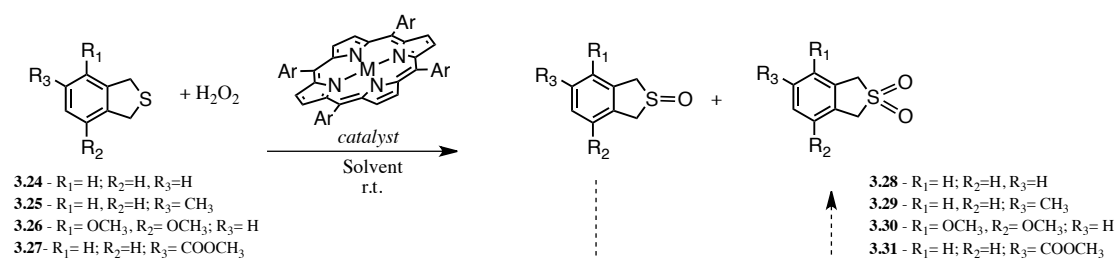
Substrate	Catalyst	S/C molar ratio	Conversion (%)	Products selectivity (%)		Time (min)
				S=O	SO <sub>2</sub>	
<b>3.24</b>	<b>I</b>	300	99.9	-	100	120
	<b>III</b>	300	99.9	0	100	90
	<b>III</b>	900	99.9	0	100	90
	<b>III</b>	1800	90.9	88.1	11.8	90
<b>3.25</b>	<b>I</b>	300	99.9	0	100	120
	<b>III</b>	300	99.9	0	100	60
<b>3.26</b>	<b>I</b>	300	99.9	18.5	81.5	90
	<b>III</b>	300	85.0	*	*	30
<b>3.27</b>	<b>I</b>	300	99.9	-	100	120
	<b>III</b>	300	99.9	-	100	90

<sup>(a)</sup>The substrate (0.3 mmol for the S/C molar ratio of 300; 0.9 mmol for the S/C molar ratio of 900; 1.8 mmol for the S/C molar ratio of 1800) was dissolved in 2.0 mL of the appropriate solvent (CH<sub>3</sub>CN for catalyst **I** and ethanol for catalyst **III**) and kept under magnetic stirring at 22-25 °C in the presence of the catalyst (**I** or **III**, 1.0 x 10<sup>-3</sup> mmol). The oxidant, diluted 1:10 in the same solvent of the reaction, was progressively added at regular intervals of 15 min in small aliquots, each corresponding to a half-substrate amount. The conversion and selectivity values are the result of at least two assays. \*The 85% of conversion after 30 min of reaction were determined by GC-MS. Under these conditions, the sulfoxide and the sulfone undergo further oxidation affording several non-identified compounds.

Both catalytic systems [catalyst **I**/H<sub>2</sub>O<sub>2</sub> and catalyst **III**/H<sub>2</sub>O<sub>2</sub>] proved to be very efficient affording excellent conversion values. In fact, for all the substrates, and using a substrate/catalyst (S/C) molar ratio of 300, it was possible to achieve conversions of 99.9 % with both catalysts tested **I** and **III**. However, the iron complex (**III**) appears to be more efficient as it allows shorter reaction times, under similar reaction conditions. At the end of the catalyzed reactions, all the substrates (**3.24-3.27**) are partially or fully converted into the corresponding dioxide products (**3.28-**



**3.31**), as represented in Scheme 3-2. In fact, this result was observed for all the assays performed with catalyst **(I)**, for which the GC-MS and  $^1\text{H}$  NMR analyses of the isolated products confirmed the structure of sulfones **3.28-3.31**. In the case of substrate **3.26**, and for the experiments involving catalyst **(III)**, the formation of sulfone **3.30** was initially detected. However, it was verified that under these conditions, the sulfone is not stable affording several non-identified compounds with lower retention time than the starting thiophene **3.26**.



Scheme 3-2

In general, when comparing the now disclosed methodology to obtain 1,3-dihydrobenzo[*c*]thiophene 2,2-dioxides (sulfones), with the already established ones, besides overcoming the principal environmental issues (chlorinated solvents are no longer required, reactions are performed at room temperature and  $\text{H}_2\text{O}_2$  is used as oxidant) this new methodology is also faster. The involvement of different catalytic active species in Mn(III) and Fe(III) macrocycles implies the use of different reaction conditions. Thus, as previously described for the catalytic experiments of sulfides (**3.1-3.2**), benzothiophenes (**3.3-3.6**) and dibenzothiophenes (**3.7-3.10**) in all the assays with catalyst **(I)** an aprotic solvent, acetonitrile, and a co-catalyst, ammonium acetate, were used, while whenever the iron catalyst **(III)** was employed the solvent needs to be a protic one, ethanol, and the reactions are performed in the absence of a co-catalyst.

Considering the above mentioned differences, the use of complex **(III)**, besides being in general more efficient, also allows the establishment of a greener procedure. Moreover, in this case the sulfone easily precipitates in the reaction medium (ethanol), as exemplified in Figure 3-13, thus contributing to a simpler and efficient purification process.

Thinking on the possibility of applying this sustainable procedure to a larger scale

conditions, additional scale-up experiments were performed in the presence of iron catalyst (**III**). Therefore, using substrate **3.24** as a model reaction, its oxidation was studied using higher quantities of substrate but maintaining the same amount of catalyst (S/C molar ratios of 900 and 1800). As can be observed in Table 3-6, the excellent efficiency, namely the selectivity for sulfone **3.28** (100%) at conversions of 99.9% is maintained for the S/C molar ratio of 900. For the S/C molar ratio of 1800, the results merit also to be highlighted, since with a conversion of 91%, the sulfoxide is now the main product (selectivity of 88%). So, depending on the S/C molar ratio, it is possible to favour efficiently the formation of the sulfone or the sulfoxide products.

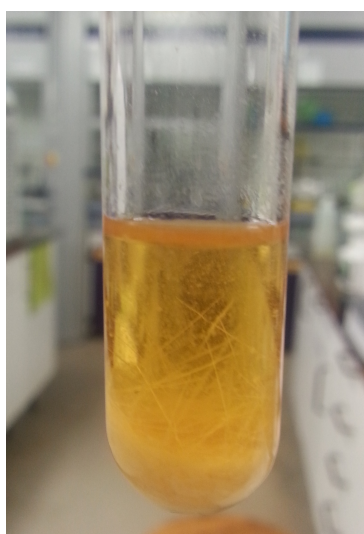


**Figure 3-13** Illustration of the sulfone precipitation at the end of reaction if performed in ethanol

### 3.2.2. CONCLUSIONS

The use of metalloporphyrin catalysts in the sulfoxidation of 1,3-dihydrobenzo[*c*]thiophenes using hydrogen peroxide, as oxidant, proved to be a highly efficient and environmentally friendly approach. For all the substrates tested excellent conversions (99.9%) were observed, generally affording the corresponding dioxide products, which were isolated and characterized.

Despite both catalysts (**I** and **III**) remain highly efficient, the iron complex (**III**) proved to be in general more active in the oxidations and allows also the use of a more sustainable synthetic procedure. The solvent used in the reactions with complex (**III**) is ethanol, no co-catalyst is necessary, and the products precipitate in the reaction medium facilitating its isolation.

### 3.3. EXPERIMENTAL

All solvents and reagents were used as received without further purification. Hydrogen peroxide (30% w/w aqueous solution) was purchased from Riedel-de-Haën and ammonium acetate was supplied by Fluka. The organosulfur compounds (**3.1-3.10**) were all purchased from Aldrich.

Relatively to the preparative TLC purification, the silica specifications and the general procedure to the plates preparation are described in section 2.4. However in the purification of colorless compounds it was required the use of silica gel 60 F<sub>254</sub> from Merck.

The GC–FID analyses were performed on a Varian 3900 chromatograph using helium as the carrier gas (30 cm/s). The GC–MS analyses were performed on a Finnigan Trace GC/MS (Thermo Quest CE instruments) using helium as the carrier gas (35 cm/s). In both cases fused silica capillary DB-5 type columns (30 m, 0.25 mm i.d., 0.25 µm film thickness) were used. The <sup>1</sup>H NMR spectra were recorded on a Bruker Avance 300 at 300.13 MHz, using CDCl<sub>3</sub> as solvent and TMS as the internal reference.

#### 3.3.1. GENERAL PROCEDURE FOR THE CATALYTIC EXPERIMENTS

All the catalytic experiments were performed following the same general procedure: the substrate (0.3 mmol), the catalyst (the amount depends on the S/C molar ratio employed) and the internal standard (0.3 mmol) were dissolved in 2.0 ml of the appropriate solvent (CH<sub>3</sub>CN for the manganese complexes **I** and **II** and ethanol for the iron complex **III**). Conversely to the experiments with catalyst **III**, where no co-catalyst is needed, with the manganese catalysts (**I** and **II**) ammonium acetate (0.12 mmol) was used as co-catalyst. The reaction mixtures were kept under magnetic stirring, in the absence of light, at 22-25°C. The oxidant [H<sub>2</sub>O<sub>2</sub> 30% (w/w) aqueous solution] was diluted (1:10) in the suitable solvent (CH<sub>3</sub>CN for **I** and **II**, ethanol for **III**) and progressively added to the reactions in aliquots corresponding to half of the substrate amount (0.5 equiv.).



### 3.3.2. GC-FID ANALYSES

The catalytic experiments with organosulfur derivatives were followed by GC-FID at intervals of 30 minutes, 1  $\mu\text{L}$  aliquots of the diluted reaction mixture being injected (1:1 in  $\text{CH}_3\text{CN}$  or ethanol). The temperature program of the chromatographic analysis was the following: column initial temperature  $70^\circ\text{C}$  for 1 min; increasing temperature rate of  $20^\circ\text{C}/\text{min}$  until the  $280^\circ\text{C}$ , where it stays for 8.5 minutes (full program with a total time of 20 min); injector temperature  $280^\circ\text{C}$ ; detector temperature  $290^\circ\text{C}$ .

The assays were stopped when, after two successive oxidant additions, no significant changes on the conversion of the substrate and on the sulfoxide/sulfone ratio were observed.

### 3.3.3. OXIDATION OF SULFIDES, BENZOTHIOPHENES AND DIBENZOTHIOPHENES

The metalloporphyrin catalyzed experiments with substrates **3.1-3.9** were performed accordingly to the already described general procedure (section 3.3.1). The manganese complexes **I**,  $\text{Mn}(\text{TDCPP})\text{Cl}$ , and **II**,  $\text{Mn}(\text{TPFPP})\text{Cl}$ , were evaluated using two S/C molar ratios 150 ( $n = 2.0 \times 10^{-3}$  mmol) and 300 ( $n = 1.0 \times 10^{-3}$  mmol) respectively. Catalyst **III** was tested for S/C molar ratios of 300, 600 ( $n = 0.5 \times 10^{-3}$  mmol) and 1200 ( $0.25 \times 10^{-3}$  mmol).

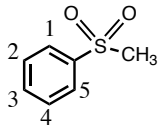
After the catalytic oxidations were finished, the reaction mixtures were directly applied in preparative TLC plates that were eluted with a  $\text{CH}_2\text{Cl}_2$ /hexane (1:2) solvent mixture. Sulfones **3.11-3.17** were isolated as the only product of the oxidation reaction of substrates **3.1-3.7**, but for substrates **3.8** (4-MDBT) and **3.9** (4,6-DEDBT), besides the sulfone products **3.19** and **3.23**, also the sulfoxide products **3.18** and **3.22** were isolated. All the isolated oxidation products were characterized by  $^1\text{H}$  NMR and the corresponding molecular weight confirmed by GC-MS.

For the 4,6-DMDBT (**3.10**), being insoluble in pure  $\text{CH}_3\text{CN}$  or ethanol at room temperature, some modifications to the aforementioned protocol were introduced. Thus, in order to increase substrate solubility, the catalytic experiments were performed with several mixtures of solvents or at higher temperature. For the optimal conditions, the established temperature was  $60^\circ\text{C}$  and the reactions were followed by TLC. After 3 h of reaction (with no evolution observed by TLC) the reactions were finished, the reaction mixtures were applied on preparative TLC plates, and 3

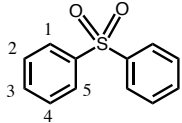
fractions were isolated using a mixture of CH<sub>2</sub>Cl<sub>2</sub>/petroleum ether (1:2) as eluent. The starting material (S.M.) and the fractions corresponding to the oxidation products, the sulfoxide (S=O) and the sulfone (SO<sub>2</sub>), were recovered, crystallized using a mixture of hexane/CH<sub>2</sub>Cl<sub>2</sub> (2:1), weighted, and characterized by <sup>1</sup>H NMR. The sulfones and the sulfoxides not yet described by single-crystal X-ray diffraction were also characterized using this technique.

### 3.3.3.1. CHARACTERIZATION OF THE COMPOUNDS

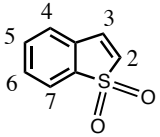
#### (methylsulfonyl)benzene dioxide (3.11)

	<sup>1</sup> H NMR (CDCl <sub>3</sub> , 300 MHz) δ (ppm): 3.06 ( <i>s</i> , 3H, CH <sub>3</sub> ), 7.56-7.61 ( <i>m</i> , 2H, H-2 and H-4), 7.86 ( <i>tt</i> , 1H, <i>J</i> = 1.6, 7.5 Hz, H-3), 7.96 ( <i>dd</i> , 2H, <i>J</i> = 1.6, 7.5 Hz, H-1 and H-5). MS (EI) m/z (rel. int., %): 156 (M <sup>+</sup> , 30), 141 (37), 94 (36), 77 (100), 65 (7), 51 (16).
---	---

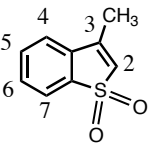
#### sulfonyldibenzene dioxide (3.12)

	<sup>1</sup> H NMR (CDCl <sub>3</sub> , 300 MHz) δ (ppm): 7.40-7.53 ( <i>m</i> , 6H, H-2, H-3, H-4), 7.88 ( <i>dd</i> , 4H, <i>J</i> = 1.5, 8.2 Hz, H-1 and H-5). MS (EI) m/z (rel. int., %): 202 (M <sup>+</sup> , 100), 185 (31), 154 (69), 125 (10), 109 (74), 97 (25), 77 (35), 65 (20), 51 (22).
---	--

#### benzo[*b*]thiophene 1,1-dioxide (3.13)

	<sup>1</sup> H NMR (CDCl <sub>3</sub> , 300 MHz) δ (ppm): 6.72 ( <i>d</i> , 1H, <i>J</i> = 6.9 Hz, H-2), 7.22 ( <i>dd</i> , 1H, <i>J</i> = 1.4, 6.9 Hz, H-3), 7.37 ( <i>dd</i> , 1H, <i>J</i> = 1.4, 7.0 Hz, H-4), 7.52 ( <i>dt</i> , 1H, <i>J</i> = 1.4, 7.0 Hz, H-6), 7.57 ( <i>dt</i> , 1H, <i>J</i> = 1.4, 7.0 Hz, H-5), 7.69-7.72 ( <i>m</i> , 1H, H-7). MS (EI) m/z (rel. int., %): 166 (M <sup>+</sup> , 65), 137 (100), 118 (13), 109 (34).
---	--

#### 3-methylbenzo[*b*]thiophene 1,1-dioxide (3.14)

	<sup>1</sup> H NMR (CDCl <sub>3</sub> , 300 MHz) δ (ppm): 2.26 ( <i>d</i> , 3H, <i>J</i> = 1.5 Hz, CH <sub>3</sub> ), 6.46 ( <i>q</i> , 1H, <i>J</i> = 1.5 Hz, H-2), 7.41 ( <i>dd</i> , 1H, <i>J</i> = 1.1, 7.3 Hz, H-4), 7.52 ( <i>dt</i> , 1H, <i>J</i> = 1.1, 7.3 Hz, H-6), 7.59 ( <i>dt</i> , 1H, <i>J</i> = 1.5, 7.3 Hz, H-5), 7.69 ( <i>dd</i> , 1H, <i>J</i> = 1.5, 7.3 Hz, H-7). MS (EI) m/z (rel. int., %): 180 (M <sup>+</sup> , 30), 151 (100), 131 (20), 91 (6), 109 (39), 77 (7).
---	---


**2-methylbenzo[*b*]thiophene 1,1-dioxide (3.15)**

	<sup>1</sup> H NMR (CDCl <sub>3</sub> , 300 MHz) δ (ppm): 2.21 ( <i>d</i> , 3H, <i>J</i> = 1.8 Hz, CH <sub>3</sub> ), 6.77-6.79 ( <i>m</i> , 1H, H-3), 7.27 (broad <i>d</i> , 1H, <i>J</i> = 7.5 Hz, H-4), 7.43 ( <i>dt</i> , 1H, <i>J</i> = 1.2, 7.5 Hz, H-5 or H-6), 7.51 ( <i>dt</i> , 1H, <i>J</i> = 1.2, 7.5 Hz, H-5 or H-6), 7.70 (broad <i>d</i> , 1H, <i>J</i> = 7.5 Hz, H-7). MS (EI) <i>m/z</i> (rel. int., %): 180 (M <sup>+</sup> , 36), 136 (100), 131 (23), 115 (29), 109 (39), 89 (9).
--	--

**2-(hydroxymethyl)benzo[*b*]thiophene 1,1-dioxide (3.16)**

	<sup>1</sup> H NMR (CDCl <sub>3</sub> , 300 MHz) δ (ppm): 2.13 ( <i>t</i> , 1H, <i>J</i> = 5.9 Hz, OH), 4.74 ( <i>dd</i> , 2H, <i>J</i> = 1.3, 5.9 Hz, CH <sub>2</sub> ), 7.07-7.09 ( <i>m</i> , 1H, H-3), 7.36 ( <i>dd</i> , 1H, <i>J</i> = 1.2, 7.4 Hz, H-4), 7.50 ( <i>dt</i> , 1H, <i>J</i> = 1.2, 7.4 Hz, H-6), 7.56 ( <i>dt</i> , 1H, <i>J</i> = 1.2, 7.4 Hz, H-5), 7.70-7.73 ( <i>m</i> , 1H, H-7). MS (EI) <i>m/z</i> (rel. int., %): 196 (M <sup>+</sup> , 10), 137 (15), 132 (51), 131 (100), 103 (23), 77 (20).
--	---

**dibenzo[*b,d*]thiophene 5,5-dioxide (3.17)**

	<sup>1</sup> H NMR (CDCl <sub>3</sub> , 300 MHz) δ (ppm): 7.59 ( <i>dt</i> , 2H, <i>J</i> = 1.1, 7.7 Hz, H-2 or H-3), 7.70 ( <i>dt</i> , 2H, <i>J</i> = 1.1, 7.7 Hz, H-2 or H-3), 7.85-7.98 ( <i>m</i> , 2H, H-1 and H-4). MS (EI) <i>m/z</i> (rel. int., %): 216 (M <sup>+</sup> , 100), 187 (31), 168 (22), 160 (16), 139 (12).
--	--

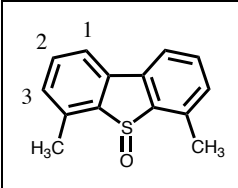
**4-methyldibenzo[*b,d*]thiophene-5-oxide (3.18)**

	<sup>1</sup> H NMR (CDCl <sub>3</sub> , 300 MHz) δ (ppm): 2.75 ( <i>s</i> , 3H, CH <sub>3</sub> ), 7.24 ( <i>d</i> , 1H, <i>J</i> = 7.7, H-3), 7.47 ( <i>t</i> , 1H, <i>J</i> = 7.7 Hz, H-2), 7.48 ( <i>dt</i> , 1H, <i>J</i> = 1.1, 7.5 Hz, H-7), 7.58 ( <i>dt</i> , 1H, <i>J</i> = 1.1, 7.5 Hz, H-8), 7.63 ( <i>d</i> , 1H, <i>J</i> = 7.5 Hz, H-6), 7.78 (broad <i>d</i> , 1H, <i>J</i> = 7.7 Hz, H-1), 7.97 ( <i>dd</i> , 1H, <i>J</i> = 1.1, 7.5 Hz, H-9). MS (EI) <i>m/z</i> (rel. int., %): 214 (M <sup>+</sup> , 70), 198 (100), 197 (84), 185 (36).
--	---

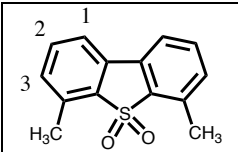
**4-methyldibenzo[*b,d*]thiophene-5,5-dioxide (3.19)**

	<sup>1</sup> H NMR (CDCl <sub>3</sub> , 300 MHz) δ (ppm): 2.72 ( <i>s</i> , 3H, CH <sub>3</sub> ), 7.27 ( <i>d</i> , 1H, <i>J</i> = 7.6, H-3), 7.50 ( <i>t</i> , 1H, <i>J</i> = 7.6 Hz, H-2), 7.52 ( <i>dt</i> , 1H, <i>J</i> = 1.2, 7.6 Hz, H-7), 7.61 ( <i>d</i> , 1H, <i>J</i> = 7.6 Hz, H-6), 7.63 ( <i>dt</i> , 1H, <i>J</i> = 1.2, 7.6 Hz, H-8), 7.78 (broad <i>d</i> , 1H, <i>J</i> = 7.6 Hz, H-1), 7.49 ( <i>dd</i> , 1H, <i>J</i> = 1.1, 7.6 Hz, H-9). MS (EI) <i>m/z</i> (rel. int., %): 230 (M <sup>+</sup> , 100), 187 (18).
--	---

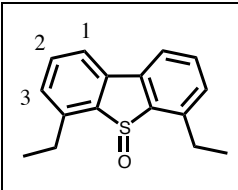
**4,6-dimethyldibenzo[b,d]thiophene-5-oxide (3.20)**

	<sup>1</sup> H NMR (CDCl <sub>3</sub> , 300 MHz) δ (ppm): 2.74 ( <i>s</i> , 6H, CH <sub>3</sub> ), 7.24 (broad <i>d</i> , 2H, <i>J</i> =7.5, H-1), 7.45 ( <i>t</i> , 2H, <i>J</i> =7.5 Hz, H-2), 7.59 ( <i>d</i> , 2H, <i>J</i> =7.5 Hz, H-3). MS (EI) <i>m/z</i> (rel. int., %): 228 (M <sup>+</sup> , 100), 212 (59), 211 (54), 197 (13), 185 (42), 184 (26).
---	--

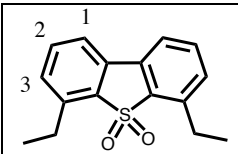
**4,6-dimethyldibenzo[b,d]thiophene-5,5-dioxide (3.21)**

	<sup>1</sup> H NMR (CDCl <sub>3</sub> , 300 MHz) δ (ppm): 2.74 ( <i>s</i> , 6H, CH <sub>3</sub> ), 7.24 (broad <i>d</i> , 1H, <i>J</i> =7.4, H-1), 7.47 ( <i>t</i> , 2H, <i>J</i> =7.4 Hz, H-2), 7.57 ( <i>d</i> , 2H, <i>J</i> =7.4 Hz, H-3). MS (EI) <i>m/z</i> (rel. int., %): 244 (M <sup>+</sup> , 100), 201 (31).
---	--

**4,6-diethyldibenzo[b,d]thiophene-5-oxide (3.22)**

	<sup>1</sup> H NMR (CDCl <sub>3</sub> , 300 MHz) δ (ppm): 1.41 ( <i>t</i> , 3H, <i>J</i> =7.6, CH <sub>3</sub> ), 3.08-3.17 ( <i>m</i> , 2H, CH <sub>2</sub> ), 7.27 (broad <i>d</i> , 1H, <i>J</i> = 7.5 Hz, H-1), 7.50 ( <i>t</i> , 1H, <i>J</i> = 7.6 Hz, H-3), 7.60 ( <i>dd</i> , 1H, <i>J</i> =1.0, 7.6 Hz, H-2). MS (EI) <i>m/z</i> (rel. int., %): 256 (M <sup>+</sup> , 100), 241 (64), 240 (53), 225 (53), 211 (38), 210 (36).
--	--

**4,6-diethyldibenzo[b,d]thiophene-5,5-dioxide (3.23)**

	<sup>1</sup> H NMR (CDCl <sub>3</sub> , 300 MHz) δ (ppm): 1.39 ( <i>t</i> , 3H, <i>J</i> =7.6, CH <sub>3</sub> ), 3.08-3.17 ( <i>q</i> , 2H, <i>J</i> = 7.6 Hz, CH <sub>2</sub> ), 7.30 (broad <i>d</i> , 1H, <i>J</i> = 7.6 Hz, H-1), 7.51 ( <i>t</i> , 1H, <i>J</i> = 7.6 Hz, H-3), 7.58 ( <i>dd</i> , 1H, <i>J</i> =1.0, 7.6 Hz, H-2). MS (EI) <i>m/z</i> (rel. int., %): 272 (M <sup>+</sup> , 100), 215 (14).
---	---

Single-crystal X-ray diffraction studies

Suitable single-crystals of compounds **3.18** to **3.23** were manually harvested directly from the crystallization vials and mounted on Hampton Research CryoLoops using FOMBLIN Y perfluoropolyether vacuum oil (LVAC 25/6) purchased from Sigma-Aldrich<sup>81</sup> with the help of a Stemi 2000 stereomicroscope equipped with Carl Zeiss lenses. Data were collected at 150(2) K on a Bruker X8 Kappa APEX II charge-coupled device (CCD) area-detector diffractometer (Mo K<sub>α</sub> graphite-monochromated radiation, λ = 0.71073 Å) controlled by the APEX2 software package,<sup>82</sup> and equipped



with an Oxford Cryosystems Series 700 cryostream monitored remotely using the software interface Cryopad.<sup>83</sup> Images were processed using the software package SAINT+,<sup>84</sup> and data were corrected for absorption by the multi-scan semi-empirical method implemented in SADABS.<sup>85</sup> Structure were solved by the direct methods of SHELXS-97,<sup>86,87</sup> and refined by full-matrix least squares on  $F^2$  using SHELXL-97.<sup>86,88</sup> All non-hydrogen atoms were directly located from difference Fourier maps and successfully refined with anisotropic displacement parameters.

Hydrogen atoms bound to carbon were placed at their idealized positions using appropriate *HFIX* instructions in SHELXL (43 for the aromatic groups, 23 for the methylene and 137 for the methyl groups) and included in subsequent least-squares refinements with an isotropic displacement parameter ( $U_{iso}$ ) fixed at 1.2 (for the aromatic and  $-CH_2-$  hydrogen atoms) or 1.5 (for the  $-CH_3$  group) of  $U_{eq}$  of the parent carbon atom.

The last difference Fourier map synthesis showed: for **3.18**, the highest peak ( $0.578 \text{ e}\text{\AA}^{-3}$ ) and deepest hole ( $-0.381 \text{ e}\text{\AA}^{-3}$ ) located at 0.94 and 0.71 Å from S2, respectively; for **3.19**, the highest peak ( $0.394 \text{ e}\text{\AA}^{-3}$ ) and deepest hole ( $-0.364 \text{ e}\text{\AA}^{-3}$ ) located at 0.82 and 0.95 Å from C14 and S1, respectively; for **3.20**, the highest peak ( $0.384 \text{ e}\text{\AA}^{-3}$ ) and deepest hole ( $-0.236 \text{ e}\text{\AA}^{-3}$ ) located at 0.81 and 0.55 Å from C14 and S1, respectively; for **3.21**, the highest peak ( $0.400 \text{ e}\text{\AA}^{-3}$ ) and deepest hole ( $-0.249 \text{ e}\text{\AA}^{-3}$ ) located at 0.70 and 1.29 Å from C8 and C14, respectively; for **3.22**, the highest peak ( $0.349 \text{ e}\text{\AA}^{-3}$ ) and deepest hole ( $-0.288 \text{ e}\text{\AA}^{-3}$ ) located at 0.69 and 0.56 Å from C12 and S1, respectively; for **3.23**, the highest peak ( $1.096 \text{ e}\text{\AA}^{-3}$ ) and deepest hole ( $-0.599 \text{ e}\text{\AA}^{-3}$ ) located at 0.90 and 1.62 Å from C7 and H3, respectively. Structural drawings have been produced using the software package Crystal Diamond.<sup>89</sup>

## Notes

‡ *Crystal data for 3.18*:  $C_{13}H_{10}OS$ ,  $M = 214.27$ , triclinic, space group  $P\bar{1}$ ,  $Z = 4$ ,  $a = 7.6012(11) \text{ \AA}$ ,  $b = 9.0726(13) \text{ \AA}$ ,  $c = 15.835(2) \text{ \AA}$ ,  $\alpha = 92.782(4)^\circ$ ,  $\beta = 90.634(4)^\circ$ ,  $\gamma = 111.267(4)^\circ$ ,  $V = 1015.9(3) \text{ \AA}^3$ ,  $\mu(\text{Mo-K}\alpha) = 0.284 \text{ mm}^{-1}$ ,  $D_c = 1.401 \text{ g cm}^{-3}$ , colourless blocks, crystal size of  $0.08 \times 0.08 \times 0.06 \text{ mm}^3$ . Of a total of 9538 reflections collected, 3713 were independent ( $R_{int} = 0.0424$ ). Final  $R1 = 0.0493$  [ $I > 2\sigma(I)$ ] and  $wR2 = 0.1192$  (all data). Data completeness to  $\theta = 25.34^\circ$ , 99.6%. CCDC 930059.



*Crystal data for 3.19:* C<sub>13</sub>H<sub>10</sub>O<sub>2</sub>S, *M* = 230.27, triclinic, space group *P* $\bar{1}$ , *Z* = 4, *a* = 7.4642(13) Å, *b* = 10.474(2) Å, *c* = 13.699(3) Å,  $\alpha$  = 92.094(12)°,  $\beta$  = 98.721(11)°,  $\gamma$  = 102.365(11)°, *V* = 1031.4(3) Å<sup>3</sup>,  $\mu(\text{Mo-K}\alpha)$  = 0.292 mm<sup>-1</sup>, *D*<sub>c</sub> = 1.483 g cm<sup>-3</sup>, colourless plates, crystal size of 0.13×0.08×0.02 mm<sup>3</sup>. Of a total of 16436 reflections collected, 3719 were independent (*R*<sub>int</sub> = 0.1718). Final *R*1 = 0.0815 [*I* > 2σ(*I*)] and *wR*2 = 0.2045 (all data). Data completeness to theta = 25.33°, 99.0%. CCDC 930060.

*Crystal data for 3.20:* C<sub>14</sub>H<sub>12</sub>OS, *M* = 228.30, monoclinic, space group *P*2<sub>1</sub>/*n*, *Z* = 4, *a* = 7.5731(3) Å, *b* = 7.6457(3) Å, *c* = 18.7201(8) Å,  $\beta$  = 91.418(2)°, *V* = 1083.59(8) Å<sup>3</sup>,  $\mu(\text{Mo-K}\alpha)$  = 0.271 mm<sup>-1</sup>, *D*<sub>c</sub> = 1.399 g cm<sup>-3</sup>, colourless blocks, crystal size of 0.12×0.09×0.07 mm<sup>3</sup>. Of a total of 16951 reflections collected, 2916 were independent (*R*<sub>int</sub> = 0.0262). Final *R*1 = 0.0334 [*I* > 2σ(*I*)] and *wR*2 = 0.0910 (all data). Data completeness to theta = 29.13°, 99.8%. CCDC 930061.

*Crystal data for 3.21:* C<sub>14</sub>H<sub>12</sub>O<sub>2</sub>S, *M* = 228.30, orthorhombic, space group *Pca*2<sub>1</sub>, *Z* = 4, *a* = 12.5035(7) Å, *b* = 7.5528(4) Å, *c* = 11.9061(6) Å, *V* = 1124.37(10) Å<sup>3</sup>,  $\mu(\text{Mo-K}\alpha)$  = 0.272 mm<sup>-1</sup>, *D*<sub>c</sub> = 1.443 g cm<sup>-3</sup>, colourless blocks, crystal size of 0.11×0.09×0.07 mm<sup>3</sup>. Of a total of 23085 reflections collected, 2995 were independent (*R*<sub>int</sub> = 0.0258). Final *R*1 = 0.0311 [*I* > 2σ(*I*)] and *wR*2 = 0.0845 (all data). Data completeness to theta = 29.13°, 99.7%. CCDC 930062.

*Crystal data for 3.22:* C<sub>16</sub>H<sub>16</sub>OS, *M* = 256.35, monoclinic, space group *P*2<sub>1</sub>/*n*, *Z* = 4, *a* = 7.8131(3) Å, *b* = 21.1480(9) Å, *c* = 8.4713(4) Å,  $\beta$  = 116.196(2)°, *V* = 1255.96(9) Å<sup>3</sup>,  $\mu(\text{Mo-K}\alpha)$  = 0.242 mm<sup>-1</sup>, *D*<sub>c</sub> = 1.356 g cm<sup>-3</sup>, colourless plates, crystal size of 0.20×0.18×0.08 mm<sup>3</sup>. Of a total of 13544 reflections collected, 3372 were independent (*R*<sub>int</sub> = 0.0326). Final *R*1 = 0.0371 [*I* > 2σ(*I*)] and *wR*2 = 0.0979 (all data). Data completeness to theta = 29.13°, 99.8%. CCDC 930063.

*Crystal data for 3.23:* C<sub>16</sub>H<sub>16</sub>O<sub>2</sub>S, *M* = 272.35, monoclinic, space group *C*2/*c*, *Z* = 4, *a* = 14.8197(18) Å, *b* = 7.6120(8) Å, *c* = 12.2153(16) Å,  $\beta$  = 110.608(8)°, *V* = 1289.8(3) Å<sup>3</sup>,  $\mu(\text{Mo-K}\alpha)$  = 0.245 mm<sup>-1</sup>, *D*<sub>c</sub> = 1.403 g cm<sup>-3</sup>, colourless blocks, crystal size of 0.12×0.12×0.07 mm<sup>3</sup>. Of a total of 4141 reflections collected, 1166 were independent (*R*<sub>int</sub> = 0.0522). Final *R*1 = 0.0674 [*I* > 2σ(*I*)] and *wR*2 = 0.2312 (all data). Data completeness to theta = 25.34°, 99.1%. CCDC 930064.



### 3.3.4. MODEL FUEL OXIDATION

For the model fuel catalytic studies, a mixture of four organosulfur derivatives (0.03 mmol each) the catalyst ( $8.0 \times 10^{-3}$  mmol in the appropriate solvent, CH<sub>3</sub>CN for catalyst **I** and ethanol for catalyst **III**) were dissolved in hexane (2.0 mL total volume). With catalyst **I** the substrates were compounds **3.3**, **3.4**, **3.5** and **3.7** and was necessary to add also a co-catalyst (ammonium acetate, 0.1 mmol). The catalytic experiments involving the iron complex (**III**) were performed with the substrates **3.3**, **3.4**, **3.8** and **3.9** and no co-catalyst was added.

The reaction mixtures were kept under magnetic stirring and in the absence of light at 22-25 °C. The oxidant (30% aqueous H<sub>2</sub>O<sub>2</sub>) diluted in the appropriate solvent (**I**-CH<sub>3</sub>CN, **III**-ethanol) (1:10) was progressively added to the reaction mixture in small aliquots, each corresponding to 0.5 equiv at every 15 min. The reaction was monitored every hour by gas chromatography and stopped when no evolution occurred after two successive analyses.

### 3.3.5. OXIDATION OF 1,3-DIHYDROBENZO[C] THIOPHENES

#### 3.3.5.1. SYNTHESIS OF THE STARTING 1,3-DIHYDROBENZO[C]THIOPHENES

The 1,3-dihydrobenzo[c]thiophenes **3.24-3.27** were obtained accordingly to well established procedures.<sup>75, 79</sup> They all have been prepared and kindly provided by Gustavo Silva.

#### 3.3.5.2. OXIDATION OF 1,3-DIHYDROBENZO[C]THIOPHENES

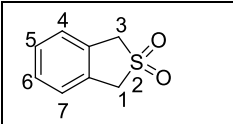
The catalytic experiments were performed accordingly to the general procedure described in section 3.3.1 and were performed with metalloporphyrins **I** and **III** which were evaluated for a S/C molar ratio of 300 ( $n = 1.0 \times 10^{-3}$  mmol).

The oxidation reactions were followed by GC-FID using the same oven temperature program described in section 3.3.2.

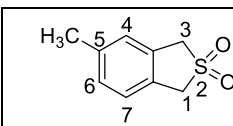
All the sulfone products (**3.28-3.31**) were isolated using preparative TLC plates, being the solvent used in the chromatographic purification a mixture of CH<sub>2</sub>Cl<sub>2</sub>/petroleum

ether (2:1). The isolated products were analyzed by  $^1\text{H}$  NMR and injected in the GC-MS to confirm the structure.

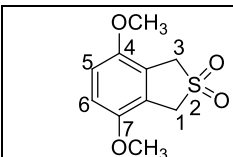
*1,3-dihydrobenzo[*c*]thiophene 2,2-dioxide (3.28)*

	$^1\text{H}$ NMR ( $\text{CDCl}_3$ , 300 MHz) $\delta$ (ppm): 4.38 ( <i>s</i> , 4H, H-1,3), 7.27-7.39 ( <i>m</i> , 4H, H-4,5,6,7) MS (EI) <i>m/z</i> : 168 $[\text{M}]^+$
---	--

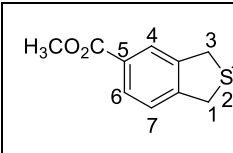
*5-methyl-1,3-dihydrobenzo[*c*]thiophene 2,2-dioxide (3.29)*

	$^1\text{H}$ NMR ( $\text{CDCl}_3$ , 300 MHz) $\delta$ (ppm): 2.39 ( <i>s</i> , 3 H, 5- $\text{CH}_3$ ), 4.35 ( <i>s</i> , 4H, 2 x $\text{CH}_2$ ), 7.14-7.28 ( <i>m</i> , 3H, H-4,6,7). MS (EI) <i>m/z</i> (rel. int., %): 182 $[\text{M}]^+$
---	---

*4,7-dimethoxy-1,3-dihydrobenzo[*c*]thiophene 2,2-dioxide (3.30)*

	$^1\text{H}$ NMR ( $\text{CDCl}_3$ , 300 MHz) $\delta$ (ppm): 3.81 ( <i>s</i> , 6H, $\text{OCH}_3$ ), 4.31 ( <i>s</i> , 4H, H-1,3), 6.80 ( <i>s</i> , 2H, H-5,6) MS (EI) <i>m/z</i> (rel. int., %): 228 $[\text{M}]^+$
---	---

*methyl 1,3-dihydrobenzo[*c*]thiophene-5-carboxylate 2,2-dioxide (3.31)*

	$^1\text{H}$ NMR ( $\text{CDCl}_3$ , 300 MHz) $\delta$ (ppm): 3.94 ( <i>s</i> , 3H, $\text{CH}_3$ ), 4.42 ( <i>s</i> , 4H, H-1,3), 7.41 ( <i>d</i> , $J=7.5$ Hz, 1H, H-7.), 8.01 ( <i>s</i> , 1H, H-4), 8.05 ( <i>d</i> , $J=7.5$ Hz, 1H, H-6) MS (EI) <i>m/z</i> (rel. int., %): 226 $[\text{M}]^+$
---	---



### 3.1. BIBLIOGRAPHY

- <sup>1</sup> X. Ma, A. Zhou, C. Song, *Catal. Today* 123 (2007) 276 and references cited therein.
- <sup>2</sup> F. Al-Shahrani, T. Xiao, S.A. Llewellyn, S. Barri, Z. Jiang, H. Shi, G. Martinie, M.L.H. Green, *Appl. Catal. B: Environ.* 73 (2007) 311 and references cited therein.
- <sup>3</sup> J.M. Campos-Martin, M.C. Capel-Sanchez, P. Peres-Presas, J.L.G. Fierro, *J. Chem. Technol. Biotechnol.* 85 (2010) 879 and references cited therein.
- <sup>4</sup> B. Pawelec, R.M. Navarro, J.M. Campos-Martin, J.L.G. Fierro, *Catal. Sci. Technol.* 1 (2011) 23 and references cited therein.
- <sup>5</sup> R. Gatan, P. Barger, V. Gembicki, *Prepr. Pap.-Am. Chem. Soc., Div. Fuel Chem.* 49 (2004) 577.
- <sup>6</sup> M. Soleimani, A. Bassi, A. Margaritis, *Biotechnol. Adv.* 25 (2007) 570.
- <sup>7</sup> R.T. Bachmann, A.C. Johnson, R.G.J. Edyvean, *Int. Biodeter. Biodegr.* 86 (2014) 225.
- <sup>8</sup> J. Zongxuan, L. Hongying, Z. Yongna, L. Can, *Chin. J. Catal.* 32 (2011) 707.
- <sup>9</sup> Y. Wang, G. Li, X. Wang, C. Jin, *Energy Fuels* 21 (2007) 1415.
- <sup>10</sup> L.F. Ramirez-Verduzco, E. Torres-Garcia, R. Gomez-Quintana, V. Gonzalez-Peña, F. Murrieta-Guevara, *Catal. Today* 98 (2004) 289.
- <sup>11</sup> S. Murata, K. Murata, K. Kidena, M. Nomura, *Energy Fuels* 18 (2004) 116.
- <sup>12</sup> A.K. Sharipov, V.R. Nigmatullin, *Chem. Technol. Fuels Oils* 41 (2005) 225.
- <sup>13</sup> G.X. Yu, S.X. Lu, H. Chen, Z. Zhu, *Energy Fuels* 19 (2005) 447.
- <sup>14</sup> D. Zhao, Y. Wang, E. Duan, *Molecules* 14 (2009) 4351 and references cited therein.
- <sup>15</sup> R. Villar, I. Encio, M. Migliaccio, M.J. Gil, V. Martinez-Merino, *Bioorg. Med. Chem.* 12 (2004) 963.
- <sup>16</sup> R. Bentley, *Chem. Soc. Rev.* 34 (2005) 609 and references cited therein.
- <sup>17</sup> K. Kamata, T. Hirano, R. Ishimoto, N. Mizuno, *Dalton Trans.* 39 (2010) 5509 and references cited therein.
- <sup>18</sup> K. Ryu, J. Kim, J. Heo, Y. Chae, *Biotech. Lett.* 24 (2002) 1535.
- <sup>19</sup> L.C. Caero, E. Hernandez, F. Pedraza, F. Murrieta, *Catal. Today* 107 (2005) 564 and references cited therein.
- <sup>20</sup> Y. Shiraishi, T. Naito, T. Hirai, *Ind. Eng. Chem. Res.* 42 (2003) 6034.
- <sup>21</sup> S Cheng., Y. Liu, J. Gao, L. Wang, X. Liu, G. Gao, P Wu., M. He, *Chin. J. Catal.* 27 (2006) 547.
- <sup>22</sup> F. Figueras, J. Palomeque, S. Loridant, C. Feche, N. Essayem, G. Gelbard, *J. Catal.* 226 (2004) 25.
- <sup>23</sup> W. Zhu, H. Li, X. Jiang, Y. Yan, J. Lu, L. He, J. Xia, *Green Chem.* 10 (2008) 641.

- <sup>24</sup> A. Di Giuseppe, M. Crucianelli, F. De Angelis, C. Crestini, R. Saladino, *Appl. Catal. B: Environ.* 89 (2009) 239.
- <sup>25</sup> H.G. Bernal, L.C. Caero, E. Finocchio, G. Busca, *Catal. Commun.* 10 (2009) 1629.
- <sup>26</sup> A.M. Cojocariu, P.H. Mutin, E. Dumitriu, A. Aboulaich, A. Vioux, F. Fajula, V. Hulea, *Catal. Today* 157 (2010) 270.
- <sup>27</sup> K. Bahrami, M.M. Khodaei, P. Fattahpour, *Catal. Sci. Technol.* 1 (2011) 389.
- <sup>28</sup> Y. Hu, Q. He, Z. Zhang, N. Ding, B. Hu, *Chem. Commun.* 47 (2011) 12194.
- <sup>29</sup> Y. Jia, G. Li, G. Ning, *Fuel Processing Technol.* 92 (2011) 106.
- <sup>30</sup> A.V. Tarakanova, M.K. Baishev, E.V. Rakhmanov, S.V. Kardashev, A.V. Anisimov, *Theor. Found. Chem. Eng.* 44 (2010) 540.
- <sup>31</sup> J.M. Campos-Martin, M.C. Capel-Sanchez, J.L.G. Fierro, *Green Chem.* 6 (2004) 557.
- <sup>32</sup> A.K. Vardhaman, S. Sikdar, C.V. Sastri, *Indian J. Chem.* 50A (2011) 427.
- <sup>33</sup> S. Otsuki, T. Nonaka, N. Takashima, W.H. Qian, A. Ishihara, T. Imai, T. Kabe, *Energy Fuels* 14 (2000) 1232.
- <sup>34</sup> Y. Shiraishi, K. Tachibana, T. Hirai, I. Komasa, *Ind. Eng. Chem. Res.* 41 (2002) 4362.
- <sup>35</sup> J. Nehlsen, J. Benziger, I. Kevrekidis, *Ind. Eng. Chem. Res.* 45 (2006) 518.
- <sup>36</sup> K. Yazu, Y. Yamamoto, T. Furuya, K. Miki, K. Ukegawa, *Energy Fuels* 15 (2001) 1535.
- <sup>37</sup> D. Huang, Y. Lu, Y. Wang, G. Luo, *Ind. Eng. Chem. Res.* 46 (2007) 6221.
- <sup>38</sup> Y. Zhang, H. Lu, L. Wang, Y. Zhang, P. Liu, H. Han, Z. Jiang, C. Li, *J. Mol. Cat. A: Chem.* 332 (2010) 59.
- <sup>39</sup> H. Lu, Y. Zhang, Z. Jiang, C. Li, *Green Chem.* 12 (2010) 1954.
- <sup>40</sup> W. Huang, W. Zhu, H. Li, H. Shi, G. Zhu, H. Liu, G. Chen, *Ind. Eng. Chem. Res.* 49 (2010) 8998.
- <sup>41</sup> X.T. Zhou, H.B. Ji, Z. Cheng, J.C. Xu, L.X. Pei, L.F. Wang, *Bioorg. Med. Chem. Lett.* 17 (2007) 4650, and references cited therein.
- <sup>42</sup> X.T. Zhou, H.B. Ji, Q.L. Yuan, J.C. Xu, L.X. Pei, L.F. Wang, *Chin. J. Chem.* 26 (2008) 1114.
- <sup>43</sup> R. Rahimi, A.A. Tehrani, M.A. Fard, B.M.M. Sadegh, H.R. Khavasi, *Catal. Commun.* 11 (2009) 232.
- <sup>44</sup> X. Zhou, S. Lv, H. Wang, X. Wang, J. Liu, *Appl. Catal. A: Gen.* 396 (2011) 101.
- <sup>45</sup> S. Rayati, S. Zakavi, H. Kalantari, *J. Porphyr. Phtalocya.* 15 (2011) 131, and references cited therein.
- <sup>46</sup> A. Rezaeifard, M. Jafarpour, H. Raissi, E. Ghiamati, A. Tootoonchi, *Polyhedron* 30 (2011) 592.
- <sup>47</sup> S. Zakavi, A. Abasi, A.R. Pourali, S. Talebzadeh, *Bull. Korean Chem. Soc.* 33 (2012) 35.



- <sup>48</sup> X. Zhou, J. Li, X. Wang, K. Jin, W. Ma, *Fuel Process. Technol.* 90 (2009) 317.
- <sup>49</sup> I. Nigel-Etinger, A. Mahammed, Z. Gross, *Catal. Sci. Technol.* 1 (2011) 578.
- <sup>50</sup> R.R.L. Martins, M.G.P.M.S. Neves, A.J.D. Silvestre, M.M.Q. Simões, A.M.S. Silva, A.C. Tomé, J.A.S. Cavaleiro, P. Tagliatesta, C. Crestini, *J. Mol. Catal. A: Chem.* 172 (2001) 33.
- <sup>51</sup> S.L.H. Rebelo, M.M.Q. Simões, M.G.P.M.S. Neves, J.A.S. Cavaleiro, *J. Mol. Catal. A: Chem.* 201 (2003) 9.
- <sup>52</sup> S.L.H. Rebelo, M.M.Q. Simões, M.G.P.M.S. Neves, A.M.S. Silva, J.A.S. Cavaleiro, *Chem. Commun.* (2004) 608.
- <sup>53</sup> S.L.H. Rebelo, M.M.Q. Simões, M.G.P.M.S. Neves, A.M.S. Silva, J.A.S. Cavaleiro, A.F. Peixoto, M.M. Pereira, M.R. Silva, J.A. Paixão, A.M. Beja, *Eur. J. Org. Chem.* (2004) 4778.
- <sup>54</sup> S.L.H. Rebelo, M.M.Q. Simões, M.G.P.M.S. Neves, A.M.S. Silva, P. Tagliatesta, J.A.S. Cavaleiro, *J. Mol. Catal. A: Chem.* 232 (2005) 135.
- <sup>55</sup> S.L.H. Rebelo, M.M. Pereira, M.M.Q. Simões, M.G.P.M.S. Neves, J.A.S. Cavaleiro, *J. Catal.* 234 (2005) 76.
- <sup>56</sup> S.L.H. Rebelo, A.R. Gonçalves, M.M. Pereira, M.M.Q. Simões, M.G.P.M.S. Neves, J.A.S. Cavaleiro, *J. Mol. Catal. A: Chem.* 256 (2006) 321.
- <sup>57</sup> R. De Paula, M.M.Q. Simões, M.G.P.M.S. Neves, J.A.S. Cavaleiro, *Catal. Commun.* 10 (2008) 57.
- <sup>58</sup> C.M.B. Neves, M.M.Q. Simões, I.C.M.S. Santos, F.M.J. Domingues, M.G.P.M.S. Neves, F.A.A. Paz, A.M.S. Silva, J.A.S. Cavaleiro, *Tetrahedron Lett.* 52 (2011) 2898.
- <sup>59</sup> R. De Paula, M.M.Q. Simões, M.G.P.M.S. Neves, J.A.S. Cavaleiro, *J. Mol. Catal. A: Chem.* 345 (2011) 1.
- <sup>60</sup> S.M.G. Pires, R. De Paula, M.M.Q. Simões, A.M.S. Silva, M.R.M. Domingues, I.C.M.S. Santos, M.D. Vargas, V.F. Ferreira., M.G.P.M.S. Neves, J.A.S. Cavaleiro, *RSC Adv.* 1 (2011) 1195.
- <sup>61</sup> S.M.G. Pires, M.M.Q. Simões, I.C.M.S. Santos, S.L.H. Rebelo, M.M. Pereira, M.G.P.M.S. Neves, J.A.S. Cavaleiro, *Appl. Catal. A: Gen.* 439-440 (2012) 51.
- <sup>62</sup> S.M.G. Pires, M.M.Q. Simões, I.C.M.S. Santos, S.L.H. Rebelo, F.A.A. Paz, M.G.P.M.S. Neves, J.A.S. Cavaleiro, *Appl. Catal. B: Environ.* 160-161 (2014) 80
- <sup>63</sup> N.A. Stephenson, A.T. Bell, *J. Mol. Catal. A: Chem.* 275 (2007) 54.
- <sup>64</sup> A. Thellend, P. Battioni, D. Mansuy, *J. Chem. Soc., Chem. Commun.* (1994) 1035.
- <sup>65</sup> I.J. Bruno, J.C. Cole, P.R. Edgington, M. Kessler, C.F. Macrae, P. McCabe, J. Pearson, R. Taylor, *Acta Cryst. B.* 58 (2002) 389.
- <sup>66</sup> R.A. Sheldon, *Chem. Soc. Rev.* 41 (2012) 1437.

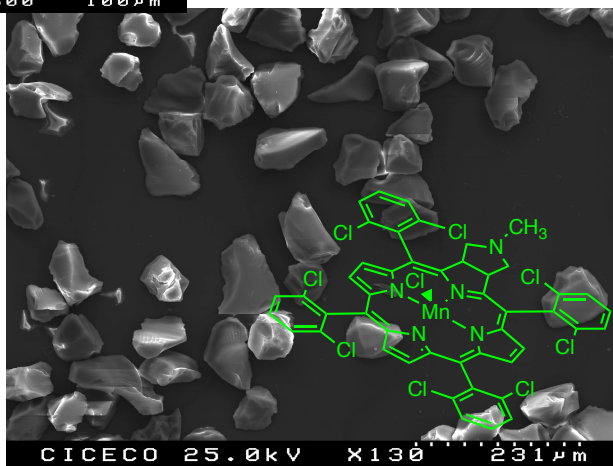
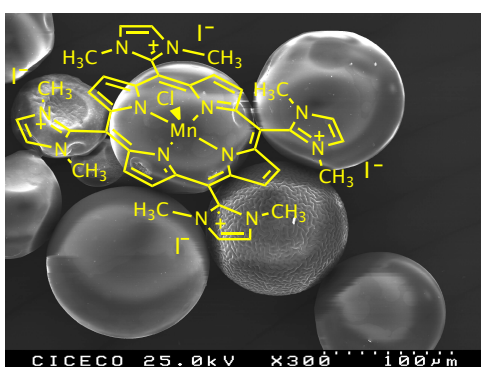
- <sup>67</sup> T. Thiemann, D. J. Walton, A. O. Brett, J. Iniesta, F. Marken, Y.-Q. Lia *Arkivoc* 9 (2009) 96.
- <sup>68</sup> J. L. Segura, N. Martin, *Chem. Rev.* 99 (1999) 3199.
- <sup>69</sup> D.C. Dittmer, A.M.S. Silva, A.C. Tomé, 1,3-Dihydrobenzo[*c*]thiophene 2,2-Dioxide. In: e-ROS Encyclopedia of Reagents for Organic Synthesis. John Wiley & Sons (2008)
- <sup>70</sup> A.C. Tomé, P.S.S. Lacerda, M.G.P.M.S. Neves, J.A.S. Cavaleiro, *Chem. Commun.* (1997) 1199.
- <sup>71</sup> A.C. Tomé, P.S.S. Lacerda, A.M.G. Silva, M.G.P.M.S. Neves, J.A.S. Cavaleiro, *J. Porphyr. Phthalocya.* 4 (2000) 532.
- <sup>72</sup> A.C. Tomé, R.F. Enes, J.P.C. Tomé, J. Rocha, M.G.P.M.S. Neves, J.A.S. Cavaleiro, J. Elguero, *Tetrahedron* 54 (1998) 11141.
- <sup>73</sup> V.L.M. Silva, A.M.S. Silva, D.C.G.A. Pinto, J.A.S. Cavaleiro, J. Elguero, *Eur. J. Org. Chem.* (2004) 4348.
- <sup>74</sup> A. Sandulache, A.M.S. Silva, J.A.S. Cavaleiro, *Tetrahedron* 58 (2002) 105.
- <sup>75</sup> A. Sandulache, A.M.S. Silva, J.A.S. Cavaleiro, *Monatsh. Chem.* 134 (2003) 551.
- <sup>76</sup> D. T. Patoilo, A.M.S. Silva, D.C.G.A. Pinto, A.C. Tomé, J.A.S. Cavaleiro, *J. Het. Chem.* 44 (2007) 1345.
- <sup>77</sup> C.M. Brito, D.C.G.A. Pinto, A.M.S. Silva, A.M.G. Silva, A.C. Tomé, J.A.S. Cavaleiro, *Eur. J. Org. Chem.* (2006) 2558.
- <sup>78</sup> R.S.G. Seixas, A.M.S. Silva, D.C.G.A. Pinto, J.A.S. Cavaleiro, *Synlett* 20 (2008) 3193.
- <sup>79</sup> M.P. Cava, A.A. Deana, *J. Am. Chem. Soc.* 81 (1959) 4266.
- <sup>80</sup> J.A. Oliver, P.A. Ongley, *Chem. Ind. (London)* (1965) 1024.
- <sup>81</sup> T. Kottke, D. Stalke, *J. App. Cryst.* 26 (1993) 615.
- <sup>82</sup> APEX2, Data Collection Software Version 2.1-RC13, Bruker AXS, Delft, The Netherlands (2006).
- <sup>83</sup> Cryopad, Remote monitoring and control, Version 1.451, Oxford Cryosystems, Oxford, United Kingdom (2006).
- <sup>84</sup> SAINT+, Data Integration Engine v. 7.23a © (1997-2005) Bruker AXS, Madison, Wisconsin, USA.
- <sup>85</sup> G.M. Sheldrick, SADABS v.2.01, Bruker/Siemens Area Detector Absorption Correction Program (1998) Bruker AXS, Madison, Wisconsin, USA.
- <sup>86</sup> G.M. Sheldrick, *Acta Cryst. A.* 64 (2008) 112.
- <sup>87</sup> G.M. Sheldrick, SHELXS-97, Program for Crystal Structure Solution, University of Göttingen (1997).



<sup>88</sup> G.M. Sheldrick, SHELXL-97, Program for Crystal Structure Refinement, University of Göttingen (1997).

<sup>89</sup> K. Brandenburg, DIAMOND, Version 3.2f. Crystal Impact GbR, Bonn, Germany (1997-2010).





## Chapter 4 HETEROGENEOUS METALLOPORPHYRIN BASED CATALYTIC SYSTEMS FOR OXIDATION OF SULFUR DERIVATIVES



## 4. HETEROGENEOUS METALLOPORPHYRIN BASED CATALYTIC SYSTEMS FOR THE OXIDATION OF ORGANOSULFUR COMPOUNDS

### 4.1. OVERVIEW

The promising results achieved with metalloporphyrin-based catalytic systems in the oxidation of several organosulfur derivatives, by hydrogen peroxide presented in previous chapter,<sup>1</sup> associated with the relevance of the research topic led us to extend it to heterogeneous conditions. As far as we know, with the exception of the work of G. Simonneaux involving a chiral metalloporphyrin,<sup>2</sup> all the porphyrin complexes used as catalysts in the oxidation of organosulfur compounds, under homogeneous<sup>1, 3, 4</sup> or heterogeneous<sup>5, 6</sup> conditions are based on symmetric *meso*-aryl derivatives. It has already been described by our group that the cationic imidazolium-based manganese porphyrin, [Mn(TDMImp)Cl]<sub>4</sub> (**V**) can be efficiently used as catalyst in olefinsepoxydation under environmentally friendly conditions.<sup>7, 8</sup> In fact the use of a cationic catalyst in this system, due to the decrease of electron density turns it more resistant to the oxidative degradation. In the particular case of **V**, the presence of the methyl substituents exhibit a steric protective effect to the macrocycle core, additionally contributing to the increasing resistance of the catalyst.<sup>7, 8</sup>

As previously mentioned, the applicability of metalloporphyrin-based biomimetic models to industrial processes is not straightforward. Besides the economic impact due to the low yields on the obtention of the starting free-bases, the arduous and many times mandatory purification steps are undoubtedly important constraints.<sup>9-10</sup> Trying to overcome this particular disadvantage, the development of the so-called heterogenized metalloporphyrin catalysts is an important issue. These hybrid materials combine the catalytic versatility of the organic moiety and the rigidity given by the support.<sup>6, 11-14</sup> Some recent examples found in literature put in evidence the great diversity of approaches using different porphyrin templates and/or supports, with the objective of developing catalyst with efficiencies and selectivities resembling those of the natural enzymes.<sup>15-18</sup>

Actually the use of the imidazole moiety can be advantageous in order to disclose an efficient immobilization methodology. Recently, the Aveiro research group has

disclosed an efficient heterogenization approach based on the covalent linkage between [Mn(TMImP)Cl] (**IV**) and Merrifield's resin support. The resulting material **IV-MR** (Figure 4-1) behaves as an efficient and reusable catalyst for alkenes' epoxidation by hydrogen peroxide.<sup>19, 20</sup>

So, in this chapter, the efficiency of the imidazole cationic catalytic system (**V**)/H<sub>2</sub>O<sub>2</sub> in the oxidation of organosulfur compounds, under homogeneous conditions will be presented and discussed first. Moreover, these results and the already proved catalytic efficiency of the immobilized [Mn(TMImP)Cl] (**IV**) in alkenes' epoxidation, prompted us to study the behavior of **IV-MR** in sulfoxidation reactions by H<sub>2</sub>O<sub>2</sub>.

Using a similar methodology, the synthesis of a new material resulting from immobilization of Fe(TF<sub>4</sub>NMe<sub>2</sub>PP)Cl (**III**) on a Merrifield's resin support was also accomplished (Figure 4-1). The results achieved with this heterogeneous material, identified as **III-MR**, in the sulfoxidation of organosulfur compounds will be also examined in this chapter.

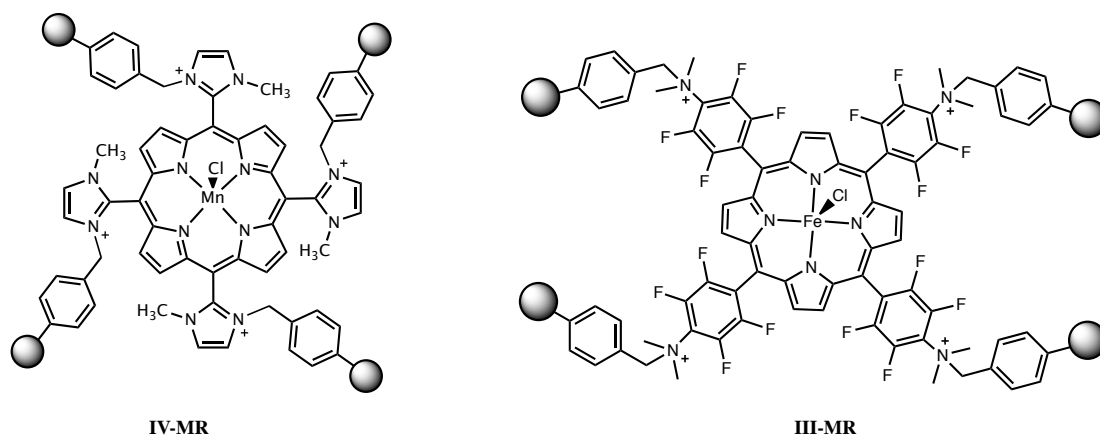
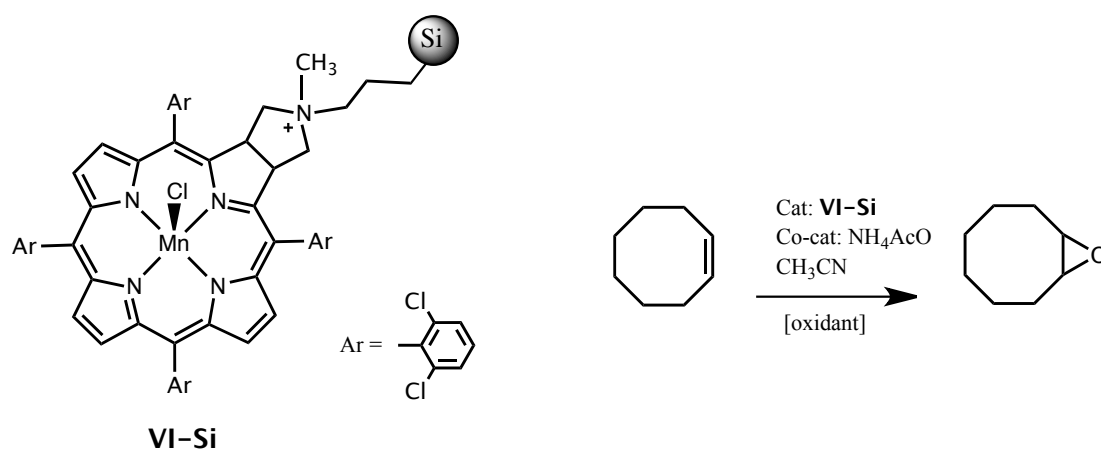


**Figure 4-1** Heterogeneous metalloporphyrin catalysts tested in sulfoxidation transformations by H<sub>2</sub>O<sub>2</sub>

Additionally, considering the good performance and recyclability demonstrated by the chlorin-based material **VI321-Si** (Scheme 4-1) in cyclooctene epoxidation led us to evaluate its efficiency in sulfoxidation transformations.<sup>21</sup> This material was developed by our group following our interest in the development of different approaches to immobilize porphyrins and analogues for catalytic studies.<sup>18, 22</sup> The chlorin-based material **VI-Si** was conveniently prepared by immobilization of a pyrrolidine functionalized manganese chlorin onto 3-bromopropylsilica, *via* a nucleophilic

substitution reaction as was mentioned in chapter 1. So, the results obtained with this material will also be presented and discussed below.



Scheme 4-1

## 4.2. CATALYTIC EXPERIMENTS WITH IMIDAZOLIUM PORPHYRIN DERIVATIVES

### 4.2.1. ASSAYS UNDER HOMOGENEOUS CONDITIONS

Our research group has previously described the low efficiency of the neutral manganese(III) complex **IV** under homogeneous conditions.<sup>23</sup> On the other hand, in 2008 De Paula *et al.* reported that it can be dramatically improved by cationization; in fact cationic derivative **V** exhibit a very high catalytic efficiency in the epoxidation of several olefins by hydrogen peroxide.<sup>7</sup>

Thus, we decided to evaluate, for the first time, the catalytic activity of this tetra-cationic derivative (**V**) in the sulfoxidation of several sulfides (**4.1** and **4.2**), BTs (**4.3-4.6**) and DBTs (**4.7-4.9**). Accordingly to the previously described experiments, all the catalytic assays involving the cationic metalloporphyrin **V** were carried out in acetonitrile and diluted H<sub>2</sub>O<sub>2</sub> was progressively added to the reaction (0.5 equiv. each addition). As described by De Paula *et al.* the catalytic behavior of this metalloporphyrin seems to be strongly dependent on the co-catalyst used; so the co-catalyst of choice was always acetic acid for catalyst **V** as demonstrated earlier.<sup>7</sup>

The results achieved in the sulfoxidation of the organosulfur derivatives **4.1-4.9**, under homogeneous conditions, are summarized in Table 4-1. All substrates reach



good to excellent conversions, ranging from 87.0 to 99.9%, using a S/C molar ratio of 150.

Even when a higher S/C molar ratio was tested (S/C molar ratio=300), with the exception of substrate **4.5**, the conversions were still high, between 80.1-99.9%.

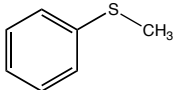
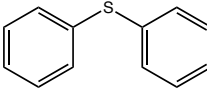
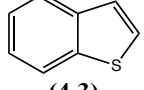
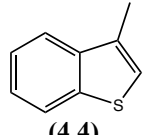
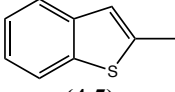
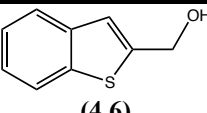
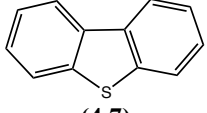
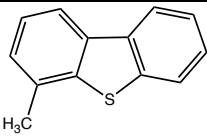
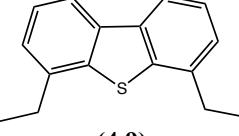
As observed with other metalloporphyrin-based catalytic systems, the easiest substrates to oxidize under the conditions tested are sulfides **4.1** and **4.2**. For the benzothiophene derivatives, catalyst **V** clearly evidences the negative impact induced by the presence of the methyl substituent at position 2 of the thiophene ring (**4.5**). The conversion value of substrate **4.5**, using a S/C molar ratio of 300 only reaches 57.9 %, while for **4.3**, **4.4** and **4.6** remains always higher than 87.0%.

The analysis of the results achieved for the most recalcitrant dibenzothiophenes allows to conclude that when alkyl substituents are present at positions 4 and 6 (**4.8** and **4.9**) the reactions require longer reaction time comparatively with non-substituted derivative **4.7**. We must emphasize here the excellent result for the unsubstituted DBT (**4.7**), with this cationic system using a S/C molar ratio of 300 giving full conversion into the corresponding sulfone after 90 minutes of reaction. Despite all the replicas performed with this particular experiment, better conversions were always achieved when a smaller amount of catalyst was used.

It is worth to mention that, concerning the absorption spectral modifications during the reactions with catalyst **V**, different behavior was registered comparatively to the *meso*-aryl manganese(III) porphyrins. Typically, for the aryl substituted Mn(III) complexes, as exemplified in Figure 4-2 for the sulfoxidation reactions in the presence of catalyst **II**, a hypsochromic shift of the Soret band is observed with oxidant additions. As the reaction takes place, the intensity of the Soret band, around 470 nm, starts to decrease giving rise to a new band appearing at shorter wavelengths, nearby the 420 nm. This new band has been assigned by Groves to an inactive species having the metal center in the oxidation state Mn(IV).<sup>24</sup>

As can be seen in Figure 4-3, the characteristic enlarged Soret band of catalyst **V**, appearing at 400 nm, suffers a bathochromic shift instead, during the reaction originating a well-defined band at 468 nm.

**Table 4-1** Results obtained for the oxidation of substrates (4.1-4.9) with H<sub>2</sub>O<sub>2</sub> catalyzed by the manganese cationic imidazole porphyrin (V).<sup>a</sup>

Substrates	S/C molar ratio	H <sub>2</sub> O <sub>2</sub> (mmol)	Conversion (%)	Products selectivity (%)		Time (min)
				S=O	SO <sub>2</sub>	
 (4.1)	600	1.2	97.3	-	100	120
	300	1.8	99.9	-	100	180
 (4.2)	300	0.9	99.7	-	100	90
	150	1.2	99.9	-	100	120
 (4.3)	300	1.8	89.2	-	100	180
	150	1.2	96.9	-	100	120
 (4.4)	300	2.1	95.4	-	100	210
	150	2.4	99.7	-	100	240
 (4.5)	300	1.5	57.9	-	100	150
	150	1.2	87.0	-	100	120
 (4.6)	300	1.8	87.9	-	100	180
	150	1.2	99.9	-	100	120
 (4.7)	300	0.9	99.9	-	100	90
	150	1.2	93.5	-	100	120
 (4.8)	300	2.1	91.7	24.1	75.9	210
	150	1.8	98.7	7.6	92.4	180
 (4.9)	300	2.1	80.1	54.7	45.3	210
	150	2.1	98.9	64.9	35.1	210

<sup>(a)</sup>The substrate (0.3 mmol) was dissolved in 2.0 mL of CH<sub>3</sub>CN and kept under magnetic stirring at 22-25 °C in the presence of V (for S/C molar ratio of 150, the catalyst amount was 2.0 x 10<sup>-3</sup> mmol; for S/C molar ratio of 300, the catalyst amount was 1.0 x 10<sup>-3</sup> mmol). The co-catalyst used was acetic acid (0.12 mmol, 24 μL). The oxidant, diluted 1:10 in CH<sub>3</sub>CN, was progressively added at regular intervals of 15 min in small aliquots, each corresponding to a half-substrate amount. The conversion and selectivity values are the result of at least two assays.

Besides displaying high stability in the presence of an excess of oxidant, the observed spectral modifications of complex V during the oxidative processes can only be

related to the interactions solvent-metal ion ( $\lambda_{\max}= 400$  nm) and oxidant-metal ion ( $\lambda_{\max}= 440$  nm). Since no changes in the position and intensity of the 2 Q bands were detected, the oxidation state of the metal ion or the structure of the macrocycle were not modified.<sup>25</sup>

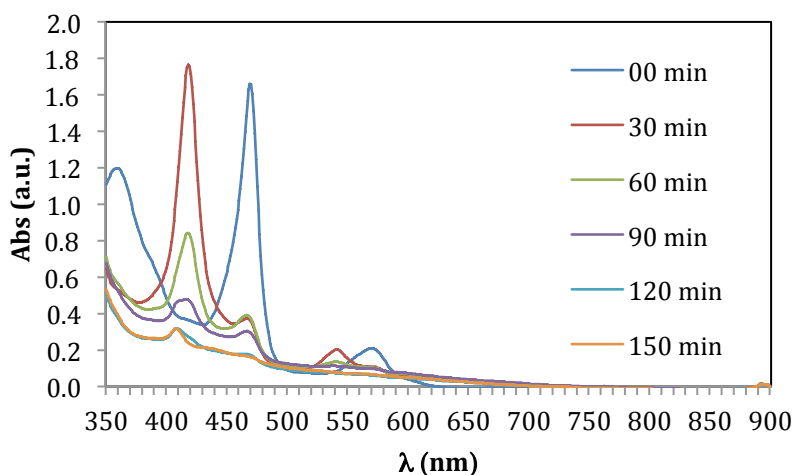


**Figure 4-2** Typical electronic absorptions spectra evolution of catalyst **II** during sulfoxidations by  $\text{H}_2\text{O}_2$ .

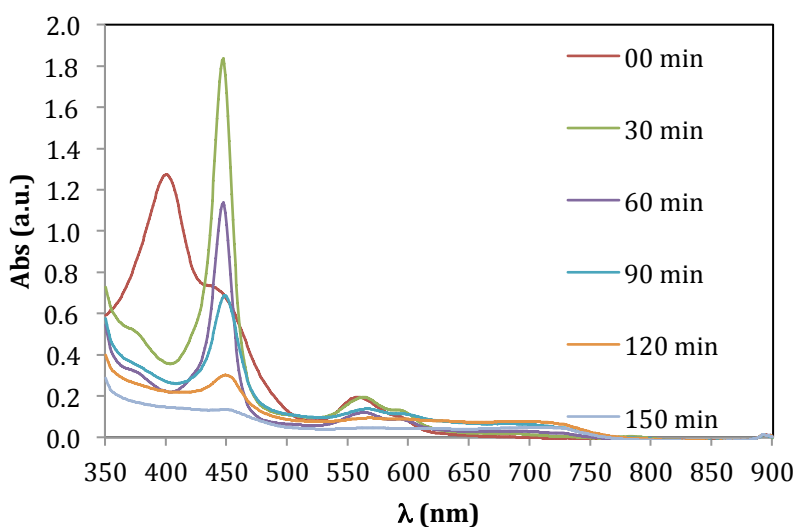


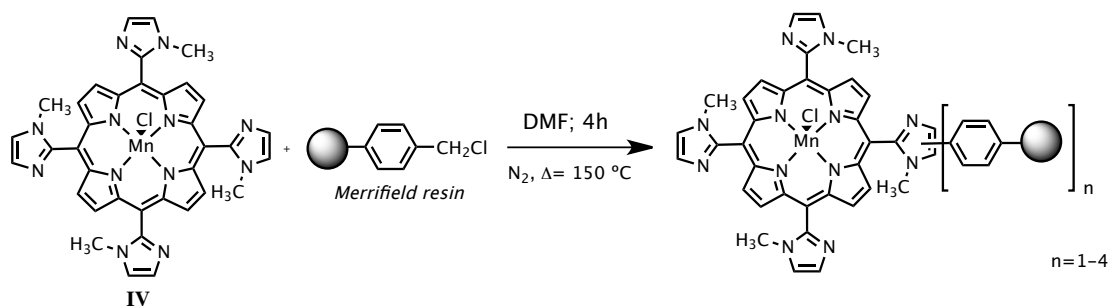
**Figure 4-3** Typical electronic absorption spectra evolution of catalyst **V** sulfoxidations by  $\text{H}_2\text{O}_2$ .

#### 4.2.2. SYNTHESIS OF THE HETEROGENEOUS CATALYSTS

The results achieved with catalyst **V** under homogeneous conditions prompted us to immobilize the neutral complex  $[\text{Mn}(\text{TMImP})\text{Cl}]$  (**IV**) in a Merrifield resin in order to



obtain the cationic heterogeneous material referred as **IV-MR**. The procedure used is based on the approach reported by Moghadam *et al.*<sup>26</sup> and also used by Du *et al.*<sup>27</sup> Thus, the optimized procedure implies the reaction of **IV** with Merrifield resin in DMF at 150°C for 4 hours, under N<sub>2</sub> atmosphere. With almost no starting porphyrin detected in solution, the dark brown solid was filtered and extensively washed with several solvents, affording a porphyrin loading of 3.6%.



Scheme 4-2

#### 4.2.3. ASSAYS UNDER HETEROGENEOUS CONDITIONS

The potential of the Merrifield resin as a support has already been highlighted, since allows the development of new metalloporphyrin-based heterogenized catalytic systems.<sup>28-30</sup> Moreover, as already mentioned, **IV-MR** demonstrated to be an efficient and recyclable heterogeneous catalyst.<sup>19,20</sup> Thus, the first experiments with **IV-MR** in sulfoxidation reactions were performed accordingly to the meanwhile disclosed procedure using **4.1** as substrate and hydrogen peroxide as oxidant. The assays were performed at room temperature (22-25°C) with additions of 0.5 equiv. of H<sub>2</sub>O<sub>2</sub> (diluted 1:10 in CH<sub>3</sub>CN) every 15 minutes. However, comparatively to the homogeneous experiments, a smaller S/C molar ratio (S/C molar ratio=75) and less solvent (500  $\mu$ L) were used. Under these conditions, the catalyzed sulfoxidation of **4.1** takes 4h to reach full conversion; then the catalyst was recovered, washed and dried before being used in a new run.

As evidenced by the results presented on Table 4-2 and in Figure 4-4, catalyst **IV-MR** maintains its efficiency in the second run since full conversion was also attained. Interestingly, the selectivity of the sulfone is higher in the 2<sup>nd</sup> run than in the first run (75.6 % versus 22.9 %). However, the efficiency of this material starts to diminish in the third run reaching a conversion of 46.9 % after four runs.



**Table 4-2** Experimental results obtained for thioanisole (**4.1**) oxidation catalyzed by heterogeneous catalyst **IV-MR** with H<sub>2</sub>O<sub>2</sub>.<sup>a)</sup>

	Run <sup>b)</sup>	Conversion (%)	S=O (%)	SO <sub>2</sub> (%)
Cat: <b>IV-MR</b> 0.5 equiv. H <sub>2</sub> O <sub>2</sub> /15min (4h)	1	99.9	77.1	22.9
	2	99.6	24.4	75.6
	3	77.7	67.7	32.3
	4	46.9	72.1	27.9
Cat.: <b>IV-MR</b> 2.0 equiv. H <sub>2</sub> O <sub>2</sub> /2h (6h)	1	99.9	78.1	21.9
	2	99.9	69.2	30.8
	3	99.9	59.6	40.4
	4	96.2	64.3	35.7
	5	78.7	73.1	26.9
	6	63.0	86.5	13.5

<sup>a)</sup> S/C molar ratio=75; substrate=0.3 mmol; catalyst=  $4 \times 10^{-3}$  mmol (80 mg); co-catalyst (acetic acid)=0.12mmol (24  $\mu$ L). All reactions were carried out in CH<sub>3</sub>CN (0.5 mL). <sup>b)</sup> The recovered catalyst was weighted and the reaction conditions adapted after each run, since some material was lost between runs.

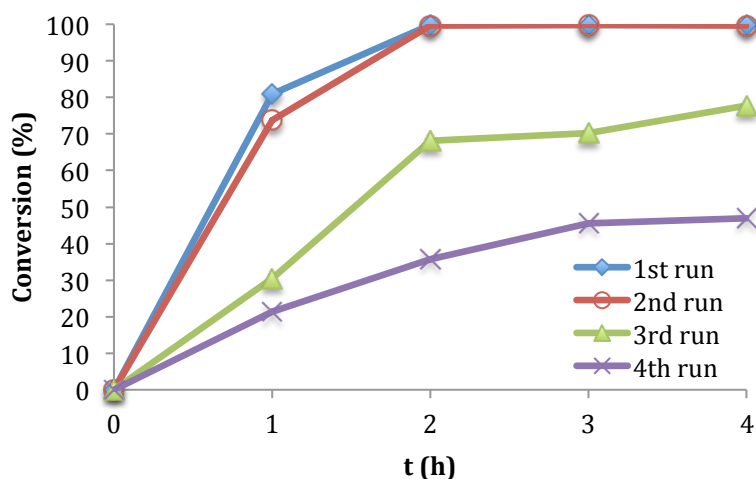


**Figure 4-4** Thioanisole (**4.1**) oxidation reaction profile with H<sub>2</sub>O<sub>2</sub> in the presence of catalyst **IV-MR** for a sub/cat molar ratio of 75 with the successive reuses.

Trying to improve the catalytic performance and recyclability of **IV-MR** the mode of oxidant addition was slightly modified. Instead of adding 0.5 equiv. of  $\text{H}_2\text{O}_2$  at every 15 minutes (1:10 in  $\text{CH}_3\text{CN}$ ), 2 equiv. of  $\text{H}_2\text{O}_2$  every two hours were added from a more concentrated solution of oxidant (1:5 in  $\text{CH}_3\text{CN}$ ). Under these conditions the addition of 6 equiv. of oxidant and the reaction was considered terminated after 6 hours. The results summarized in Table 4-2 and in Figure 4-5 show that we were able to significantly increase the number of runs and **IV-MR** could be used in 6 consecutive cycles with appreciable catalytic efficiency; after the 6<sup>th</sup> run a reasonable conversion of *ca* 60 % was still attained.

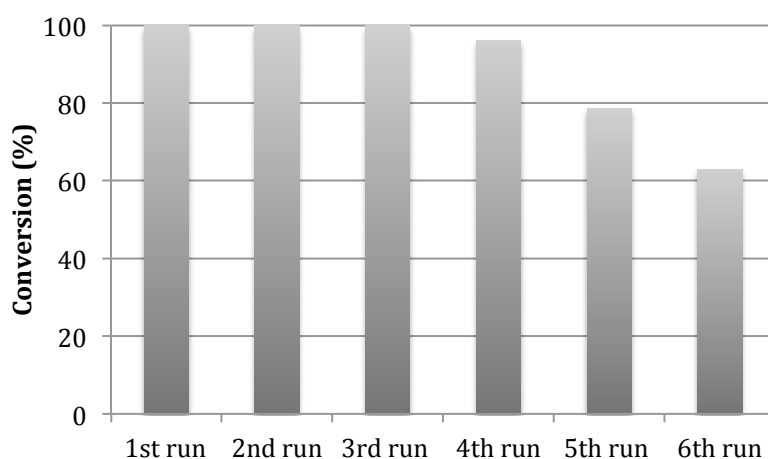


**Figure 4-5** Recyclability of **IV-MR** catalytic system in the oxidation of thioanisole **4.1**, under the following conditions: S/C molar ratio=75; substrate=0.3 mmol; catalyst=  $4 \times 10^{-3}$  mmol (80 mg); co-catalyst(acetic acid)= 0.12mmol (24  $\mu\text{L}$ ), 2 equiv.  $\text{H}_2\text{O}_2$  (diluted 1:5 in  $\text{CH}_3\text{CN}$ ) added at every 2 hours. The recovered catalyst was weighted and the reaction conditions adapted after each run.

In all the experiments with this **IV-MR**/ $\text{H}_2\text{O}_2$  catalytic system, no bleaching of the porphyrin from the support was observed, and the solvent always remained uncolored during the experiments. So, the lower efficiency observed with the increasing number of runs was attributed mainly to its possible degradation/inactivation.

As can be observed in Figure 4-6, the recovered material after the catalytic experiments seems to lose some color, presenting a lighter brown color. Furthermore, the comparison of diffuse reflectance spectra between the starting material and the material after being used in the catalytic experiments (Figure 4-7) shows important modifications. In the starting **IV-MR** material, the bands at 482, 596 and 710 nm prove the immobilization of manganese(III) porphyrin **IV** in the support; after being subject to 6 catalytic cycles those bands are much less pronounced.

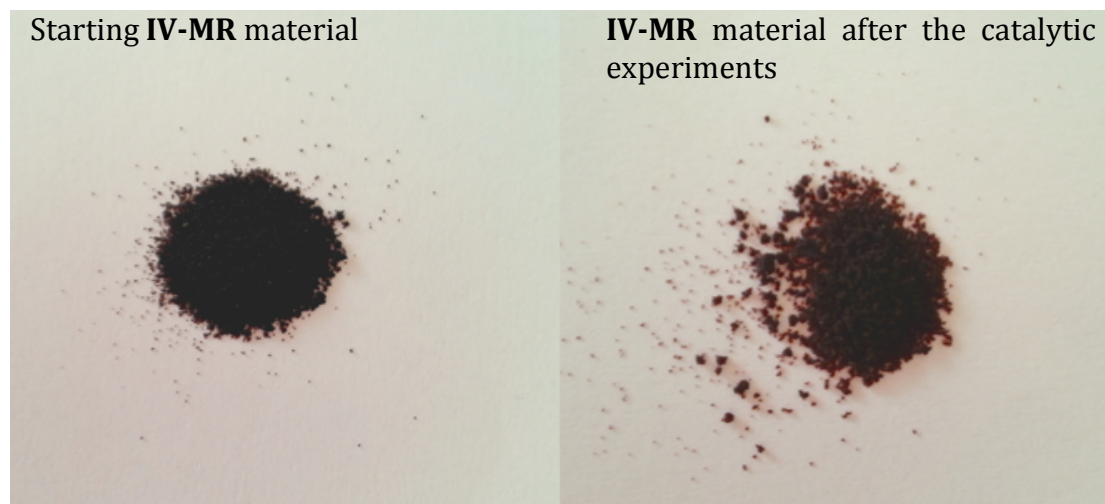


**Figure 4-6** Comparative image of IV-MR heterogeneous catalyst before (left) and after (right) the catalytic experiments

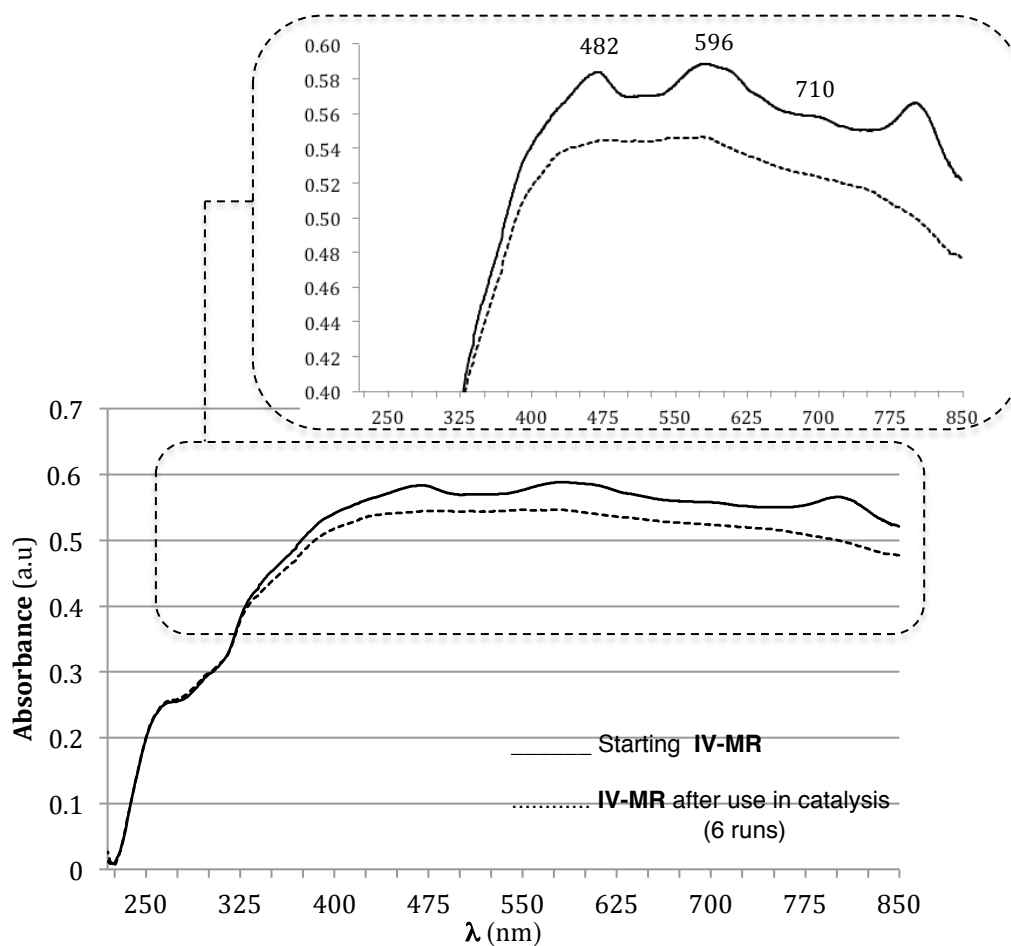


**Figure 4-7** Comparison of the diffuse reflectance spectra of the IV-MR material before and after the catalytic experiments (6 runs)

It is important to refer that control experiments were carried out, under similar reaction conditions but using an equal amount of Merrifield resin instead of catalyst **IV-MR**. The conversion obtained was lower than 4%, confirming that the reaction only takes place in the presence of **IV-MR**.

The results achieved in the sulfoxidation of **4.1** with **IV-MR** prompted us to test the efficiency of this promising heterogeneous catalyst in the sulfoxidation of an envisaged model fuel consisting of a mixture of five organosulfur compounds BTs **4.2** and **4.4**, and DBTs **4.7-4.9** in hexane (Figure 4-8). The GC-FID chromatograms of the reaction mixture at  $R_t = 0$  minutes and  $R_t = 24$  hours (end of reaction) are presented in Figure 4-9. Under the optimized conditions, additions of  $H_2O_2$  (2 equiv. each) at every 2 hours for 6 hours of reaction and then leaving the mixture under stirring for 24 hours, it was possible to accomplish just 48.0 % of conversion of the starting model fuel. Although no full conversion was reached, it is interesting to note that the oxidation products of compounds **4.2**, **4.4** and **4.7-4.9** were detected, respectively at 10.11, 9.30, 10.35, 11.69, 12.64 minutes [Figure 4-9 (B)]. Diphenylsulfide **4.2** is completely oxidized, since the peak at 8.53 disappeared affording the corresponding sulfone ( $R_t$  10.11 minutes). However, the more recalcitrant derivatives are much harder to oxidize, and thus all of them are still present at the end of reaction.

Organosulfur derivatives used in the model fuel:

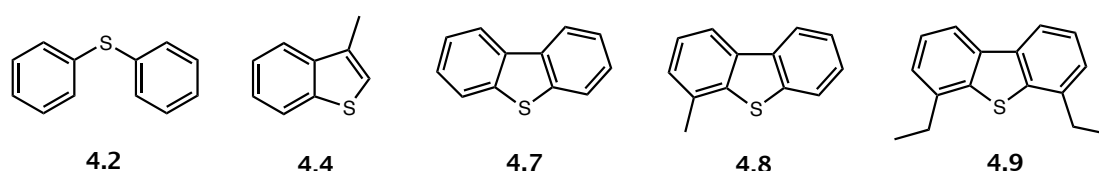


**Figure 4-8** Sulfur derivatives used as a model fuel mixture in catalytic experiments with **IV-MR**

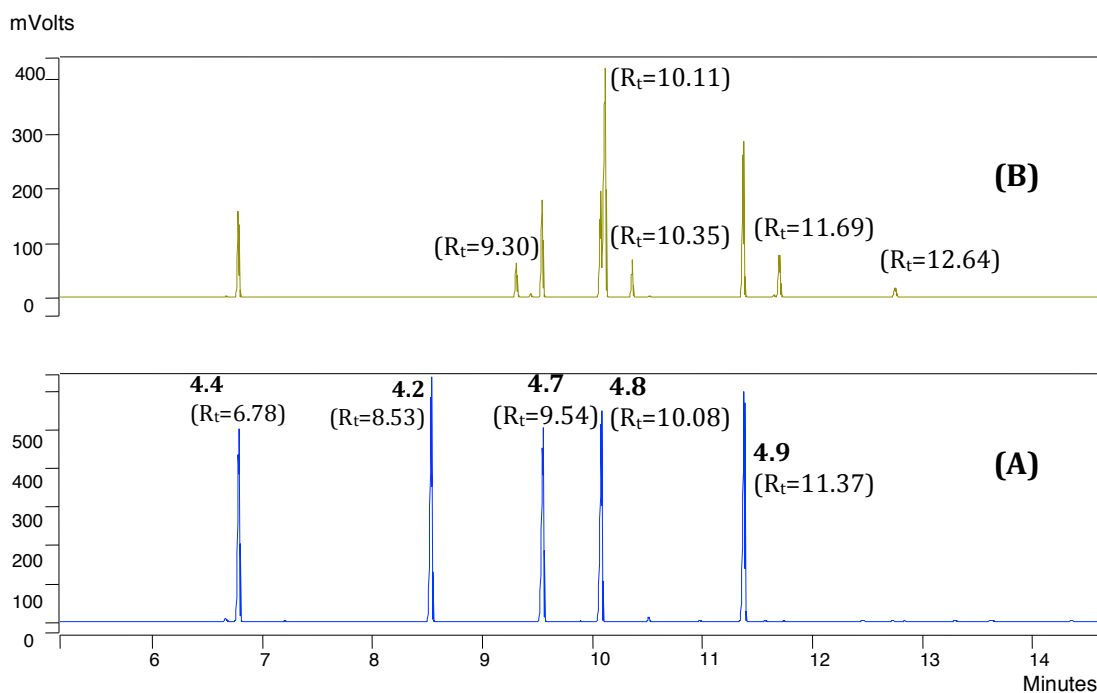


**Figure 4-9** GC-FID chromatograms of the model fuel oxidation using catalyst **IV-MR** before oxidant addition (A) and after 24 hours of reaction (B).

### 4.3. IMMOBILIZATION OF AN IRON PORPHYRIN ON A MERRIFIELD RESIN AND CATALYTIC EXPERIMENTS

As iron(III) complex **III** [Fe(TF<sub>4</sub>NMe<sub>2</sub>PP)Cl] presents the *p*-fluor atoms substituted by an amine, the possible application of the immobilization strategy described for the imidazole porphyrin was envisaged. So, a solution of **III** in DMF under N<sub>2</sub> atmosphere was refluxed for 3 hours. In this case and taking into account the lower reactivity of the amine, NaI was used to facilitate the nucleophilic substitution. The recovered solid, corresponding to **III-MR** heterogeneous catalyst, after being extensively washed with different solvents (CH<sub>2</sub>Cl<sub>2</sub>, methanol, ethanol and acetone) presents a brown color inducing that at least part of the porphyrin was effectively linked to the support. The content of immobilized porphyrin in the support was ascertained by UV-Vis and by the mass of the recovered starting porphyrin, affording a loading of 2.6%.

During the homogeneous catalytic experiments described in chapter 3, the iron(III) porphyrin (**III**)/H<sub>2</sub>O<sub>2</sub> revealed to be the most efficient catalytic system in the oxidation of organosulfur compounds. This led us to evaluate also the catalytic performance of the new synthesized material **III-MR** for this reaction. Heterogeneous

**III-MR** was tested using similar reaction conditions to those described for **IV-MR**; however, some modifications for the use of an iron(III) complex were necessary. The solvent selected for the reaction and to dilute the oxidant was ethanol and the experiments were performed in the absence of co-catalyst. Moreover, the lower loading of the immobilized porphyrin implies the use of a large amount of catalyst to the previous 0.5 mL of solvent. Thus, it was decided to use only 0.1 mmol of substrate in these experiments.

**Table 4-3** Experimental results obtained for thioanisole (**4.1**) oxidation catalyzed by heterogeneous catalyst **III-MR** with H<sub>2</sub>O<sub>2</sub>.<sup>a)</sup>

Cat.: <b>III-MR</b>	Run <sup>b)</sup>	Conversion (%)	S=O (%)	SO <sub>2</sub> (%)
3 x 2 equiv. of H <sub>2</sub> O <sub>2</sub> (24 h)	1	83.4	84.4	15.5
	2	68.7	90.1	9.9
	3	43.8	96.4	3.6

<sup>a)</sup> S/C molar ratio=75; substrate=0.1 mmol; catalyst=  $1.3 \times 10^{-3}$  mmol (60 mg); three additions of 2 equiv. H<sub>2</sub>O<sub>2</sub> were done at 0, 2, and 4 hours of reaction. The reaction mixture was then reacted for 24 hours. All reactions were carried out in ethanol (0.5 mL). <sup>b)</sup> The recovered catalyst was weighted and the reaction conditions adapted after each run, since some material was lost between runs.

As the reaction is slower than when **IV-MR** was used, after the addition of 6 equiv. of H<sub>2</sub>O<sub>2</sub> the reaction mixture was maintained under stirring for 24 hours. The achieved results are summarized in Table 4-3 and in Figure 4-10. The conversion values after 24 hours of reaction did not go further than 83.4% and in the next two cycles a significant decrease of catalyst efficiency is also noticed.

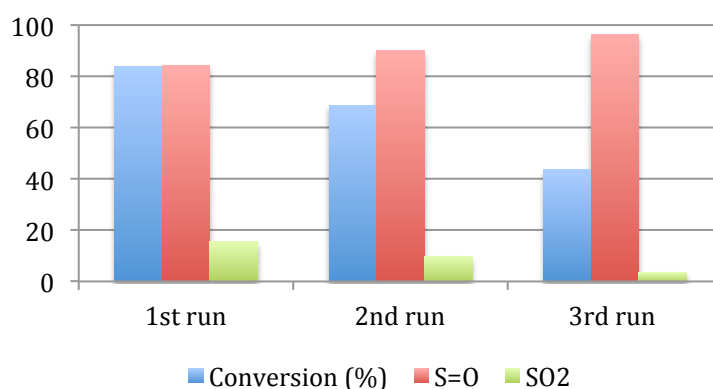


**Figure 4-10** Results from the catalytic experiments with thioanisole **4.1** involving heterogeneous catalyst **III-MR**, under the following conditions: S/C molar ratio=75; substrate=0.1 mmol in ethanol

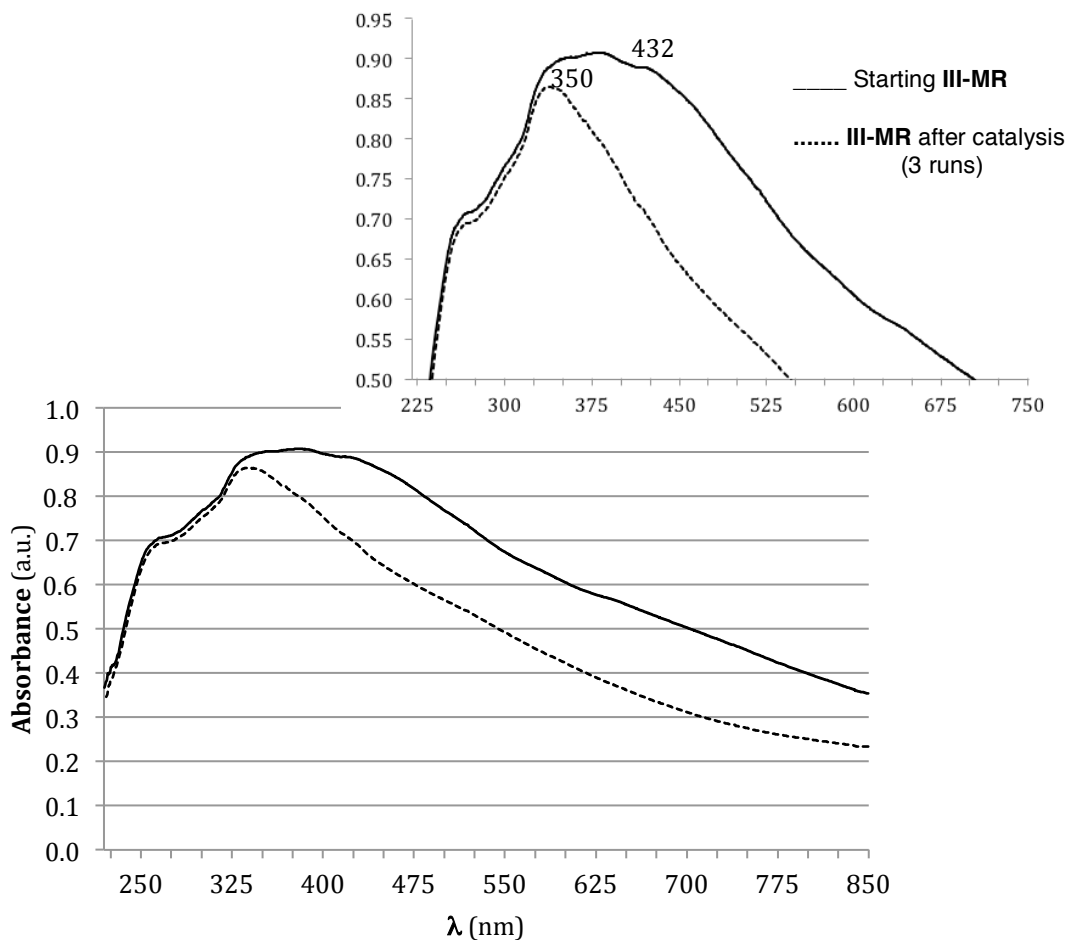


**Figure 4-11** Comparison of catalytic diffuse reflectance spectra of material **III-MR** before and after being used in catalytic experiments

Although during these experiments no bleaching of the catalyst was detected, the recycling experiments put in evidence that this material cannot be efficiently reused. The diffuse reflectance spectrum of **III-MR** after being used in catalytic sulfoxidation of thioanisole (**4.1**) by  $\text{H}_2\text{O}_2$  shows that the Soret band at 432 is almost undetectable after three uses in catalytic tests (Figure 4-11).

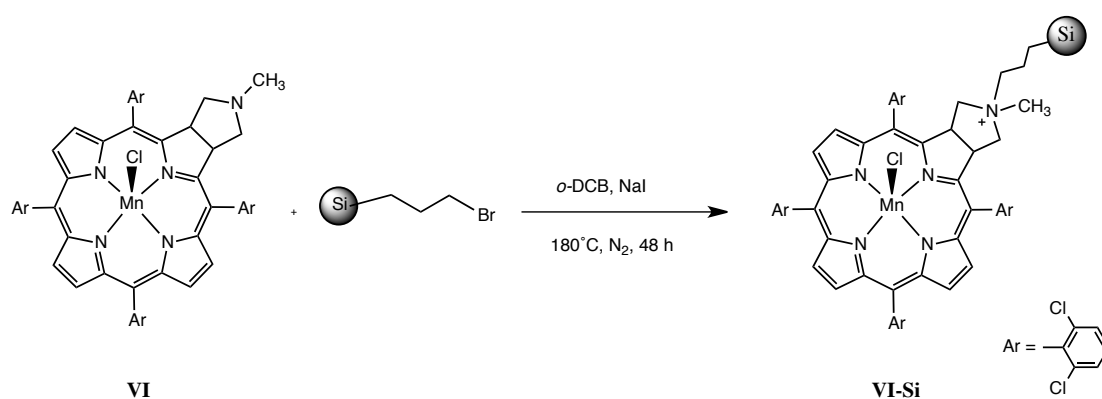
#### 4.4. CATALYTIC EXPERIMENTS WITH THE HETEROGENEOUS CHLORIN VI-Si

The stability of the silica support under oxidative conditions turns it an optimal choice to heterogenization processes of tetrapyrrolic macrocycles. Furthermore, the easy access to chlorin **VI** and to its immobilization in solids supports<sup>21, 28</sup> led us to



synthesize material **VI-Si** and to evaluate its efficiency in sulfoxidation reactions by hydrogen peroxide.

The synthesis of this chlorin-based material is not new and involved the reaction of chlorin **VI** with 3-bromopropylsilica in *o*-dichlorobenzene (*o*-DCB) as represented in Scheme 4-3.<sup>21</sup> Relatively to the original procedure, and in order to facilitate the reaction, sodium iodide was added in catalytic amount (iodide ion is a better leaving group than bromide ion).



Scheme 4-3

After 48 hours the reaction mixture was filtered and exhaustively washed with several solvents. At the end a dark green solid was recovered (Figure 4-12) and, since the reaction was not complete, the recovered unreacted chlorin was weighted, and the mass obtained was compared with the loading determined by UV-Vis. Both loading values are in agreement and the content of immobilized chlorin was 2.8%.

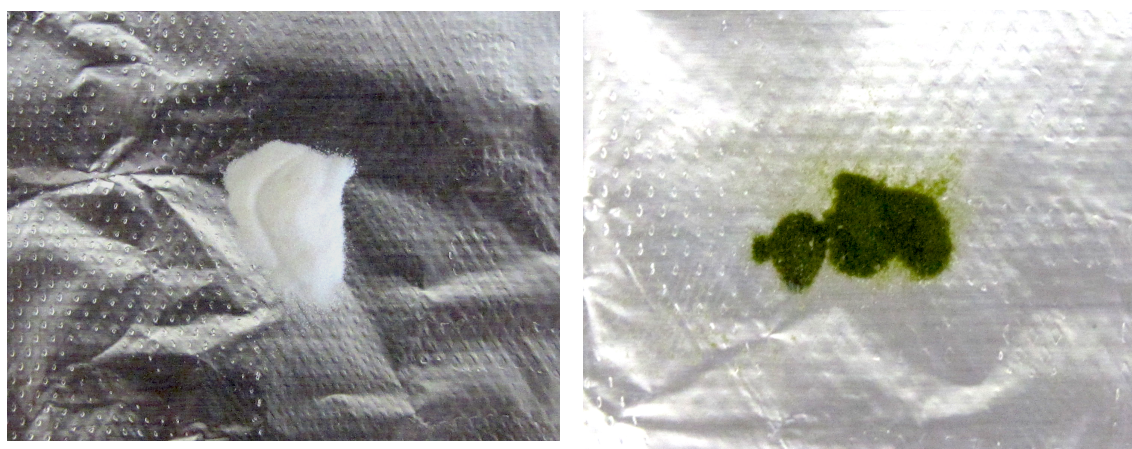


Figure 4-12 Comparison between the starting silica (left) and after the chlorin immobilization reaction (right).



The immobilized chlorin **VI-Si** was evaluated in the sulfoxidation of substrate **4.1** by  $\text{H}_2\text{O}_2$  under similar reaction conditions to the previously reported for the oxidation of cyclooctene. So, in the catalytic study a S/C molar ratio of 75 was employed, ammonium acetate was used as co-catalyst and the oxidant (diluted 1:10 in  $\text{CH}_3\text{CN}$ ) added in several aliquots of 0.5 equiv. at every hour. The results obtained are summarized in Table 4-4 and **VI-Si** proves to be efficient in the thioanisole (**4.1**) catalytic oxidation by hydrogen peroxide.

**Table 4-4** Experimental results obtained for thioanisole (**4.1**) oxidation catalyzed by heterogeneous catalyst **VI-Si** with  $\text{H}_2\text{O}_2$ .<sup>a)</sup>

Catalyst: <b>VI-Si</b>	Run <sup>b)</sup>	Conversion (%)	S=O (%)	SO <sub>2</sub> (%)
0.5 equiv./h $\text{H}_2\text{O}_2$ (1:10) (5 h)	1	98.0	57.0	43.0
	2	90.3	63.1	36.9
	3	72.7	78.8	21.2
	4	54.3	84.6	15.3

<sup>a)</sup> S/C molar ratio=75; substrate=0.3 mmol; catalyst=  $4 \times 10^{-3}$  mmol (150 mg); co-catalyst (ammonium acetate)= 15 mg. Each oxidant addition corresponds to a half of the initial substrate concentration (*i.e.*, 0.15 mmol) performed at every hour. All reactions were carried out in  $\text{CH}_3\text{CN}$  (0.5 mL). <sup>b)</sup> The recovered catalyst was weighted and the reaction conditions adapted after each run, since some material was lost between runs

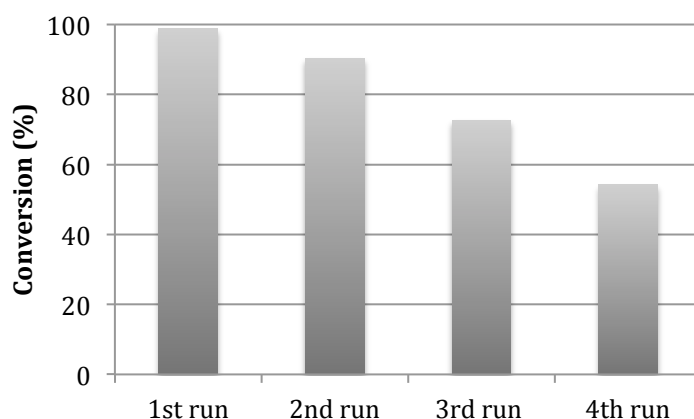


**Figure 4-13** Recyclability of **VI-Si** catalytic system in the oxidation of thioanisole **4.1** by  $\text{H}_2\text{O}_2$

Moreover, this chlorin-based material affords conversions above 50% after four consecutive runs, as highlighted in Figure 4-13. In this particular case, the decreasing efficiency along the runs performed may be associated to some leaching of **VI** from the support. The solvent of the reaction does not appear colorless as at the beginning

of the reaction; it presents a red-brown tone. However, the UV-Vis analysis of the supernatant liquid does not allow a definite conclusion.

Besides some possible leaching, the diffuse reflectance spectra put also in evidence the delocalization of chlorin Soret band to minor wavelengths, from 489 to 420 nm. As mentioned earlier, this is a typical modification detected in symmetric porphyrin macrocycles and is normally associated with the formation of an inactive catalytic species. So, this fact can also justify the decrease in efficiency observed with the recycle of this material. However, the typical band at 651 nm of chlorin derivatives and also the starting Soret band are still observed after the fourth runs, indicating that the catalyst is not completely destroyed.

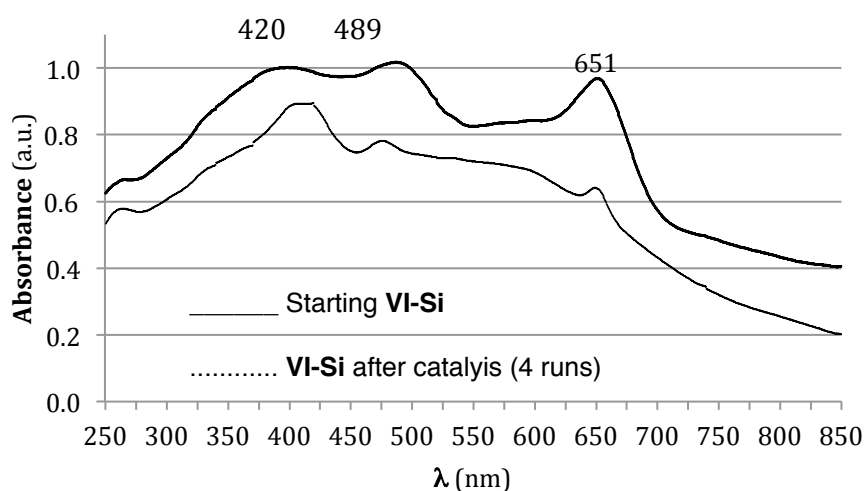


**Figure 4-14** Comparison of diffuse reflectance spectra of the **VI-Si** material before and after catalytic experiments

#### 4.5. CONCLUSIONS

Herein the catalytic efficiency of a cationic symmetric imidazole porphyrin derivative (**V**) was studied for the first time in sulfoxidation reactions by hydrogen peroxide of several organosulfur compounds. The catalytic system **V**/ $\text{H}_2\text{O}_2$ /acetic acid demonstrated comparable efficiency to the widely used and well studied complexes **I**, **II**, and **III**. For sulfides **4.1** and **4.2**, it was possible to reach excellent conversions (>97%) into the corresponding sulfones with the S/C molar ratios tested (150 and 300). The conversions reached for the benzothiophenes **4.3-4.6** (87.0-99.9%) and dibenzothiophenes **4.7-4.9** (93.5-99.9%) at S/C molar ratios of 150 are also



meaningful. It is interesting to note that DBTs are usually considered the most recalcitrant, but the worst result was achieved for the 2-methylsubstituted BT derivative (**4.5**).

The imidazole moiety was successfully used to promote the immobilization of the neutral complex **IV** into a Merrifield resin support, thus obtaining the also cationic heterogeneous catalyst **IV-MR**. From the catalytic experiments involving **IV-MR**/H<sub>2</sub>O<sub>2</sub>/acetic acid catalytic system it is possible to conclude that this is able to efficiently oxidize thioanisole (99.9% in the first use) besides having appreciable recycling capacity. After 6 runs **IV-MR** catalyst gives more than 60% of conversion.

The efficiency of two additional heterogeneous catalysts, **III-MR** and **VI-Si** was also evaluated for the first time in the oxidation of **4.1**. Comparatively to the imidazole-based material, the iron(III) porphyrin immobilized on a Merrifield resin (**III-MR**) demonstrated lower efficiency, allowing just 83.4% of conversion in the 1<sup>st</sup> run. Interestingly, the chlorin-based heterogeneous catalyst **VI-Si** proved to be highly efficient in the oxidation of **4.1**. Using hydrogen peroxide as oxidant it was possible to perform 4 runs with a conversion of 54.3 % in the 4<sup>th</sup> run.

## 4.6. EXPERIMENTAL

The Merrifield resin (30-40 mesh, 2.0 mmol/g, 1% cross-linked) and the functionalized silica (200-400 mesh, 1.5 mmol/g) were both purchased from Aldrich. The DMF used as solvent in the synthesis of **VI-Si** was dried in molecular sieves previously activated in the muffle furnace at 350 °C for 4 hours.

The diffuse reflectance measurements were performed using a Jasco V-560 spectrophotometer equipment with the accessory to reflectance.

The GC-FID apparatus specifications and the acquisition programs used for the oxidation tests were already described in chapter 3.

### 4.6.1. SYNTHESIS OF PORPHYRIN-BASED CATALYSTS IMMOBILIZED ON A MERRIFIELD RESIN

To a conic flask containing a solution of **IV** in DMF (15.0 mg of **IV** in 6 mL of DMF), 250 mg of the Merrifield resin were added. The mixture, maintained protected from light, was vigorously stirred at reflux temperature (T=155°C) for 4 hours.

After cooling, the material was collected by filtration and thoroughly washed with DMF, methanol, water, ethanol and chloroform, and acetone in this order, and dried in the oven (T=50°C) overnight.

In the particular case of the immobilization of iron(III) porphyrin (**III**) the procedure was similar, however a catalytic amount of NaI was used and the reaction was stopped only after 24 hours.

In both cases the recovered unreacted porphyrin was weighted and analyzed by UV-Vis in order to ascertain the quantity of immobilized porphyrin. In the case of **IV-MR** the loading was 3.6 %, and for **III-MR** the loading was 2.6%.

#### 4.6.2. SYNTHESIS OF PORPHYRIN-BASED CATALYSTS IMMOBILIZED ON A FUNCTIONALIZED SILICA

To a pear shaped flask of 10 mL, 500 mg of 3-bromopropylsilica were added, followed by the chlorin complex **VI** (10 mg) diluted in 5.0 mL of *o*-DCB, and a catalytic amount of NaI. The reaction mixture, kept under strong magnetic stirring, N<sub>2</sub> atmosphere and protected from light, was left at reflux temperature (190 °C) for 48 hours.

After confirming the obtention of a dark green solid base by TLC, the mixture was cooled to room temperature, and the solid filtered under vacuum using filter paper. The recovered solid was extensively washed with different solvents (petroleum ether, CH<sub>3</sub>CN, CH<sub>2</sub>Cl<sub>2</sub>, CHCl<sub>3</sub>/metanol (10%) and acetone) in order to remove all the unreacted chlorin. The solid material was dried in the oven at a T=50 °C for 12 h.

Since the reaction is not complete, the unreacted starting chlorin was recovered, weighted and quantified by UV-Vis to allow the determination of **VI** linked to the support. The loading of the immobilized chlorin was 2.8%

#### 4.6.3. CATALYTIC STUDIES

##### 4.6.3.1. CATALYTIC TESTS USING CATIONIC CATALYST **V** UNDER HOMOGENEOUS CONDITIONS

Accordingly to the procedure already established in our laboratory, all the catalytic assays involving imidazole derivatives were carried in acetonitrile and acetic acid was



used as the co-catalyst. For the experiments with **V** under homogeneous conditions, the substrate (0.3 mmol), the I.S. (0.3 mmol), the catalyst ( $1 \times 10^{-3}$  mmol for a S/C molar ratio=300;  $2 \times 10^{-3}$  mmol for a S/C molar ratio= 150), the co-catalyst (24  $\mu$ L) and the solvent (2.0 mL in total) were maintained under stirring in a 5 mL round bottom flask, protected from light. The oxidant, 30% (w/w) aqueous H<sub>2</sub>O<sub>2</sub> diluted in acetonitrile (1:10), was progressively added to the reaction mixture at every 15 minutes in aliquots corresponding to 0.5 equivalents of the substrate amount. The reactions were monitored by GC–FID and GC–MS analysis, using chlorobenzene as internal standard.

#### 4.6.3.2. CATALYTIC TESTS WITH METALLOPORPHYRIN-BASED MATERIALS UNDER HETEROGENEOUS CONDITIONS

For the experiments involving the heterogeneous catalyst **IV-MR** the above described procedure was optimized and slightly modified. Generally, instead of 2.0 mL of solvent, 0.5 mL were used, and a bigger amount of catalyst (S/C molar ratio 75) was necessary. The oxidant was also diluted but only 1:5 in CH<sub>3</sub>CN, and additions of 2 equiv. were performed at every 2 hours. At the end of reaction, in order to recover the catalyst, the reaction mixture was centrifuged, the solid material extensively washed with different solvents, namely CH<sub>3</sub>CN, CH<sub>2</sub>Cl<sub>2</sub>, MeOH and acetone, and finally dried at 50 °C overnight before new utilization under similar reaction conditions.

When **III-MR** was used as catalyst, the solvent was ethanol and no co-catalyst was necessary. In order to use a lower amount of catalyst, the tests were performed with 0.1 mmol of substrate instead of 0.3 mmol. The experiments concerning the evaluation of the chlorin-based material **III-Si** besides using a different co-catalyst, namely ammonium acetate (15 mg), also involves the addition of 0.5 equiv. at each 15 minutes of diluted H<sub>2</sub>O<sub>2</sub> in CH<sub>3</sub>CN (1:10).

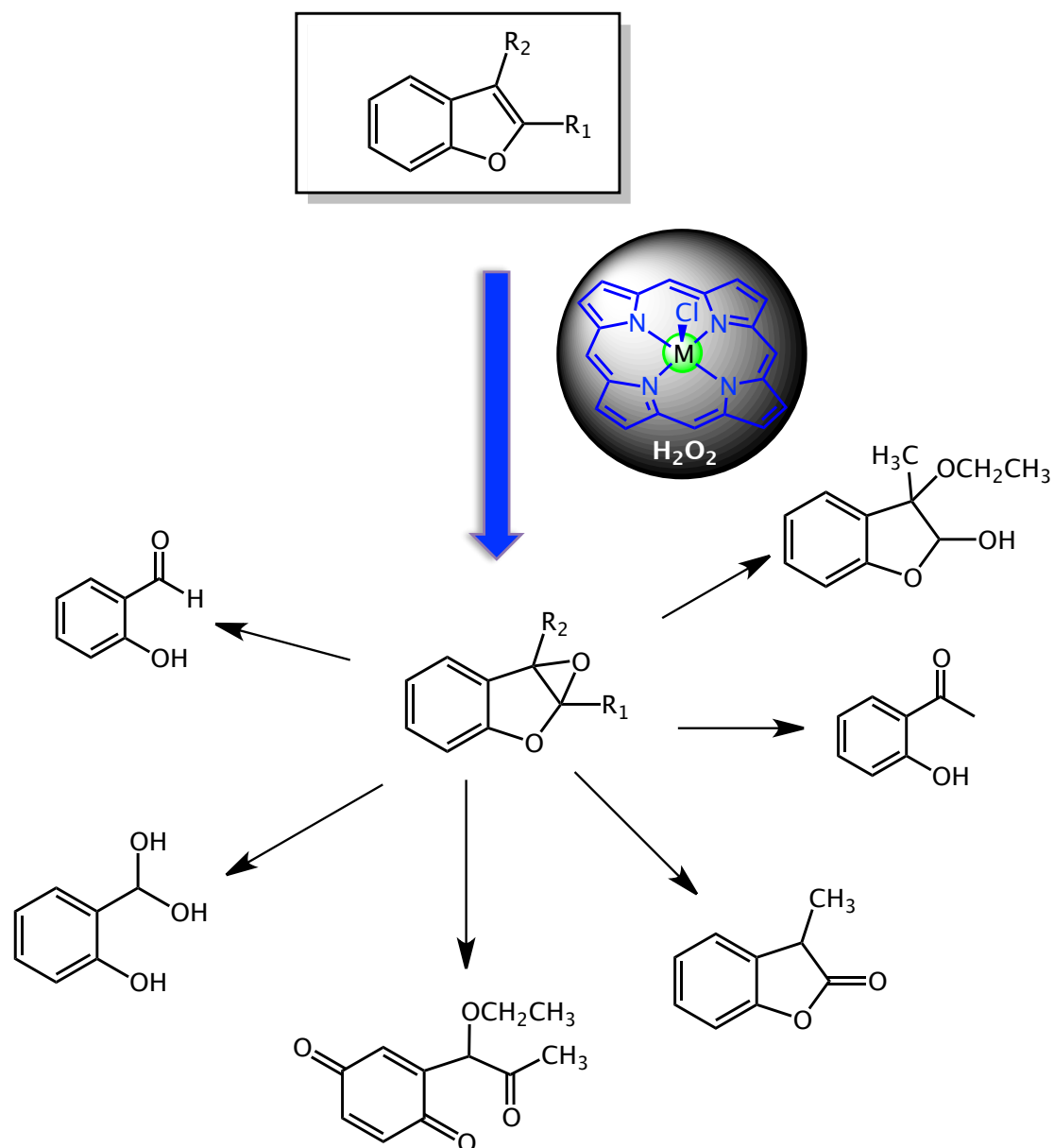
#### 4.7. BIBLIOGRAPH

- <sup>1</sup> a) S.M.G. Pires, M.M.Q. Simões, I.C.M.S. Santos, S.L.H. Rebelo, M.M. Pereira, M.G.P.M.S. Neves, J.A.S. Cavaleiro, *Appl. Catal. A: Gen.* 439-440 (2012) 51. b) S.M.G. Pires, M.M.Q. Simões, I.C.M.S. Santos, S.L.H. Rebelo, F.A.A. Paz, M.G.P.M.S. Neves, J.A.S. Cavaleiro, *Appl. Catal. B: Environ.* 160-161 (2014) 80.
- <sup>2</sup> P. Le Maux, G. Simonneaux, *Chem. Commun.* 47 (2011) 6957.
- <sup>3</sup> X. Zhou, G. Ren, H. Ji, *J. Porphyr. Phthalocya.* 17 (2013) 1105.
- <sup>4</sup> E. Baciocchi, M.F. Gerini, A. Lapi, *J. Org. Chem.* 69 (2004) 3586.
- <sup>5</sup> X. Zhou, S. Lv, H. Wang, X. Wang, J. Liu, *Appl. Catal. A: Gen.* 396 (2011) 101.
- <sup>6</sup> A. Rezaeifard, M. Jafarpour, P. Farshid, A. Naeimi, *Eur. J. Inorg. Chem.* (2012) 5515.
- <sup>7</sup> R. De Paula, M.M.Q. Simões, M.G.P.M.S. Neves, J.A.S. Cavaleiro, *Catal. Commun.* 10 (2008) 57.
- <sup>8</sup> R. De Paula, M.M.Q. Simões, M.G.P.M.S. Neves, J.A.S. Cavaleiro, *J. Mol. Catal. A: Chem.* 345 (2011) 1.
- <sup>9</sup> J. Połtowicz, E.M. Serwicka, E. Bastardo-Gonzalez, W. Jonesb, R. Mokaya, *Appl. Catal. A: Gen.* 1-2 (2001) 211.
- <sup>10</sup> S. Tangestaninejad, M.H. Habib, V. Mirkhani, M. Moghadam, *J. Chem. Res.-S* 10 (2001) 444.
- <sup>11</sup> K. S. Suslick, in *"The Porphyrin Handbook"*, K. Kadish, K. Smith, R. Guillard (Eds.), Academic Press, New York (1999).
- <sup>12</sup> C. Che, J. Huang, *Chem. Commun.* (2009) 3996.
- <sup>13</sup> E. Brulé, Y.R. de Miguel, *Org. Biomol. Chem.* 4 (2006) 599.
- <sup>14</sup> D. Mansuy, *C. R. Chimie* 10 (2007) 392.
- <sup>15</sup> C.-X. Liu, Q. Liu, C.-C. Guo, *Catal. Lett.* 138 (2010) 96.
- <sup>16</sup> X.-L. Yang, M.-H. Xie, C. Zou, Y. He, B. Chen, M. O' Keeffe, C.-D. Wu, *J. Am. Chem. Soc.* 134 (2012) 10638.
- <sup>17</sup> R. Rahimi, S.Z. Ghoreishi, M.G. Dekamin, *Monatsh. Chem.* 143 (2012) 1031.
- <sup>18</sup> K.A.D.F. Castro, M.M.Q. Simões, M.G.P.M.S. Neves, J.A.S. Cavaleiro, F. Wypych, S. Nakagaki, *Catal. Sci. Technol.* 4 (2014) 129.
- <sup>19</sup> R. De Paula, I.C.M.S. Santos, M.M.Q. Simões, M.G.P.M.S. Neves, J.A.S. Cavaleiro, *J. Catal.*, submitted.
- <sup>20</sup> R. De Paula, PhD Thesis, University of Aveiro (2009).
- <sup>21</sup> S.M.G. Pires, R. De Paula, M.M.Q. Simões, M.G.P.M.S. Neves, I.C.M.S. Santos, A.C. Tomé, J.A.S. Cavaleiro, *Catal. Commun.* 11 (2009) 24.



- <sup>22</sup> S.L.H. Rebelo, A.R. Gonsalves, M.M. Pereira, M.M.Q. Simões, M.G.P.M.S. Neves, J.A.S. Cavaleiro, *J. Mol. Catal. A: Chem.* 256 (2006) 321.
- <sup>23</sup> R. De Paula, M.M.Q. Simões, M.G.P.M.S. Neves, J.A.S. Cavaleiro, In: *Evaluation of Five-Membered Heterocyclic Ring Meso-Substituted Metalloporphyrins as Catalysts in Oxidative Reactions*, 4th Spanish-Portuguese-Japanese Organic Chemistry Symposium, Santiago de Compostela/Spain (2006) PO-26, p. 86.
- <sup>24</sup> J.T. Groves, J. Lee, S.S. Marla, *J. Am. Chem. Soc.* 113 (1996) 209.
- <sup>25</sup> R. De Paula, PhD Thesis, University of Aveiro (2009) Chapter 3.
- <sup>26</sup> M. Moghadam, S. Tangestaninejad, M.H. Habibi, V. Mirkhani, *J. Mol. Catal. A: Chem.* 217 (2004) 9.
- <sup>27</sup> C.-P. Du, Z.-K. Li, X.-M. Wen, J. Wu, X.-Q. Yu, M. Yang, R.-G. Xie, *J. Mol. Catal. A: Chem.* 216 (2004) 7.
- <sup>28</sup> G.R. Newkome, E. He, C.N. Moorefield, *Chem. Rev.* 99 (1999) 1689.
- <sup>29</sup> S. Ribeiro, A. Serra, A. Gonsalves, *J. Catal.* 256 (2008) 331.
- <sup>30</sup> A. Ciammaichella, A. Leoni, P. Tagliatesta, *New J. Chem.* 34 (2010) 2122.





## Chapter 5 BIOMIMETIC OXIDATION OF BENZOFURAN DERIVATIVES



## 5. BIOMIMETIC OXIDATION OF BENZOFURAN DERIVATIVES

### 5.1. OVERVIEW

During the last years the chemistry of naturally occurring and synthetic benzofurans has attracted much attention due to their broad spectrum of pharmacological activities. Several examples of bioactive compounds containing the benzofuran moiety (Figure 5-1), showing antibacterial,<sup>1</sup> antimicrobial,<sup>2</sup> anti-inflammatory,<sup>3</sup> antitumor,<sup>4</sup> anticonvulsant, antioxidant,<sup>5</sup> among other activities,<sup>6</sup> have been reported. Moreover, a series of benzofuran derivatives are already used to treat Alzheimer's disease.<sup>7</sup> So, the synthesis of this core backbone has always attracted chemists' attention and has been extensively investigated. So far, many efficient synthetic methods have been disclosed. However, they often involve either multi-step, rigorous reaction conditions, or expensive reagents.<sup>8-13</sup> Among these methods, the annulation reaction is perhaps the most powerful and straightforward way to afford polyfunctional heterocyclic molecules.<sup>13,14</sup> Nematollahi *et al.*<sup>15</sup> and Pei *et al.*<sup>16</sup> reported efficient strategies for the one-pot synthesis of polyhydroxylated benzofurans involving the oxidation of catechols. In 2007, Witayakran *et al.* have disclosed for the first time the cascade synthesis of benzofuran derivatives by using a biocatalyst (laccase/ Sc(OTf)<sub>3</sub>) under mild conditions.<sup>17</sup>

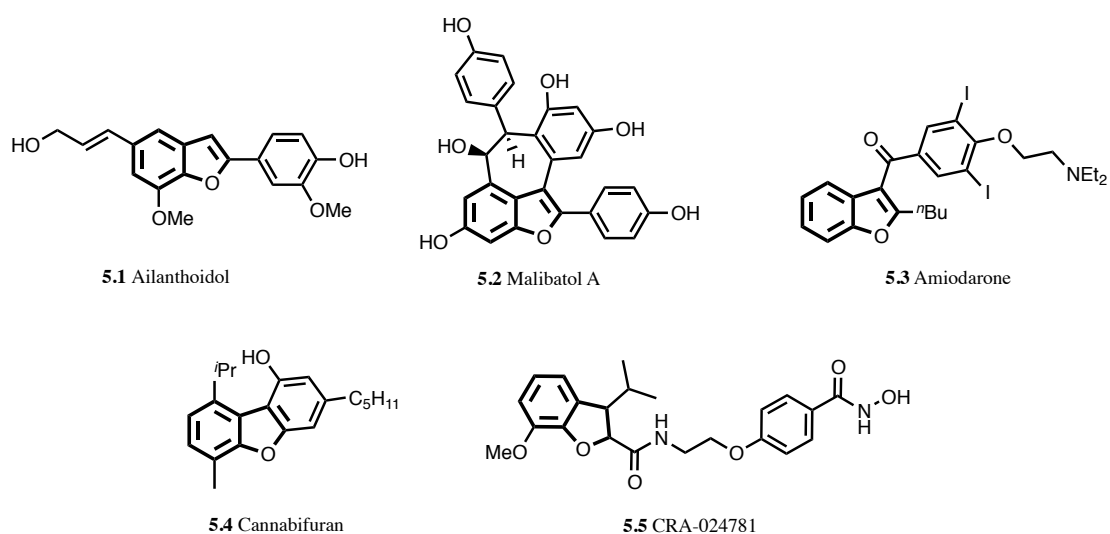
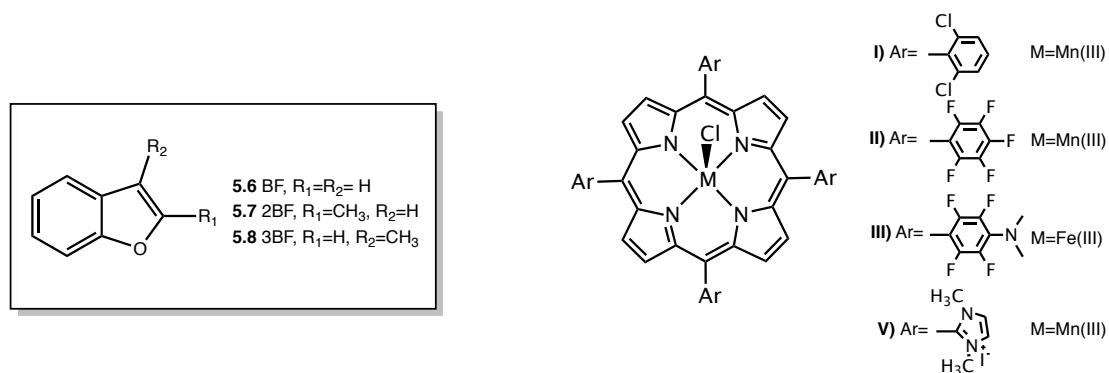


**Figure 5-1** Examples of naturally occurring, pharmaceuticals and biological active compounds containing the benzofuran moiety.

Besides their relevance as important biological active molecules, 2,3-benzofurans (2,3-BFs) are important pollutants in the environment, resulting from waste incineration<sup>18</sup> and from exhaust gases of gasoline and diesel engines.<sup>19</sup> Additionally, some studies revealed that 2,3-BFs are potential carcinogenic to humans.<sup>20</sup> Nevertheless, further studies are necessary in order to understand the role of the metabolism of 2,3-BFs in the disclosed toxicity.

The advantages brought by the use of biomimetic enzymatic models to the development of new synthetic strategies have already been discussed in this dissertation (please see chapter 1, section 1.3). In this sense, an important contribution to the achievement of new relevant compounds, otherwise impossible to obtain, but also to the understanding of metabolic pathways of living organisms can be expected.<sup>21, 22</sup> For instance, it has already been postulated that heteroarene epoxides, such as benzofuran epoxides, are the main responsible for the cytotoxicity detected after benzofurans oxidative activation by CYP-450. So, a suitable screening of their reactivity, for instance through the preparation of authentic samples, is highly important.<sup>23</sup> Synthetic metalloporphyrins can play a crucial role, contributing to the search for benign and environmentally clean oxidation procedures and, as surrogates of CYP-450, for deeper knowledge about benzofurans' metabolism.

As far as we are aware, the study of benzofurans oxidation using a biomimetic, environmentally sustainable approach has not been described yet. Thus, in here we decided to study the oxidation of benzofuran derivatives **5.6-5.8** by hydrogen peroxide in the presence of metalloporphyrin complexes **I, II, III** and **V** (Figure 5-2). The results obtained in these homogeneous catalytic experiments will be presented and discussed below.

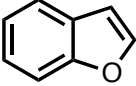
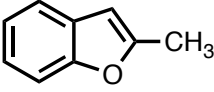
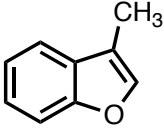


**Figure 5-2** Benzofurans (**5.6-5.8**) and metalloporphyrin catalysts (**I-III** and **V**) involved in the catalytic experiments.

## 5.2. CATALYTIC EXPERIMENTS WITH BENZOFURAN SUBSTRATES

The oxidation of benzofuran derivatives **5.6-5.8** by hydrogen peroxide in the presence of the manganese catalysts **I**, **II** and **V** and of the iron(III) complex **III** was performed accordingly to the established and already described procedures. All the assays were carried out at room temperature and were monitored by GC-FID every 30 minutes. The reactions were stopped when a full conversion was reached or when no evolution was detected in two successive analyses. The conversions obtained using S/C ratios of 300 and 150 are summarized in Table 5-1.

**Table 5-1** Results from the catalytic assays with substrates **5.6-5.8** using metalloporphyrins **I-III** and **V**

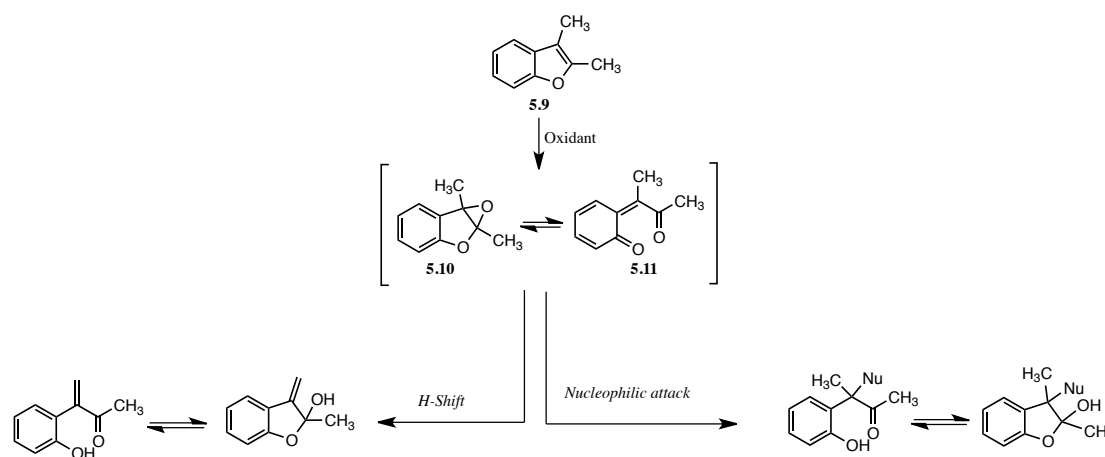
Substrate	Catalyst	Co-Catalyst	S/C Molar Ratio	Conversion (%)	Time (Min)
	I	NH <sub>4</sub> AcO	300	98.7	180
	I	NH <sub>4</sub> AcO	150	99.9	180
	II	NH <sub>4</sub> AcO	300	95.5	180
	II	NH <sub>4</sub> AcO	150	99.9	180
	III	-	300	91.8	120
	III	-	150	99.9	90
	V	AcOH	300	93.5	180
	V	AcOH	150	96.5	120
	I	NH <sub>4</sub> AcO	300	96.9	240
	I	NH <sub>4</sub> AcO	150	97.3	240
	II	NH <sub>4</sub> AcO	300	81.3	210
	II	NH <sub>4</sub> AcO	150	99.9	240
	III	-	300	99.9	120
	III	-	150	99.9	60
	V	AcOH	300	97.5	180
	V	AcOH	150	99.9	180
	I	NH <sub>4</sub> AcO	300	99.7	120
	I	NH <sub>4</sub> AcO	150	99.9	90
	II	NH <sub>4</sub> AcO	300	79.9	270
	II	NH <sub>4</sub> AcO	150	84.3	180
	III	-	300	99.9	60
	V	AcOH	300	99.8	120
	V	AcOH	150	99.9	90

<sup>a)</sup> Reaction conditions: substrate= 0.3 mmol; for S/C molar ratio of 150, the catalyst amount was  $2.0 \times 10^{-3}$  mmol; for S/C molar ratio of 300, the catalyst amount was  $1.0 \times 10^{-3}$  mmol; internal standard (chlorobenzene)= 0.3 mmol; solvent= 2.0 mL total volume (CH<sub>3</sub>CN for manganese catalysts **I**, **II** and **V**, and ethanol for catalyst **III**). Oxidant (H<sub>2</sub>O<sub>2</sub>) additions of 0.5 equiv. each were made at every 15 minutes.

Blank experiments were also performed for the three benzofurans, under similar conditions but in the absence of catalyst and no significant conversions were noticed

(always below 10%). Generally, all the porphyrin complexes (**I-III** and **V**) studied exhibit high catalytic efficiency in the oxidation of benzofuran derivatives affording conversions ranging from 79.9-99.9%. Nevertheless, the quantification and identification of the oxidation products of benzofurans was much more complex than expected, probably due to the high reactivity of the epoxides.

In fact, very few examples regarding the isolation of epoxides from this type of substrates are known. For instance, epoxide **5.10** obtained from benzofuran **5.9** is considered one of the most stable in this series (Scheme 5-1). However, the strong electrophilicity of its valence-isomeric *cis*-ene dione **5.11** and also the epoxide rearrangement to the corresponding allylic alcohol by an H-shift are considered the main reaction features responsible for the high reactivity of this unique epoxide. The NMR characterization of these molecules is possible only at very low temperatures (between -30 and -55 °C). Just to have an idea, derivative **5.10** is able to add methanol without acid assistance at a temperature of -78 °C.<sup>24</sup>



Scheme 5-1

The oxidation of different substituted benzofurans has already been studied with *m*-CPBA and dimethyldioxirane (DMD) as oxidants, being the most relevant isolated products represented in Figure 5-3.<sup>23, 25</sup> In fact, these particular epoxides can easily rearrange and isomerize, even at room temperature; the evolution pathway in these oxidative processes is dependent on the substituents present in the furan backbone.

The reactions studied here gave different products, depending on the substrate, the reaction catalyst, co-catalyst or solvent used. Thus, for a question of simplicity, the analysis of the results in the next sections, is organized by benzofuran derivative; first

the results with benzofuran **5.6** will be presented followed by those obtained with the methyl-substituted benzofurans **5.7** and **5.8**.

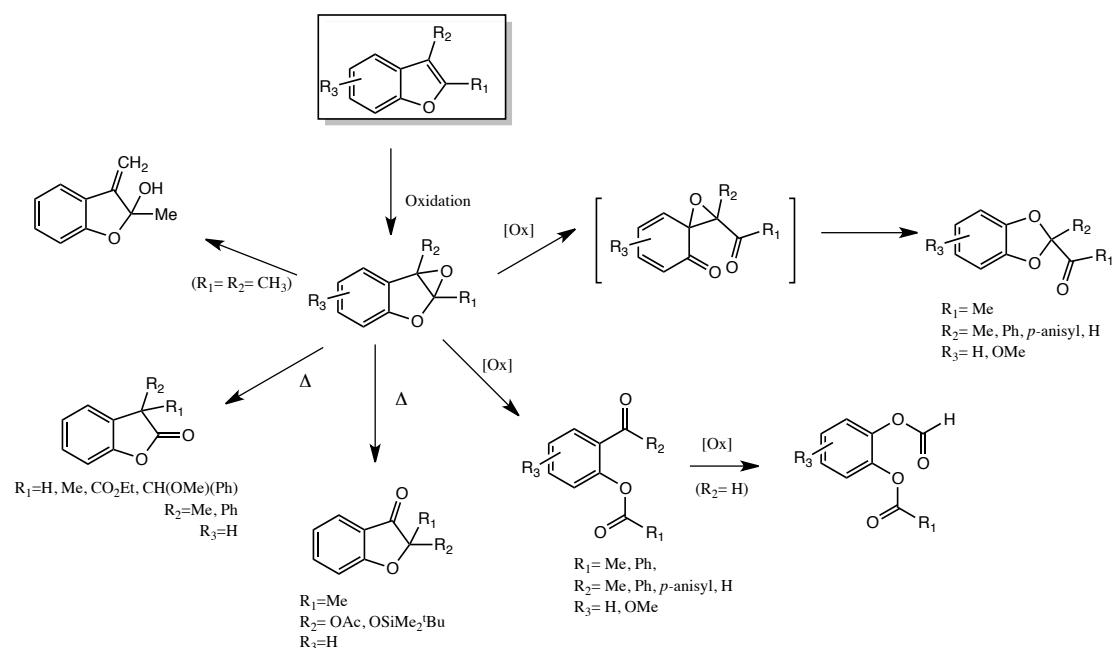


**Figure 5-3** Most common isolated oxidation products from benzofuran derivatives with *m*-CPBA or DMD (adapted from references 23 and 25)

### 5.2.1. CATALYTIC OXIDATION OF BENZOFURAN (**5.6**)

Starting with the experiments involving Mn(III) complexes **I** and **II**, the reaction controls by GC-FID during the oxidation of substrate **5.6** put in evidence the first problem associated with the detection of the oxidation products obtained - the consume of benzofuran was not in agreement with the amount of the products obtained. In a typical GC chromatogram (Figure 5-4), only a very small new peak at 4.39 min is observed.

The analysis of the reaction mixture by GC-MS allowed to identify the new peak as salicylaldehyde **5.12** (MW=122.12). As the peak corresponding to **5.12** was too small for the theoretical amount expected (0.3 mmol) we decided to investigate the possible formation of other non-volatile products, by analyzing the NMR of a reaction mixture.

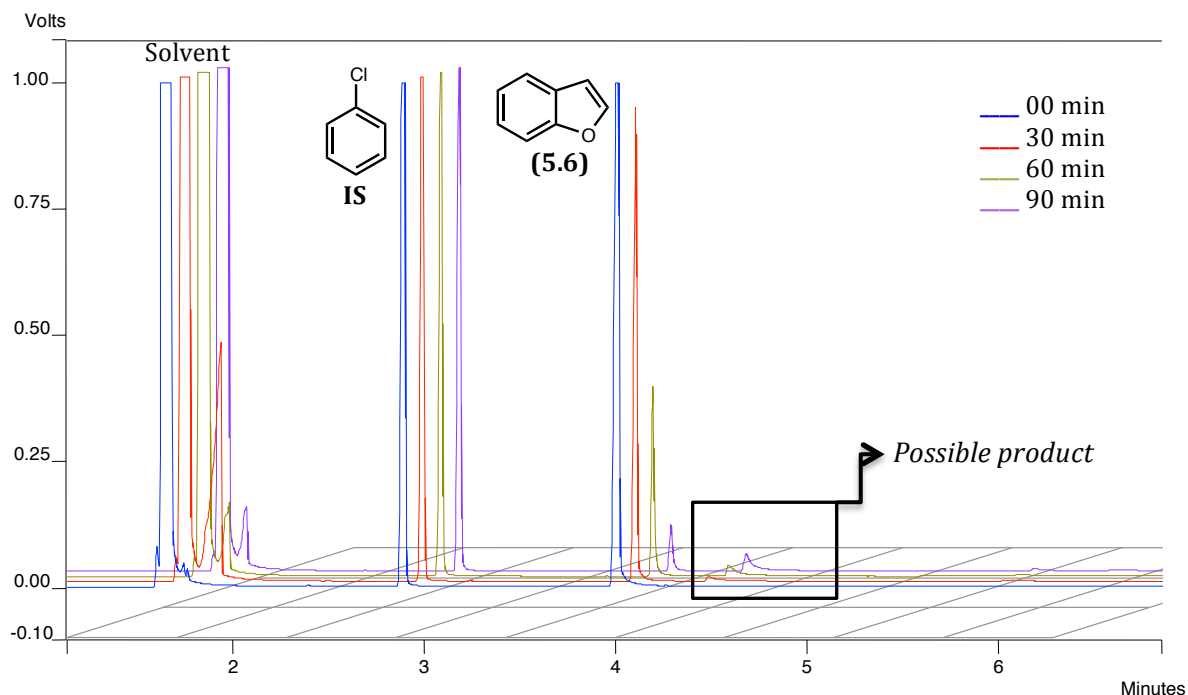
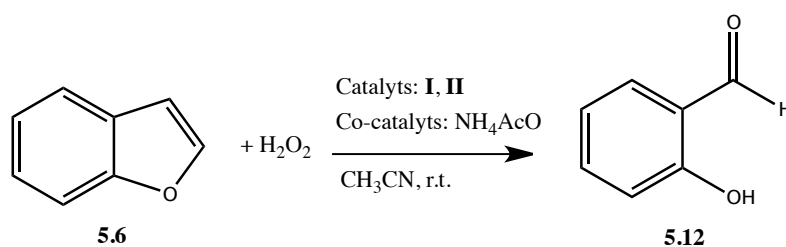


**Figure 5-4** GC-FID chromatograms for substrate **5.6** oxidation by  $\text{H}_2\text{O}_2$  using catalyst **I**

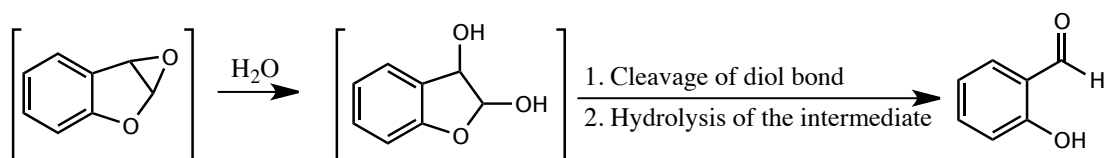
It should be mentioned that before this analysis is necessary to separate the paramagnetic manganese(III) catalyst; it was found that the most appropriate procedure involves the separation of the catalyst through a small alumina column using  $\text{CH}_2\text{Cl}_2$  as eluent followed by its evaporation under vacuum (bath temperature  $30^\circ\text{C}$ ). The GC, TLC and NMR analysis confirmed the formation of the aldehyde **5.12** as the only product of the reaction (Scheme 5-2).



**Scheme 5-2**

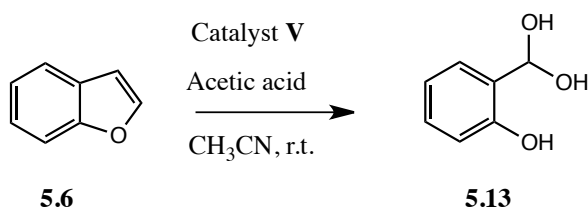
The formation of **5.12** can be explained according to the pathway presented in Scheme 5-3: i) epoxidation of furan ring double bond; ii) epoxide ring opening by water nucleophilic attack; iii) cleavage of the diol C-C bond, followed by hydrolysis of the obtained intermediate.





Scheme 5-3

The oxidation of benzofuran **5.6** by  $\text{H}_2\text{O}_2$  reveals to be highly sensitive to the reaction conditions and, in the case of catalyst **V**, where the co-catalyst is acetic acid instead of ammonium acetate, a different product is detected ( $R_t = 6.12$  min). Moreover, the above-mentioned problem concerning the intensity of the peak corresponding to **5.12**, is maintained in the new oxidation product detected. At the end of reaction, and after removing complex **V** from the mixture, the mono and bidimensional NMR analysis allowed the unequivocal identification of proton and carbon resonances that support the proposed structure **5.13** as the only oxidation product (Scheme 5-4). In  $^1\text{H}$  NMR the typical resonance of the aldehyde proton (singlet at  $\delta = 9.91$  ppm) is not detected. It is described in the literature that aldehydes (and also ketones), in aqueous media and under acid conditions, present the ability to efficiently form geminal diols, by hydration of the carbonyl group. Possibly, the use of acetic acid as co-catalyst favors the formation of the hydrate **5.13** with the catalytic system **V**/ $\text{H}_2\text{O}_2$ .



Scheme 5-4

Finally, for the catalytic system **III** /  $\text{H}_2\text{O}_2$  evaluated with this substrate, the use of ethanol and the absence of a co-catalyst result in the formation of a more complex mixture of products, as can be observed in Figure 5-5. Despite all the efforts to identify the products, using the available characterization techniques such as NMR and MS, it was not possible to assign a correct structure to any of the reaction products. The application of the usual procedure to remove the catalyst, followed by NMR analysis of the reaction mixture led to an extremely complex spectrum. Also, the attempted purification of the detected products by TLC, over silica plates with indicator, using  $\text{CH}_2\text{Cl}_2$  as eluent, resulted in their degradation being thus impossible

to disclose any putative structure. The chromatograms obtained from the monitoring of the reaction put in evidence the efficiency of the catalyst, since after 3 hours of reaction almost all the substrate is converted. All the products detected present higher retention times comparatively to the already disclosed products for the Mn(III) catalytic systems. We hope to finish this part of the work in a near future.

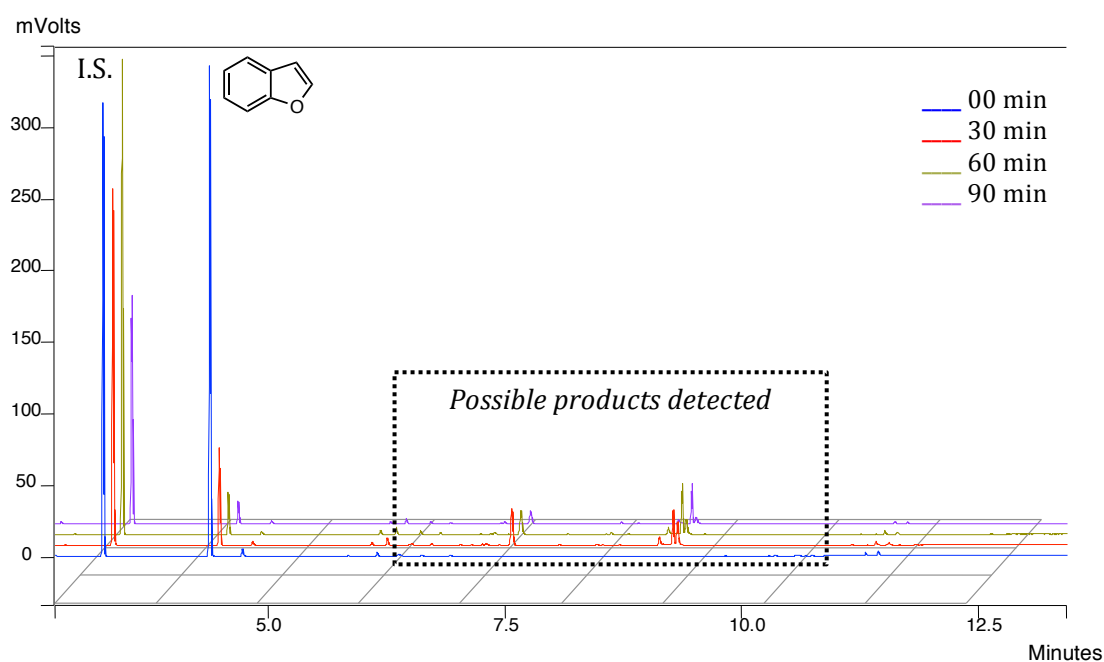


**Figure 5-5** GC-FID chromatograms for the oxidation of **5.6** by H<sub>2</sub>O<sub>2</sub> using catalyst **III**

### 5.2.2. CATALYTIC OXIDATION OF 2-METHYLBENZOFURAN (5.7)

The catalytic experiments using the selected metalloporphyrin complexes, substrate **5.7** and H<sub>2</sub>O<sub>2</sub> as oxidant, also emphasize the high reactivity of the epoxide intermediate formed. Under the evaluated conditions in the presence of Mn(III) porphyrins, despite the total consumption of the substrate, no products were detected by GC-FID, as can be observed in Figure 5-6 for catalyst **I**. However, the separation of metalloporphyrin catalyst from the reaction crude allowed the obtention of the NMR spectra of the reaction mixtures, which confirmed the presence of several products (at least three). The characteristic **5.12** NMR signals at  $\delta = 9.91$  and  $\delta = 11.03$  ppm allowed the identification of this aldehyde as one of the reaction products. The GC-MS analysis of the reaction mixture from the NMR tube confirmed the presence of three major compounds with MW= 122.0, 164.2 and 254.2. The

compound with MW= 122.0 is in agreement with the identified salicylaldehyde by NMR.

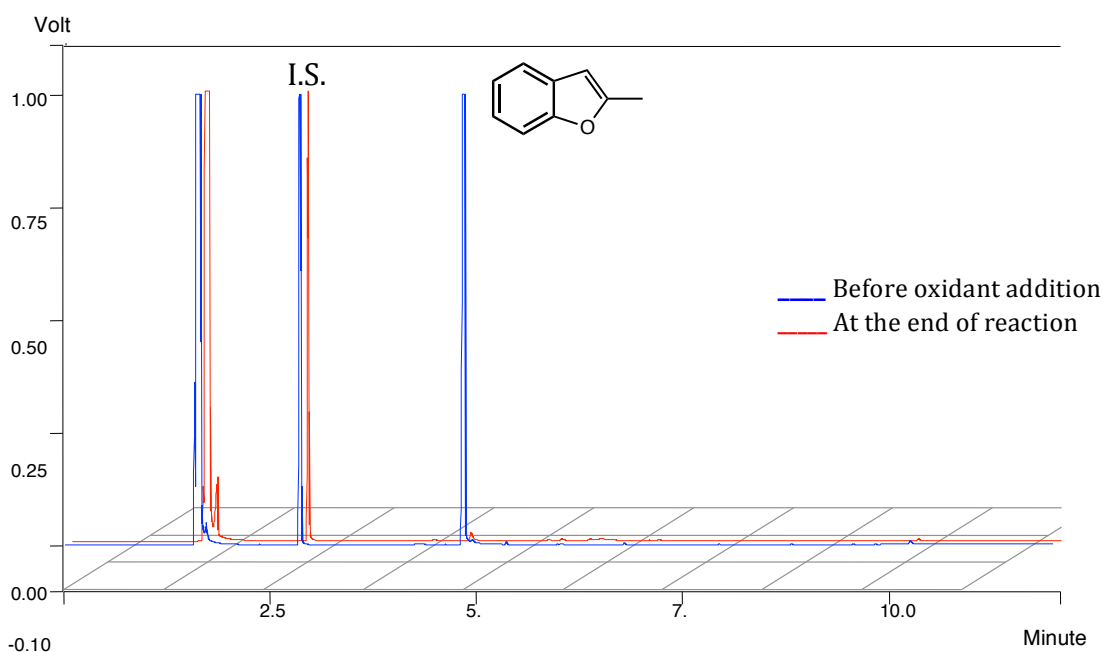
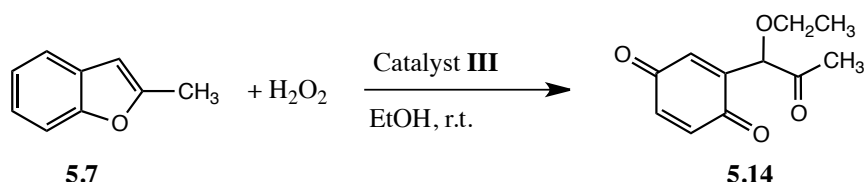


**Figure 5-6** GC-FID chromatograms of the oxidation of **5.7** by H<sub>2</sub>O<sub>2</sub> using catalyst **I**

Although by NMR analysis of the mixtures some important resonances are detected, namely singlets at 12.3 and 8.76 ppm and doublets at 4.10 and 5.56 ppm, only with this data it was impossible to disclose the structure of the other products. So, it was tried to purify the reaction mixture by chromatography but without success. Also, it was tried to silylate the products obtained, using trimethylchlorosilane in order to facilitate their identification by GC-MS. Unfortunately all these attempts did not allow to identify the other two major compounds. The possible explanations for this failure can lie on the instability of the achieved compounds towards the purification processes.

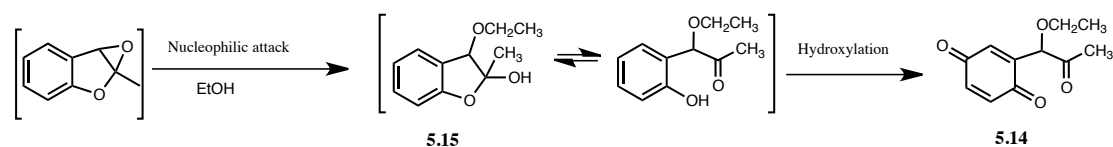
With the iron porphyrin catalyst **III** a different reaction profile was observed. A main intermediate seen at the beginning of the reaction is almost converted at the end of the reaction in a stable product. The <sup>1</sup>H and <sup>13</sup>C NMR spectra (mono and bi-dimensional experiences) of the final reaction mixture after filtration by a small alumina column to remove **III**, allowed to propose structure **5.14** for the only oxidation product obtained (Scheme 5-5). The <sup>1</sup>H NMR spectrum presents resonances ranging between 6.75-6.82 ppm due to the quinone protons and the <sup>13</sup>C spectrum presents the carbon resonances

at 186.2 and 187.0 ppm consistent with the presence of quinone carbonyl groups in the ring; the carbon with higher chemical shift at 204.4 ppm is in agreement with the alkyl substituted ketone. The resonances in the aliphatic region are in agreement with the proposed structure.



Scheme 5-5

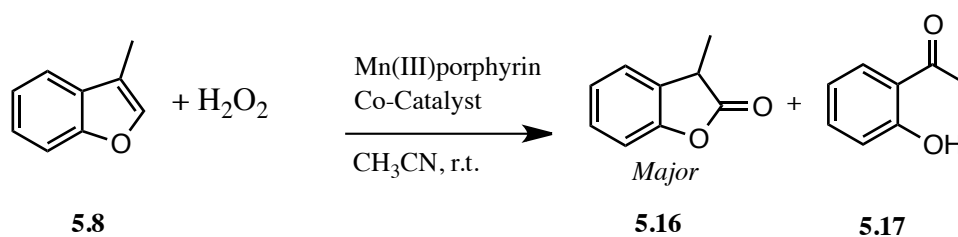
The observations by GC-MS and the formation of quinone **5.14** can be explained by the proposed route shown in Scheme 5-6. The epoxide after being formed in the first step, undergoes nucleophilic attack by ethanol affording intermediate **5.15** with  $R_t=7.44$  min and MW= 194.1. Further hydroxylation of the aromatic ring affords quinone **5.14** (MW= 208,  $R_t=7.88$  min) as the final oxidation product. Interestingly this extra hydroxylation of aromatic ring was only detected with the iron complex **III** and not with Mn(III)porphyrins.



Scheme 5-6

### 5.2.3. CATALYTIC OXIDATION OF 3-METHYLBENZOFURAN (**5.8**)

In the oxidation of substrate **5.8** by hydrogen peroxide in the presence of the manganese(III) porphyrin complexes, the GC-FID analysis showed a similar profile for all the catalysts: **5.8** is fully converted into two products presenting retention times of 5.25 and 6.01 minutes, being the last one clearly the more abundant. After the established procedure to separate the catalyst from the crude reaction, the NMR analysis confirms the obtention of two products, which were identified as lactone **5.16**, the major product, and acetophenone **5.17** (Scheme 5-7).



Scheme 5-7

As demonstrated in Figure 5-7, the characteristic and distinct resonances of -CH<sub>3</sub> protons of both products are easily identified, appearing at high fields, one with lower chemical shift (1.57 ppm) belonging to **5.16** and the other (2.64 ppm) to 2'-hydroxyacetophenone **5.17**. On the opposite side of the spectrum the singlet attributed to the resonance of the proton of the hydroxyl group of **5.17** (12.3 ppm) is also easily distinguished.

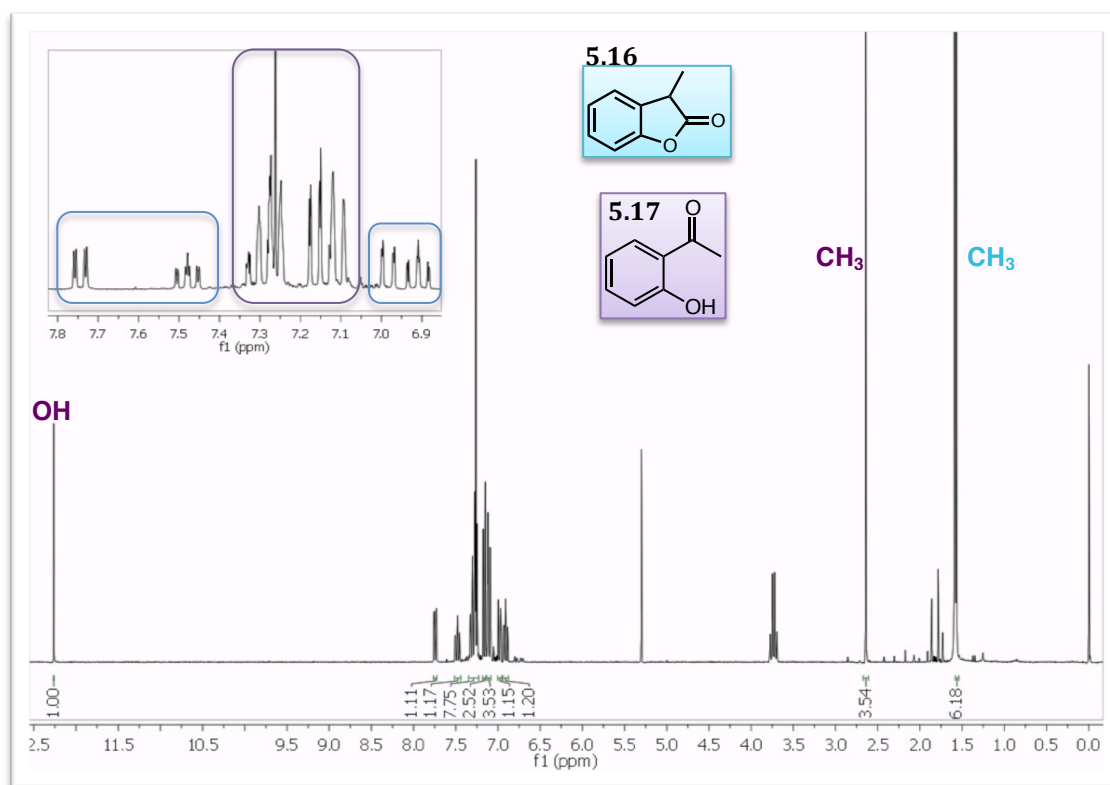


**Figure 5-7** <sup>1</sup>H NMR spectrum of the reaction mixture for substrate **5.8** oxidation using catalyst **I** and H<sub>2</sub>O<sub>2</sub>

In terms of the selectivity exhibited by the three Mn(III) porphyrins, as emphasized in Table 5-2, the preferential formation of **5.16** (determined by GC-FID) is notorious; the cationic complex **V** behaves as the most selective, giving almost exclusively **5.16**.



The formation of benzofuranones as **5.16** has already been described, and results from the thermal rearrangement of the corresponding epoxide.<sup>23</sup> It is interesting to note that **5.16** can also be obtained from **5.7** by a 1,2-alkyl migration. However in our experiments with **5.7**, under the same reaction conditions, we were not able to detect its formation. Relatively to the obtention of **5.17**, this is the corresponding product obtained by a similar pathway as salicylaldehyde **5.12** in the oxidation **5.6**.

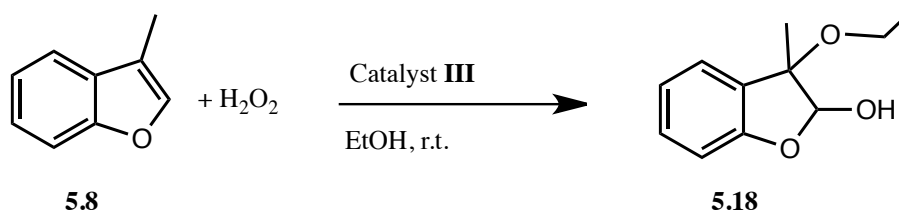
The GC-MS analysis of **5.16** and **5.17** corroborate the proposed structures by NMR; both were identified by the library of the apparatus, and the major product formed presents a  $m/z=147.8$  (in accordance with the MW=148.16 of benzofuranone **5.16**) whereas the other has a  $m/z=136.15$  (in agreement with the MW=136.15 of acetophenone **5.17**).

**Table 5-2** Selectivity observed with Mn(III) catalysts **I**, **II**, **V** in the oxidation of benzofuran **5.8** by H<sub>2</sub>O<sub>2</sub>

Catalyst	S/C Molar Ratio	Conversion (%)	Time (Min)	Selectivity <sup>a</sup>	
				<b>5.16</b>	<b>5.17</b>
I	300	99.7	120	91.9	8.1
I	150	99.9	90	88.3	11.7
II	300	79.9	270	86.8	13.2
II	150	84.3	180	87.0	13.0
V	300	99.8	120	98.8	1.1
V	150	99.9	90	98.4	1.6

<sup>a</sup> calculated from the GC-FID peak integration areas and are the result of the average of two assays

As observed for the other two benzofuran derivatives (**5.6** and **5.7**) the oxidation of **5.8** by H<sub>2</sub>O<sub>2</sub> using metalloporphyrin **III** also affords a distinct product, resulting not only from the involvement of an iron(III) catalyst but also from the different reaction conditions. After the usually performed characterization techniques, it was possible to suggest structure **5.18** to the only product detected from the oxidation of **5.8** by H<sub>2</sub>O<sub>2</sub> using catalyst **III** (Scheme 5-8). The GC-MS shows a peak at  $m/z=194.0$  which is in accordance with the molecular weight (MW=194.2) of **5.18**. Similarly to the oxidation of benzofuran **5.7**, under similar conditions, the corresponding epoxide suffers ring opening by ethanol nucleophilic attack.



Scheme 5-8

Interestingly, and contrary to what happened with substrate **5.7**, under similar reaction conditions the hydroxylation on the aromatic ring of **5.8** was not detected by NMR. Despite that, a small peak with higher retention time at  $m/z= 210.1$  can be seen by GC-MS which can indicate that, in fact, this occurs even at much lower extension.

### 5.3. CONCLUSIONS

The catalytic experiments with metalloporphyrins **I-III** and **V**, involving the oxidation of benzofurans by H<sub>2</sub>O<sub>2</sub>, proved the high efficiency of these catalytic systems since conversions higher than 80% are always attained, for both S/C molar ratios used (300 and 150). Moreover, for all the experiments performed the preferential pathway seems to be the epoxidation of the double bond of the furan ring. Despite that, the Fe(III) complex **III** was able to catalyze the hydroxylation of the aromatic ring in substrates **5.7** and **5.8**.

Nevertheless, despite all the problems related with the identification of some of the attained products (some not solved yet and further experiments will be needed), it was possible to identify several products resulting always from the decomposition of the unstable and very reactive epoxides. From the structures of the oxidation products already disclosed, the influence of the catalyst employed and of the reaction conditions (namely the solvent or the co-catalyst) is evident. The unsubstituted benzofuran **5.6**, besides affording different products with Mn(III) or Fe(III) also presents a distinct reactivity in the presence of catalyst **V**/acetic acid/H<sub>2</sub>O<sub>2</sub> catalytic system.

To our knowledge, the work described seems to be the first application of such biomimetic catalytic systems to the oxidation of benzofuran derivatives. Although the work is not finished, this approach and the already achieved results can significantly contribute to the understanding of the reactivity of these organic compounds.



## 5.4. EXPERIMENTAL

All the reagents and solvents described in this chapter were used as received without further purification. The benzofurans **5.6-5.8** were purchased from Aldrich.

All the purifications were carried out using silica gel 60 F<sub>254</sub> from Merck. The description of all the equipment involved in the NMR, GC-FID and GC-MS analyses can be seen in section 3.3 of this dissertation.

### 5.4.1. CATALYTIC EXPERIMENTS

The catalytic experiments involving substrates **5.6-5.8** were performed according to the general procedure described in 3.3.1. However, it must be emphasized herein that after the end of the reactions in order to properly characterize the resulting compounds, the careful protection from the light is advised and the use of vacuum should be avoided. Whenever possible, the purification of the products was performed by direct application of the reaction mixture over a small alumina column using CH<sub>2</sub>Cl<sub>2</sub> as eluent. The evaporation of the solvent was always done at the lowest temperature possible.

The GC-FID analyses to monitor the evolution of the oxidative transformations was carried out every 30 minutes using the following temperature program: column initial temperature 70 °C for 1 min.; increasing temperature rate of 20°C/min up to 270 °C, for 1 min (full program total time of 12 minutes); injector temperature 270 °C; detector temperature 280°C.

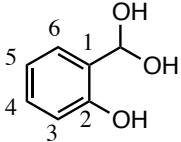
### 5.4.2. CHARACTERIZATION OF THE ISOLATED OXIDATION PRODUCTS

#### *Salicylaldehyde (5.12)*

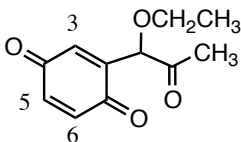
	<sup>1</sup> H NMR (CDCl <sub>3</sub> , 300 MHz) δ (ppm): 6.99-7.06 ( <i>m</i> , 2H, Ar-H), 7.52-7.59 ( <i>m</i> , 2H, Ar-H), 9.91 ( <i>s</i> , 1H, CHO), 11.03 ( <i>s</i> , 1H, -OH). MS (EI) <i>m/z</i> : 122 [M] <sup>+</sup>
--	---



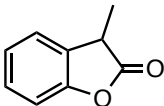
*(2-hydroxyphenyl)methanediol (5.13)*

	$^1\text{H NMR}$ (DMSO- $d_6$ , 300 MHz) $\delta$ (ppm): 2.04 ( <i>s</i> , 2H, -OH geminal), 5.78 ( <i>s</i> , 1H, -C-H), 6.89-6.97 ( <i>m</i> , 2H, H-3,4), 7.32 ( <i>dt</i> , 1H, $J=1.3$ and $J=7.8$ Hz, H-5), 7.40 ( <i>dd</i> , 1H, $J=1.3$ and $J=7.8$ Hz H-6). $^{13}\text{C NMR}$ (DMSO- $d_6$ , 75 MHz) $\delta$ (ppm): 78.7 (-C(OH) $_2$ ), 110.3 (C-3), 121.0 (C-4), 123.9 (C-2), 127.1 (C-6), 131.3 (C-5), 160.0 (-C-1). MS (EI) $m/z$ : 140 [M] $^{+}$
---	--

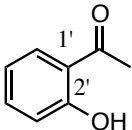
*2-(1-ethoxy-2-oxopropyl)cyclohexa-2,5-diene-1,4-dione (5.14)*

	$^1\text{H NMR}$ (CDCl $_3$ , 300 MHz) $\delta$ (ppm): 1.26 ( <i>t</i> , 3H, $J=7.0$ Hz, -CH $_2$ -CH $_3$ ), 2.29 ( <i>s</i> , -CH $_3$ ), 3.60 ( <i>q</i> , 2H, $J=7.0$ Hz, -CH $_2$ ), 4.83 ( <i>s</i> , 1H, -C-H), 6.75-6.80 ( <i>m</i> , 2H, H-5,6) 6.83 ( <i>s</i> , 1H, H-3). $^{13}\text{C NMR}$ (CDCl $_3$ , 75 MHz) $\delta$ (ppm): 15.1 (-CH $_2$ -CH $_3$ ), 26.6 (-CH $_3$ ), 67.0 (-CH $_2$ ), 80.8 (C-H), 133.0 (C-3), 136.5 (C-5 and C-6), 186.2 (C-1 or C-4), 187.0 (C-1 or C-4), 204.5-(C=O) MS (EI) $m/z$ : 208 [M] $^{+}$
---	--

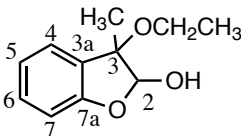
*3-methylbenzofuran-2(3H)-one (5.16)*

	$^1\text{H NMR}$ (CDCl $_3$ , 300 MHz) $\delta$ (ppm): 1.58 (broad <i>d</i> , 3H, $J=7.4$ Hz, -CH $_3$ ), 3.72 ( <i>q</i> , 1H, $J=7.4$ Hz, -CH), 7.11 (broad <i>d</i> , 1H, $J=7.7$ Hz, -H-Ar), 7.16 ( <i>dd</i> , 1H, H-Ar) 7.25-7.33 ( <i>m</i> , 2H, H-Ar). MS (EI) $m/z$ : 147 [M] $^{+}$
--	---

*2'-hydroxyacetophenone (5.17)*

	$^1\text{H NMR}$ (CDCl $_3$ , 300 MHz) $\delta$ (ppm): 2.64 ( <i>s</i> , 3H, -CH $_3$ ), 6.90 ( <i>ddd</i> , 1H, $J=1.0$ , $J=6.6$ and $J=8.5$ Hz, H $'$ -4 or H $'$ -5), 6.98 ( <i>dd</i> , 1H, $J=1.0$ and $J=8.5$ Hz, H-3'), 7.48 ( <i>ddd</i> , 1H, $J=1.7$ , $J=6.6$ and $J=8.5$ Hz, H $'$ -4 or H $'$ -5), 7.74 ( <i>dd</i> , 1H, $J=1.7$ and $J=8.5$ Hz, H-3' or H-6'). MS (EI) $m/z$ : 135 [M] $^{+}$
---	--

*3-ethoxy-3-methyl-2,3-dihydrobenzofuran-2-ol (5.18)*

	$^1\text{H NMR}$ (CDCl $_3$ , 300 MHz) $\delta$ (ppm): 1.13 ( <i>t</i> , 3H, $J=4.2$ Hz, -CH $_2$ -CH $_3$ ), 1.58 ( <i>s</i> , -CH $_3$ ), 3.26-3.50 ( <i>m</i> , 2H, -CH $_2$ ), 4.83 ( <i>d</i> , 1H, $J=7.0$ Hz, -O-H), 5.50 ( <i>d</i> , 1H, $J=7.0$ Hz, -CH), 6.84-6.93 ( <i>m</i> , 2H, H-Ar) 7.24-7.28 ( <i>m</i> , 2H, H-Ar). $^{13}\text{C NMR}$ (CDCl $_3$ , 125 MHz) $\delta$ (ppm): 15.4 (-CH $_2$ -CH $_3$ ), 19.8 (-CH $_3$ ), 58.8 (-CH $_2$ ), 78.2 (C-3), 106.8 (C-2), 110.8 (C-4 or C-7), 120.4 (C-5 or C-6), 124.8 (C-4 or C-7), 127.3 (C-3a) 130.7 (C-5 or C-6), 157.5 (C-7a) MS (EI) $m/z$ : 194 [M] $^{+}$
---	--

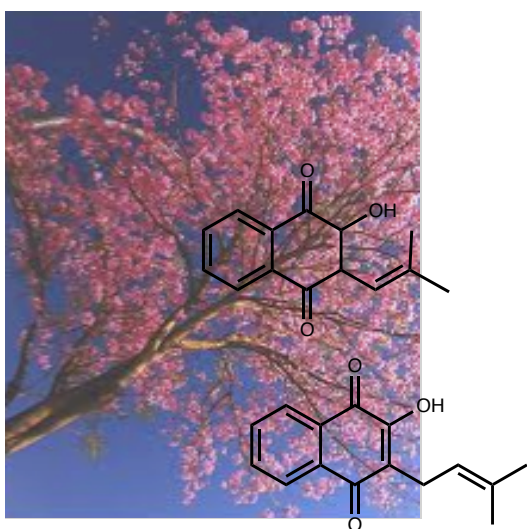


## 5.5. BIBLIOGRAPHY

- <sup>1</sup> G.K. Rao, K.N. Venugopala, P.N.S. Pai, *J. Pharmacol. Toxicol.* 2 (2007) 481.
- <sup>2</sup> a) M. Koca, S. Servi, C. Kirilmis, M. Ahmedzade, C. Kazaz, B. Özbek, G. Ötük, *Eur. J. Med. Chem.* 40 (2005) 1351. b) A. Urzúa, M.C. Rezende, C. Mascayano, L. Vásquez, *Molecules* 13 (2008) 882. c) K. Manna, Y.K. Agarwal, *Bioorg. Med. Chem. Lett.* 19 (2009) 2688.
- <sup>3</sup> a) L. Santana, M. Teijeira, E. Uriarte, C. Teran, B. Liñares, R. Villar, R. Laguna, E. Cano, *Eur. J. Pharm. Sci.* 7 (1999) 161. b) K.M. Dawood, H. Abdel-Gawad, E.A. Rageb, M. Ellithey, H.A. Mohamed, *Bioorg. Med. Chem.* 1 (2006) 3672.
- <sup>4</sup> a) L. Pieters, S.V. Dyck, M. Gao, R. Bai, E. Hamel, A. Vlietinck, G. Lemièrre, *J. Med. Chem.* 42 (1999) 5475. b) I. Hayakawa, R. Shioya, T. Agatsuma, H. Furukawa, S. Naruto, Y. Sugano, *Bioorg. Med. Chem. Lett.*, 14 (2004) 455. c) S.A. Galal, E.A. Abd, M.M. Abdullah, H. EL-Diwani, *Bioorg. Med. Chem. Lett.* 19 (2009) 2420.
- <sup>5</sup> A.H. Banskota, Y. Tezuka, K. Midorikawa, K. Matsushige, S. Kadota, *J. Nat. Prod.* 63 (2000) 1277.
- <sup>6</sup> a) P.G. Wyatt, M.J. Allen, J. Chilcott, C.J. Gardner, D.G. Livermore, J.E. Mordaunt, F. Nerozzi, M. Patel, M.J. Perren, G.G. Weingarten, S. Shabbir, P. M. Woollard, P. Zhou, *Bioorg. Med. Chem. Lett.* 12 (2002) 1405. b) B. Carlsson, B.N. Sing, M. Temcius, S. Nilsson, Y.-L. Li, C. Mellin, J. Malm, *J. Med. Chem.* 45 (2002) 623. c) K. M. Zareba, *Drugs Today* 42 (2006) 75.
- <sup>7</sup> M. Ono, H. Kawashima, A. Nonaka, T. Kawai, M. Haratake, H. Mori, M. Kung, H.F. Kung, H. Saji, M. Nakayama, *J. Med. Chem.* 49 (2006) 2725.
- <sup>8</sup> N.T. Patil, Y. Yamamoto, *Chem. Rev.* 108 (2008) 3395.
- <sup>9</sup> W.A.L. van Otterlo, C.B. de Koning, *Chem. Rev.* 109 (2009) 3743.
- <sup>10</sup> B. Godoi, R. F. Schumacher, G. Zeni, *Chem. Rev.* 111 (2011) 2937.
- <sup>11</sup> A.R. Katritzky, S. Rachwal, *Chem. Rev.* 111 (2011) 7063.
- <sup>12</sup> X.-F. Wu, H. Neumann, M. Beller, *Chem. Rev.* 113 (2013) 1.
- <sup>13</sup> R. Zhu, J. Weia, Z. Shi, *Chem. Sci.* 4 (2013) 3706.
- <sup>14</sup> A. Abu-Hashem, H.A.R. Hussein, A.S. Aly, M.A. Gouda, *Synth. Commun.: Int. J. Rapid Commun. Synth. Org. Chem.* 44 (2014) 2899.
- <sup>15</sup> a) D. Nematollahi, Z. Forooghi, *Tetrahedron* 58 (2002) 4949. b) D. Nematollahi, D.J. Habibi, *J. Org. Chem.* 69 (2004) 2637. c) D. Nematollahi, M.J. Rafiee, *Electroanal. Chem.* 566 (2004) 31. d) D. Nematollahi, M. Rafiee, *Green Chem.* 7 (2005) 638.
- <sup>16</sup> L.-X. Pei, Y.-M. Li, X.-Z. Bu, L.-Q. Gu, A.S.C. Chan, *Tetrahedron Lett.* 47 (2006) 2615.
- <sup>17</sup> S. Witayakran, L. Gelbaum, A.J. Ragauskas, *Tetrahedron* 63 (2007) 10958.

- <sup>18</sup> G.A Junk., C.S. Ford, *Chemosphere* 9 (1980) 187.
- <sup>19</sup> D.E. Seizinger, B. Dimitriades, *J. Air Pollut. Control Assoc.* 22 (1972) 47.
- <sup>20</sup> J.C. Connelly, S.C. Connor, S. Monte, N.J.C. Bailey, N. Borgeaud, E. Holmes, J. Troke, J.K. Nicholson, C.L. Gavaghan, *Drug Met. Dispos.* 30 (2002) 1357.
- <sup>21</sup> M.M.Q Simões, M.G.P.M.S. Neves, J.A.S. Cavaleiro, *Jordan J. Chem.* 1 (2006) 1.
- <sup>22</sup> M.M.Q. Simões, R. De Paula, M.G.P.M.S. Neves, J.A.S. Cavaleiro, *J. Porphyrins Phthalocyanines* 13 (2009) 589.
- <sup>23</sup> M. Sauter, W. Adam, *Acc. Chem. Res.* 28 (1995) 289.
- <sup>24</sup> W. Adam, M. Sauter, *Tetrahedron* 50 (1994) 11441.
- <sup>25</sup> W. Adam, M. Ahrweiler, M. Saute, *Chem. Ber.* 127 (1994) 941.





## Chapter 6 BIOMIMETIC OXIDATION OF NAPHTHOQUINONES



Chapter based on the following publication:

- "Novel biomimetic oxidation of lapachol with  $H_2O_2$  catalyzed by a manganese(III) porphyrin complex", S.M.G Pires, R. De Paula, M.M.Q. Simões, A.M.S Silva, M.R.M Domingues, I.C.M.S. Santos, M.D. Vargas, V.F. Ferreira, M.G.P.M.S. Neves, J.A.S. Cavaleiro, *RSC Advances*. 1 (2011) 1195.

## 6. BIOMIMETIC OXIDATION OF NAPHTHOQUINONES

### 6.1. OVERVIEW

It is already established that the presence of the quinone structure in several naturally occurring compounds is associated with their potential biological activity.<sup>1-3</sup> Usually this activity is related with quinones ability to accept electrons and sometimes to their acid-base properties. In fact these molecules demonstrate the capacity to interact with topoisomerases and to generate semiquinone radicals and reactive oxygen species inside the cell.<sup>4</sup> Plants containing naphthoquinones are widely used in Southeast Asia and South America to treat malignant and parasitic diseases.<sup>5,6</sup>

Lapachol (**6.1**) is the most abundant, naturally occurring naphthoquinone, found in the heartwood of several trees of the *bignoniaceae* family, and pure is a light to dark yellow crystalline powder.<sup>5,7</sup> Since it was first isolated by Arnaudon in 1858,<sup>8</sup> lapachol has been studied by several authors and proved to be one of the most versatile biologically active compounds.<sup>9-15</sup> Besides the extraction<sup>16</sup> it can also be synthesized with good yields in six chemical steps using Pd-catalyzed allylation of lawsone with isopentenyl alcohol or isopentenyl methyl ether.<sup>17</sup> More recently, other methodologies have been described like coupling of lawsone phenyliodonium ylide with activated arenes and aromatic aldehydes<sup>18</sup> or the reduction of *o*-quinone methides to the corresponding 3-alkyl-2-hydroxy-1,4-naphthoquinones.<sup>19</sup>

Lapachol (**6.1**) and several of its derivatives (Figure 6-1), especially *ortho*- and *para*-naphthoquinones (**6.3-6.7**), are associated to a broad spectrum of biological activities ranging anti-tumour, antibiotic, anti-malarial, anti-inflammatory and anti-ulcer, antibacterial, fungicidal and trypanocidal activity. Supported by structural and biological properties of these naphthoquinones, they are nowadays considered privileged structures in medicinal chemistry.<sup>5,20,21</sup> Very recently, Epifano *et al.* published a review regarding the anticancer activity of several 1,4-naphthoquinones, including **6.1**. Authors thoroughly discussed the phytochemical properties and pharmacological effects of the parent compound **6.1** always in the perspective of its potential therapeutic benefits for the future.<sup>22</sup>

For the cited reasons, **6.1** is undoubtedly an ideal candidate for planned structural

modifications in order to develop an understanding of its structure-activity associations and thus, eventually, to develop analogues with improved activity. Besides that, it is also important to identify the metabolites resulting from *in vivo* oxidation of these putative drugs, in order to prevent possible secondary effects reducing unwanted toxicity.

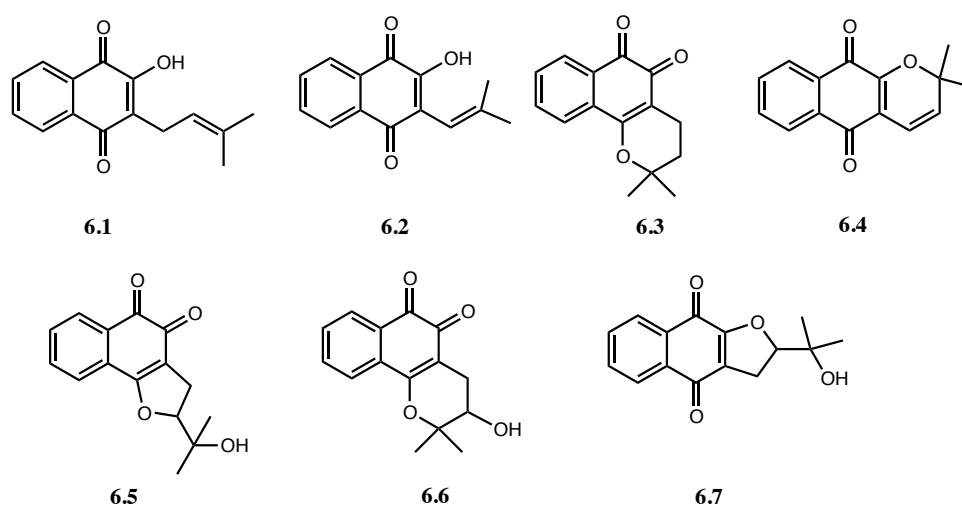


**Figure 6-1** Lapachol (**6.1**) and some of its known derivatives' structure (**6.2-6.7**).

As discussed in chapter 1, many drug metabolites are formed by oxidative processes catalyzed primarily by cytochrome containing enzymes, mainly by cytochrome P-450 monooxygenase enzymes. Several studies have reported potential oxidative metabolites of bioactive compounds, revealing that epoxidation, aliphatic and aromatic hydroxylation or oxidation of the heteroatoms are the most common reactions.<sup>23</sup>

Although the oxidation of (**6.1**) and some of its analogues, especially  $\beta$ -lapachone (**6.3**), have been studied for several decades, almost all the procedures reported so far implicated the use of very aggressive oxidizing conditions and demonstrated little or none environmental concerns. The use of powerful and hazardous oxidants like alkaline  $\text{KMnO}_4$ <sup>24</sup> or *m*-chloroperoxybenzoic acid (*m*-CPBA)<sup>25</sup> is a common feature to all methodologies.

However, in 1999 *Cunningham et al*<sup>26</sup> published a different approach in which they have performed the oxidation of some quinone derivatives in much milder reaction conditions using the iron complex of 5,10,15,20-tetrakis(pentafluorophenyl)porphyrin as catalyst and hydrogen peroxide as oxidant. The use of metalloporphyrins, beyond



mimicking the *in vivo* activity of natural enzymes, allows the oxidation reactions to occur under more environmentally friendly conditions.<sup>27-30</sup>

Taking into account the relevance of the biomimetic oxidation studies of this type of naphthoquinones, and the existing partnership between our group and the group of Professor Victor Ferreira, from Fluminense Federal University, it was possible to perform an interesting work, partly already published, concerning two naphthoquinone derivatives **6.1** and **6.2**.

In the next sections of this chapter the results from the experiments with the catalytic system Mn(TDCPP)Cl (**I**)/H<sub>2</sub>O<sub>2</sub> for the two substrates **6.1** and **6.2** kindly supplied by the Brazilian group will be presented and discussed. For comparative reasons the results of the pioneering approach applied to quinone derivatives are compared to the attained with the traditional oxidation procedure using *m*-CPBA. Furthermore, with substrate **6.1**, in order to ascertain the influence of the porphyrin macrocycle structure in the catalyst performance as also in the isolated products distribution, the catalytic systems Mn(TPFPP)Cl (**II**)/H<sub>2</sub>O<sub>2</sub> and Mn(TDMImP)Cl (**V**)/ H<sub>2</sub>O<sub>2</sub> were also tested.

## 6.2. BIOMIMETIC OXIDATION OF LAPACHOL (6.1) WITH Mn(TDCPP)Cl AS CATALYST

In order to perform the oxidation of lapachol (**6.1**), two distinct approaches were followed: route **A** (using *m*-CPBA) and route **B** (using H<sub>2</sub>O<sub>2</sub> and catalyst **I**), which is a much more environmentally benign procedure. The reactions have been followed by TLC and, in both cases, a total conversion of (**6.1**) was observed. The reactions were complete after 48 hours following route **A**, using 2.5 molar equivalents of *m*-CPBA. For route **B**, the reactions are more efficient and can be performed in 1 hour, depending on the substrate/catalyst molar ratio used. After work-up, the reaction products were purified by preparative TLC and characterized by <sup>1</sup>H and <sup>13</sup>C NMR and by mass spectrometry.

The reaction products obtained, **6.5** and **6.6**, following route **A** (*m*-CPBA) are already known and the structural characterizations are in agreement with those described in the literature.<sup>31-33</sup> On the other hand, the products obtained following route **B** (catalyst (**I**)/H<sub>2</sub>O<sub>2</sub>) are completely different. Just by comparison of the <sup>1</sup>H NMR spectra of **A** and **B** reaction mixtures (Figure 6-2), it is possible to observe the differences between

the products obtained. With *m*-CPBA, almost only *o*-quinones (**6.5**) and (**6.6**) are observed. In contrast, for metalloporphyrin catalyzed reactions the selectivity is completely different and *p*-quinones (**6.4**) and (**6.7**) are preferentially formed.

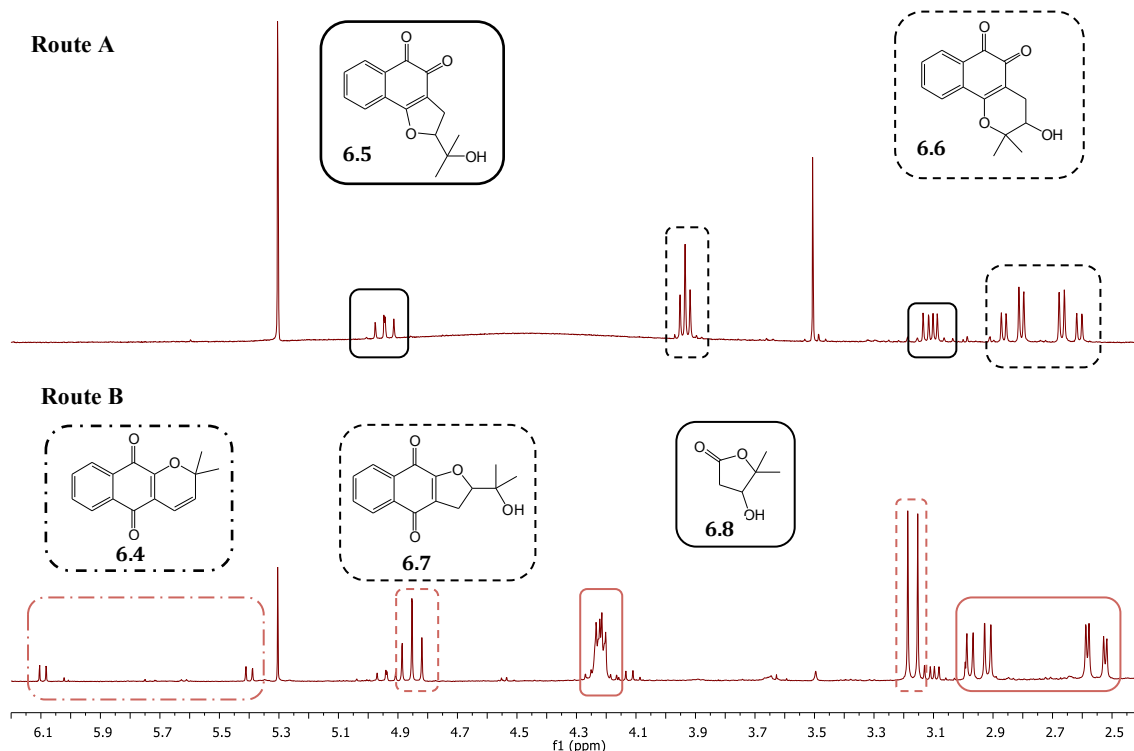


**Figure 6-2** Details of the aliphatic region of <sup>1</sup>H NMR spectra of the oxidation reaction mixtures (Routes A and B) in CDCl<sub>3</sub>.

Comparing with the classical oxidation methodology, the catalytic procedure gives rise at least to three different products. Furthermore, in the catalyzed reactions, a new lactone (**6.8**) is observed. The characterization of **6.8** by <sup>1</sup>H NMR (Figure 6-3), besides allowing the identification of two methyl groups ( $\delta$  1.39 and  $\delta$  1.45 ppm) just put in evidence its non-aromatic character since no protons are detected in the aromatic region of the spectra. The presence of a non-aromatic compound can be justified by the cleavage of lapachol (**6.1**) molecule. This hypothesis is supported by the <sup>13</sup>C NMR spectrum of (**6.8**) since only one carbonyl is observed ( $\delta$  174.4 ppm) and a small number of carbons are registered. The structural confirmation of lactone **6.8** comes also from mass spectrometry; the MS spectrum of **6.8** shows the ion  $[M + H]^+$  at  $m/z$  131. The MS/MS spectrum of this molecular ion allows the identification

of a characteristic fragment ion at  $m/z$  113 (-18 Da) which corresponds to the loss of  $H_2O$ .

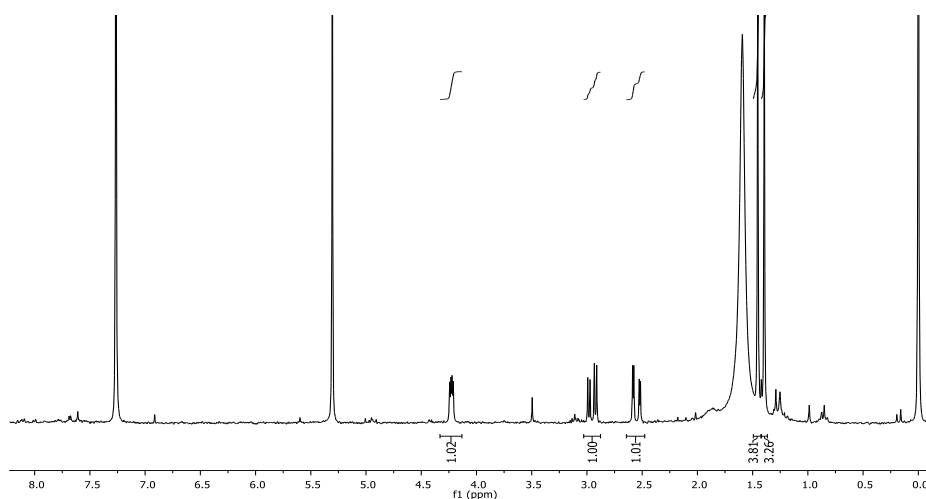


**Figure 6-3**  $^1H$  NMR spectrum of lactone (**6.8**) in  $CDCl_3$

The oxidation results for routes **A** and **B** are summarized in Table 6-1, where the yields have been determined by  $^1H$  NMR, using the spectra of each reaction mixture and the average result from at least two experiments. Mechanistically the obtention of derivatives **6.4** to **6.7** is justified, as presented in Scheme 6-1, within the keto–enol tautomerism of the starting material. The attack of the hydroxyl group to each carbon of the epoxide results in the formation of the corresponding *ortho*- and *para*-naphthoquinones.

Route **B** was performed using different sub/cat molar ratios, namely 75, 150 and 300. From the results obtained, it is possible to conclude that with the increment of catalyst quantity the yield for lactone (**6.8**) increases and the yield for compounds (**6.4**), (**6.5**) and (**6.7**) decreases. The presence of catalyst **I** not only allows the epoxidation of the side chain double bond of (**6.1**), but also the epoxidation of the double bond present in the quinone ring, which gives access to the molecule cleavage. Epoxidation of the quinone ring of **6.1** seems to be a common process to this type of metalloporphyrin catalysts in naphthoquinones oxidation<sup>26</sup> and it is very similar to what is observed with certain microorganisms.<sup>34</sup>

The identification of (**6.8**) showed to be an important feature in order to understand what happens in the oxidation of (**6.1**) following route **B**. From the beginning of the work with this catalytic approach, a weight loss in the recovered material was noticed



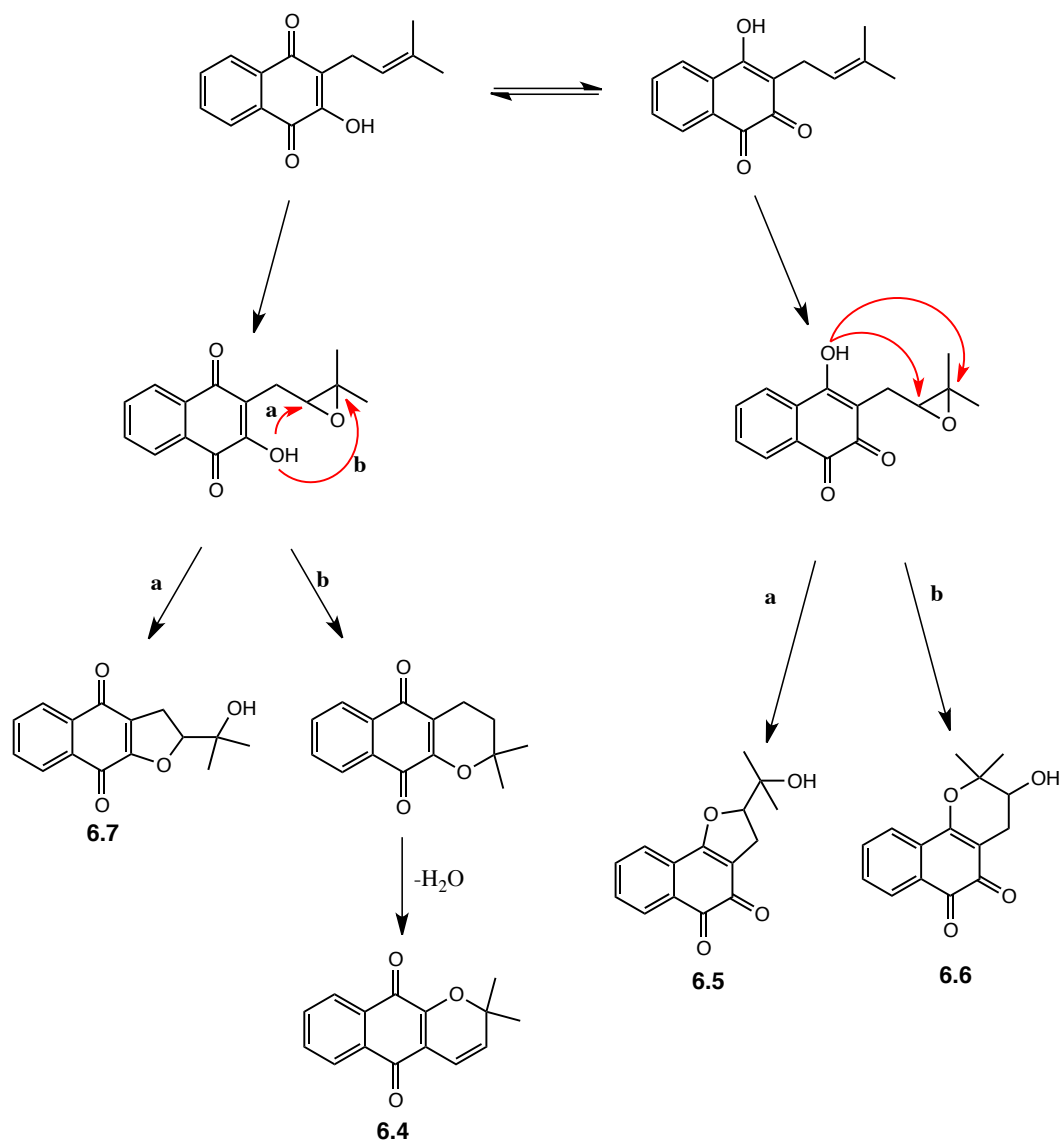
at the end of the reactions. At that point, it proved to be almost impossible, using the already mentioned characterization techniques, to identify other products or even the remaining part of lapachol molecule, even after identifying compound (6.8). Two possible explanations were considered: i) some products formed in the reactions could be lost in the work-up procedure, or ii) the reactions originate some volatile compounds that cannot be isolated by TLC.

**Table 6-1** Oxidation of lapachol (6.1) using routes A<sup>(a)</sup> and B<sup>(b)</sup>. Products (6.4 – 6.8) yields (%) were determined by <sup>1</sup>H NMR

	Route A	Route B		
	<i>m</i> -CPBA	Sub/Cat molar ratio 75:1 (after 60 min)	Sub/Cat molar ratio 150:1 (after 90 min)	Sub/Cat molar ratio 300:1 (after 145 min)
(6.4)	-	4.0	16.4	18.3
(6.5)	26.5	5.9	9.1	12.6
(6.6)	73.5	-	-	-
(6.7)	-	24.5	42.6	44.7
(6.8)	-	65.6	31.9	24.4

<sup>(a)</sup>The substrate (0.075 mmol) was dissolved in 2.0 mL of CH<sub>2</sub>Cl<sub>2</sub> under magnetic stirring at 22 ± 2 °C in the presence of *m*-CPBA (2.5 equiv.).

<sup>(b)</sup>The substrate (0.075 mmol) was dissolved in 2.0 mL of CH<sub>3</sub>CN and kept under magnetic stirring at 22 ± 2 °C in the presence of **I** (for sub/cat molar ratio of 75, the catalyst amount was 1.0 × 10<sup>-3</sup> mmol; for sub/cat molar ratio of 150, the catalyst amount was 5.0 × 10<sup>-4</sup> mmol; for sub/cat molar ratio of 300, the catalyst amount was 2.5 × 10<sup>-4</sup> mmol). The co-catalyst used was NH<sub>4</sub>CH<sub>3</sub>CO<sub>2</sub> (0.12 mmol). The oxidant was progressively added at regular intervals of 15 min in small aliquots, each corresponding to a half-substrate amount.



Scheme 6-1

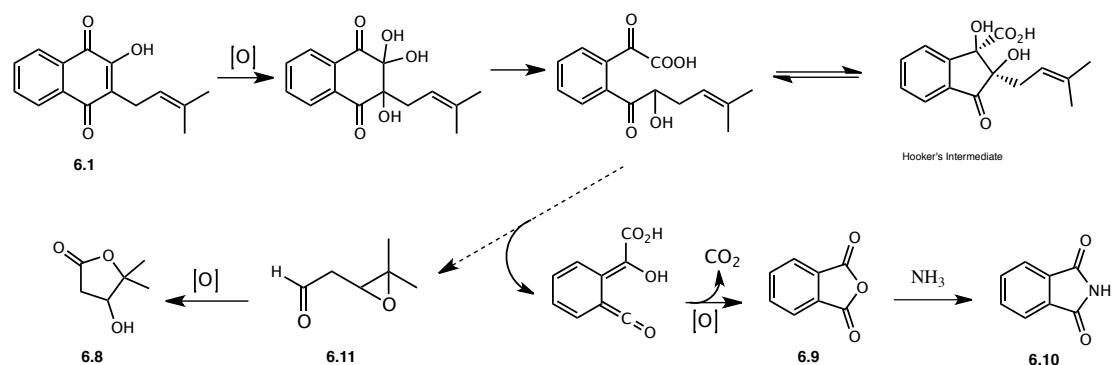
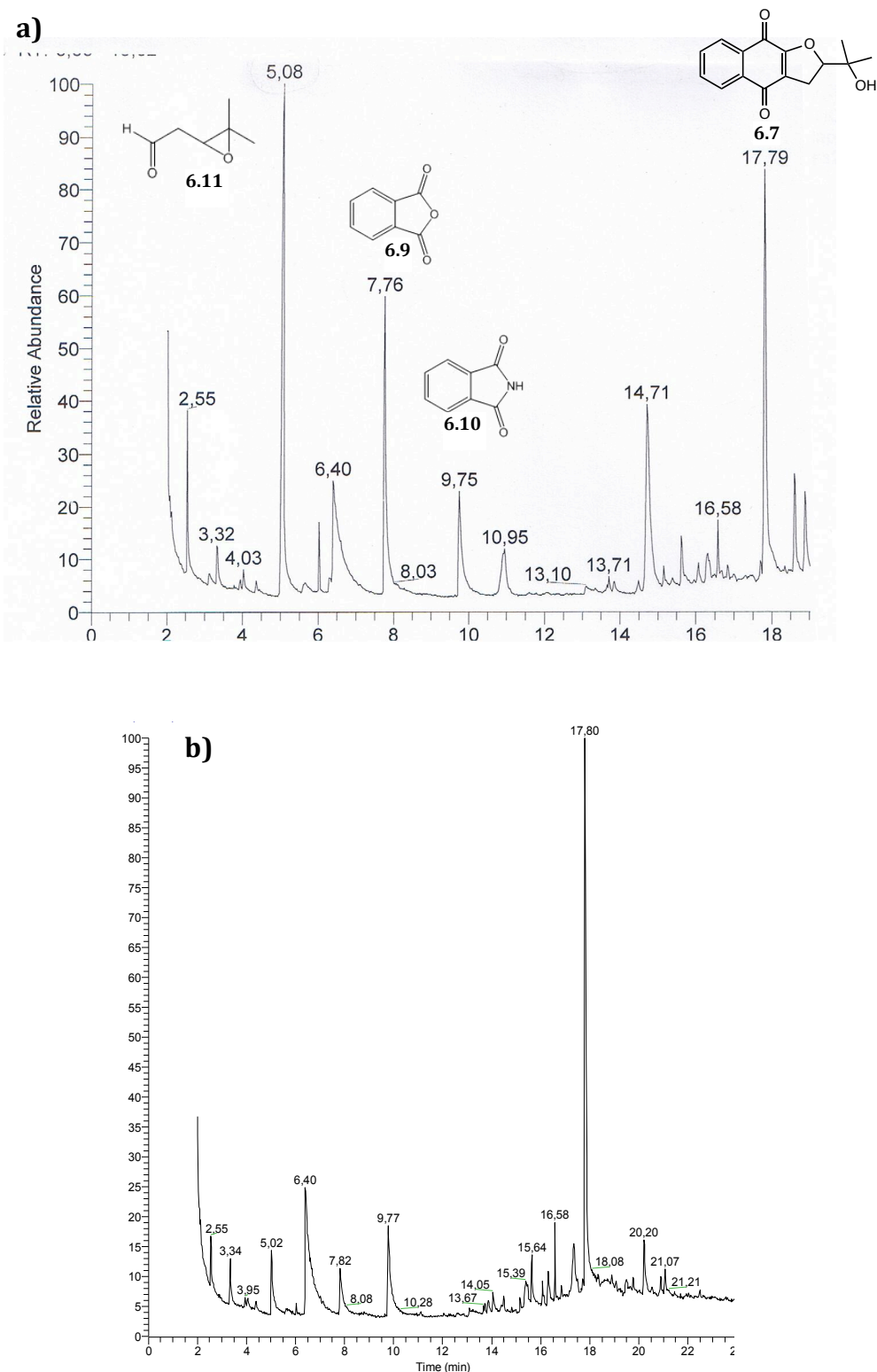


Figure 6-4 Mechanistic proposal to formation of lactone 6.8 and other oxidation products



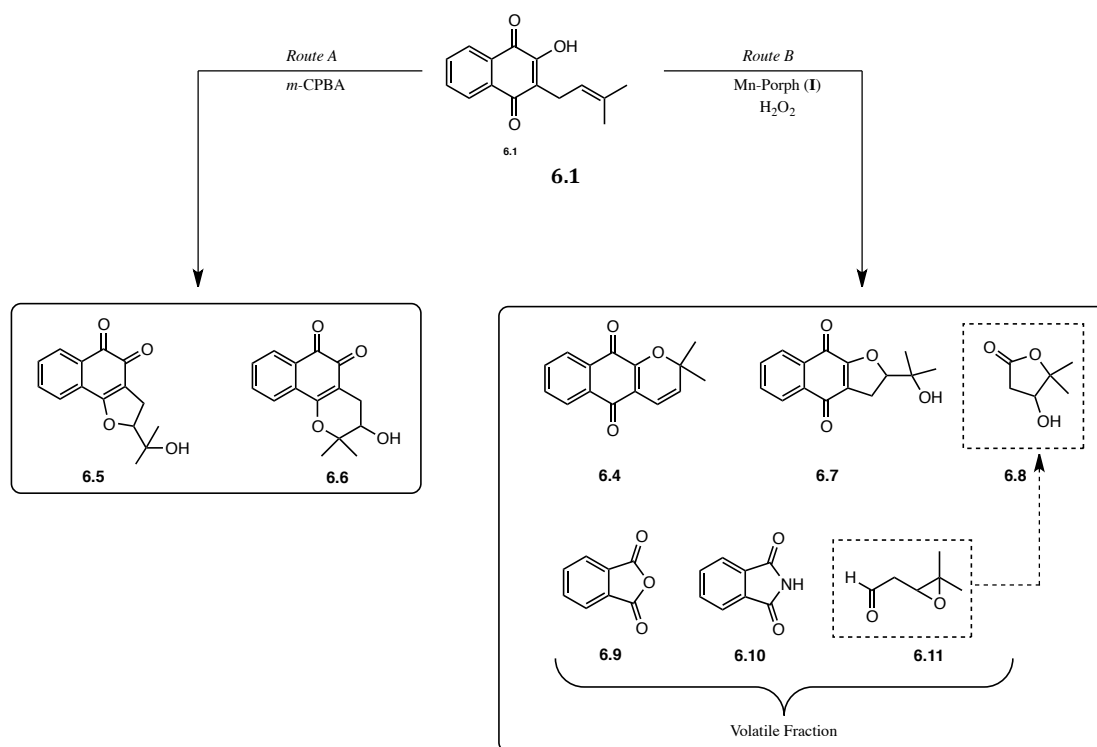
**Figure 6-5** Catalyzed oxidation of 6.1 (Route B) GC-MS Chromatograms a) before the work up and b) after the work up

In order to ascertain the volatile products formation, an aliquot from a Mn-Porph catalyzed reaction was analyzed by GC-MS before and after work-up. The GC-MS

chromatograms obtained before the work-up procedure clearly reveal the presence of the expected phthalic anhydride **6.9** and, at least, two additional products, ortho-phthalimide **6.10** (which is explained by the presence of ammonium acetate as co-catalyst) and epoxide **6.11**, that is actually the precursor of **6.8**, as proposed in Figure 6-4. The C–C cleavage is similar to the first step of Hooker oxidation,<sup>24</sup> the epoxidation of the prenyl moiety and the hydroxyl ketone C–C cleavage give rise to **6.11**. Further oxidation of the aldehyde followed by the ring-opening of the epoxide can justify the formation of lactone **6.8**. Another reaction having **6.9** as substrate was performed under similar conditions; and gave rise to product **6.10**.

The chromatogram of the reaction mixture obtained after work-up [Figure 6-5 b)] showed that almost all the previously detected peaks disappear; only the peak corresponding to quinone (**6.7**) remained unchanged after work-up. This means that the missing volatile reaction products are soluble in water and may be lost during the usual work-up procedure, when the reaction mixture is washed with water.

The products formed with both methodologies (Scheme 6-2) reveal that, besides the lower selectivity achieved with route **B**, different and interesting products are obtained, specially compounds (**6.4**) and (**6.7**), due to their known, important biological activities.<sup>34, 35</sup>



Scheme 6-2

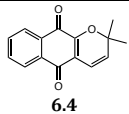
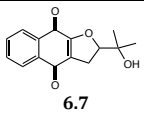
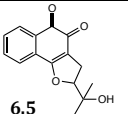
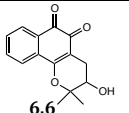


6.2.1. BIOMIMETIC OXIDATION OF LAPACHOL **6.1** IN THE PRESENCE OF Mn(III)  
METALLOPORPHYRINS **II** AND **V**

The good results achieved in the experiments with **6.1** using the catalytic system Mn(TDCPP)Cl/H<sub>2</sub>O<sub>2</sub> prompted us to extend this approach to manganese complexes **II** and **V**. The aim was to study the influence of metalloporphyrin structure in terms of catalytic performance and also in the oxidation products distribution. On Table 6-2 are summarized the achieved results from the assays with **II** and **V** and, at first sight, it is clear the marked influence of the macrocycle structure on the results. The lactone **6.8** is not detected with these metalloporphyrins. Furthermore, the use of the cationic porphyrin **V** results in closer selectivity to that observed with *m*-CPBA. If with **I** and **II** the identified compounds are the *para*-quinones **6.4** and **6.7**, with catalyst **V** the *ortho*-quinones **6.5** and **6.6** were preferentially formed (total selectivity  $\approx 70\%$ ). With this catalyst it was only detected the *para*-quinone **6.7** (selectivity of  $\approx 30\%$ ). Despite all the efforts, we were not able yet to disclose the possible structure of one of the products detected with catalyst **II** [Mn(TPFPP)Cl]. The unknown product (U.P. Table 6-2) after the usual work-up/chromatography suffered a significant loss as we can conclude by comparing the selectivities obtained presented in Table 6-2, entries 1 and 4. In entry 1, the reaction mixture was subjected to the usual work-up procedure and purification and in entry 4 this last step was not performed. The putative structure of this product is still under evaluation and more experiments should be envisaged. From the results presented is possible to infer that along with the efficiency presented for all the metalloporphyrin/H<sub>2</sub>O<sub>2</sub> catalytic systems in oxidation of **6.1**, the use of different complexes can favour the formation of *ortho* or *para*-quinones.



**Table 6-2** Results from the catalytic tests using manganese (III) metalloporphyrins **II** and **V**

	Catalyst	S/C	T (min)	H <sub>2</sub> O <sub>2</sub> (equiv.)				U.P. <sup>c</sup>	
					<b>6.4</b>	<b>6.7</b>	<b>6.5</b>		<b>6.6</b>
1	<b>II</b> <sup>a)</sup>	75	60	2.5	16.6	58.8	-	24.6	-
2	<b>II</b> <sup>a)</sup>	150	90	3.0	-	69.5	-	30.5	-
3	<b>II</b> <sup>a)</sup>	300	120	3.5	-	67.7	-	32.3	-
4	<b>II</b> <sup>b)</sup>	75	60	2.0	5.7	19.0	-	74.6	-
5	<b>V</b> <sup>a)</sup>	75	90	3.0	-	*	*		*
6	<b>V</b> <sup>a)</sup>	150	120	3.5	-	30.5	24.3	-	45.2
7	<b>V</b> <sup>a)</sup>	300	165	5.0	-	30.7	25.6	-	43.7

<sup>a)</sup> The substrate (0.075 mmol) was dissolved in 2.0 mL of CH<sub>3</sub>CN and kept under magnetic stirring at 22 ± 2 °C in the presence of **II** or **V** (for sub/cat molar ratio of 75, the catalyst amount was 1.0 x 10<sup>-3</sup> mmol; for sub/cat molar ratio of 150, the catalyst amount was 5.0 x 10<sup>-4</sup> mmol; for sub/cat molar ratio of 300, the catalyst amount was 2.5 x 10<sup>-4</sup> mmol). In the presence of catalyst **II** ammonium acetate (0.12 mmol) was used as co-catalyst and in the presence of cationic catalyst **V** was acetic acid (0.12 mmol). Reactions subjected to the general work-up. Distribution of products determined by <sup>1</sup>H NMR.

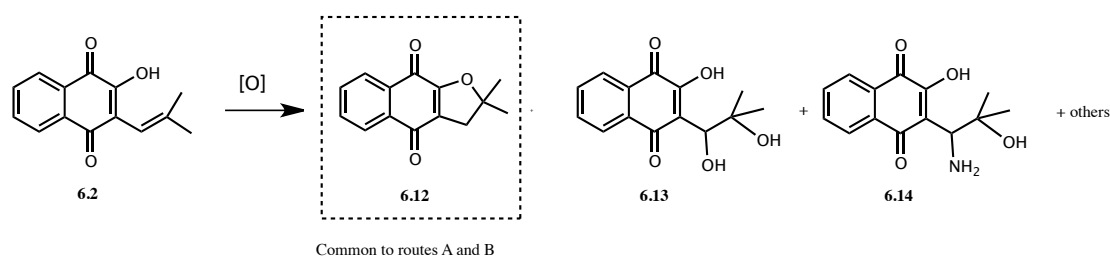
<sup>b)</sup> After the end of reaction, the mixture was directly purified in a small alumina column, using CH<sub>2</sub>Cl<sub>2</sub> as eluent, just to remove the catalyst

<sup>c)</sup> Unknown product.

\* The <sup>1</sup>H NMR spectra do not allow the determination of product distribution.

### 6.3. BIOMIMETIC OXIDATION OF *nor*-LAPACHOL (6.2)

As for substrate **6.1**, also *nor*-lapachol **6.2** the assays were performed comparing two different oxidation procedures: Route A concerning the traditional oxidation methodology with *m*-CPBA and Route B concerning the use of a catalytic system Mn(TDCPP)Cl (**I**)/H<sub>2</sub>O<sub>2</sub>. All the experiments for procedures A and B were performed in the same reaction conditions used for **6.1** and were monitored by TLC. With Route B, after 90 minutes of reaction and for a S/C molar ratio of 75 is possible to achieve total conversion being the presence of the starting material **6.2** no longer detected by TLC. Nevertheless, a complex mixture of products is formed, and the purification in preparative TLC plates using a mixture of solvents, CH<sub>2</sub>Cl<sub>2</sub>/ethyl acetate (20:1), permits the isolation of three major fractions. The small quantities of the isolated products only permitted the <sup>1</sup>H NMR analysis and from that it was possible to propose the structures **6.12-6.14** as the major obtained products. Product **6.12** is common to Routes A and B, and products **6.13** and **6.14** were only obtained under catalytic conditions (Scheme 6-3). The formation of **6.12** is quite intriguing since it does not result from oxidation - a simple intramolecular cyclization affords this product. However, the same procedure performed in the absence of **I** does not afford **6.12**.



Scheme 6-3

Comparatively to **6.1**, and for both Routes A and B, in the case of *nor*-lapachol **6.2** the formation of much more complex mixtures is detected. Moreover, if for lapachol **6.1** and using *m*-CPBA, the expected mass of the achieved *ortho*-quinones **6.5** and **6.7** was recovered, for substrate **6.2** only a minor amount was recovered.

In this case it was not possible to perform the quantification of the reaction products by  $^1\text{H}$  NMR by two main reasons: due to the complexity and to the small amount of the samples.

#### 6.4. CONCLUSIONS

The procedure involving the use of the manganese porphyrin complex not only allows the study of some metabolites formed during lapachol (**6.1**) oxidation, but also provides a totally different selectivity towards cyclised quinones formed in the reaction. Using Mn(III) complex **I** as catalyst and  $\text{H}_2\text{O}_2$  as oxidant, the *para*-quinones are highly favoured, in contrast to what happens in classical oxidation with *m*-CPBA. Moreover, it should be noted that catalyzed reactions seem more selective for furanonaphthoquinones than those with *m*-CPBA reaction.

The extension of Route B to other metalloporphyrins, namely **II** and **V**, proved that the structure of the macrocycle affects the course of the oxidation in terms of performance and selectivity. With the cationic catalyst **V**, a mixed behaviour between *m*-CPBA and Mn-Porh **I** and **II** catalyzed oxidations is observed; thus, depending on the catalyst of choice, it is possible to obtain completely different oxidation products. Moreover, the approach involving metalloporphyrin catalyzed reactions allowed the use of a benign, environmentally clean oxidant ( $\text{H}_2\text{O}_2$ ), instead of *m*-CPBA which generates *meta*-chlorobenzoic acid as by-product.

For substrate **6.2** a more complex situation was detected in both conditions and we were able to identify only products **6.12-6.14**. Further studies are necessary in order to optimize the reaction conditions and to obtain less complex reaction mixtures.

## 6.5. EXPERIMENTAL

All the solvents and reagents were used as received without further purification; phthalic anhydride was purchased from Sigma-Aldrich. The silica used in the preparative TLC plates was always silica gel 60 F<sub>254</sub> from Merck. For details concerning the preparation of preparative TLC plates please consult chapter 2, section 2.4. The NMR and GC-MS equipment's specifications are described in 3.3.2. Positive ESI-MS analysis was performed on a Q-TOF2 mass spectrometer (Micromass, Manchester, UK) using a flow rate of 10  $\mu\text{L min}^{-1}$ , cone voltage of 35 V, capillary voltage of 3 kV. The source temperature was 80 °C and the desolvation temperature was 150 °C.

### 6.5.1. GENERAL PROCEDURES

#### 6.5.1.1. OXIDATION OF LAPACHOL DERIVATIVES (**6.1** AND **6.2**) USING *m*-CPBA – ROUTE A

Lapachol (**6.1** or **6.2**) (0.075 mmol) was dissolved in 2.0 ml of CH<sub>2</sub>Cl<sub>2</sub> and *m*-CPBA was added (2.5 equiv). The mixture was kept under magnetic stirring and protected from light at 22  $\pm$  2 °C for 48 h. After that time, the substrate was completely consumed (confirmed by TLC). The mixture was dissolved in CH<sub>2</sub>Cl<sub>2</sub> and washed with basic water (K<sub>2</sub>CO<sub>3</sub>). The organic layer was recovered through anhydrous sodium sulphate and evaporated under reduced pressure.

#### 6.5.1.2. GENERAL PROCEDURES OXIDATION OF LAPACHOL (**6.1** AND **6.2**) USING MN(III) PORPHYRINS – ROUTE B

In a typical experiment based on earlier work of our group, lapachol (**6.1** or **6.2**) (0.075 mmol), catalyst (depending on catalyst/substrate molar ratio) and co-catalyst (0.12 mmol) were dissolved in CH<sub>3</sub>CN (2.0 ml). With catalyst **I** and **II** the co-catalyst was always ammonium acetate, with catalyst **V** acetic acid was used as co-catalyst.



The mixture was kept under magnetic stirring at room temperature ( $22 \pm 2$  °C) and protected from light. The oxidant, 30% H<sub>2</sub>O<sub>2</sub> (w/w) diluted in acetonitrile (1:10) was added at regular intervals of 15 minutes in aliquots corresponding to a half-substrate amount ( $3.7 \times 10^{-2}$  mmol). The reactions were followed by TLC and stopped when all the substrate was totally consumed or when no more evolution was observed, after two successive analyses.

The reaction mixture was then diluted in CH<sub>2</sub>Cl<sub>2</sub> and washed with water. The organic layer was recovered through anhydrous sodium sulfate and evaporated. After that, the obtained material was submitted to silica preparative TLC using a mixture of ethyl acetate/hexane (2:1) as eluent.

### 6.5.2. CHARACTERIZATION OF THE COMPOUNDS

dehydro- $\alpha$ -lapachone (**6.3**) [MW(C<sub>15</sub>H<sub>12</sub>O<sub>3</sub>)= 240.25]

<sup>1</sup>H NMR (CDCl<sub>3</sub>, 300 MHz)  $\delta$  (ppm): 1.45 (*s*, 6H, 2CH<sub>3</sub>), 5.40 (*d*, 1H, *J* = 6.6 Hz, -CH=CH-), 6.10 (*d*, 1H, *J* = 6.6 Hz, -CH=CH-), 7.70-7.90 (*m*, 4H, H-Ar). <sup>13</sup>C (CDCl<sub>3</sub>, 75 MHz)  $\delta$  (ppm): 18.0, 23.9, 83.7, 86.0, 98.5, 123.6, 126.5, 126.6, 131.6, 133.0, 133.3, 134.8, 161.8, 177.6, 181.0. ESI-MS *m/z* 265.1 corresponding to the hydroquinone C<sub>15</sub>H<sub>14</sub>O<sub>3</sub> [M+Na]<sup>+</sup>.

*nor*-hydroxy- $\beta$ -lapachone (**6.4**) [MW(C<sub>15</sub>H<sub>14</sub>O<sub>4</sub>)=258.27]

<sup>1</sup>H NMR (CDCl<sub>3</sub>, 300 MHz)  $\delta$  (ppm): 1.39 (*s*, 3H, CH<sub>3</sub>), 1.46 (*s*, 3H, CH<sub>3</sub>), 3.10-3.13 (*m*, 2H, -CH<sub>2</sub>-), 4.94 (*t*, 1H, *J* = 9.3 Hz, -O-CH-), 7.57-7.66 (*m*, 2H, H-Ar), 8.07-8.13 (*m*, 2H, H-Ar). ESI-MS *m/z* 281.1 [M+Na]<sup>+</sup>.

hydroxy- $\beta$ -lapachone (**6.5**) [MW(C<sub>15</sub>H<sub>14</sub>O<sub>4</sub>)=258.27]

<sup>1</sup>H NMR (CDCl<sub>3</sub>, 300 MHz)  $\delta$  (ppm): 1.46 (*s*, 3H, CH<sub>3</sub>), 1.52 (*s*, 3H, CH<sub>3</sub>), 2.63 (*dd*, 1H, *J* = 5.1 Hz and *J* = 17.7 Hz, -CH-), 2.83 (*dd*, 1H, *J* = 5.1 Hz and *J* = 17.7 Hz, -CH-), 3.93 (*t*, 1H, *J* = 5.1 Hz, -O-CH-), 7.53 (*td*, 1H, *J* = 1.4 Hz and *J* = 7.6 Hz, H-Ar), 7.67 (*td*, 1H, *J* = 1.1 Hz and *J* = 7.6 Hz, H-Ar), 7.85 (*dd*, 1H, *J* = 1.1 Hz and *J* = 7.6 Hz, H-Ar), 8.07 (*dd*, 1H, *J* = 1.4 Hz and *J* = 7.6 Hz, H-Ar). ESI-MS *m/z* 281.1 [M+Na]<sup>+</sup>.

*nor*-hydroxy- $\alpha$ -lapachone (**6.6**) (C<sub>15</sub>H<sub>14</sub>O<sub>4</sub>) [MW(C<sub>15</sub>H<sub>14</sub>O<sub>4</sub>)= 258.27]

<sup>1</sup>H NMR (CDCl<sub>3</sub>, 300 MHz)  $\delta$  (ppm): 1.26 (*s*, 3H, CH<sub>3</sub>), 1.41 (*s*, 3H, CH<sub>3</sub>), 3.17 (*d*, 2H, *J*= 10.0 Hz, -CH<sub>2</sub>-) 4.86 (*t*, 1H, *J*= 10 Hz, -O-CH-) 7.66-7.76 (*m*, 2H, H-Ar), 8.06-8.10 (*m*, 2H, H-Ar). <sup>13</sup>C (CDCl<sub>3</sub>, 75 MHz)  $\delta$  (ppm): 24.0, 25.8, 28.4, 92.1, 133.0, 134.2, 159.9, 177.7, 182.2. ESI-MS *m/z* 281.1 [M+Na]<sup>+</sup>

4-hydroxy-5,5-dimethyldihydrofuran-2(3*H*)-one (**6.8**) [MW(C<sub>6</sub>H<sub>10</sub>O<sub>3</sub>)=130.14]

<sup>1</sup>H NMR (CDCl<sub>3</sub>, 300 MHz)  $\delta$  (ppm): 1.39 (*s*, 3H, CH<sub>3</sub>), 1.45 (*s*, 3H, CH<sub>3</sub>), 2.55 (*dd*, 1H, *J* = 1.9 Hz and *J* = 10.8 Hz, -CH<sub>2</sub>-), 2.95 (*dd*, 1H, *J* = 3.8 Hz and *J* = 10.8 Hz, -CH<sub>2</sub>-), 4.21-4.23 (*m*, 1H, -CH-OH), <sup>13</sup>C (CDCl<sub>3</sub>, 75 MHz)  $\delta$  (ppm) : 21.0 (-CH<sub>3</sub>), 25.8 (-CH<sub>3</sub>), 38.2 (-CH<sub>2</sub>-), 73.8 (C-OH), 87.2 (-C(CH<sub>3</sub>)<sub>2</sub>), 174.3 (-C=O). ESI-MS *m/z* 131.0 [M+H]<sup>+</sup>.

phthalic anhydride (**6.9**) [MW(C<sub>8</sub>H<sub>4</sub>O<sub>3</sub>)=148.12]

MS (EI) *m/z* (rel. int., %): 149 (3), 148 (M<sup>+</sup>, 38), 104 (100), 76 (63), 50 (25).

*o*-phthalimide (**6.10**) [MW(C<sub>8</sub>H<sub>5</sub>NO<sub>2</sub>)=147.13]

MS (EI) *m/z* (rel. int., %): 148 (9), 147 (M<sup>+</sup>, 100), 104 (44), 76 (38), 50 (13).

3,4-epoxy-4-methylpentanal (**6.11**) [MW(C<sub>6</sub>H<sub>10</sub>O<sub>2</sub>)=114.1]

MS (EI) *m/z* (rel. int., %): 115 (4), 85 (41), 59 (100), 58 (39), 43 (46), 42 (34), 41 (39), 39 (16).

*nor*- $\alpha$ -lapachone **6.12** [MW(C<sub>14</sub>H<sub>12</sub>O<sub>3</sub>)=228.2]

<sup>1</sup>H NMR (CDCl<sub>3</sub>, 300 MHz)  $\delta$  (ppm): broad 1.58 (*s*, 6H, 2 -CH<sub>3</sub>), 3.01 (*s*, 2H, -CH<sub>2</sub>), 7.66 (*td*, 1H, *J* = 1.5, *J* = 7.3 and *J* = 7.7 Hz, H-Ar), 7.72 (*td*, 1H, *J* = 1.5, *J* = 7.3 and *J* = 7.7 Hz, H-Ar) 8.06-8.10 (*m*, 2H, H-Ar) <sup>13</sup>C (CDCl<sub>3</sub>, 75 MHz)  $\delta$  (ppm): 28.3, 40.1, 92.0, 123.4, 126.0, 126.3, 131.6, 132.8, 133.1, 134.1, 158.9, 178.4, 182.6. ESI-MS *m/z* 251.1 [M+Na]<sup>+</sup>.

Mixture of compounds **6.13** [MW(C<sub>14</sub>H<sub>14</sub>O<sub>5</sub>)=262.1] and **6.14** [MW(C<sub>14</sub>H<sub>15</sub>NO<sub>4</sub>)=261.3]



$^1\text{H}$  NMR ( $\text{CDCl}_3$ , 300 MHz)  $\delta$  (ppm): 1.51 (*s*, 6H, 2  $-\text{CH}_3$ ), 1.62 (*s*, 6H,  $-\text{CH}_3$ ), 2.95 (*s*, 1H, CH-NH<sub>2</sub>), 5.09 (*s*, 1H, CH-OH) 7.55-7.76 (*m*, 5H, H-Ar), 7.55-7.76 (*m*, 5H, H-Ar), 8.08-8.12 (*m*, 3H, H-Ar)  $^{13}\text{C}$  ( $\text{CDCl}_3$ , 75 MHz)  $\delta$  (ppm): 20.2, 26.5, 28.4, 29.7, 39.3, 76.3, 77.2, 93.7, 94.9, 123.6, 124.6, 126.1, 126.6, 128.8, 129.3, 131.0, 131.7, 131.8, 133.0, 133.2, 134.4, 134.5, 160.0, 175.7, 178.8, 182.9.

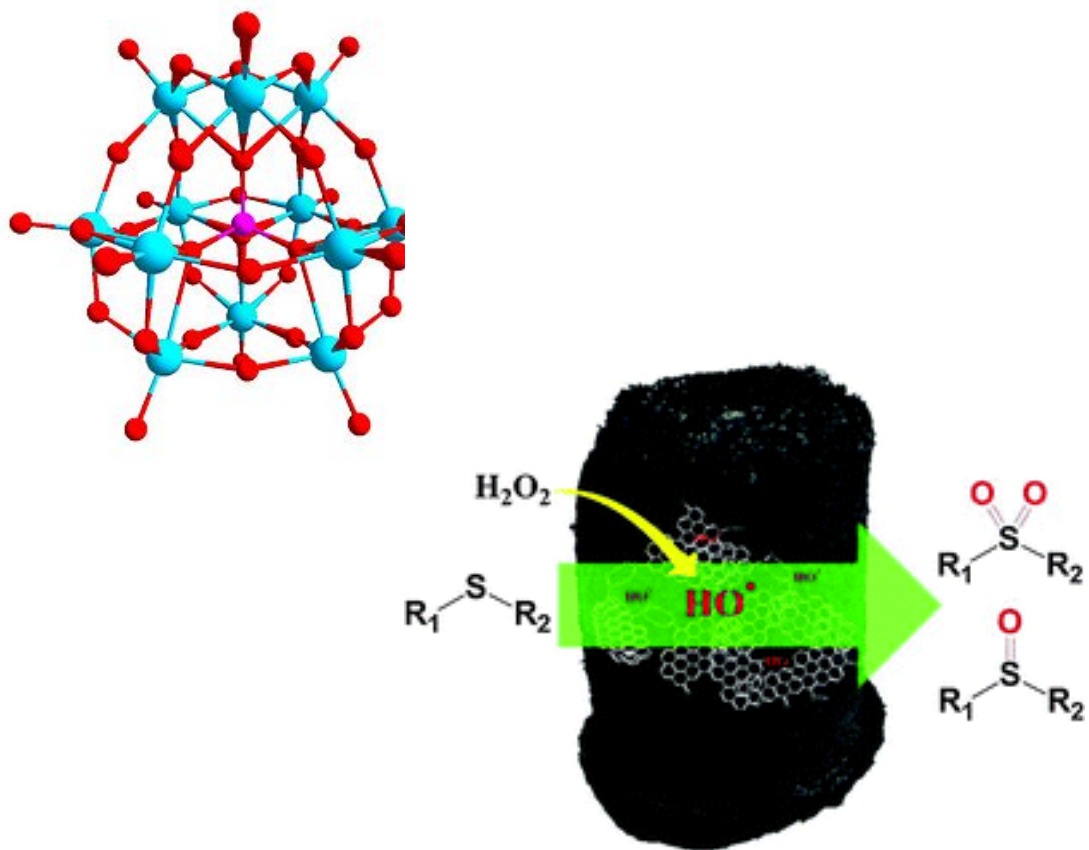
## 6.6. BIBLIOGRAPHY

- <sup>1</sup> P. O'Brien, *J. Chem. Biol. Interact.* 80 (1991) 1.
- <sup>2</sup> A.V. Pinto, S.L. de Castro, *Molecules* 14 (2009) 4570.
- <sup>3</sup> E.N. da Silva Junior, M.A.B.F. de Moura, A.V. Pinto, M.C.F.R. Pinto, M.C.B.V. de Souza, A.J. Araújo, C. Pessoa, L.V. Costa-Lotuf, R.C. Montenegro, M.O. de Moraes, V.F. Ferreira, M.O. F. Goulart, *J. Braz. Chem. Soc.* 20 (2009) 635.
- <sup>4</sup> M.N. da Silva, M.C.B.V. da Souza, V.F. Ferreira, A.V. Pinto, M.C.R.F. Pinto, S.M.S.V. Wardell, J.L. Wardell, *Arkivoc X* (2003) 156.
- <sup>5</sup> H. Hussain, K. Krohn, V.U. Ahmad, G.A. Miana, I.R. Green, *Arkivoc II* (2007) 145.
- <sup>6</sup> M.N. Silva, V.F. Ferreira, M.C.B.V. Souza, *Quim. Nova.* 26 (2003) 407.
- <sup>7</sup> E.N. da Silva Júnior, M.C.F.R. Pinto, K.C.G. de Moura, C.A. de Simone, C.J. Nascimento, C.K.Z. Andrade, A.V. Pinto, *Tetrahedron Lett.* 50 (2009) 1575.
- <sup>8</sup> M. Arnaudon, *Comptes Rendus Hebdomadares. Des Sianes'L'Acord. Des Science* 46 (1858) 1152.
- <sup>9</sup> S.C. Hooker *J. Chem. Soc.* 61 (1892) 611.
- <sup>10</sup> S.C. Hooker *J. Am. Chem. Soc.* 58 (1936) 1181.
- <sup>11</sup> E. Paterno, *Gazz. Chim. Ital.* 12 (1882) 337.
- <sup>12</sup> L.F. Fieser, F.C. Chang, W.G. Dauben, C. Heidelberger, H. Heymann, M. Seligman, *J. Pharmacol. Exp. Ther.* 94 (1948) 85.
- <sup>13</sup> N. McHardy, A.T. Hudson, D.W.T. Morgan, D.G. Rae, T.T. Dolan, *Res. Vet. Sci.* 35 (1983) 347.
- <sup>14</sup> P. Boehm, K. Cooper, A.T. Hudson, J.P. Elphick, N. McHardy, *J. Med. Chem.* 24 (1981) 295.
- <sup>15</sup> F.G.G. Miranda, J.C. Vilar, I.A.N. Alves, S.C.H. Cavalcanti, A.R. Antonioli, *BMC Pharmacology* 1 (2001) 6.
- <sup>16</sup> V. F. Ferreira, *Quim. Nova na Escola* 4 (1996) 35.
- <sup>17</sup> G. Kazantzi, E. Malamidou-Xenikaki, S. Spyroudis, *Synlett* (2007) 427.
- <sup>18</sup> E. Glinis, E. Malamidou-Xenikaki, H. Skouros, S. Spyroudis M. Tsanakopoulou *Tetrahedron* 66 (2010) 5786.
- <sup>19</sup> S.B. Ferreira, D.R. da Rocha, J.W.M. Carneiro, W.C. Santos, V.F. Ferreira, *Synlett* (2011) 1551.
- <sup>20</sup> M.N. Silva, V.F. Ferreira, M.C.B.V. Souza, *Quim. Nova* 26 (2003) 407.
- <sup>21</sup> S. Claessens, P. Habonimana, N. De Kimpe, *Org. Biomol. Chem.* 8 (2010) 3790.
- <sup>22</sup> F. Epifano, S. Genovese, S. Fiorito, V. Mathieu, R. Kiss, *Phytochem. Rev.* 13 (2014) 37.



- <sup>23</sup> F. P. Guengerich, *Chem. Res. Toxicol.* 14 (2006) 611.
- <sup>24</sup> S.C. Hooker, *J. Am. Chem. Soc.* 58 (1936) 1168.
- <sup>25</sup> M. Cortes, J. Katalinic, J. Valderrama, *An. Quim.* 79C (1983) 202.
- <sup>26</sup> I.D. Cunningham, T.N. Danks, K.T.A. O'Connell, P. Scott, *J. Org. Chem.* 64 (1999) 7330.
- <sup>27</sup> R.A. Sheldon (Ed.), in "*Metalloporphyrins in Catalytic Oxidations*", Marcel Dekker Inc., New York (1994).
- <sup>28</sup> J.T. Groves, In "*Cytochrome P-450: Structure, Mechanism and Biochemistry*", Ortiz de Montellano (Ed.), 3<sup>rd</sup> edition, Springer, New York (2005) pp 1-43.
- <sup>29</sup> S.L.H. Rebelo, M.M.Q. Simões, M.G.P.M.S. Neves, A.M.S. Silva, J.A.S. Cavaleiro, *Chem. Commun.* (2004) 608.
- <sup>30</sup> S.L.H. Rebelo, M.M. Pereira, M.M.Q. Simões, M.G.P.M.S. Neves, J.A.S. Cavaleiro, *J. Catal.* 234 (2005) 76.
- <sup>31</sup> J. Mock, S.T. Murphy, E. Richie, W.C. Taylor, *Aust. J. Chem.* 26 (1973) 1121.
- <sup>32</sup> M. Onitsuka, M. Fujiu, N. Shinma, H.B. Maruyama, *Chem. Pharm. Bull.* 31 (1983) 670.
- <sup>33</sup> M. Girard, J.C. Ethier, D. Kindack, B.A. Dawson, D.V.C. Awang, *J. Nat. Prod.* 50 (1987) 1149.
- <sup>34</sup> S. Otten, J.P. Rosazza, *Appl. Environ. Microbiol.* 35 (1978) 554.
- <sup>35</sup> P.S. Sacau, A. Estévez-Braun, A.G. Ravelo, E.A. Ferro, H. Tokuda, T. Mukainaka, H. Nishino, *Biorg. Med. Chem.* 11 (2003) 483.





Chapter 7 OTHER CATALYTIC SYSTEMS  
IN THE OXIDATION OF SULFUR  
COMPOUNDS



Part of this chapter was based on the following publication:

- *“Three-dimensional graphene oxide: a promising green and sustainable catalyst for oxidation reactions at room temperature”*, G.A.B. Gonçalves, S.M.G. Pires, M.M.Q. Simões, M.G.P.M.S. Neves, P.A.A.P. Marques, *Chem. Commun.* 50 (2014) 7673.

## 7. OTHER CATALYTIC SYSTEMS IN THE OXIDATION OF ORGANOSULFUR COMPOUNDS

### 7.1. OVERVIEW

It was widely discussed in chapter 3 of this dissertation the importance of the development of new and environmentally friendly processes able to treat the most recalcitrant organosulfur contaminants present in fuels. Through the oxidative desulfurization (ODS) the refractory sulfur compounds are oxidized into more polar molecules that are then easily extracted using appropriate methodologies.  $H_2O_2$  is largely used as an oxidant in ODS mainly because it is eco-sustainable and the presence of an efficient catalyst in the oxidation step of the ODS procedure is crucial for the success of this process.

In this sense, several reports appeared recently in literature claiming the efficiency of Keggin-type polyoxometalate (POM) derivatives  $[XM_{12}O_{40}]^{m-}$  in ODS processes.<sup>1-5</sup> Nevertheless, most of these studies involve the use of temperatures between 60-80 °C and sometimes the use of toxic organic solvents. Inspired by the results achieved in the oxidation of organosulfur compounds catalyzed by manganese(III) porphyrins under very mild conditions (chapter 3), it was possible to study the application of a similar approach with a Mn-POM catalyst. The tetrabutylammonium (TBA) salt of a Keggin-type polyoxotungstate with the formula  $[BW_{11}Mn(H_2O)O_{39}]^{6-}$ , **Mn-POM**, was evaluated in the oxidation of different organosulfur derivatives, namely benzothiophene, 2-methylbenzothiophene, 3-methylbenzothiophene, dibenzothiophene, 6-methyldibenzothiophene and 4,6-diethyldibenzothiophene, by hydrogen peroxide at room temperature. **Mn-POM** demonstrated special efficiency with most of the recalcitrant dibenzothiophenes studied, and thus a simulated ODS procedure was developed. In the following sections the efficiency of **Mn-POM** as catalyst in the oxidation of a designed model fuel can be envisaged, along with the effectiveness of an environmentally sustainable and simple sulfur extraction methodology.

In the path towards green and sustainable chemistry, a constant goal is the use of non-toxic, sustainable catalysts with minimal environmental footprint. In the pursuit of



this objective, the successful application of two carbocatalysts, namely graphene oxide (**2DGO**) and a three-dimensional graphene nanostructure (**3DGO**) in the sulfoxidation of thioanisole will be also described in this chapter. Beyond the good catalytic activity, heterogeneous **3DGO** also proved to be recyclable.<sup>6</sup>

## 7.2. POLYOXOMETALATE CATALYSTS: POTENTIAL APPLICATION IN ODS

As widely highlighted on chapter 3, the search for new and highly efficient catalytic systems for the oxidation of sulfides to sulfoxides and sulfones is nowadays a research area of great relevance.<sup>7-10</sup> First, the sulfoxides and sulfones, besides being important intermediates in organic synthesis, are also biological active molecules.<sup>11-13</sup> Secondly, oxidative desulfurization constitutes an alternative with high potential in terms of efficiency and environmental sustainability, which gained the interest of the scientific community.<sup>14-16</sup>

POMs belong to a class of metal oxygen cluster anions that have been applied in several fields, namely in catalysis, medicine and materials science. Despite being known since the XIX century, POMs still attract wide interest mainly driven by the high versatility of disclosed structures, presenting a wide range of physical and chemical properties serving a large domain of applications.<sup>17-19</sup> The above mentioned development of POMs is much due to the advances on instrumentation (especially single-crystal X-ray crystallography techniques) and to new synthetic approaches.<sup>20, 21</sup>

Perhaps the most important fields for which this metal oxygen cluster anions have been applied is acid and oxidative catalysis. In fact, comparatively to many organometallic complexes (including metalloporphyrins), POMs present an all set of important properties: strong Brønsted acidity, good redox properties under mild conditions, good solubility in different solvents (according with the counter-ion) and, not less important, a high thermal and oxidative stability, which make them very interesting catalysts.<sup>1, 22-24</sup> Among the various POM structures, the Keggin-type ( $[\text{XM}_{12}\text{O}_{40}]^{n-}$ ) and the lacunary Keggin-type polyoxometalates with a general formula  $[\text{XW}_{11}\text{MO}_{39}]^{m-}$  for which one  $\text{MO}^{4+}$  unit was removed are perhaps the most studied in catalysis. If, in the former case, the POM properties can be modulated by the substitution of M and X by different metal centers, the latter contain free oxygen

atoms at the lacuna that can coordinate to other transition metals or lanthanides. Their success as catalysts is thus associated with the easy tuning of the structures and properties.<sup>25-27</sup>

The efficiency of this type of catalysts in ODS processes has already been demonstrated in several reports.<sup>28-32</sup> Moreover, as was fully discussed in chapters 3 and 4, our research group has developed a catalytic oxidation system of organosulfur derivatives under mild conditions using metalloporphyrin complexes.<sup>33, 34</sup> Thus, based on our experience on the synthesis as well as in POMs catalytic application<sup>35-39</sup> and taking advantage of the fact that manganese POMs have been poorly studied in this area,<sup>40</sup> the evaluation of the Mn-POM catalytic efficiency in the oxidation of several benzothiophenes **7.1-7.3** and dibenzothiophenes **7.4-7.6** by H<sub>2</sub>O<sub>2</sub> was proposed (Figure 7-1).

As in the previous work involving metalloporphyrin catalysts, in order to prove the potential of BW<sub>11</sub>Mn/H<sub>2</sub>O<sub>2</sub> catalytic system for ODS two distinct model fuels were also studied, generally consisting in a mixture of four BTs and DBTs in hexane. Significantly and in order to simulate all the ODS procedure, the final extraction of the oxidized sulfones was also assessed.

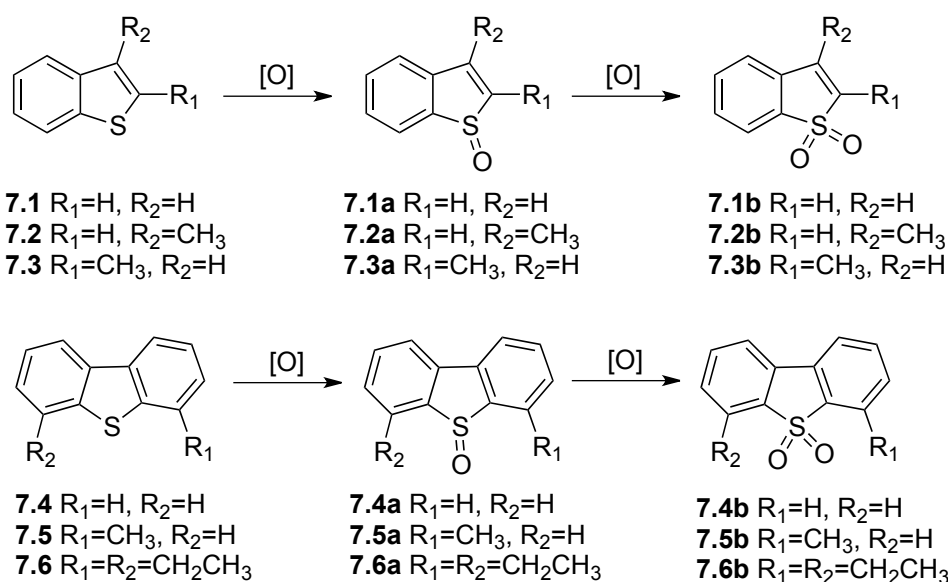


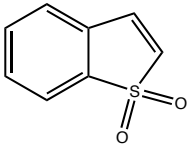
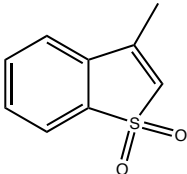
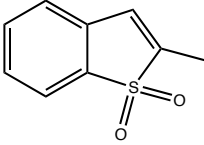
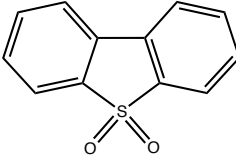
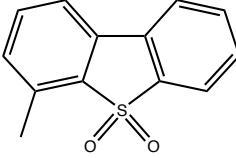
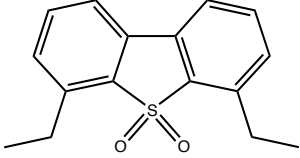
**Figure 7-1** Benzothiophenes and dibenzothiophenes tested in catalysis and their oxidation products



### 7.2.1. CATALYTIC EXPERIMENTS USING A $BW_{11}Mn$

The catalytic performance of the polyoxometalate  $TBA_4H_2[BW_{11}Mn(H_2O)O_{39}] \cdot 2H_2O$  (**Mn-POM**), prepared and kindly supplied by Master Tiago Duarte, was evaluated in sulfoxidation reactions by  $H_2O_2$  under homogeneous conditions. The catalytic tests were performed with substrates **7.1-7.6** (Figure 7-1) and the results are summarized on Table 7-1.

**Table 7-1** Results obtained for the oxidation of substrates (**7.1-7.6**) with  $H_2O_2$  catalyzed by the manganese polyoxometalate (Mn-POM). <sup>a)</sup>

Substrate	Ratio SUB/CAT	Conversion (%) <sup>a)</sup>	Product	t <sub>r</sub> (min)
<b>7.1</b>	300	47.0		180
	150	97.0		180
<b>7.2</b>	300	90.0		180
	150	99.9		180
<b>7.3</b>	300	93.0		180
	150	99.9		180
<b>7.4</b>	300	99.9		180
	150	99.9		180
<b>7.5</b>	300	98.3		180
	150	99.9		60
<b>7.6</b>	300	71.6		180
	150	97.7		180

<sup>a)</sup>Reaction conditions: the substrate (0.3 mmol), the catalyst corresponding to a substrate/catalyst molar ratio of 150 and 300, the internal standard (chlorobenzene, 0.3 mmol) and the 30% (w/w)  $H_2O_2$  (6 equiv.) were stirred in 2.0 mL of  $CH_3CN$  at room temperature. <sup>b)</sup> conversion values determined by GC-FID.

The values presented were determined by the GC-FID analysis. To monitor the sulfoxidation reactions aliquots, from the reaction mixture were directly injected into the GC-FID apparatus at each 30 minutes, being stopped after 3 hours of reaction when a plateau of conversion was reached.

In order to compare the efficiency of the **Mn-POM** catalyst with the Metalloporphyrins under homogeneous conditions (results presented in chapter 3 of this dissertation) the experiments were carried out using similar reaction conditions. Thus, in both cases the solvent of choice was CH<sub>3</sub>CN, the oxidant was H<sub>2</sub>O<sub>2</sub> and the assays were performed at room temperature (22-24 °C). It is important to refer that for porphyrin complexes the oxidant is used diluted and added in small aliquots (half of the substrate amount at each 15 minutes) to protect the catalyst from the oxidation conditions. For the studies employing the manganese POM, due to its higher chemical resistance, hydrogen peroxide 30% (w/w) is used directly and added all at once at the beginning of the reactions.

From the results obtained it is possible to infer that good to excellent conversions, ranging from 47.0 to 99.9%, were attained with most substrates for both S/C molar ratios tested (300 and 150). As expected, the use of a higher amount of catalyst (S/C molar ratio = 150) affords better results. Furthermore, for benzothiophene **7.1** and 4,6-diethyldibenzothiophene **7.6** a significative difference between the two S/C ratios was detected. It must be emphasized that this is the first example of a Keggin-type catalyst efficiently used at room temperature in a sulfoxidation process. Usually the use of POM catalysts in sulfoxidation processes requires temperatures around the 60-80 °C, or even higher; thus the efficiency demonstrated by **Mn-POM** at room temperature is quite remarkable. Noteworthy, **Mn-POM** remains especially efficient with DBTs **7.4** and **7.5**. In fact, this constitutes a very promising result since the most difficult or the most recalcitrant organosulfur derivatives to treat through an ODS procedure are DBTs.

Figure 7-2 illustrates the evolution of the attained conversion vs. time to each substrate in the catalytic assays with **Mn-POM** for a SUB/CAT molar ratio of 300. This puts in evidence the higher efficiency of **Mn-POM** with DBTs. After 60 minutes of reaction, the higher conversion values were attained for **7.4**, **7.5** and **7.6**, by this order, thus unsubstituted BT **7.1** giving the worst result.

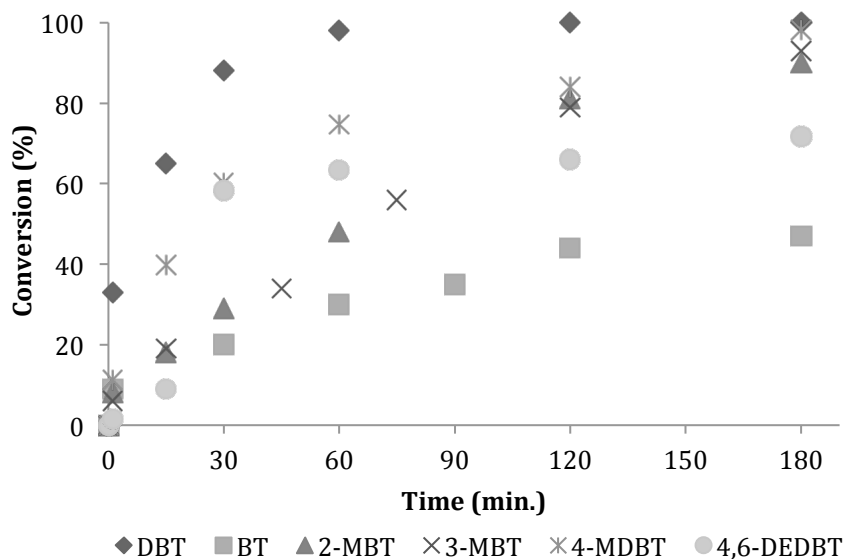


**Figure 7-2** Conversion profile vs time of reaction for all the organosulfur compounds tested (7.1-7.6) in the presence of Mn-POM (substrate/catalyst molar ratio of 300), with H<sub>2</sub>O<sub>2</sub> at room temperature in CH<sub>3</sub>CN.

Unexpectedly, in the case of benzothiophenes the presence of the methyl substituents seems to have a positive effect in the course of sulfoxidation (substrates 7.2 and 7.3 are easily oxidized if compared with 7.1). In the case of DBTs the steric hindrance appears as the main factor affecting the catalytic results. So, despite some differences in conversion from the very beginning of the reaction, the presence of a methyl substituent does not affect significantly the results attained after 180 min for 7.5 if compared with 7.4; in the case of 7.6, possessing two ethyl substituents, a significant decrease on the conversion after 3 hours of reaction is detected, when a SUB/CAT molar ratio of 300 is used.

Based on the good results achieved for the S-containing compounds above, the performance of Mn-POM was also evaluated for the oxidation of a model fuel, consisting of a mixture of substrates 7.1-7.4 in hexane (MF1), the same mixture tested with metalloporphyrin I (chapter 3).

Figure 7-3 illustrates the GC monitoring of the oxidation of MF1 by H<sub>2</sub>O<sub>2</sub> in the presence of Mn-POM, after 3 hours of reaction. Only a small amount of BT 7.1 remains in solution. More than 99% of the starting MF1 is fully converted into the corresponding oxidized products and, in accordance to the above-mentioned results, Mn-POM seems to be more efficient for the DBTs oxidation. After 60 min, the most



recalcitrant substrates of **MF1**, DBT **7.5** ( $R_t = 9.50$  min), is almost undetected in the chromatogram [Figure 7-3(B)].

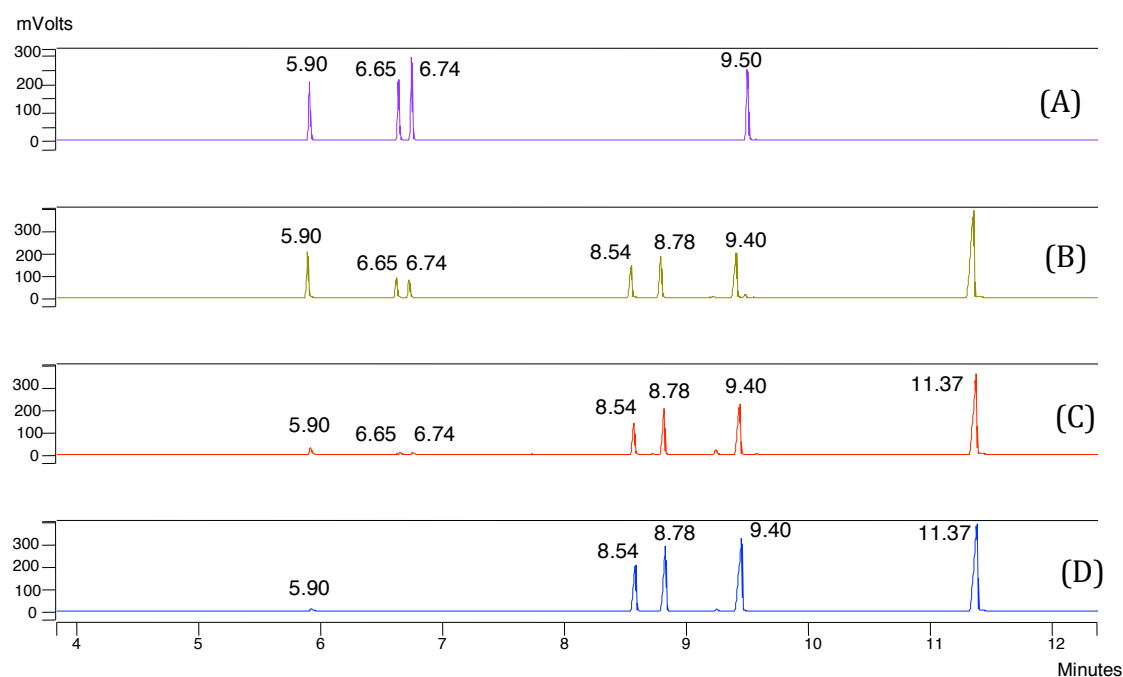


**Figure 7-3** Typical GC-FID chromatograms illustrating **MF1** oxidation reaction profile with  $H_2O_2$  in the presence of **Mn-POM** for a sub/cat molar ratio of 150. (A) Initial reaction mixture before the addition of  $H_2O_2$ ; (B) after 60 min of reaction; (C) after 120 min of reaction and (D) after 180 min of reaction. The model fuel is a solution of **7.1** ( $R_t = 5.90$ ), **7.2** ( $R_t = 6.65$ ), **7.3** ( $R_t = 6.74$ ), and **7.4** ( $R_t = 9.50$ ) in hexane (with 0.03 mmol each).

Considering the potential application of the developed procedure in an ODS process, and knowing that DBTs are the most recalcitrant contaminants present in fuels, the demonstrated high efficiency of **Mn-POM** for this substrates led us to test this catalyst in the oxidation of a harder model fuel (**MF2**). So, this new **MF2**, composed by three DBTs (**7.4**, **7.5** and **7.6**) and one benzothiophene (**7.3**) was oxidized by  $H_2O_2$  in the presence of the Mn-POM, for 3 hours under similar reaction conditions as for **MF1**.

In Figure 7-4 the chromatograms obtained before (A) and after 3 hours of  $H_2O_2$  addition (B), due to the overlap of some of the starting peaks with those correspondent to the oxidized products, may not be entirely clear to demonstrate the total conversion of the starting **MF2**. Therefore, the unambiguous identification of each peak was performed by GC-MS and the peak at 9.44 minutes corresponds to sulfone **7.3b** ( $M^+ = 180$ ), the peak at 11.39 was identified as product **7.4b** ( $M^+ = 216$ )

and finally the peaks at 11.65 and 12.68 were assigned as sulfones **7.5b** ( $M^+ = 230$ ) and **7.6b** ( $M^+ = 272$ ) respectively.

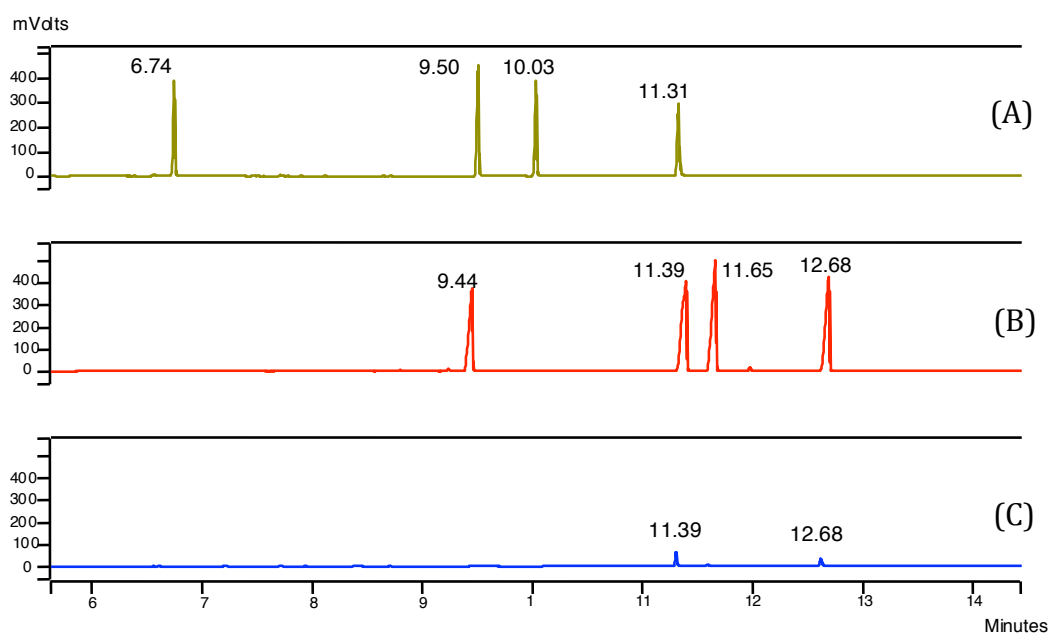


**Figure 7-4** Typical GC-FID chromatograms illustrating **MF2** oxidation reaction profile with  $H_2O_2$  in the presence of Mn-POM for a sub/cat molar ratio of 150. (A) Initial reaction mixture before the addition of  $H_2O_2$ ; (B) after 180 min of reaction; (C) after the extraction procedure. The model fuel (**MF2**) is a solution of **7.3** ( $R_t = 6.74$ ), **7.4** ( $R_t = 9.50$ ), **7.5** ( $R_t = 10.03$ ), and **7.6** ( $R_t = 11.31$ ) in hexane (with 0.03 mmol each).

Proven the efficiency of the oxidation methodology, the next step in order to simulate the entire ODS process, is the extraction of the oxidized products from hexane. After a few attempts using different extraction solvents, we were able to perform a successful extraction procedure, using 2.0 mL of a mixture ethanol/ $H_2O$  (1:1) and stirring for 10 minutes. In the photography shown in Figure 7-5 is possible to observe that the addition of ethanol/ $H_2O$  causes the products precipitation in the middle of the two observed phases. Therefore, and to allow the phases to properly separate the reaction mixture was left reposing for 10 minutes. The GC analysis of the hexane fraction after the described extraction procedure [Figure 7-4(C)] clearly put in evidence the success of the extraction methodology, since more than 98% of the organic compounds were removed. The developed extraction methodology, besides being efficient and very simple, using only ethanol and water as solvents, respects the environmental and safety issues required to ODS.

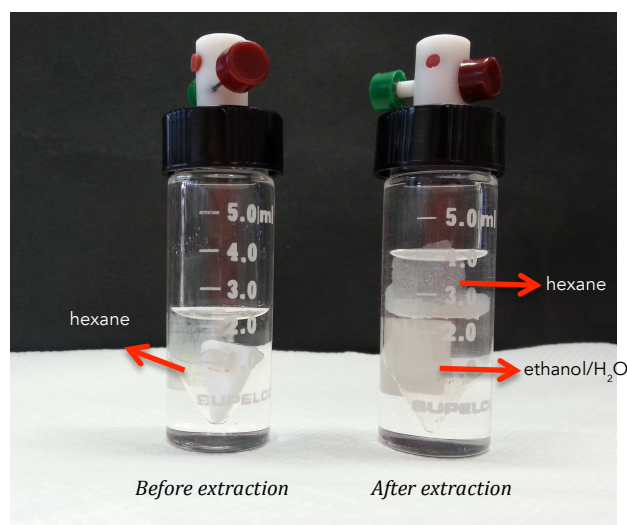


**Figure 7-5** Photography of the reactors used during the ODS of MF2

### 7.3. CATALYTIC EXPERIMENTS USING GRAPHENE OXIDE

Graphene and other two-dimensional  $sp^2$ -hybridized carbon nanomaterials has sparked huge interest among researchers in several areas from modern chemistry, physics, to materials science and engineering.<sup>41, 42</sup> Their outstanding electrical, optical, electrochemical and mechanical properties, associated to the significant advances in synthetic and processing methods to access this materials significantly contributed to this increasing interest.<sup>43-47</sup> Beyond the referred applications, the use of graphene and chemically modified graphenes as “carbocatalysts”, despite being a relatively new area, is of enormous potential. Contributing to the development of new sustainable metal-free heterogeneous catalysts<sup>48-50</sup> is very attractive in respect to low cost and natural abundance of the used carbon materials.<sup>51, 52</sup>

Graphene oxide (GO), produced by the exfoliation of graphite oxide, is an intermediate product to achieve mass production of graphene by solution chemistry. Structurally it holds carboxylic acid groups at the edges and hydroxyl as well as epoxide groups at the basal planes, which makes it a promising 2D nanoplatform for further chemical functionalization giving rise to new materials. Undoubtedly the oxygen-containing functional groups, its acidic nature, low density and hydrophilicity are very attractive features in view of their application as catalysts. In this sense GO has been used as a support scaffold for various catalytic active species,<sup>53</sup> and as the

catalyst itself.<sup>54</sup> The potential catalytic properties of GO have been explored in some reactions,<sup>52-54</sup> namely hydration of alkynes,<sup>55</sup> oxidation,<sup>48, 55, 56</sup> oxidative coupling,<sup>52</sup> Friedel-Crafts addition,<sup>57</sup> Aza-Michael addition,<sup>58, 59</sup> polymerization,<sup>60</sup> and photo-oxidation.<sup>61</sup>

Recently, the focus of scientists' attention has moved towards more elaborated systems such as chemically modified graphene taking profit of the oxygen functionalities present at its surface,<sup>62</sup> giving rise to chemically modified GO, and therefore expanding the range of reactions that can be catalyzed by this carbocatalyst.<sup>63, 64</sup> On the other hand, the preparation of a three-dimensional (3D) graphene nanostructure is believed to be one step closer to more extensive applications.<sup>65-69</sup> The large surface areas of these foams arouse our interest, and in a collaboration with TEMA from the Department of Mechanical Engineering at the University of Aveiro, we planned to study its ability to catalyse the oxidation of an organosulfur compound, namely thioanisole, in comparison to its 2D counterpart.

The preparation of both catalysts, 2DGO and 3DGO, as well all the necessary characterization was ensured by TEMA resarch team. The starting GO was obtained accordingly to already reported procedures,<sup>62</sup> concerning the oxidation of graphite powder, which through hydrothermal treatment efficiently affords the 3DGO foam (Figure 7-6 a).

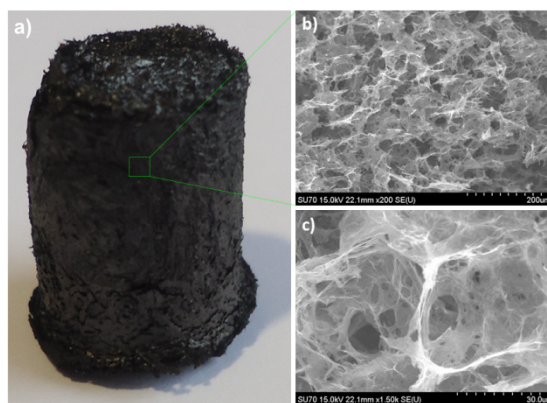


**Figure 7-6** a) Photograph of the 3DGO foam; b) and c) SEM images of 3DGO internal microstructure with different magnifications.

This material is an open-cell foam with a 3D porous network as imaged by scanning electron microscopy of the freeze-dried samples (Figure 7-6 b and c). The

characteristic N<sub>2</sub> adsorption–desorption isotherm for 3DGO has an H3 hysteresis loop, which is typical for plate-like particles (Figure 7-7). Moreover, the curve reveals the existence of both micro and mesoporosity, while the distinct upward turn at  $p/p_0$  close to 1 implies additional macroporosity.<sup>70</sup> This is in accordance with the pore size distribution obtained (Figure 7-8.). The determined BET surface area (SA) for 3DGO was 210 m<sup>2</sup> g<sup>-1</sup>. No reproducible SA values for 2DGO were obtained. It is known that upon drying, GO sheets form dense aggregates with complex structure and porosity,<sup>71</sup> thus hindering the nitrogen molecules to penetrate into the interlayer space of dried GO.

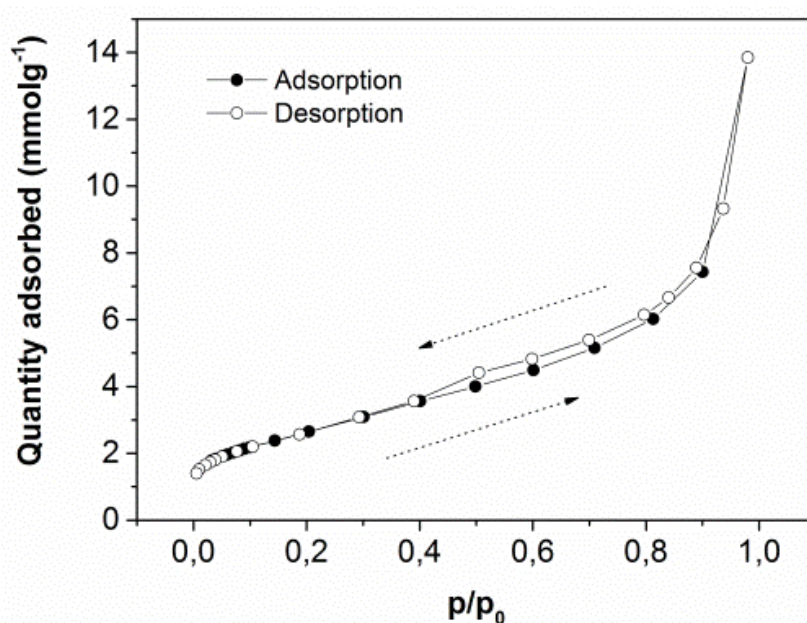


Figure 7-7 Nitrogen adsorption-desorption isotherm of 3DGO

XPS analysis was used to evaluate the degree of unsaturation and oxyfunctionalization of the two materials. The 3DGO presents a  $sp^2/sp^3C$  ratio of 1.32 against 0.28 for the 2DGO, which is indicative of a reduction process during the hydrothermal treatment. Although some carbonyl and carboxylic groups are still present in the 3DGO structure, the C-O/C-OH groups initially present at 2DGO (54.89 at%) are predominantly removed during the foam formation (Figure 7-9 and Table 7-2).

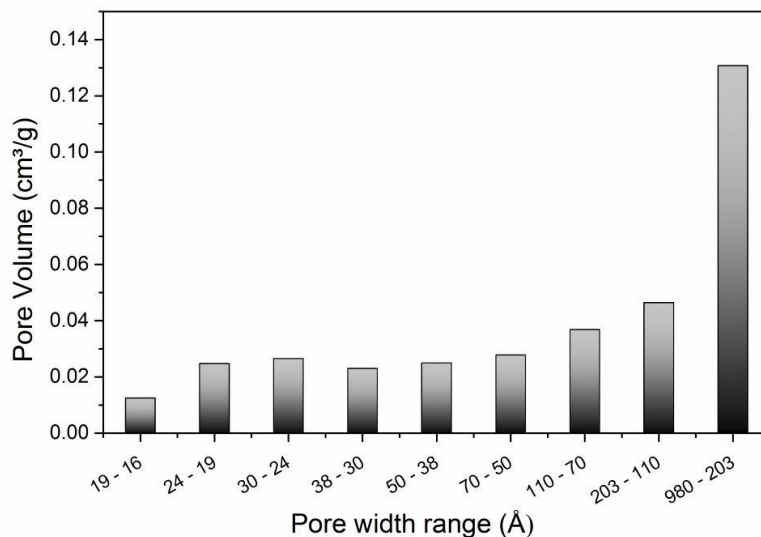
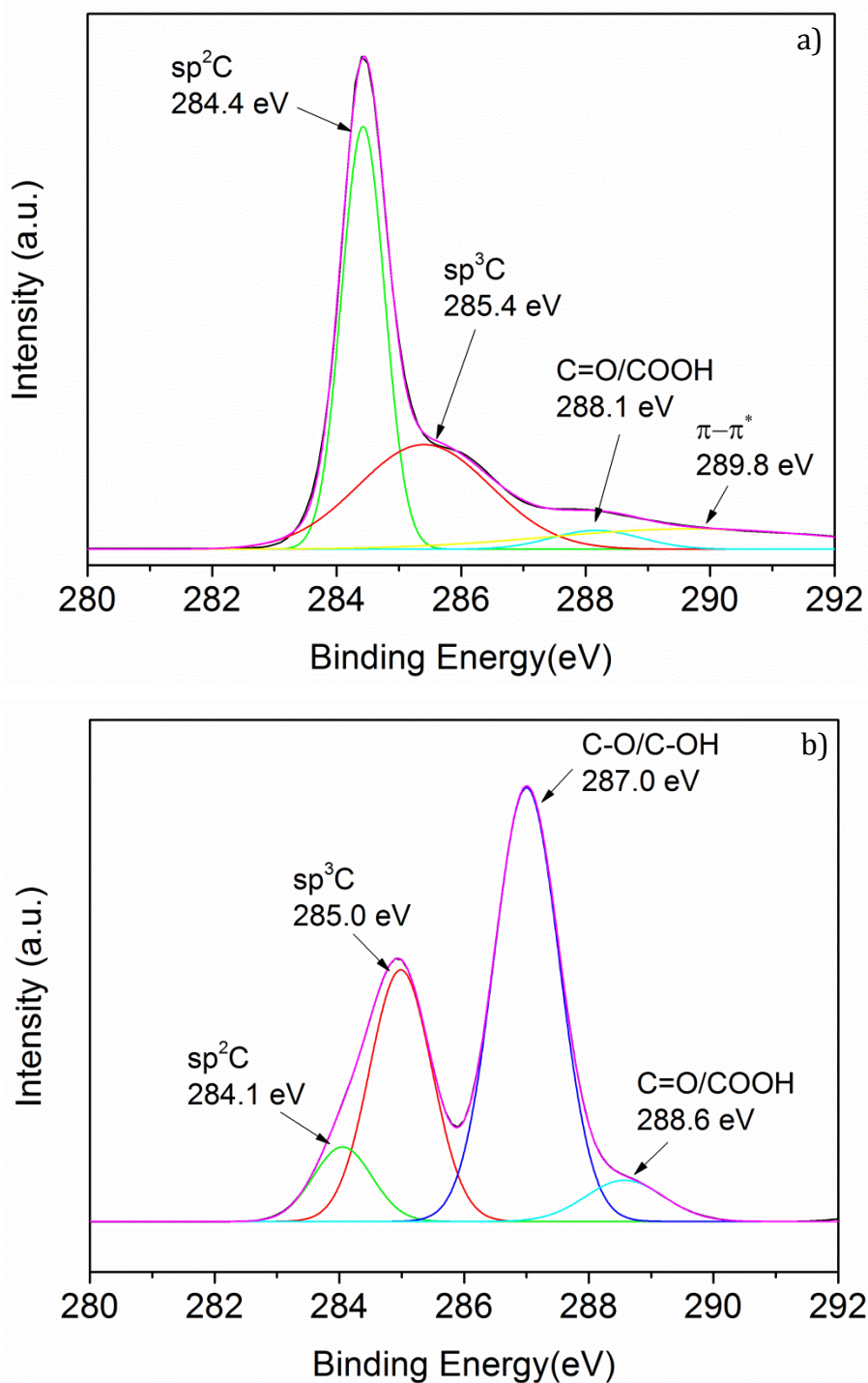


Figure 7-8 Pore width range distribution.

Table 7-2 Results of XPS analysis of the C1s content on the 3DGO and 2DGO

Chemical Bonds <sup>1</sup>	3DGO		2DGO	
	BE (eV)	AC (at.%)	BE (eV)	AC (at.%)
sp <sup>2</sup> C	284.4	46.1	284.1	8.44
sp <sup>3</sup> C	285.3	35.0	285.0	30.45
C-O/C-OH	<0.1	<0.1	287	54.89
C=O/COOH	288.1	4.23	288.6	6.22
π-π* <sup>2</sup>	289.7	14.68	-	-
<b>Ratio</b> sp <sup>2</sup> /sp <sup>3</sup> C	1.32		0.28	
<b>Ratio</b> C/O	2.10		0.75	

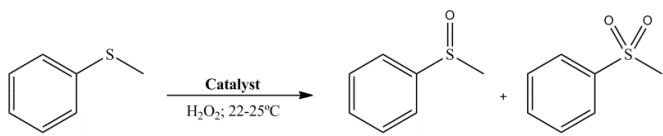


**Figure 7-9** Curve-fitting of C1s XPS spectra of a) 3DGO and b) 2DGO

For the catalytic experiments, both 2DGO and 3DGO nanostructures were compared. The results of the oxidation reactions with the two heterogeneous catalysts (2DGO and 3DGO) are summarized in Table 7-3. The 3DGO foam proved to be a more efficient catalyst in the oxidation of thioanisole affording the corresponding sulfoxide and sulfone at very high conversion. In fact, the results clearly show that on the first

cycle of the oxidation reaction the conversion is ~65% for 2DGO and ~87% for 3DGO. More interestingly, the conversion using 3DGO increases after recycling the material (97.2% of conversion for the 2<sup>nd</sup> cycle, 97.0% for the 3<sup>rd</sup> cycle and 99.7% for the 4<sup>th</sup> cycle), in opposition to the 2DGO (34.6% of conversion for the 2<sup>nd</sup> cycle, 28.2% for the 3<sup>rd</sup> cycle and 29.5% for the 4<sup>th</sup> cycle) as clearly put in evidence in Figure 7-10.

**Table 7-3** Oxidation of thioanisole with aqueous H<sub>2</sub>O<sub>2</sub> catalysed by 2DGO and a 3DGO foam<sup>a</sup>

Reaction scheme	Catalyst	Cycle <sup>b</sup>	Conversion (%)	Selectivity <sup>c</sup>	
				S=O	SO <sub>2</sub>
	2DGO	1 <sup>st</sup>	64.6	60.5	39.5
		2 <sup>nd</sup>	37.5	79.7	20.3
		3 <sup>rd</sup>	28.8	80.6	19.4
		4 <sup>th</sup>	30.7	74.6	25.4
	3DGO	1 <sup>st</sup>	86.7	91.2	8.8
		2 <sup>nd</sup>	97.2	89.8	10.2
		3 <sup>rd</sup>	97.0	74.8	25.2
		4 <sup>th</sup>	99.7	93.1	6.9

<sup>a</sup> Reaction conditions: thioanisole (0.3 mmol), catalyst (2DGO or 3DGO, 4.0 mg), internal standard (chlorobenzene, 0.3 mmol); CH<sub>3</sub>CN, for a total reaction volume of 2.0 mL; three 31 μL aliquots (0.3 mmol each) of H<sub>2</sub>O<sub>2</sub> 30 % (w/w) aqueous solution were added at the beginning, after 24 h, and after 48 h of reaction; room temperature. <sup>b</sup> Each cycle have the duration of 72 h. <sup>c</sup> Determined by GC with chlorobenzene as the IS.

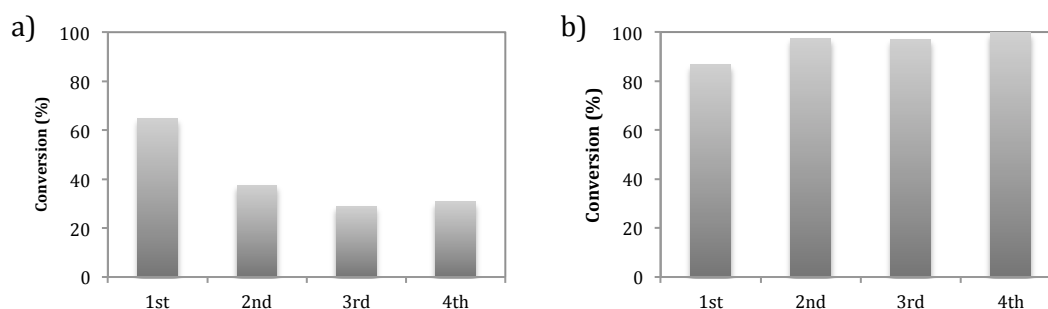


**Figure 7-10** Comparative graphics of the conversion obtained in the catalytic cycles carried out using a) 2DGO and b) 3DGO

FTIR analysis of the 3DGO catalyst before and after the catalysis reactions (Figure 7-11) shows an increment of oxygen functional groups on its surface, especially



carboxylic groups, and a decrease on C=C bonds during the catalytic process. XPS analysis after the 4<sup>th</sup> cycle shows effectively an increase on the carbonyl/carboxylic groups, concomitantly to a decrease on the C=C sp<sup>2</sup>, and a reciprocal increment on the sp<sup>3</sup> carbons after the catalysis reactions (Table 7-4). In fact, the sp<sup>2</sup>C/sp<sup>3</sup>C and the C/O ratios both decrease, suggesting an increase of oxygen contents on carbon structure after catalysis reactions. This increase can be due to the availability of oxygen species in the reaction medium, and seems to have an important contribution in the oxidation of organosulfur compounds. Although 2DGO has a higher percentage of oxygen on its structure than the 3DGO foam (Figure 7-8 and Table 7-2), the conversion of thioanisole into the corresponding oxidation products is less efficient for 2DGO. This suggests that the thioanisole oxidation reaction is promoted by the carbon double bonds that react with H<sub>2</sub>O<sub>2</sub> by forming oxygen functional groups on the 3DGO surface and oxygen free radicals able to oxidise the organosulfur compound, which is in accordance with the literature.<sup>54</sup> Still, we have tested the presence of radicals by adding known radical scavengers (KI and 1,4-benzoquinone) to the reaction medium, specific to scavenge the •OH and •O<sub>2</sub><sup>-</sup> radicals, respectively.<sup>72</sup> The results show that no conversion of thioanisole occurs by adding KI and only 23% of conversion is observed by adding 1,4-benzoquinone. This point out to two very important conclusions: 1) the oxidation of thioanisole with H<sub>2</sub>O<sub>2</sub> as oxidant, using 3DGO as a heterogeneous catalyst, seems to be a radicalar reaction, and 2) the radicals responsible for the oxidation reaction process seem to be essentially the •OH. Moreover, in the blank experiments performed in the presence of 3DGO, but without the addition of H<sub>2</sub>O<sub>2</sub> or alternatively, just in the presence of the oxidant, no products from the oxidation of thioanisole were detected.

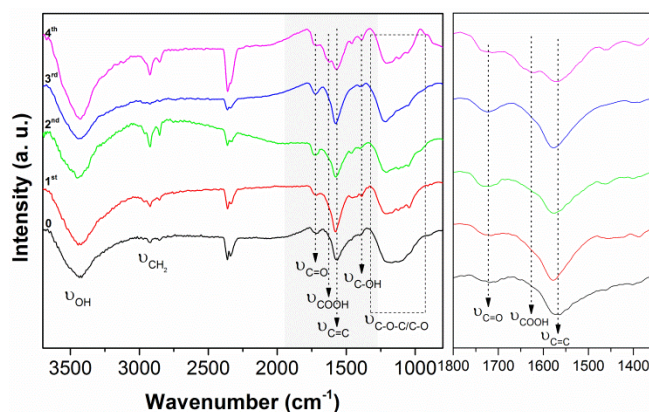


**Figure 7-11** FTIR spectra of 3DGO (0), and after the 1<sup>st</sup>, 2<sup>nd</sup>, 3<sup>rd</sup> and 4<sup>th</sup> catalytic cycles in the oxidation of thioanisole with aqueous H<sub>2</sub>O<sub>2</sub>



We propose that the formation of  $\bullet\text{OH}$  may occur by the homolytic cleavage of  $\text{H}_2\text{O}_2$  mediated by 3DGO with the formation of oxygen functional groups on its surface (C-OH on Figure 7-11).

**Table 7-4** XPS analysis of 3DGO before catalysis and after the 4<sup>th</sup> cycle

Chemical Bonds	3DGO		3DGO (after 4 <sup>th</sup> cycle)	
	BE (eV)	AC (at.%)	BE (eV)	AC (at.%)
sp <sup>2</sup> C	284.4	46.1	284.4	43.1
sp <sup>3</sup> C	285.3	35.0	285.3	38.5
C-O/C-OH	-	< 0.1	-	< 0.1
C=O/COOH	288.1	4.23	288.2	11.9
$\pi$ - $\pi^*$	289.7	14.68	290.9	6.6
Ratio sp <sup>2</sup> C/sp <sup>3</sup> C	1.32		1.12	
Ratio C/O	2.10		1.92	

These radicals are then able to oxidize the organosulfur compound at room temperature. The products' selectivity is similar for both catalysts, always with higher selectivity for sulfoxide over sulfone (Table 7-3). In general, 3DGO is more selective for the sulfoxide than 2DGO along the 4 cycles. The higher selectivity for sulfone in the case of 2DGO can also be related to the higher amount of oxygen functional groups on the GO surface, namely hydroxyl groups, potentially available to form  $\bullet\text{OR}$  radicals and the subsequent over-oxidation of the sulfoxide to the sulfone.

The 3DGO catalyst was also tested under similar conditions for the oxidation of diphenyl sulfide, an organosulfur compound typically present in fuels. The conversion of diphenyl sulfide is  $\approx 45\%$ , which is lower than for thioanisole (87%), probably due to higher steric hindrance.

The 3DGO catalysts stand out from other metal-free catalysts not only for its high catalytic activity ( $>90\%$ ) for the oxidation of thioanisole, but also by presenting the particularity to increase the catalytic activity with the number of cycles (Table 7-3). In fact, similar catalytic studies using fullerenes,<sup>73,74</sup> periodic mesoporous silicas,<sup>75</sup> and cyclodextrins<sup>76</sup> showed lower conversion values.

## 7.4. CONCLUSIONS

From the work presented firstly in this chapter, involving the catalytic experiments with the  $\text{TBA}_4\text{H}_2[\text{BW}_{11}\text{Mn}(\text{H}_2\text{O})\text{O}_{39}] \cdot 2\text{H}_2\text{O}$  (**Mn-POM**)/ $\text{H}_2\text{O}_2$  catalytic system, a new, environmental friendly, and efficient oxidation procedure for BTs (7.1-7.3) and DBTs (7.4-7.6) at room temperature is disclosed. As far as we know this is the first example of a POM as catalyst at room temperature with such an efficiency. Under very mild conditions, excellent conversion values were obtained (97.0-99.9% for a substrate/catalyst molar ratio of 150) with this **Mn-POM**.

Comparatively to the metalloporphyrin complexes, which proved to be more efficient catalyzing BTs sulfoxidation by  $\text{H}_2\text{O}_2$ , the **Mn-POM** under similar reaction conditions evidences better performance for DBTs. The high potential of **Mn-POM** for application in ODS was verified through the worthy results achieved in the oxidation of two model fuels by  $\text{H}_2\text{O}_2$ : one mainly composed by BTs (7.1-7.4) and the other mainly by DBTs (7.3-7.6), both with conversions close to 100% were attained after 3 hours of reaction.

Envisaging the simulation of the entire ODS procedure, a simple, efficient and environmentally sustainable extraction approach of the sulfone products from **MF2** was also developed, using an ethanol/ $\text{H}_2\text{O}$  mixture to successfully extract the sulfone products from hexane. The GC-FID analysis after 20 minutes of extraction showed that more than 98% of the organosulfur compounds were removed.

Relatively to the experiments involving graphene oxide catalysts, some advantages can be pointed out to 3DGO foam, since it is a metal-free and inexpensive catalyst, additionally to its facile recovery from the reaction media and subsequent reutilization. Contrarily to the results usually found in the literature, requiring high ratios (60-400 wt%) of GO for typical oxidative reactions,<sup>52, 54</sup> the ratio of 3DGO used in the present reactions is very low, around 11 wt% relatively to the substrate, and the reactions are run at room temperature, two major gains of the present system. These advantages indicate that 3DGO, when compared with other metal-free catalysts acts more efficiently for the thioanisole oxidation.



## 7.5. EXPERIMENTAL

### 7.5.1. INSTRUMENTS AND METHODS

To consult all the experimental details relatively to reagents, solvents and the apparatus involved in the performed experiments please go to section 3.3 of this dissertation. The GC-FID method was the same described in 3.3.2.

The conversion and selectivities values presented were estimated from the corresponding chromatographic peak areas, using chlorobenzene as internal standard. To confirm the structure of the products achieved, their retention times in the GC-FID were compared with those of authentic samples, and they were also injected in the GC-MS.

### 7.5.2. SYNTHESIS OF **MN-POM** AND **GRAPHENE OXIDE CATALYSTS**

Starting by the homogeneous catalyst,  $\text{TBA}_4\text{H}_2[\text{BW}_{11}\text{Mn}(\text{H}_2\text{O})\text{O}_{39}] \cdot 2\text{H}_2\text{O}$ , this was prepared and characterized according to previously described procedures.<sup>77</sup> The obtained compounds were characterized by elemental analysis (C, H, N, W, Mn), thermogravimetry and infrared spectroscopy and the results were in agreement with the previously published values.<sup>77</sup>

Relatively to the heterogeneous material, GO sheets were prepared by the oxidation of graphite powder under harsh oxidizing conditions.<sup>19</sup> The GO sheets were then thoroughly washed and purified by dialysis. To obtain the 3DGO foam an hydrothermal treatment of an aqueous suspension of GO sealed in a Teflon-lined autoclave at 180 °C for 12 h was performed.

### 7.5.3. TYPICAL PROCEDURE FOR THE OXIDATION REACTIONS USING **MN-POM**

For  $\text{BW}_{11}\text{Mn}$  the reactions were typically carried out as follows: the substrates **7.1** to **7.6** (0.3 mmol); the amount of catalyst corresponding to the appropriate substrate/catalyst molar ratio (150 and 300); the required amount of 30% (w/w) aqueous  $\text{H}_2\text{O}_2$  is 6 eq., 2.0 mL of acetonitrile and the internal standard

(chlorobenzene, 0.3 mmol) were stirred in a close vessel at room temperature for 3 hours in the absence of light.

For the model fuel catalytic studies, the procedure is very similar, however after dissolving the reactants and catalyst in 500  $\mu\text{L}$  of  $\text{CH}_3\text{CN}$  the total reaction volume (2.0 mL) were completed with hexane. Instead of using 0.3 mmol of substrate only 0.12 mmol were used (0.03 mmol of each sulfur derivative); **MF1** contains substrates **7.1-7.4** and **MF2** contains substrates **7.3-7.6**.

#### 7.5.4. TYPICAL PROCEDURE FOR THE OXIDATION REACTIONS USING GRAPHENE OXIDE

For a typical oxidation experiment the substrate (thioanisole, 0.3 mmol), the catalyst (2DGO or 3DGO, 4.0 mg), and the internal standard (chlorobenzene, 0.3 mmol) were placed in  $\text{CH}_3\text{CN}$ , for a total reaction volume of 2.0 mL. Three 31  $\mu\text{L}$  aliquots (0.3 mmol each) of the oxidant, a  $\text{H}_2\text{O}_2$  30 % (w/w) aqueous solution, were added at the beginning, after 24 h, and after 48 h of reaction. The course of the oxidation reactions was followed by GC-FID using chlorobenzene as the internal standard. Both 2DGO and 3DGO materials were recovered by centrifugation, carefully washed with different solvents ( $\text{CH}_3\text{CN}$ ,  $\text{CH}_2\text{Cl}_2$ , and acetone, in this order) and dried at open air for two days, before its reutilization under similar conditions.



## 7.6. BIBLIOGRAPHY

- <sup>1</sup> Y.X. Ding, W.S. Zhu, H.M. Li, W. Jiang, M. Zhang, Y.Q. Duan, Y.H. Chang, *Green Chem.* 13 (2011) 1210.
- <sup>2</sup> J.H. Xu, S. Zhao, W. Chen, M. Wang, Y.F. Song, *Chem. A Eur. J.* 18 (2012) 4775.
- <sup>3</sup> W.S. Zhu, W.L. Huang, H.M. Li, M. Zhang, W. Jiang, G.Y. Chen, C.R. Han, *Fuel Proces. Technol.* 92 (2011) 1842.
- <sup>4</sup> W. Trakarnpruk, K. Rujiraworawut, *Fuel Proces. Technol.* 90 (2009) 411.
- <sup>5</sup> J.L. Garcia-Gutierrez, G.A. Fuentes, M.E. Hernandez-Teran, F. Murrieta, J. Navarrete, F. Jimenez-Cruz, *Appl. Catal. A: Gen.* 305 (2006) 15.
- <sup>6</sup> G.A.B. Gonçalves, S.M.G. Pires, M.M.Q. Simões, M.G.P.M.S. Neves, P.A.A.P. Marques, *Chem. Commun.* 50 (2014) 7673.
- <sup>7</sup> T. Yamaura, K. Kamata, K. Yamaguchi, N. Mizuno, *Catal. Today* 203 (2012) 76.
- <sup>8</sup> M. Bagherzadeh, M.M. Haghdoost, M. Amini, P.G. Derakhshandeh, *Catal. Commun.* 23 (2012) 14.
- <sup>9</sup> J.M. Campos-Martin, M.C. Capel-Sanchez, P. Peres-Presas, J.L.G. Fierro, *J. Chem. Technol. Biotechnol.* 85 (2010) 879 and references cited therein.
- <sup>10</sup> B. Pawelec, R.M. Navarro, J.M. Campos-Martin, J.L.G. Fierro, *Catal. Sci. Technol.* 1 (2011) 23 and references cited therein.
- <sup>11</sup> L. Xu, J. Cheng, M.L. Trudell, *J. Org. Chem.* 68 (2003) 5388.
- <sup>12</sup> R. Villar, I. Encio, M. Migliaccio, M.J. Gil, V. Martinez-Merino, *Bioorg. Med. Chem.* 12 (2004) 963.
- <sup>13</sup> R. Bentley, *Chem. Soc. Rev.* 34 (2005) 609 and references cited therein.
- <sup>14</sup> Z. Jiang, H. Lü, Y. Zhang, C. Li, *Chin. J. Catal.* 32 (2011) 707.
- <sup>15</sup> A. Stanislaus, A. Marafi, M.S. Rana, *Catal. Today* 153 (2010) 1.
- <sup>16</sup> W. Zhu, H. Li, X. Jiang, Y. Yan, J. Lu, J. Xia, *Energy Fuels* 21 (2007) 2514.
- <sup>17</sup> J.T. Rhule, C.L. Hill, D.A. Judd, R.F. Schinazi, *Chem. Rev.* 98 (1998) 327.
- <sup>18</sup> D.L. Long, E. Burkholder, L. Cronin, *Chem. Soc. Rev.* 36 (2007) 105.
- <sup>19</sup> C. L. Hill, *J. Mol. Catal. A: Chem.* 262 (2007) 1.
- <sup>20</sup> M.T. Pope, A. Müller, *Angew. Chem. Int. Ed. Engl.* 30 (1991) 34.
- <sup>21</sup> Special issue for polyoxometalates (Guest Editor: C. L. Hill), *Chem. Rev.* (1998) 98.
- <sup>22</sup> D. E. Katsoulis, *Chem. Rev.* 98 (1998) 359.
- <sup>23</sup> W. G. Klemperer, C. G. Wall, *Chem. Rev.* 98 (1998) 297.
- <sup>24</sup> N. Mizuno, K. Yamaguchi, K. Kamata, *Coord. Chem. Rev.* 249 (2005) 1944.
- <sup>25</sup> O.A. Kholdeeva, R.I. Maksimovskaya, *J. Mol. Catal. A: Chem.* 262 (2007) 7.

- <sup>26</sup> A.C. Estrada, M.M.Q. Simões, I.C.M.S. Santos, M.G.P.M.S. Neves, A.M.S. Silva, A.M.V. Cavaleiro, *Appl. Catal. A: Gen.* 366 (2009) 275.
- <sup>27</sup> N. Wu, B. Li, Z. Liu, C. Han, *Catal. Commun.* 46 (2014) 156.
- <sup>28</sup> Y.-F. Song, R. Tsunashima, *Chem. Soc. Rev.* 41 (2012) 7384.
- <sup>29</sup> X. Xue, W. Zhao, B. Ma, Y. Ding, *Catal. Commun.* 29 (2012) 73.
- <sup>30</sup> Y. Ding, W. Zhu, H. Li, W. Jiang, M. Zhang, Y. Duan, Y. Chang, *Green Chem.* 13 (2011) 1210.
- <sup>31</sup> S. Ribeiro, C.M. Granadeiro, P. Silva, F.A.A. Paz, F.F. de Biani, L. Cunha-Silva, S.S. Balula, *Catal. Sci. Technol.* 3 (2013) 2404.
- <sup>32</sup> S. Ribeiro, A.D.S. Barbosa, A.C. Gomes, M. Pillinger, I.S. Gonçalves, L. Cunha-Silva, S.S. Balula, *Fuel Proces. Technol.* 116 (2013) 350.
- <sup>33</sup> S.M.G. Pires, M.M.Q. Simões, I.C.M.S. Santos, S.L.H. Rebelo, M.M. Pereira, M.G.P.M.S. Neves, J.A.S. Cavaleiro, *Appl. Catal. A: Gen.* 439–440 (2012) 51.
- <sup>34</sup> S.M.G. Pires, M.M.Q. Simões, I.C.M.S. Santos, S.L.H. Rebelo, F.A.A. Paz, M.G.P.M.S. Neves, J.A.S. Cavaleiro, *Appl. Catal. B: Environ.* 160–161 (2014) 80.
- <sup>35</sup> A.C. Estrada, M.M.Q. Simões, I.C.M.S. Santos, M.G.P.M.S. Neves, J.A.S. Cavaleiro, A.M.V. Cavaleiro, *Monatsh. Chem.* 141 (2010) 1223.
- <sup>36</sup> J.L.C. Sousa, I.C.M.S. Santos, M.M.Q. Simões, J.A.S. Cavaleiro, H.I.S. Nogueira, A.M.V. Cavaleiro, *Catal. Commun.* 12 (2011) 459.
- <sup>37</sup> I.C.M.S. Santos, S.S. Balula, M.M.Q. Simões, L. Cunha-Silva, M.G.P.M.S. Neves, B. de Castro, A.M.V. Cavaleiro, J.A.S. Cavaleiro, *Catal. Today* 203 (2013) 87.
- <sup>38</sup> S.S. Balula, I.C.M.S. Santos, L. Cunha-Silva, A.P. Carvalho, J. Pires, C. Freire, J.A.S. Cavaleiro, B. Castro, A. M. V. Cavaleiro, *Catal. Today* 203 (2013) 95.
- <sup>39</sup> T.A.G. Duarte, I.C.M.S. Santos, M.M.Q. Simões, M.G.P.M.S. Neves, A.M.V. Cavaleiro, J.A.S. Cavaleiro, *Catal. Lett.* 144 (2014) 104
- <sup>40</sup> Y. Zhang, H. Lü, L. Wang, Y. Zhang, P. Liu, H. Han, Z. Jiang, C. Li, *J. Mol. Catal. A: Chem.* 332 (2010) 59.
- <sup>41</sup> K.S. Novoselov, A.K. Geim, S.V. Morozov, D. Jiang, Y. Zhang, S.V. Dubonos, I.V. Grigorieva, A. A. Firsov, *Science* 306 (2004) 666.
- <sup>42</sup> J.-H. Chen, C. Jang, S. Xiao, M. Ishigami, M. S. Fuhrer, *Nat. Nanotechnol.* 3 (2008) 206.
- <sup>43</sup> A.H.C. Neto, F. Guinea, N.M.R. Peres, K.S. Novoselov, A.K. Geim, *Rev. Mod. Phys.* 81 (2009) 109.
- <sup>44</sup> T.G. Pedersen, C. Flindt, J. Pedersen, A.-P. Jauho, N.A. Mortensen, K. Pedersen, *Phys. Rev. B* 77 (2008) 245431;



- <sup>45</sup> F. Scarpa, S. Adhikari, A.S. Phani, *Nanotechnology* 20 (2009) 65709.
- <sup>46</sup> S. Stankovich, D.A. Dikin, G.H.B. Dommett, K.M. Kohlhaas, E.J. Zimney, E.A. Stach, R.D. Piner, S.T. Nguyen, R.S. Ruoff, *Nature* 442 (2006) 282.
- <sup>47</sup> R. Arsat, M. Breedon, M. Shafiei, P.G. Spizziri, S. Gilje, R.B. Kaner, K. Kalantar-Zadeh, W. Wlodarski, *Chem. Phys. Lett.* 467 (2009) 344.
- <sup>48</sup> H.P. Jia, D.R. Dreyer, C.W. Bielawski, *Tetrahedron* 67 (2011) 4431.
- <sup>49</sup> A. Dhakshinamoorthy, M. Alvaro, M. Puche, V. Fornes, H. Garcia, *Chem. Cat. Chem.* 4 (2012) 2026.
- <sup>50</sup> H.P. Jia, D.R. Dreyer, C.W. Bielawski, *Adv. Synth. Catal.* 353 (2011) 528.
- <sup>51</sup> J. Pyun, *Angew. Chem. Int. Ed.* 50 (2011) 46.
- <sup>52</sup> C. Su, M. Acik, K. Takai, J. Lu, S. Hao, Y. Zheng, P. Wu, Q. Bao, T. Enoki, Y.J. Chabal, K.P. Loh, , *Nat. Commun.* 3 (2012) 1298.
- <sup>53</sup> B.F. Machado, P. Serp, *Catal. Sci. Technol.* 2 (2012) 54.
- <sup>54</sup> D.R. Dreyer, C.W. Bielawski, *Chem. Sci.* 2 (2011) 1233.
- <sup>55</sup> D.R. Dreyer, H.P. Jia, C.W. Bielawski, *Angew. Chem. Int. Ed.* 49 (2010) 6813.
- <sup>56</sup> D.R. Dreyer, H.P. Jia, A.D. Todd, J.X. Geng, C.W. Bielawski, *Org. Biomol. Chem.* 9 (2011) 7292.
- <sup>57</sup> A.V. Kumar, K.R. Rao, *Tetrahedron Lett.* 52 (2011) 5188.
- <sup>58</sup> S. Verma, H.P. Mungse, N. Kumar, S. Choudhary, S.L. Jain, B. Sain, O.P. Khatri, *Chem. Commun.* 47 (2011) 12673.
- <sup>59</sup> Y. Kim, S. Some, H. Lee, *Chem. Commun.* 49 (2013) 5702.
- <sup>60</sup> D.R. Dreyer, C.W. Bielawski, *Adv. Funct. Mater.* 22 (2012) 3247.
- <sup>61</sup> Y.H. Pan, S. Wang, C.W. Kee, E. Dubuisson, Y.Y. Yang, K.P. Loh, C.H. Tan, *Green Chem.* 13 (2011) 3341.
- <sup>62</sup> G. Gonçalves, P.A.A.P. Marques, C.M. Granadeiro, H.I.S. Nogueira, M.K. Singh, J. Gracio, *Chem. Mater.* 21 (2009) 4796.
- <sup>63</sup> J.L. Long, X.Q. Xie, J. Xu, Q. Gu, L.M. Chen, X.X. Wang, *ACS Catal.* 2 (2012) 622.
- <sup>64</sup> J.Y. Ji, G.H. Zhang, H.Y. Chen, S.L. Wang, G.L. Zhang, F.B. Zhang, X.B. Fan, *Chem. Sci.* 2 (2011) 484.
- <sup>65</sup> Y.X. Xu, K.X. Sheng, C. Li, G.Q. Shi, *ACS Nano* 4 (2010) 4324.
- <sup>66</sup> X.H. Cao, Y.M. Shi, W.H. Shi, G. Lu, X. Huang, Q.Y. Yan, Q.C. Zhang, H. Zhang, *Small* 7 (2011) 3163.
- <sup>67</sup> D. Zhou, T.L. Zhang, B.H. Han, *Micropor. Mesopor. Mat.* 165 (2013) 234.
- <sup>68</sup> H. Huang, P.W. Chen, X.T. Zhang, Y. Lu, W.C. Zhan, *Small* 9 (2013) 1397.



- <sup>69</sup> Z. Fan, D.Z.Y. Tng, S.T. Nguyen, J.D. Feng, C.F. Lin, P.F. Xiao, L. Lu, H.M. Duong, *Chem. Phys. Lett.* 561 (2013) 92.
- <sup>70</sup> K.S.W. Sing, D.H. Everett, R.A.W. Haul, L. Moscou, R. A. Pierotti, J. Rouquerol, T. Siemieniowska, *Pure Appl. Chem.* 57 (1985) 603.
- <sup>71</sup> R.L.D. Whitby, V.M. Gunko, A. Korobeinyk, R. Busquets, A.B. Cundy, K. Laszlo, J. Skubiszewska-Zieba, R. Lebeda, E. Tombacz, I.Y. Toth, K. Kovacs, S.V. Mikhalovsky, *ACS Nano* 6 (2012) 3967.
- <sup>72</sup> J.M. Monteagudo, A. Duran, I. San Martin, A. Carnicer, *Appl. Catal. B: Environ.* 106 (2011) 242.
- <sup>73</sup> A.W. Jensen, B.S. Maru, X. Zhang, D.K. Mohanty, B.D. Fahlman, D.R Swanson, D.A. Tomalia, *Nano Lett.* 5 (2005) 1171.
- <sup>74</sup> A.W. Jensen, C. Daniels, *J. Org. Chem.* 68 (2003) 207.
- <sup>75</sup> R.A. Garcia, V. Morales, T. Garces, *J. Mater. Chem.* 22 (2012) 2607.
- <sup>76</sup> H.M. Shen, H.B. Ji, *Carbohydr. Res.* 354 (2012) 49.
- <sup>77</sup> a) I.C.M.S. Santos, PhD Thesis (2004) University of Aveiro, b) M.S.S. Balula, I.C.M.S. Santos, M.M.Q. Simões, M.G.P.M.S. Neves, J.A.S. Cavaleiro, A.M.V. Cavaleiro, *J. Mol. Catal. A: Chem.* 222 (2004) 159.



## **Chapter 8 GENERAL CONCLUSIONS AND FUTURE PERSPECTIVES**



In this dissertation a biomimetic and environmentally benign approach, using M-Porph/H<sub>2</sub>O<sub>2</sub> catalytic systems for the oxidation of several organosulfur compounds, namely sulfides, benzothiophenes and dibenzothiophenes, were presented. Despite the high efficiency demonstrated by Mn(III) complexes, (Mn(TDCPP)Cl and Mn(TPFPP)Cl, allowing to obtain conversions above 95% into the corresponding sulfoxides and/or sulfones for all the substrates tested, the Fe(TF<sub>4</sub>NMe<sub>2</sub>PP)Cl, besides a superior catalytic performance, permits the establishment of an even more clean approach. With the Fe(III) catalyst the assays were carried out in ethanol and in the absence of a co-catalyst. The good results achieved can bring an important future contribute to the application of this type of methodologies in the decontamination of fuels. In fact, the preliminary results on the oxidation of envisaged model fuels consisting of a mixture of benzo and dibenzothiophenes in hexane using both catalytic systems Mn(TDCPP)Cl/H<sub>2</sub>O<sub>2</sub> and Fe(TF<sub>4</sub>NMe<sub>2</sub>PP)Cl/H<sub>2</sub>O<sub>2</sub> are quite promising.

A similar methodology was applied to the oxidation of 1,3-dihydrobenzo[*c*]thiophenes, which gave the corresponding sulfones, important dienophiles for Diels-Alder reactions. This constitutes the first eco-friendly procedure for the synthesis of this kind of sulfones.

The good results achieved with metalloporphyrin catalysts in the oxidation of sulfur derivatives by H<sub>2</sub>O<sub>2</sub> under homogeneous conditions led us to envisage the development of an efficient heterogeneous system. The potential of this approach resides on the possibility of the catalyst to be recovered and reused. With the experience of our group in the area, three heterogeneous metalloporphyrin-based catalysts have been synthesized, and their catalytic efficiency evaluated in the sulfoxidation of thioanisole. For two of the Mn(III) complexes, one linked to a Merrifield support and the other to a silica support, this preliminary study afforded interesting results. However, when the catalytic tests were extended to more recalcitrant substrates, the efficiency of this catalysts showed to be limited.

The catalytic experiments with metalloporphyrins as catalysts were also extended to other substrates, namely benzofurans and naphthoquinones. Starting by benzofuran derivatives, the preferential oxidation route seems to be the epoxidation on the furan ring. Despite that, the instability of the epoxides formed led to different products, depending on the catalyst employed and on the reaction conditions. The identification of the obtained products with such biomimetic models can bring further and relevant



knowledge related with the toxicity of benzofuran epoxides. In this sense, further studies are needed to complete the work, namely to identify the unknown products. The development of a comprehensive two-dimensional gas chromatography analysis (GC-GC) procedure was envisaged in order to evaluate the formation of any other products, beyond those already identified, and also to bring some answers to the more complex samples.

Relatively to the catalyzed oxidation of naphthoquinones, the tests with lapachol using a Mn(III)porphyrin show that, in comparison to the previous results using *m*-CPBA, different products are detected, as well as a different selectivity. With Mn(TDCPP)Cl/H<sub>2</sub>O<sub>2</sub> catalytic system, the formation of *para*-naphthoquinones seems to be highly favored and a new lactone is isolated and characterized. It has also been noticed that the use of different metalloporphyrins led to different selectivity as well to new products. More catalytic experiments should be addressed in a near future with the two naphthoquinones studied, namely lapachol and *nor*-lapachol, in order to identify the unknown products with Mn(TPFPP)Cl and Mn(TDMI<sub>2</sub>P)Cl, and to confirm the proposed structures for *nor*-lapachol.

In addition to metalloporphyrins, it was possible to study also other catalysts, namely a POM and a graphene oxide foam 3D. The first was tested in the oxidation of benzothiophenes (BTs) and dibenzothiophenes (DBTs) by hydrogen peroxide. Remarkably, it proved to be highly efficient at room temperature, and showing a special ability for the oxidation of most recalcitrant DBTs. The use of POM catalysts in the oxidative desulfurization of fuels, evidenced by the herein presented results, is thus an area full of potential for future developments.

Finally, a heterogeneous material, the three-dimensional graphene oxide foam, (3DGO) was found to be a highly efficient and recyclable catalyst for the oxidation of thioanisole. Moreover, 3DGO reveals to be more efficient than 2DGO, and its efficiency increases with the number of cycles for 3DGO, in contrast to the 2D counterpart. These more elaborated systems, presenting high surface areas with oxygen functionalities, attracted scientist's interest, as it is believed that they can be applied in an increased number of applications. 3DGO is a metal-free, inexpensive carbocatalyst, able to work under very mild conditions and this topic should be retaken in a near future.

